Public

Report

Document ID	Version	Status	Reg no	Page
1454226	1.0	Approved		1 (130)
Author Jan Hernelind/5T Engineering AB			Date 2014-12-07	
Reviewed by Lisette Åkerman (QA)			Reviewed date 2015-01-08	
Approved by Jan Sarnet			Approved date 2015-01-08	

Hydrostatic pressure for detailed BWR/PWR-canisters

Abstract

The BWR and PWR canisters have to be designed to withstand the loads caused by the swelling pressure in the buffer plus the load caused by a thick ice sheet. The effect of such loads has been investigated by finite element calculations and the results are compared with a previous study (Dillström et al. 2010).

A three-dimensional finite element mesh of the canister has been created and simulation of an assumed hydrostatic load has been performed using the FE-code ABAQUS (ABAQUS 2013).

The obtained results, evaluated using changes in kinetic energy as well following ASME VIII (6-153) (ASME 1995), show that both the PWR and BWR canisters withstand the design loads with a satisfying safety factor, see “Evaluation and Conclusions”.

Sammanfattning

Både BWR- och PWR-kapseln måste dimensioneras för att klara svälltrycket i bufferten plus lasten under en tjock inlandsis. Effekten av dylik glaciärlast har undersökts med hjälp av finita elementberäkningar.
En tredimensionell finita element modell av kapseln har skapats varefter simulering av ett antaget hydrostatiskt tryck har utförts med FE-programmet ABAQUS (ABAQUS 2013).

Erhållna resultat, evaluerade via ändring i kinetisk energi samt också via ASME VIII (6-153) (ASME 1995), visar att både PWR- och BWR- kapseln klarar designlasten med tillfredsställande säkerhetsfaktor, se “Evaluation and Conclusions”.

Svensk Kärnbränslehantering AB
Swedish Nuclear Fuel and Waste Management Co
PO Box 250, SE-101 24 Stockholm
Visiting address Blekholmstorget 30
Phone +46-8-459 84 00 Fax +46-8-579 386 10
www.skb.se
556175-2014 Seat Stockholm

Contents

1 Introduction and simulation strategy

1.1 Introduction

According to the design premises set out by SKB, see Table 2-1 in SKB (2010), "The canister shall withstand an isostatic load of 45 MPa, being the sum of maximum swelling pressure and maximum groundwater pressure". SKB has requested results of impact on the canister at 60, 90 and 100 MPa as applied hydrostatic pressure on the outer surface of the copper shell which will imply a possibility to estimate the safety factor of the design.
In addition, SKB also explores the possibilities to increase the load in the design premises from 45 MPa to 50 MPa. An assessment on potential safety factor in relation to such a requirements for the given canister designs is also asked for.
Comparison is then performed with one of several previous studies (Dillström et al. 2010) which mainly consist of 2-dimensional analyses evaluated with the ASME-code (ASME 1995).

In the present work, the geometry definition for the BWR and PWR canister is created based on 3-dimensional CAD-drawings with as few simplifications as possible.

Four cases are requested for each of the BWR and the PWR designs:

- Design based on nominal measures
- Design based on manufacturing tolerances (the channel tubes are moved 10 mm in radial direction)
- Design based on manufacturing tolerances where one cylindrical defect has been defined (height 50 mm with radius 20 mm for the BWR insert and 40 mm for the PWR insert)
- Sensitivity on yield surface for the insert. Design based on manufacturing tolerances where one cylindrical defect has been defined and the yield surface for the nodular cast iron used for the insert has been reduced (89% of the original yield surface).

Since large deformations and discontinuities due to contacts are expected, an explicit solver is used to avoid possible convergence issues with an implicit solver.

1.2 Modelling and labeling of analyzes

The performed simulations are based on the same geometry as in previous analyses (Hernelind 2010) for the copper shell. The insert and channel tubes are defined by all details in the drawings for BWR /PWR inserts. The channel tubes are connected by support plates welded to the channel tubes. The support plates are glued to the cast iron insert which also applies to the base plates and base screws. Otherwise, the channel tubes are constrained by contact conditions. All screw heads are simplified to a cylindrical shape and a few extremely small holes that appear in the drawings are removed (these holes doesn't exist in reality and have been removed). The steel lid is fixed by a screw in the centre. The default model is based on nominal dimensions without considering tolerances and three models for both the BWR and the PWR insert are defined by moving the steel channels (channel tubes) as much as possible (10 mm) in the radial direction due to allowed tolerances (SKB 2010).
Table 1-1 shows job-names for all analyses described in this report.

Table 1-1. Definition of simulation cases.

Model name	No nodes	No elements	Description
pwr_centric_full_PD	451890	342869	PWR insert based on nominal dimensions
pwr_eccentric_full_PD	440610	334069	PWR insert based on manufacturing tolerances
pwr_eccentric_defect_full_PD	370434	273837	PWR insert based on manufacturing tolerances with one cylindrical defect included.
pwr_eccentric_defect_full_PD2	370434	273837	PWR insert based on manufacturing tolerances with one cylindrical defect included and reduced yield surface.
bwr_centric_rotated_PD	627897	493624	BWR insert based on nominal dimensions with model from previous shearing analyses.
bwr_eccentric_rotated_PD	717632	576456	BWR insert based on manufacturing tolerances with model from previous shearing analyses.
bwr_eccentric_defect_PD	1173271	925726	BWR insert based on manufacturing tolerances with one cylindrical defect.
bwr_eccentric_defect_PD2	1173271	925726	BWR insert based on manufacturing tolerances with one cylindrical defect and reduced yield surface.

2 Meshes

The geometry used for the hydrostatic load consists of the insert (made of nodular cast iron), the insert lid (made of steel), the channel tubes (made of steel), the fixing centre screw and the copper shell. The geometry is based on CAD-geometries received from SKB, "Ritningsförteckning för kapselkomponenter" (SKBdoc 1203875, ver 2) and should therefore correspond to the current design.

Regardless of a BWR or PWR insert, the outer dimension of the insert is the same, implying that also the surrounding copper shell, the insert lid and the fixing centre screw are identical

Since geometrical instability is expected, the initially symmetric geometry will be lost and thus the complete insert has been modelled. The mesh is then generated by 3-dimensional solid elements, mainly 8-noded hexahedral (most of them using full integration technique) and a few 6-noded wedge elements.

Figures 2-1 to 2-3 show geometry and mesh for the PWR model. Figures 2-4 to 2-6 show the corresponding plots for the BWR model.

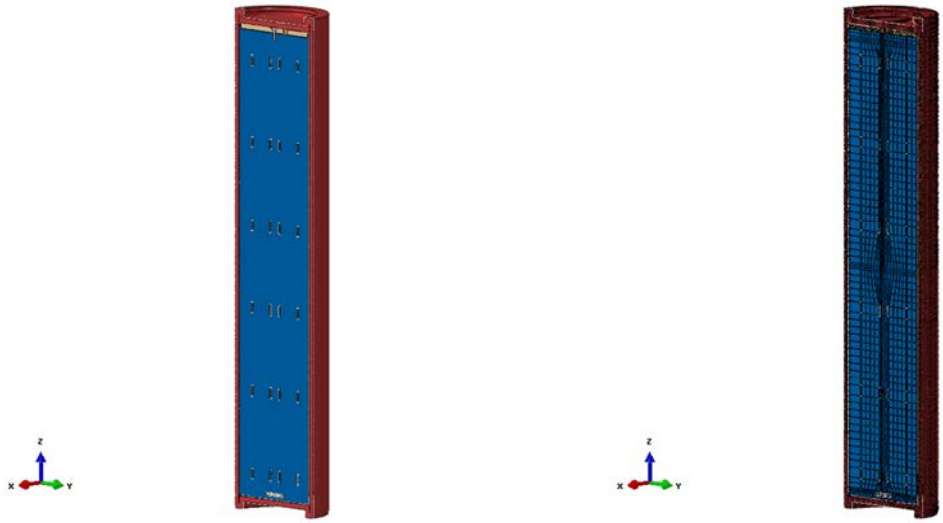

Figure 2-1. *The PWR model (half of the model is shown), with the copper shell (red), insert lid (brown), insert (blue), channel tubes (white) and screw (grey).*

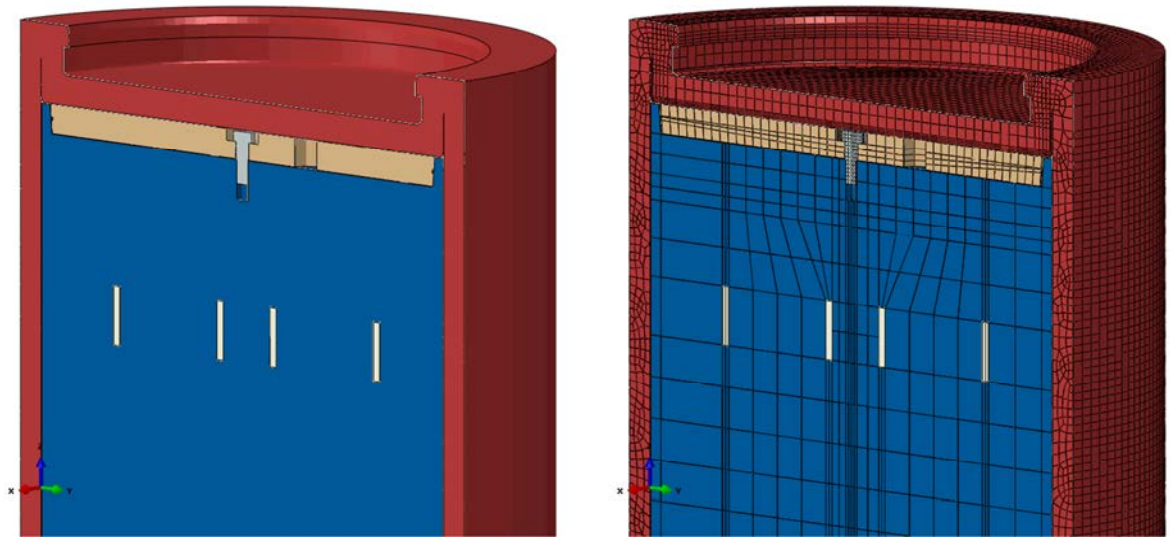

Figure 2-2. *Details of the upper part of the PWR model, with the copper shell (red), insert lid (brown), insert (blue), channel tubes (white) and screw (grey).*

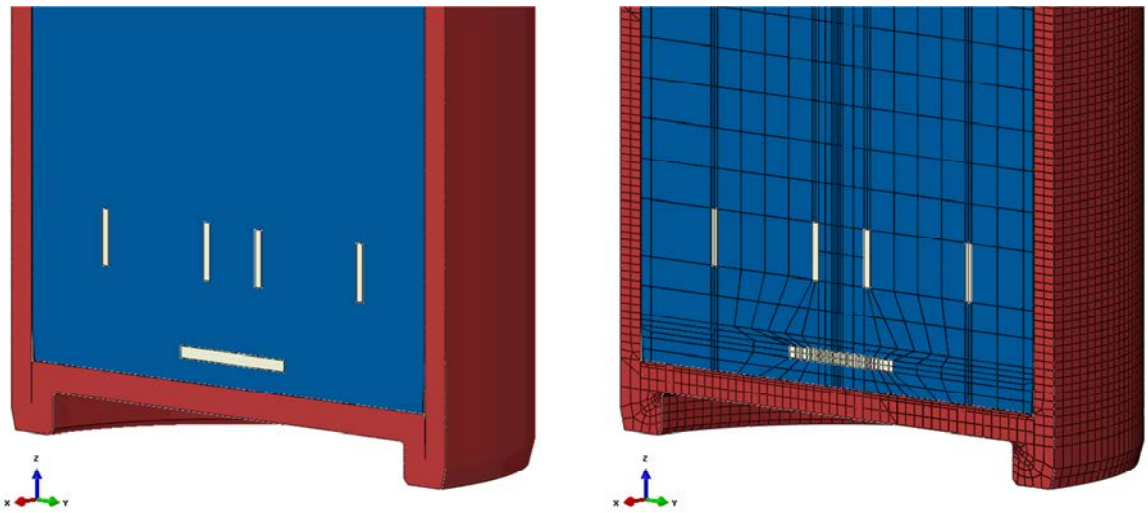

Figure 2-3. *Details of lower part of the PWR model, with the copper shell (red), insert (blue) and channel tubes (white).*

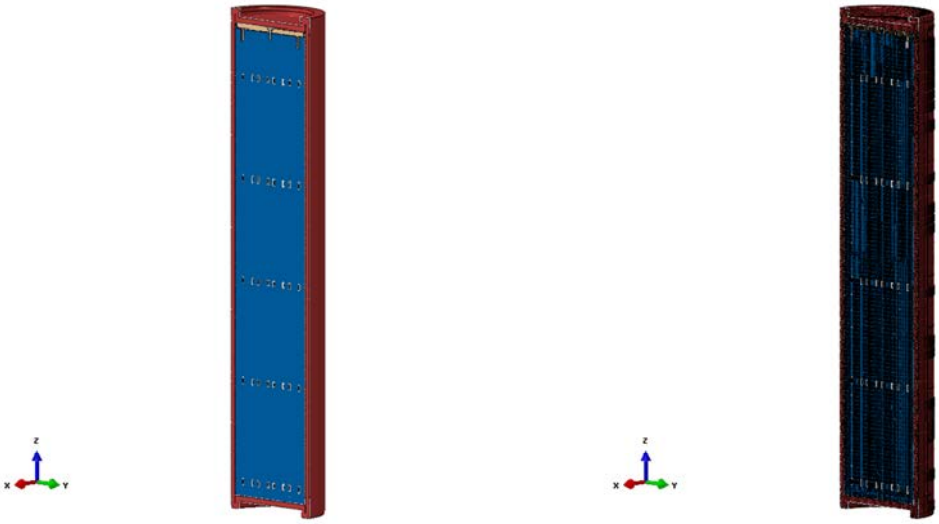

Figure 2-4. *The BWR model (half of the model is shown), with the copper shell (red), insert lid (brown), insert (blue), channel tubes (white) and screw (grey).*

Figure 2-5. *Details of the upper part of the BWR model, with the copper shell (red), insert lid (brown), insert (blue), channel tubes including support plates (white) and screw (grey).*

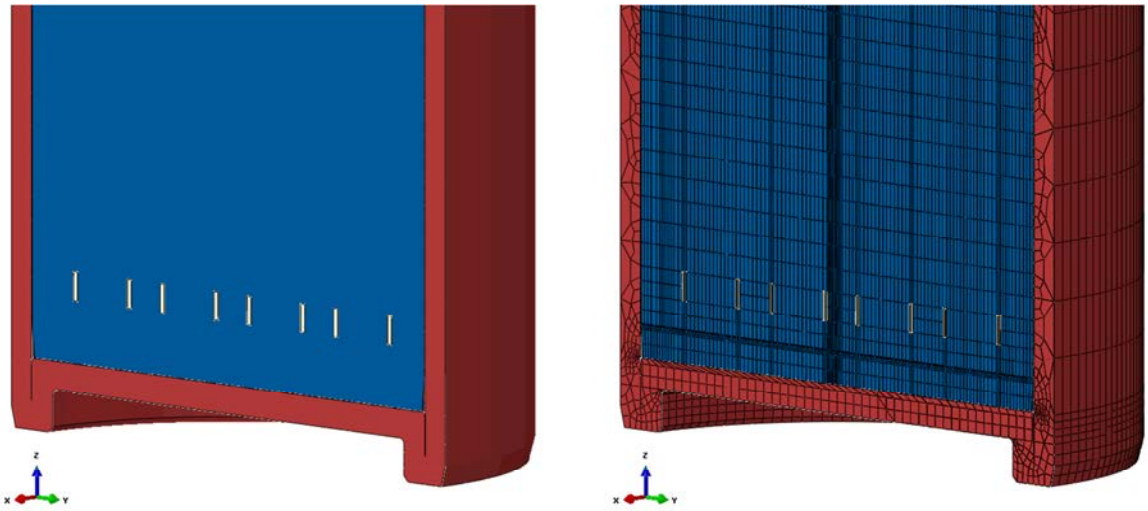

Figure 2-6*. Details of the lower part of the BWR model, with the copper shell (red), insert (blue) and channel tubes including support plates (white).*

3 Geometry of parts

3.1 Copper shell

The copper shell, common to the BWR and PWR inserts, surrounds the insert and interacts with the insert. The copper shell has been modelled rather accurately in order to catch “hot spots” where large strains and large strain gradients are expected, e.g. the fillets at the base and top (the copper lid). The lid is welded to the flange and will act as one part, see Figures 3-1 to 3-3.

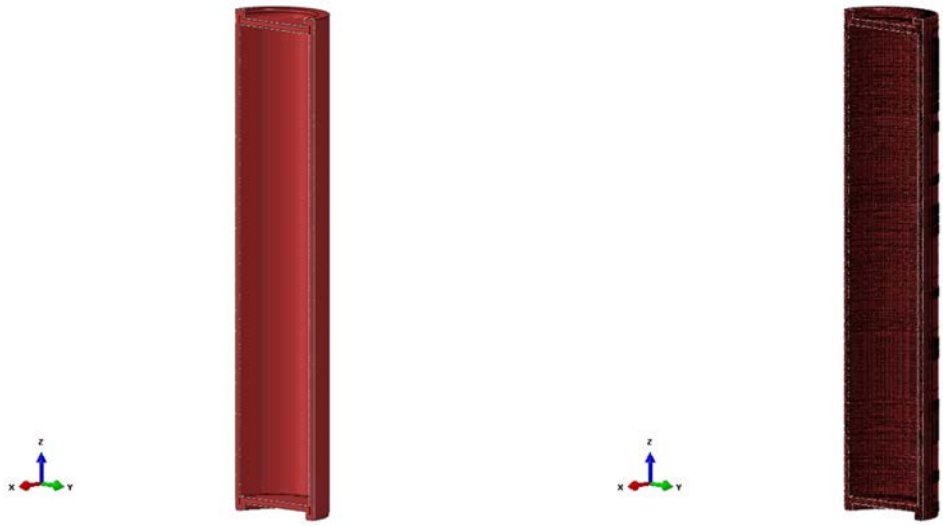

Figure 3-1*. Copper shell geometry (left) and mesh (right). Half the model is shown.*

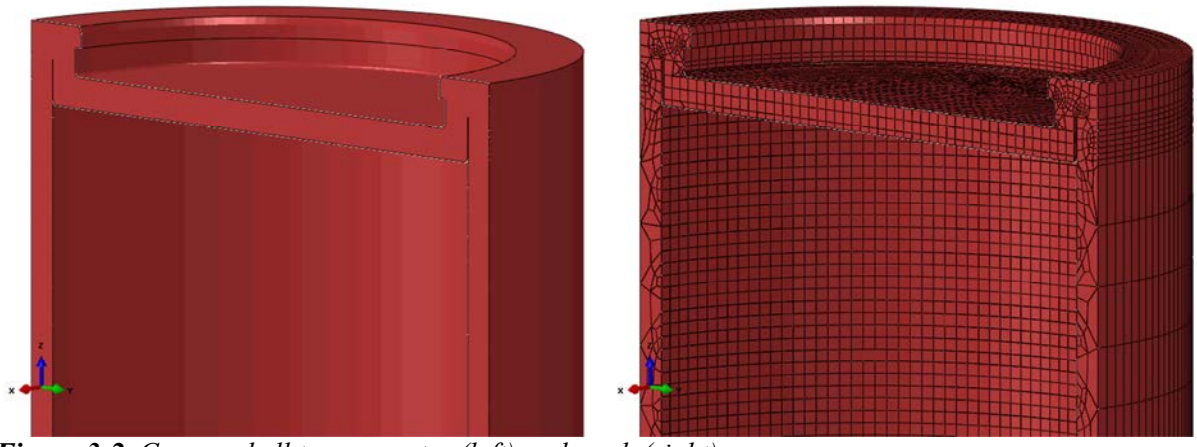

Figure 3-2*. Copper shell top geometry (left) and mesh (right).*

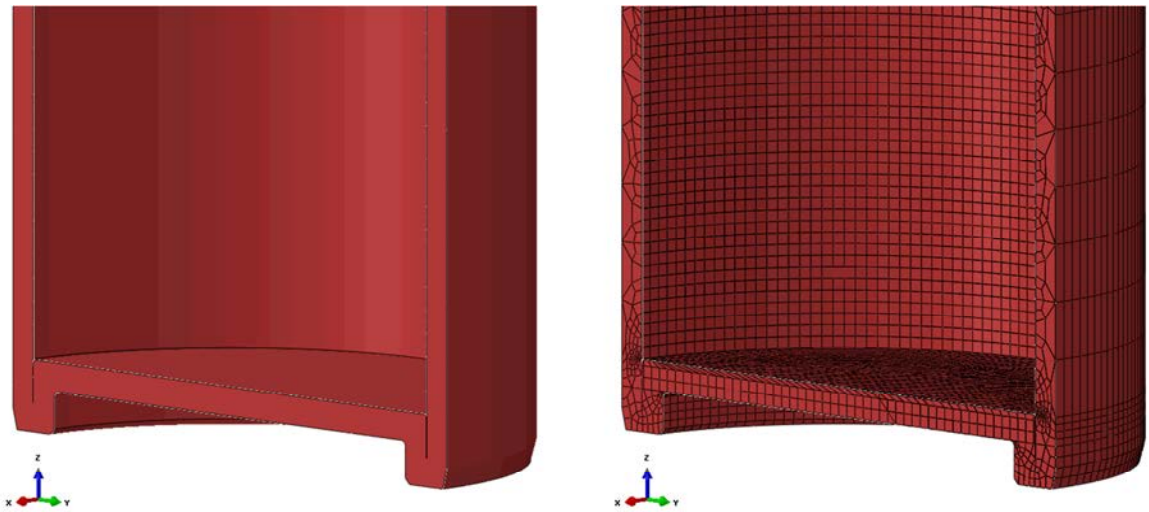

***Figure 3-3**. Copper shell base geometry (left) and mesh (right).*

3.2 Insert (nodular cast iron)

The insert is made of nodular cast iron. The steel channel tubes with plates are placed inside the cast. One set-up is for BWR and PWR using nominal values and another where the tolerances have been included.

3.3 BWR insert

The BWR insert is modelled as a homogeneous part with 3D solids based on SKB drawings, see Figures 3-4 to 3-9 for models using symmetry. A few simplifications have been made:

- The screw head geometry is modified to a cylindrical shape.
- A few small cylindrical holes that appear in the drawings have been removed (these holes doesn't exist in reality).
- The conical screw hole bottom is modified to cylindrical shape.

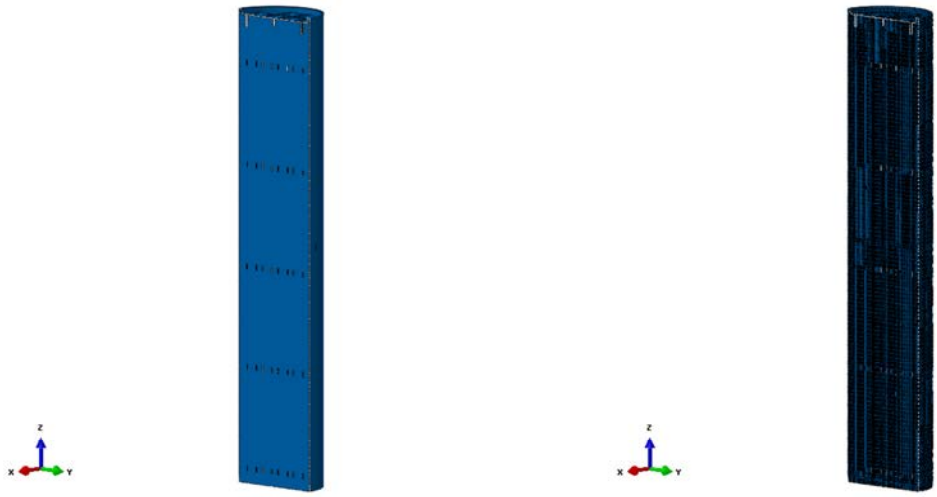

***Figure 3-4**. BWR insert geometry (left) and mesh (right). Half the model is shown.*

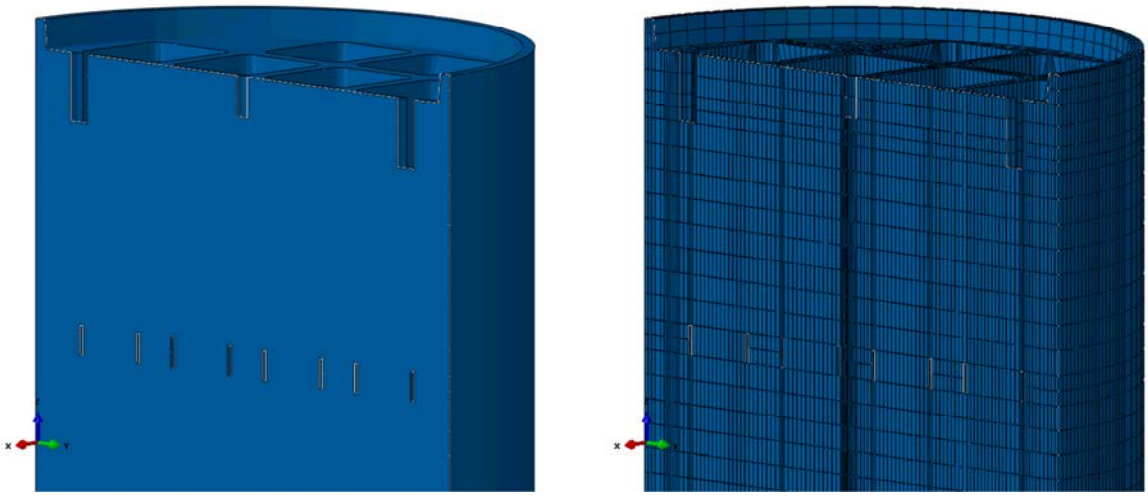

Figure 3-5. *BWR insert, upper geometry (left) and mesh (right).*

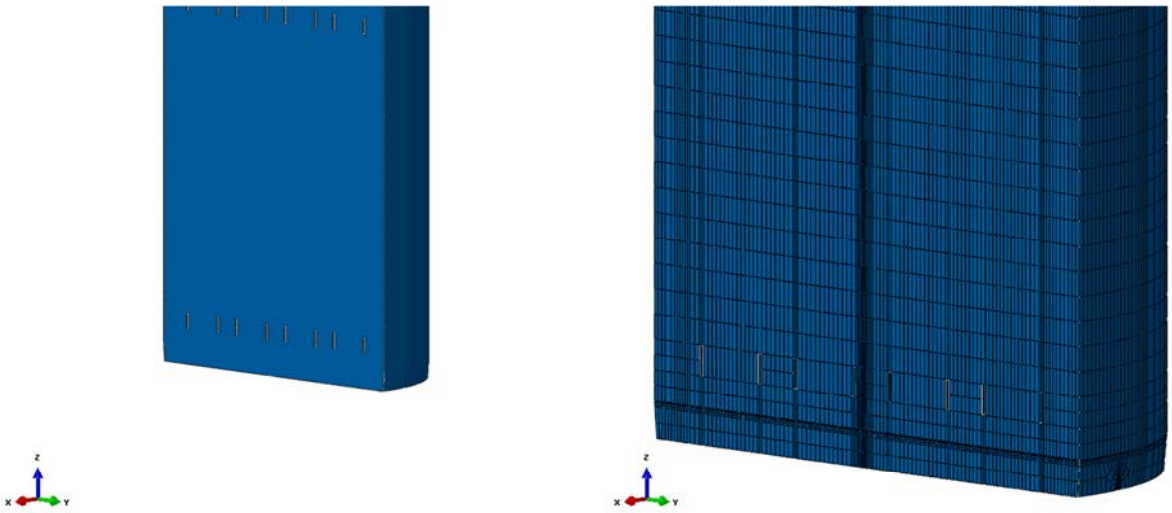

Figure 3-6. *BWR insert, lower geometry (left) and mesh (right).*

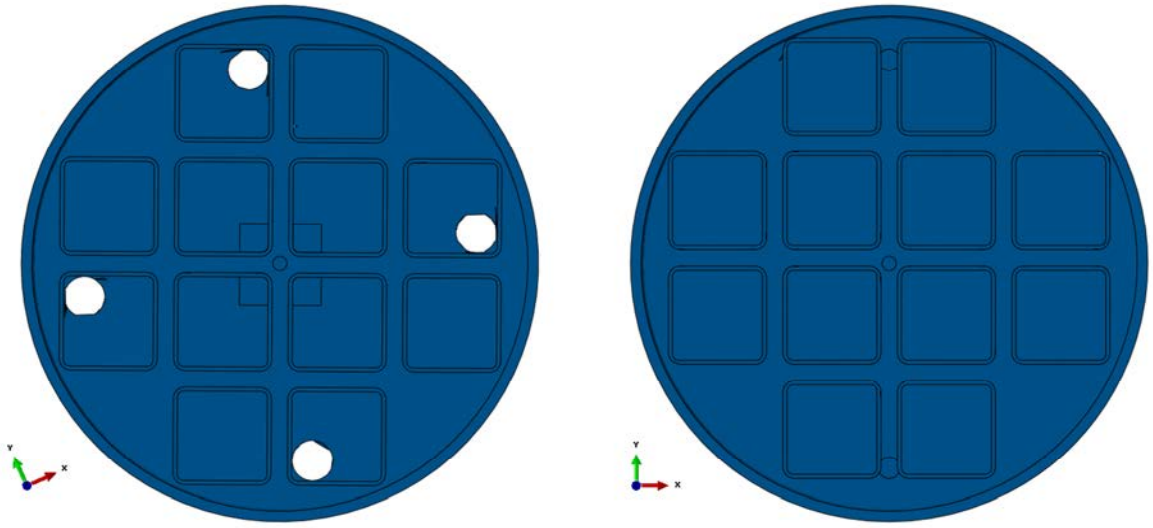

Figure 3-7*. BWR insert with channel tubes symmetrically positioned (left) and eccentrically positioned (right) – top view.*

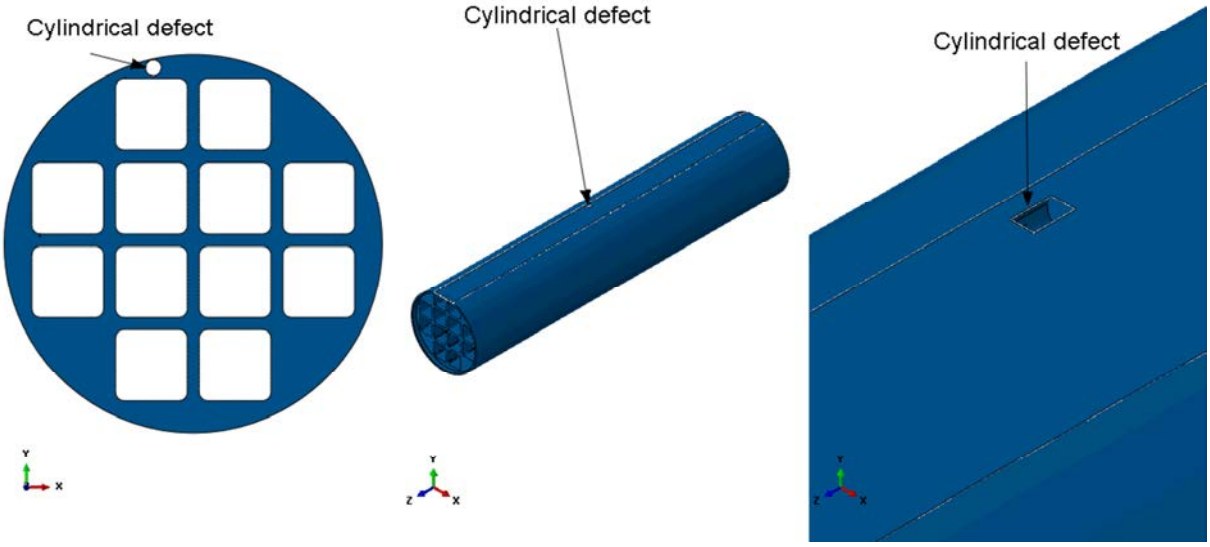

Figure 3-8*. BWR insert with a cylindrical defect, top view (left) and isometric view (middle and right).*

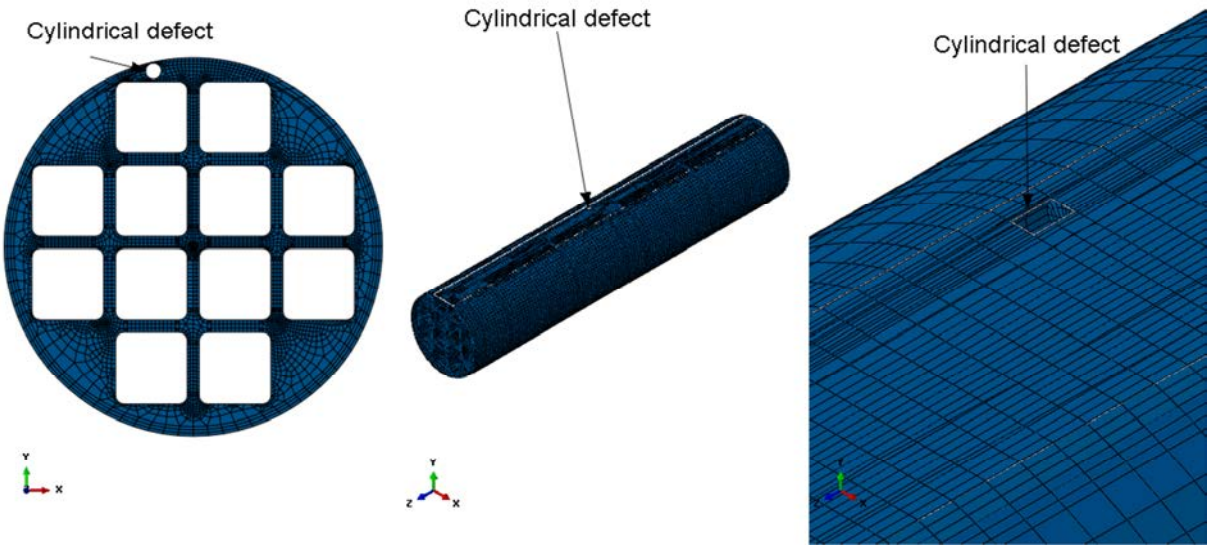

Figure 3-9. *BWR insert mesh with a cylindrical defect, top view (left) and isometric view (middle and right).*

3.4 Steel channel tubes (BWR)

The BWR steel channel tubes are connected by support plates which are tied to the insert, see Figures 3-10 to 3-13.

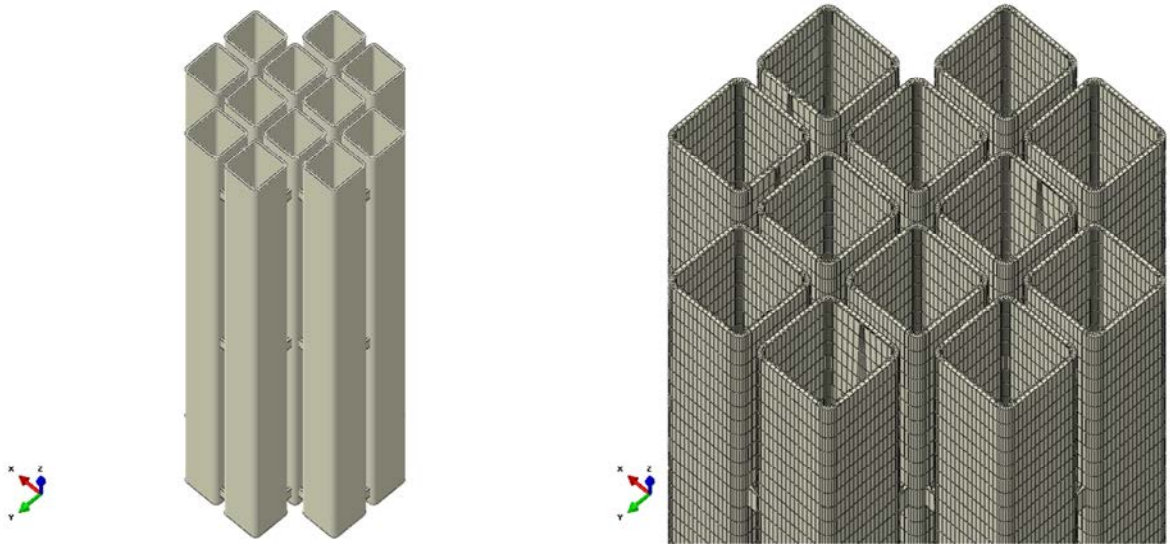

Figure 3-10. *Upper part of the steel channel tubes geometry (left) and mesh (right) – top view.*

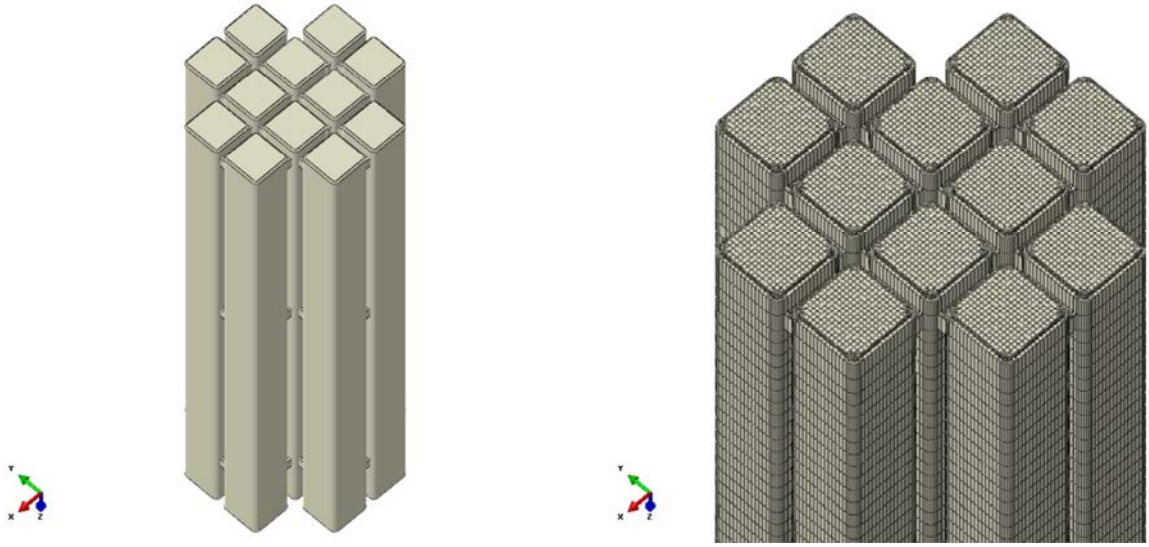

Figure 3-11. *Steel channel tubes geometry (left) and mesh (right) – base view.*

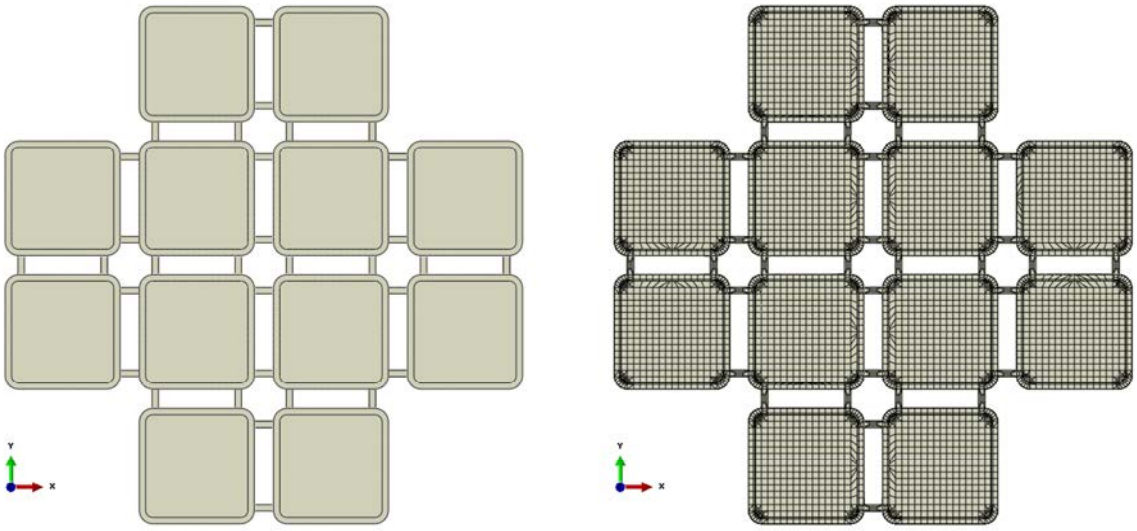

Figure 3-12. *Steel channel tubes geometry (left) and mesh (right) – top view showing also the support plates.*

The welds for the support plates have been included by modifying the geometry, see Figure 3-13, where also the corner radius is shown.

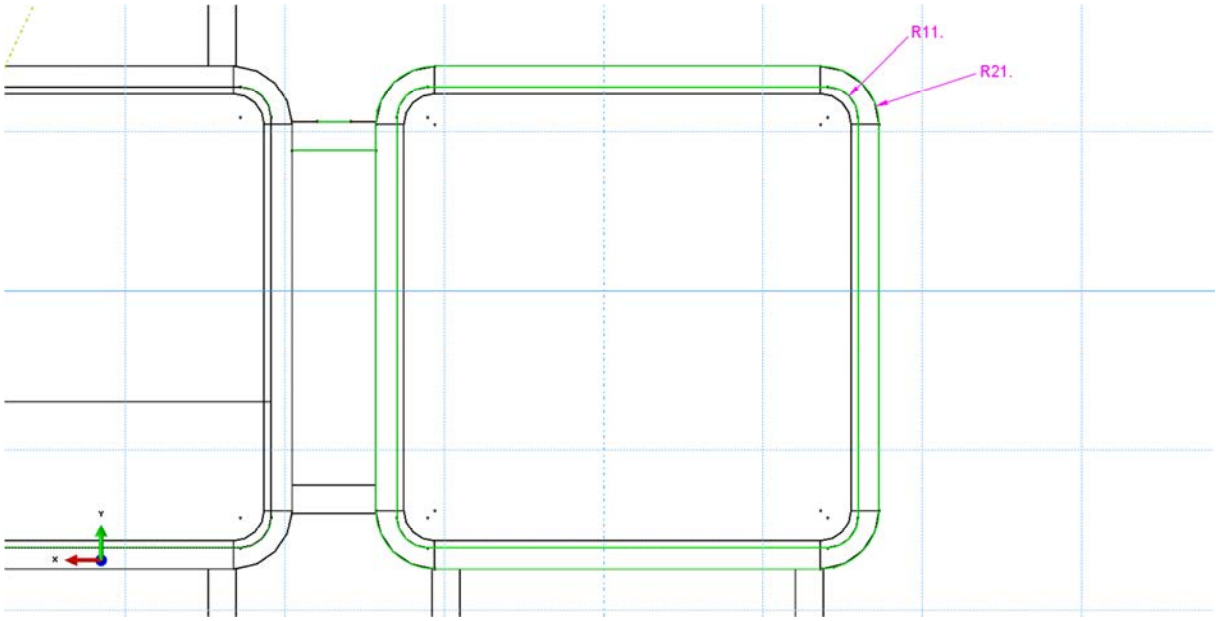

Figure 3-13. *Plot that shows corner radius for the channel tubes. Also the modified geometry for the support plates with the weld is included. Also note that the inner weld string from manufacturing of welded tubes (shown at the CAD-drawing) has been removed.*

3.5 PWR insert

The PWR insert is modelled as a homogeneous part with 3D solids based on SKB drawings, see Figures 3-14 to 3-19 for models using symmetry. A few simplifications have been made:

- The screw head geometry is modified to a cylindrical shape.
- A few small cylindrical holes that appear in the drawings have been removed (these holes doesn't exist in reality).
- The conical screw hole bottom is modified to cylindrical shape.

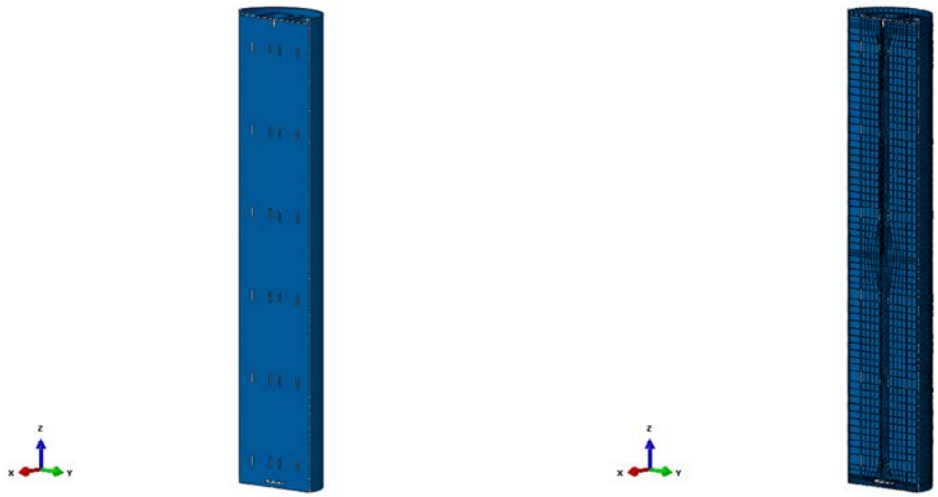

Figure 3-14. *PWR insert, geometry (left) and mesh (right). Half the model is shown.*

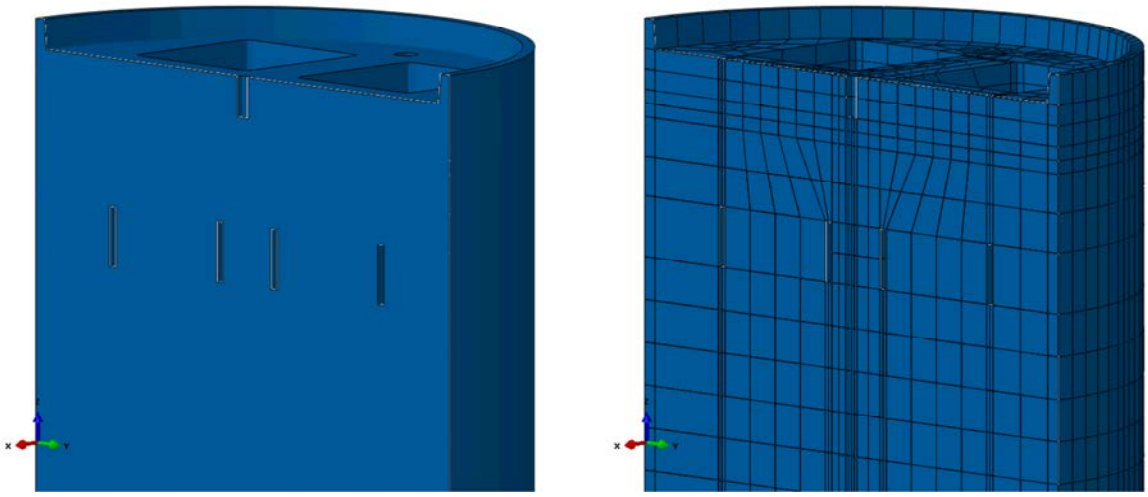

Figure 3-15. *PWR insert, upper geometry (left) and mesh (right).*

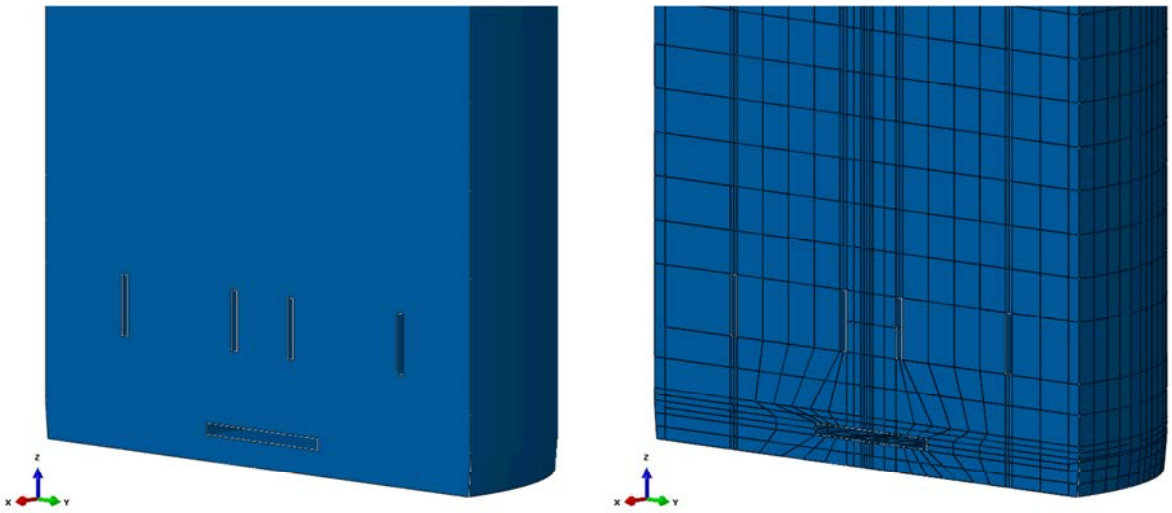

Figure 3-16. *PWR insert, lower geometry (left) and mesh (right).*

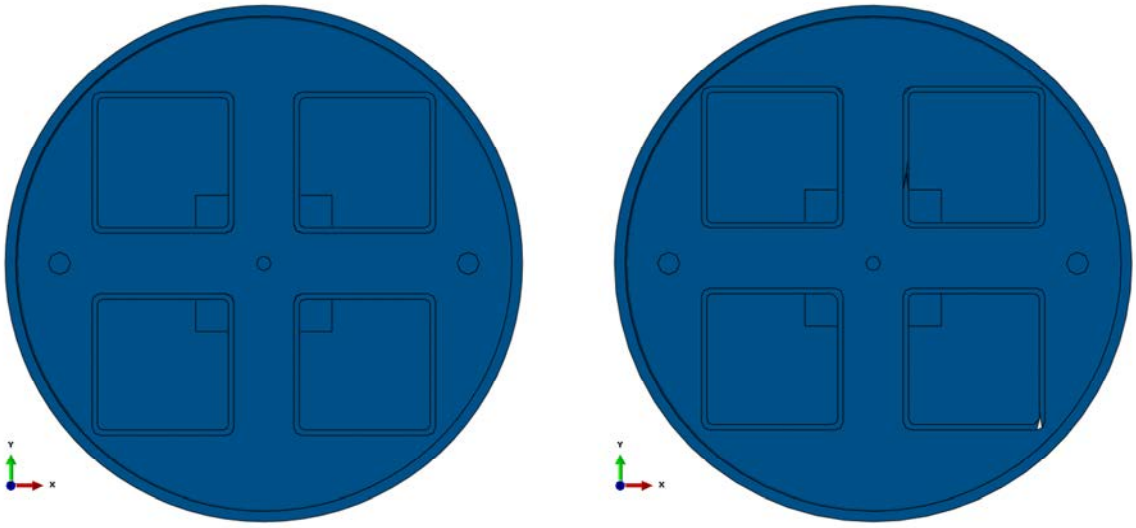

Figure 3-17*. PWR insert with channel tubes symmetrically positioned (left) and eccentrically positioned (right) – top view.*

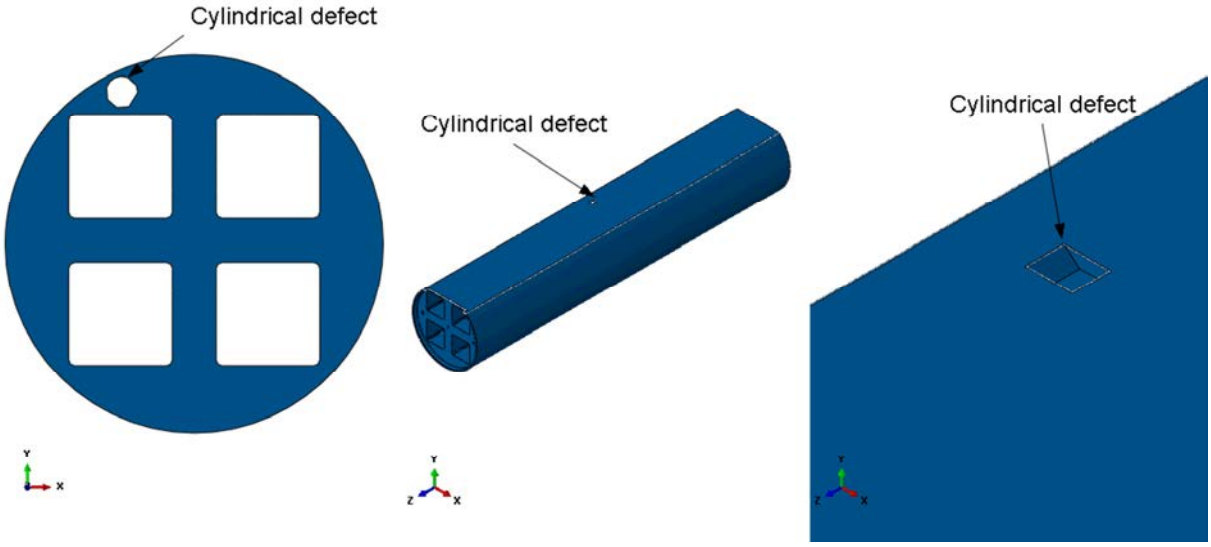

Figure 3-18*. PWR insert with a cylindrical defect, top view (left) and isometric view (middle and right).*

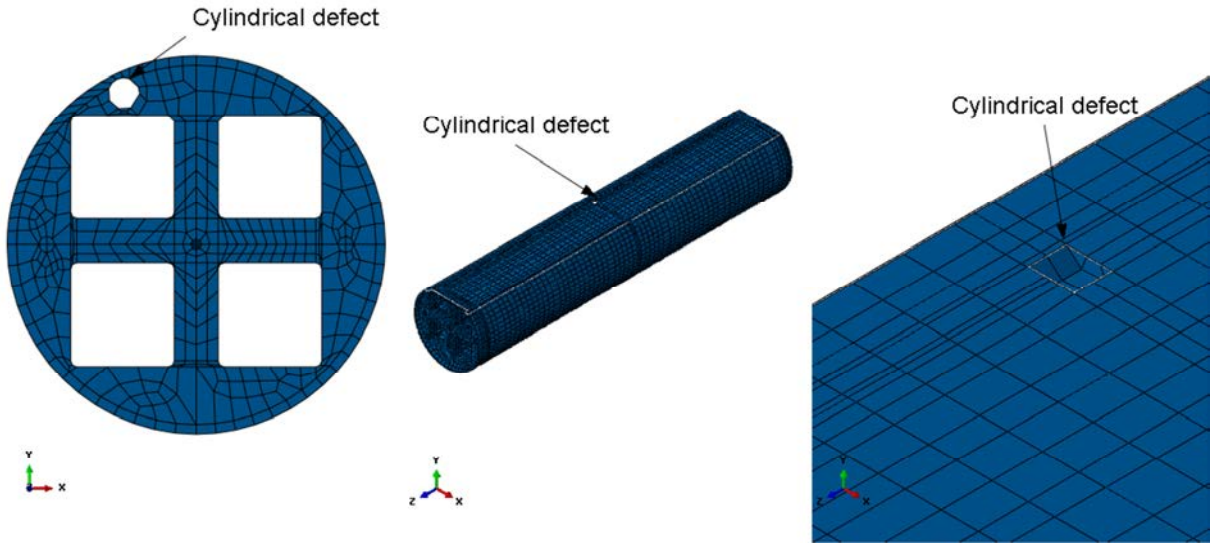

Figure 3-19. *PWR insert mesh with a cylindrical defect, top view (left) and isometric view (middle and right).*

3.6 Steel channel tubes (PWR)

The PWR steel channel tubes are connected by support plates which are tied to the insert, see Figures 3-20 to 3-22.

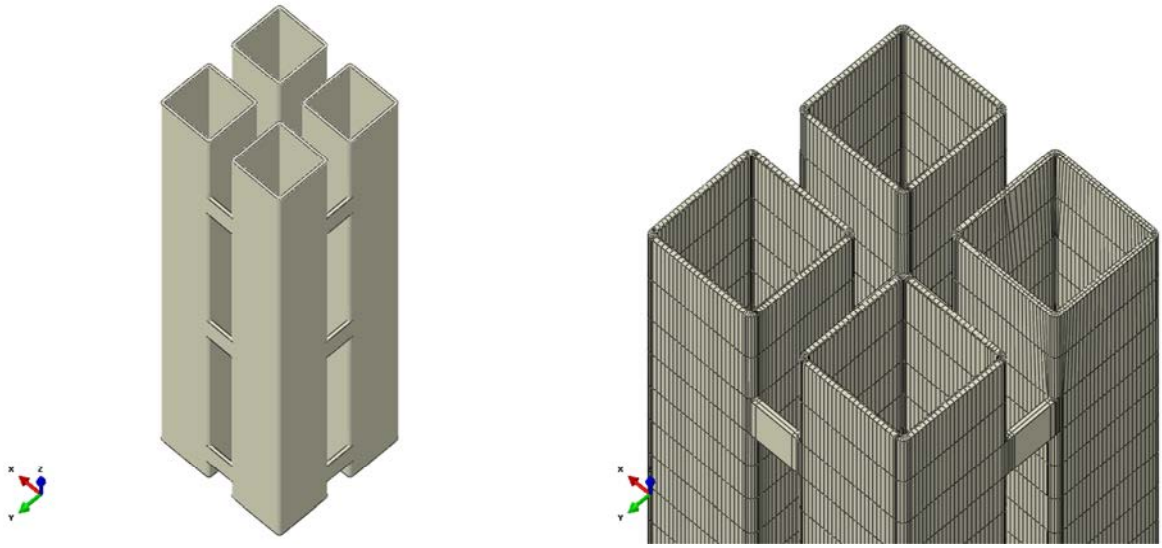

Figure 3-20. *Upper part of the steel channel tubes geometry (left) and mesh (right) – top view.*

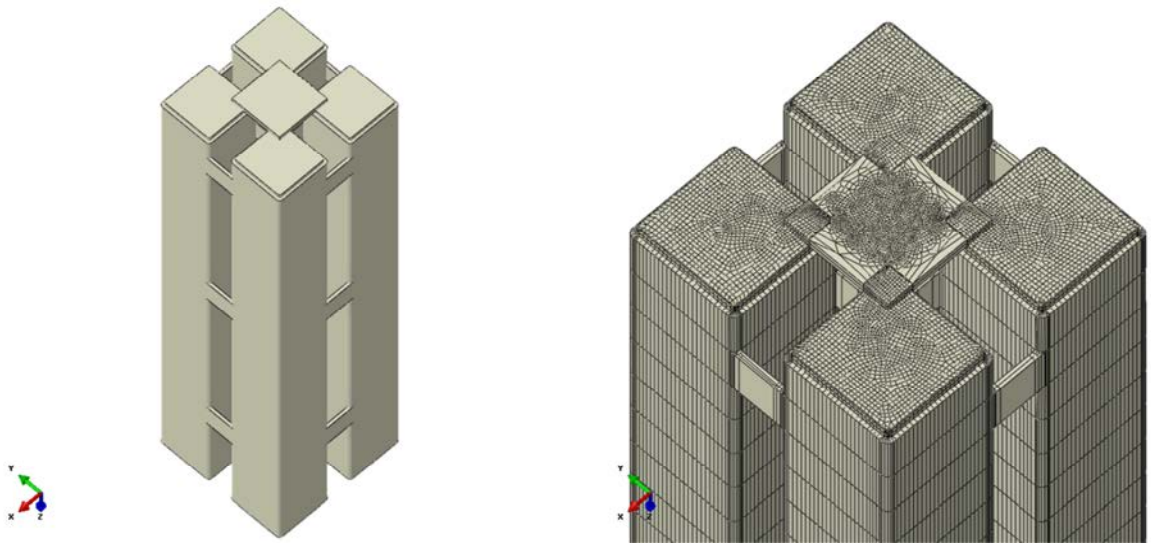

Figure 3-21. *Steel channel tubes geometry (left) and mesh (right) – base view.*

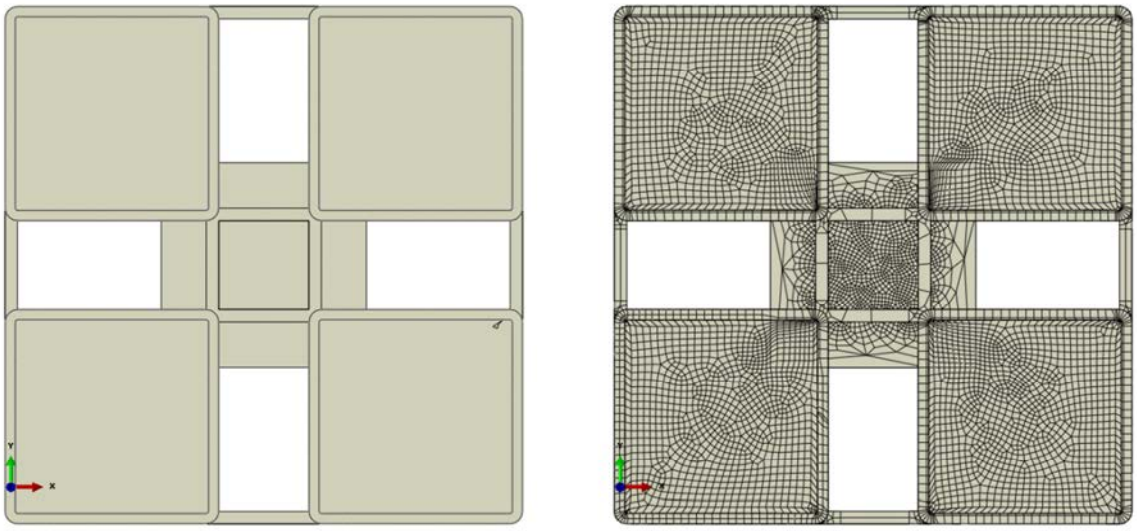

Figure 3-22. *Steel channel tubes geometry (left) and mesh (right) – top view showing also the support plates.*

3.7 Insert lid

The insert lid is made of steel and is modelled with 3D solids, see Figure 3-23. The surrounding gasket is not included which is assumed to have a minor effect on the stress distribution in the contact zone. Also a few details in the vent hole have been neglected since they hardly have any effect on the stiffness of the steel lid.

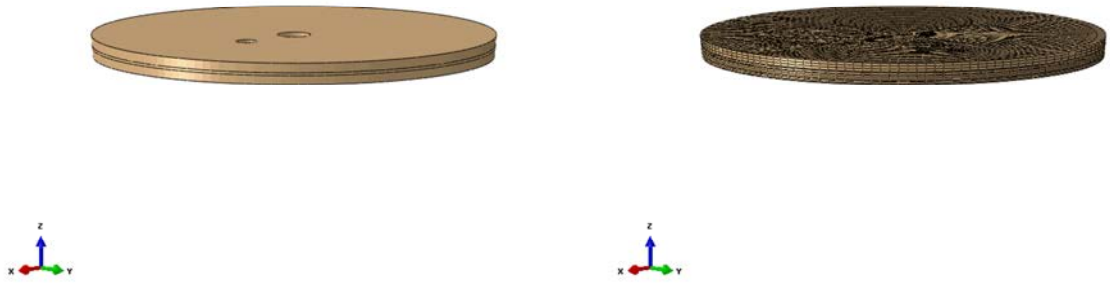

Figure 3-23. *Insert lid geometry (left) and mesh (right).*

3.8 Screw

The screw fixing the steel lid to the insert is modelled with 3D solids, see Figure 3-24.

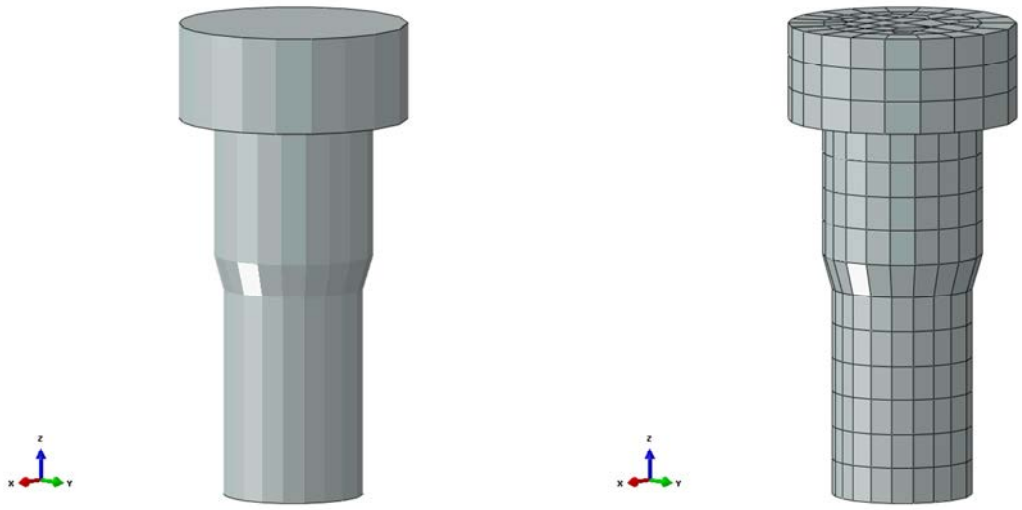

Figure 3-24*. Screw geometry (left) and mesh (right) – used to fix the steel lid to the insert.*

4 Material models

The finite element code ABAQUS version 6.12 (ABAQUS 2013) was used for the calculations. Since the obtained results should be compared with (Dillström et al. 2010) the same material properties have been used also in this study.

The materials have been modelled as elastic-plastic with stress-strain properties that correspond to each material. The material definitions are not valid for very large deformations.

Note that in ABAQUS values outside the definition range will be constant at the last value defined.

4.1 Nodular cast iron (used for the insert)

The material model for the insert is based on a von Mises material model with elastic behaviour defined by Young's modulus and the Poisson's ratio and the plastic behaviour defined through yield surface (true stress) versus plastic strain (defined as logarithmic strain), see Dillström et al. (2010) and is named Iron_insert_PD.

The material definition is shown in Table 4-1 and Fig. 4-1. Note that also one case with reduced yield surface is studied (89% of the default yield surface), named iron_insert_PD2.

Data is available up to 50% plastic equivalent strain, which covers the range of obtained results for the performed analyses.

The experiments providing the data were performed at 20^{o} C.

Table 4-1. True stress-true strain definition for BWR and PWR inserts (Iron_insert_PD).

Plastic Strain (%)	Mises [MPa]
0	270
2	333
4	394
6	429
10	482
20	534
50	550
100	550

Young's modulus E = 166 GPa and Poisson's ratio $\nu = 0.3$ (Dillström et al. 2010).

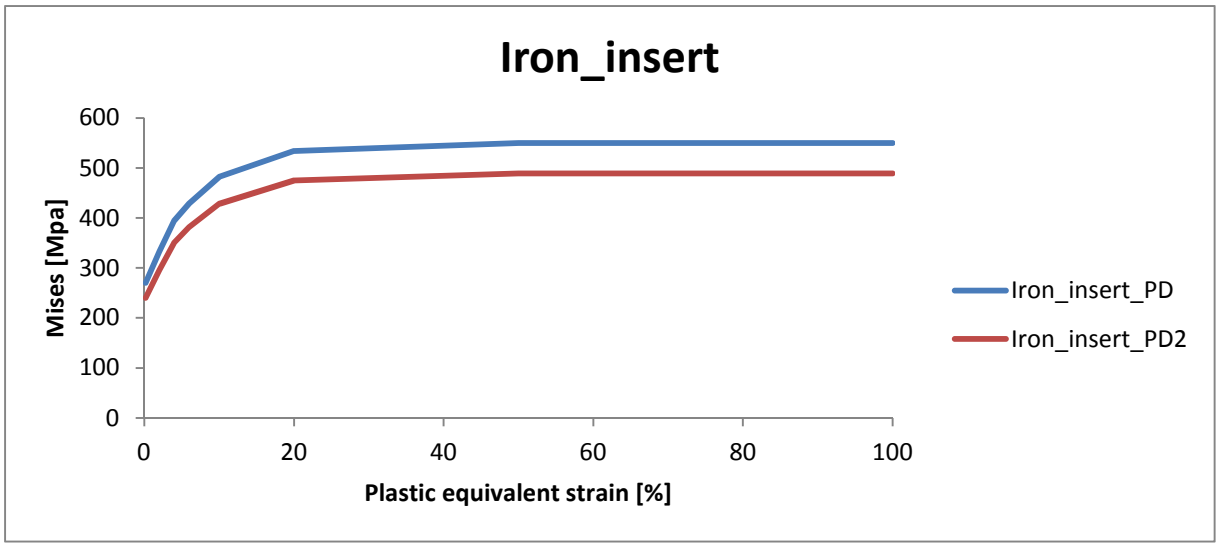

Figure 4-1. *Insert yield surface (nodular cast iron), true stress, [MPa] versus logarithmic plastic equivalent strain. Iron_insert_PD is the default definition and Iron_insert_PD2 is the definition where the yield surface is reduced by a scale factor 89%.*

4.2 Steel (used for the channel tubes in the insert)

The material model for the channel tubes in the insert is based on a von Mises material model with elastic behaviour defined by Young's modulus and the Poisson's ratio. The plastic behaviour is defined through yield surface (true stress) versus plastic strain (using logarithmic strain).

The steel channel tubes are manufactured by steel S355J2H, for example Domex 355 MC B. SKB has earlier supplied test data for the yield point of their material, however no stress-strain data to be used in a plastic analysis. The stress-strain curve for Domex 355 MC B (SSABDirect 2008) can be scaled using the yield stress and tensile ultimate strength measured by SKB, Re = 412 MPa (yield stress) and Rm = 511MPa (ultimate stress). With this procedure, a simplified stress-strain curve is obtained and described by Table 4-2 and Figure 4-2.

Table 4-2. Stress-strain definition for channel tubes used in the insert.

Strain (%)	Stress (MPa)	Log Strain (%)	True Stress (MPa)	Plastic equivalent strain (%)
0	0	0	0	0
0.196	412	0.196	412	0
15	509	14.3	587	14.0
20	511	18.5	613	18.2

Furthermore, Young's modulus E = 210 GPa and Poisson's ratio v = 0.3 according to Table 4-3 in Raiko et al. (2010).

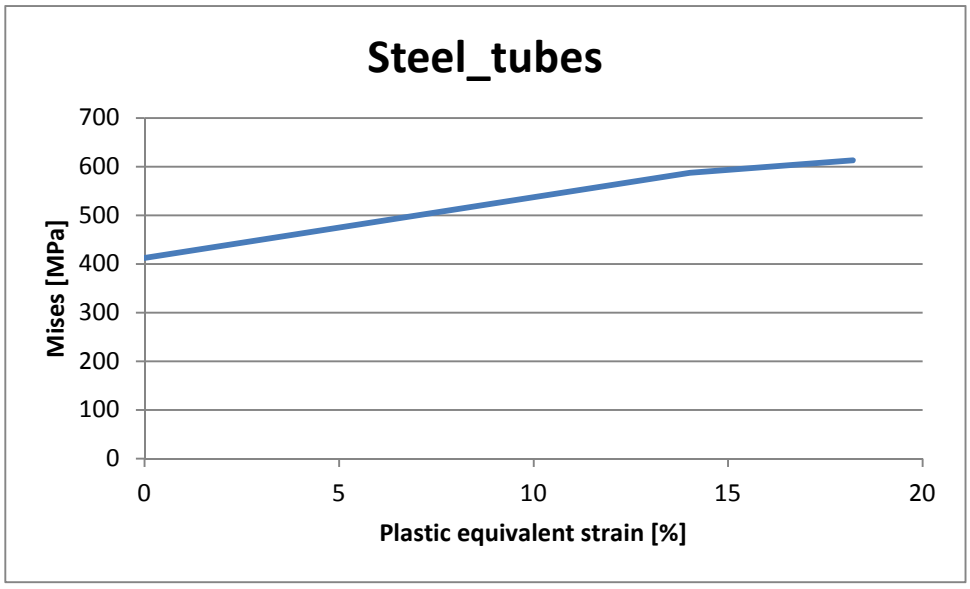

Figure 4-2. *Channel tube yield surface, true stress [MPa], as a function of the logarithmic plastic equivalent strain.*

The dataset with the lowest value from the experiments has been chosen for the yield surface. However, the plasticity definition for the steel channel tubes has very minor influence on the overall results. Furthermore, the obtained results from the performed analyses are within the range for the available material data.

4.3 Steel (used for the insert lid, support plates, bottom plates and screws)

The material model for the insert lid is based on a von Mises material model with elastic behaviour defined by Young's modulus and the Poisson's ratio. The plastic behaviour is defined through yield surface (true stress) versus plastic strain (calculated as logarithmic strain).

Manufacturing drawings for the lid specify steel S355J2G3. Strain versus stress for steel Domex 355 MC B with *Re* = 389 MPa (yield stress) and *Rm* = 484 MPa (ultimate stress) can be found from SSABDirekt (2008). According to SS-EN 10025-2:2004, the material S355 with nominal thickness 40-63 mm has *Re* = 335 MPa (yield stress) and *Rm* = 470-630 MPa (ultimate stress). Scaling stress-strain curves for Domex 355 by the minimum values given in SS-EN 10025-2:2004 implies the simplified material definition (engineering data) shown in Table 4-3 and Figure 4-3.

Table 4-3. Stress-strain definition for the insert lid.

Strain (%)	Stress (MPa)	Log Strain (%)	True Stress (MPa)	Plastic equivalent strain (%)
0	0	0	0	0
0.1595	335	0.1593	335	0
15	470	13.98	540	13.7
20	470	18.2	564	17.9

Furthermore, Young's modulus E = 210 GPa and Poisson's ratio ν = 0.3 according to table 4-3 in Raiko et al (2010).

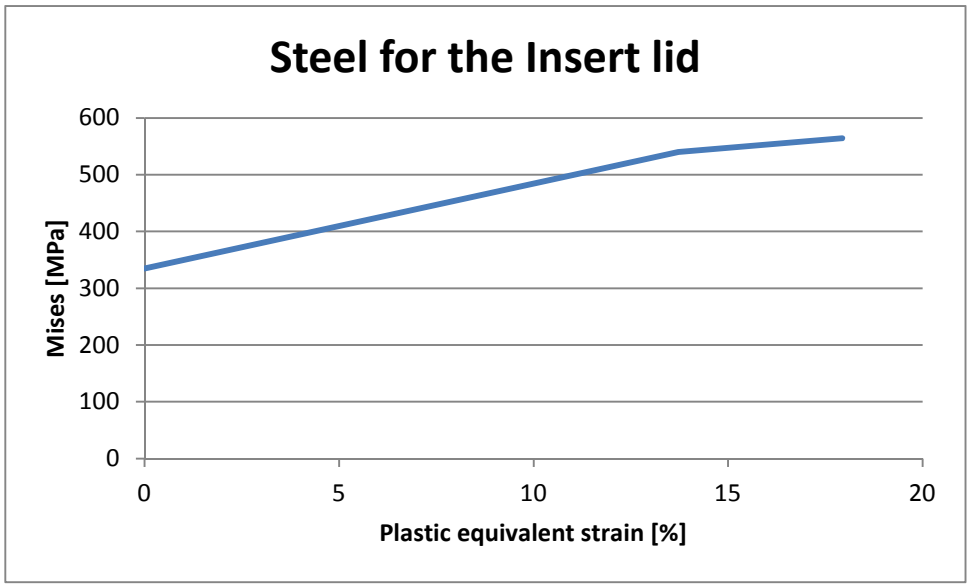

Figure 4-3. *Insert lid yield surface, true stress [MPa], as a function of the logarithmic plastic equivalent strain.*

The dataset with the lowest value from the experiments (SS-EN 10025-2:2004) has been chosen for the yield surface. However, the plasticity definition for the insert lid has very minor influence on the overall results. Furthermore, the obtained results are within the range of the available material data.

4.4 Copper material model (used for the copper shell)

Also the material definition for copper, named Copper_PD, is taken from (Dillström et al. 2010), see Figure 4-5 and Table 4-5.

Data is available up to 100% plastic equivalent strain but is not valid for such large strains.

Table 4-5. Elastic-plastic material data for the copper (Copper_PD).

Elastic part		Plastic part: von Mises stress σ_j (MPa) at the following plastic strains (ε_p)				
E (MPa)	*v*	0	0.10	0.20	0.59	1.00
$1.14 \cdot 10^5$	0.35	58	165	240	341	428

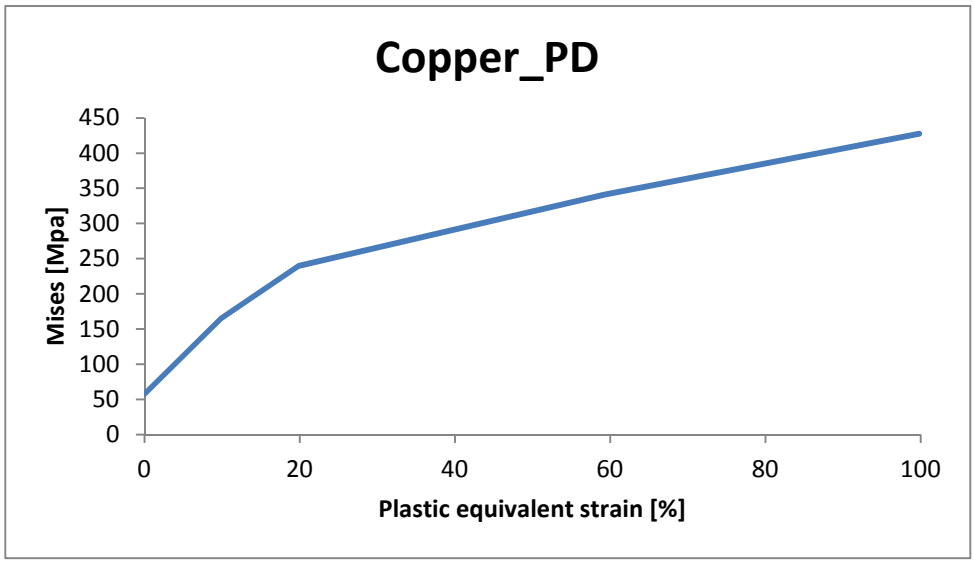

Figure 4-5. *Copper shell yield surface, true stress, [MPa] as a function of the logarithmic plastic equivalent strain.*

5 Contact definitions

All the boundaries of the copper shell, the insert and the insert lid interact through contact surfaces allowing finite sliding. All contact surfaces have friction at sliding with no cohesion and the friction coefficient 0.1, i.e. the friction angle (ϕ) is 5.7˚ and the cohesion (c) is 0 kPa.

The contact is released when the contact pressure is lost.

Contact pairs between support plates and the insert are tied together (tied means that the surfaces are constrained together and will not allow for opening/closing or sliding) which is assumed to be a reasonable assumption since the gravity and the pre-stress in the screw implies pressure in the axial direction.

6 Initial conditions

Initial conditions are defined as:

- Temperature for all nodes in the model as 300 K. The temperature is assumed to not change during the analysis.

7 Boundary conditions

No boundary conditions are needed since the loading should not imply any rigid body motion.

8 Loading

The applied hydrostatic pressure is increased with time, see Fig 8-1 for the BWR insert and Fig 8-2 for the PWR insert. Note that the pressure is increased smoothly combined with constant magnitude for some time at specific pressure magnitudes (6, 45, 60, 90, 100, 120 and 150 MPa). A new stable configuration is indicated by a decrease in the magnitude of the kinetic energy without any change in displaced geometry. Note that the time for applying the pressure combined with mass-scaling aim to have a response close to static response.

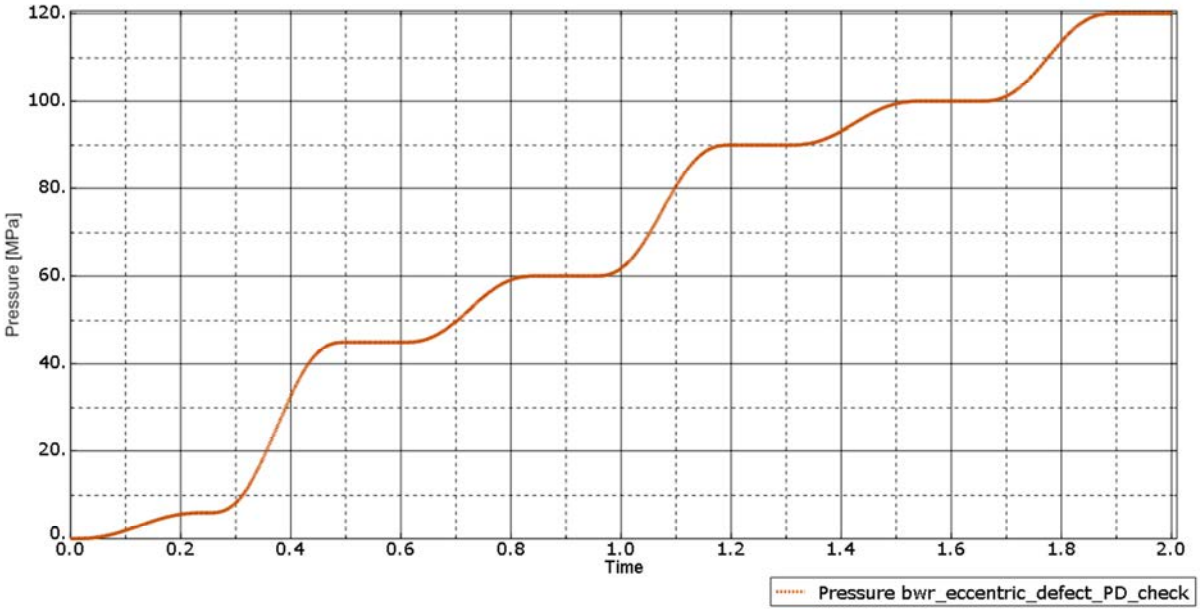

Figure 8-1. *Hydrostatic pressure applied to the copper shell external surface for the BWR insert.*

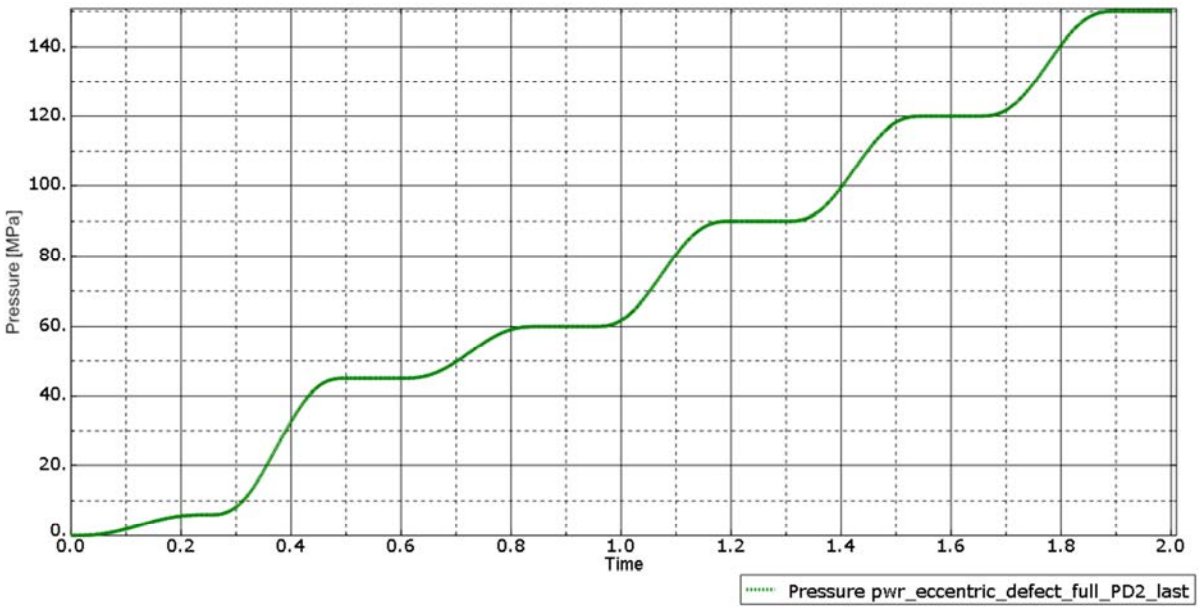

Figure 8-2*. Hydrostatic pressure applied to the copper shell external surface for the PWR insert.*

For the two most severe cases (eccentric placed channel tubes containing one defect and at the same time using a reduced yield surface for the insert) additional analyses have been performed where the kinetic energy is reduced before the first instability is passed. This is achieved by keeping the load

constant for some time at pressure magnitude 90 MPa. For the PWR insert the load then is increased to 110 MPa and kept at that level to check if the design still is stable, see Fig 8-3.

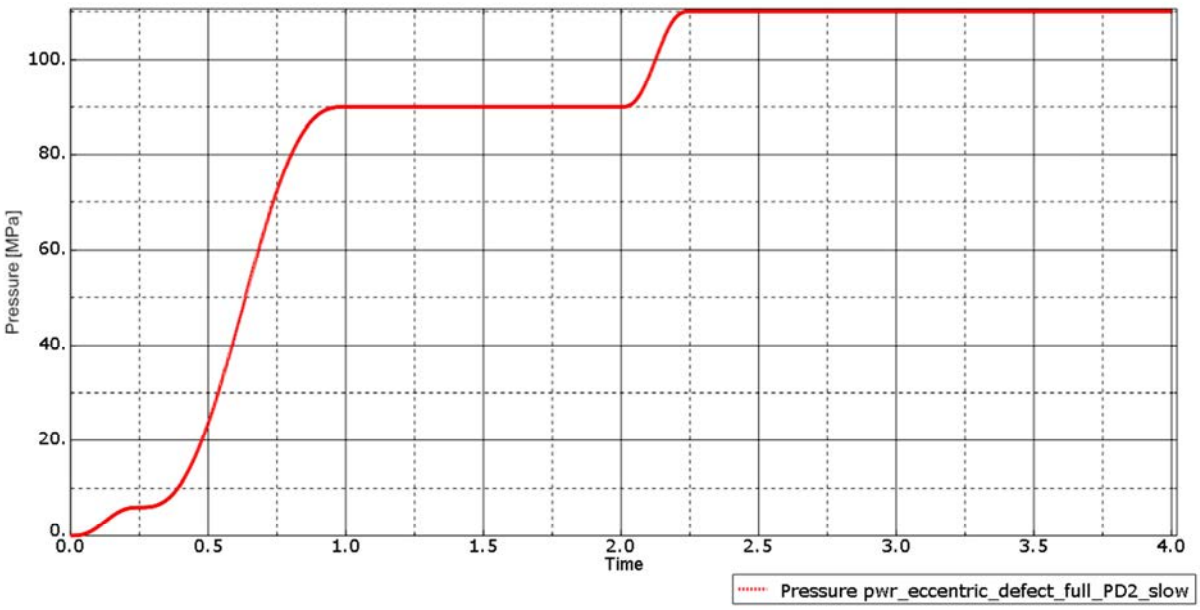

***Figure 8-3**. Hydrostatic pressure applied to the copper shell external surface for the PWR insert when the load is applied slowly.*

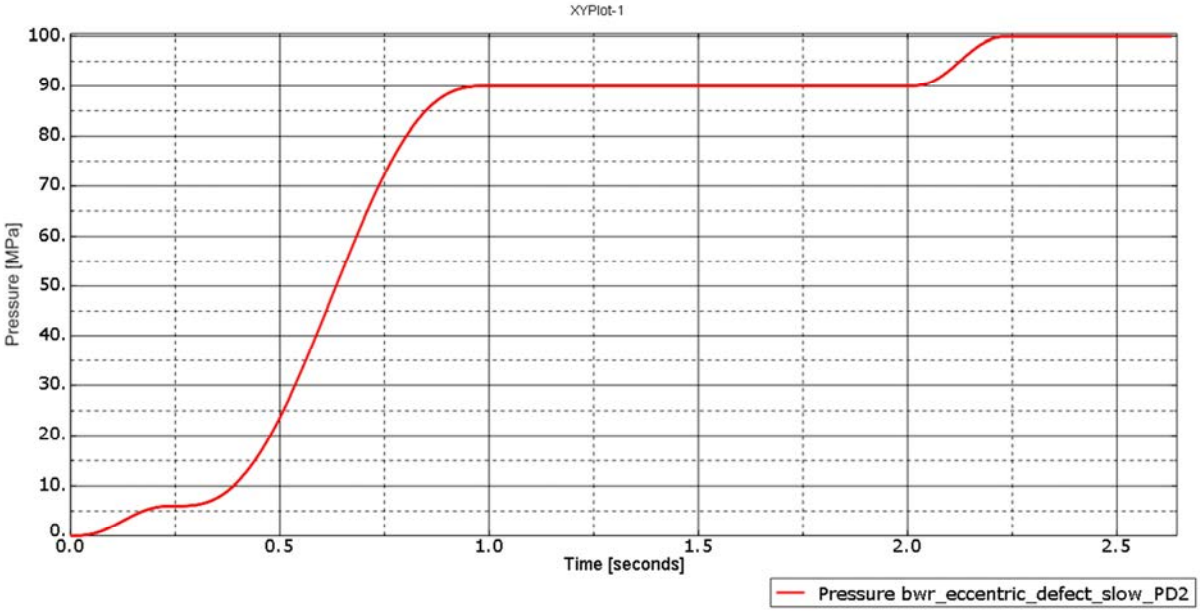

***Figure 8-4**. Hydrostatic pressure applied to the copper shell external surface for the BWR insert when the load is applied slowly.*

Figures 8-4 and 8-5 show the applied hydrostatic load for the case “slow loading” with different magnitudes where the load is kept constant.

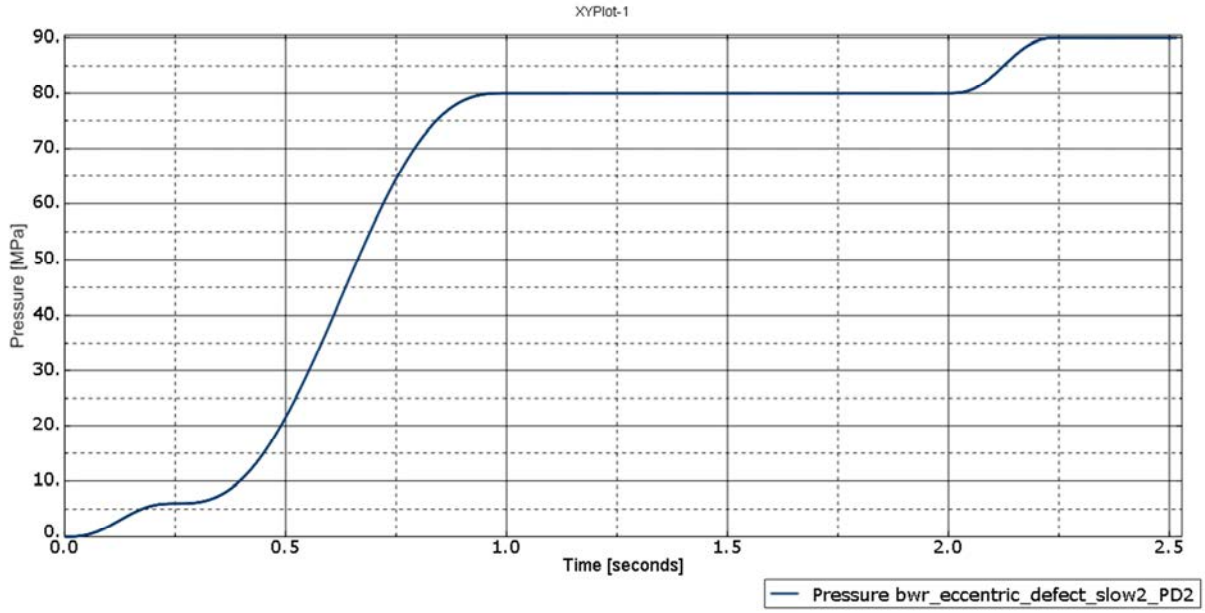

***Figure 8-5**. Hydrostatic pressure applied to the copper shell external surface for the BWR insert when the load is applied slowly and with constant load before the first expected instability to stabilize the solution.*

9 Calculations

9.1 General

The performed study aims to investigate the risk for collapse of the insert and therefore a dynamic approach has been selected where the load is monotonically increased until the structure becomes unstable. Also the stress and strain state is of interest during the load increase.

9.1.1 Hydrostatic pressure

The analyses have been performed by increasing the pressure from 0 up to 100 MPa for the BWR insert and from 0 up to 200 MPa for the PWR insert.

9.1.2 Analysis approach

The numerical calculations are performed using the FE-code ABAQUS/Explicit version 6.13 (ABAQUS 2013) assuming non-linear geometry and material definitions. This means that all non-linearities defined by the input will be considered, such as large displacements, large deformations, non-linear interactions (contact) and non-linear materials.

Some selective mass-scaling, see ABAQUS (2013), has been used to have reasonable calculation times. However, the amount of mass-scaling has been checked to assure a quasi-static solution but sudden changes (e.g. at contact changes) can result in high frequency non-physical noise. This could e.g. be filtered by a cut-off for frequencies above a specified level. Figure 9-1 shows an example of filtering the kinetic energy with a cut-off at 100 Hz.

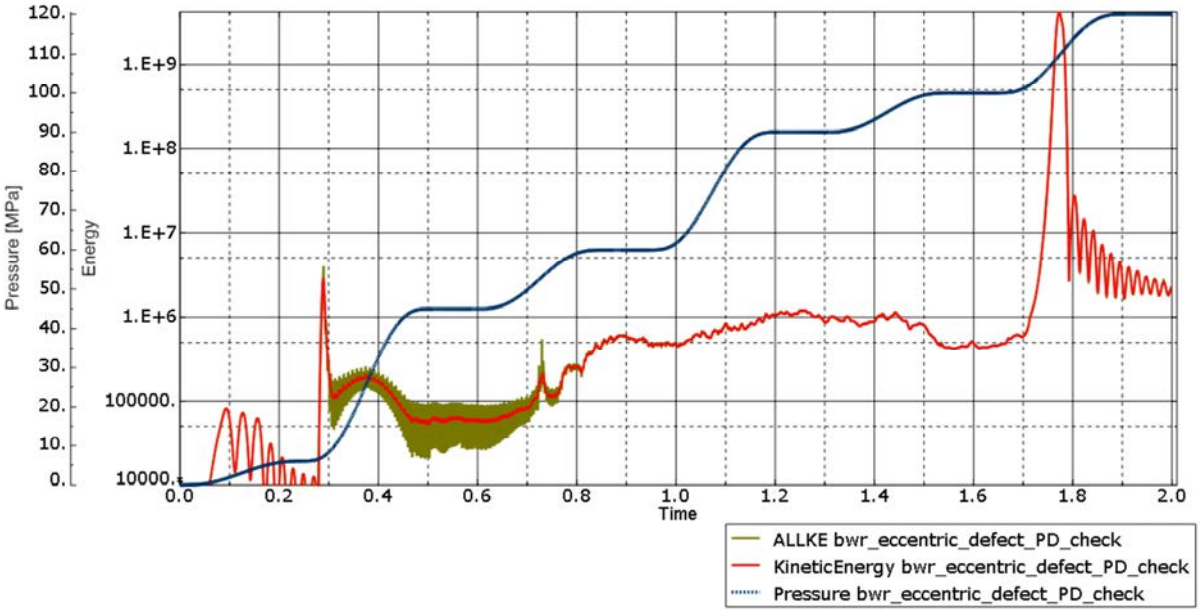

***Figure 9-1**. Example of filtering with cut-off at 100 Hz. The high frequency noise after initial contact between insert and copper shell at about 0.3 seconds disappears completely. Time scale in seconds.*

10 Interpretation of contour plot

The FE-analyses calculates stresses and strains in each element at the integration points where the defined relation between stresses and strains is used. The obtained results are then presented as contour plots where the integration point values are extrapolated for each element to the nodal points and then eventually averaged. The default rule is that the averaging is performed for nodal values. The extent to which values are averaged at nodes within each region is controlled by the averaging threshold (default is 75% and is shown at the legend table) as follows:

$$\text{relative nodal variation} = \frac{(\text{maximum at node} - \text{minimum at node})}{(\text{maximum within region} - \text{minimum within region})}$$

If the relative nodal variation for each node included in the plot is less than the averaging threshold, values of contributing elements are averaged at that node. If the relative nodal variation exceeds the setting, the values are not averaged.

The lower the averaging threshold value is, the more the displayed values depict the individual element results. Conversely, a higher averaging threshold produces a smoother effect with fewer noticeable discontinuities at element boundaries and lower maximum magnitude.

At regions with large gradients, the choice of averaging threshold affects the produced plots significantly but with small gradients the threshold has very small influence on the plots.

For the performed analyses, the peak values for stresses and strains are much localized around the corners defining the channel tubes. This results in large gradients and in most cases, heavily distorted elements, affecting the corresponding contour plots. To avoid too distorted elements, a much finer mesh is needed or the geometry has to be further simplified. It seems reasonable to neglect results from these highly distorted elements, especially since the element size is very small, see Figs. 10-1 – 10-3.

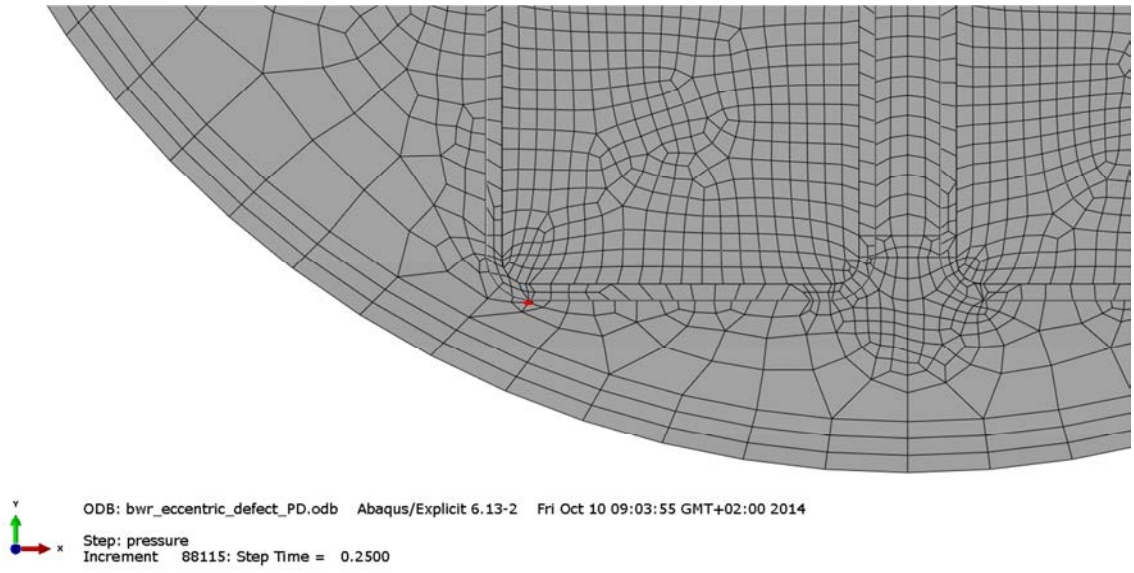

Figure 10-1*. Example of bad elements creating unrealistically high stress and strain magnitudes (red colour).*

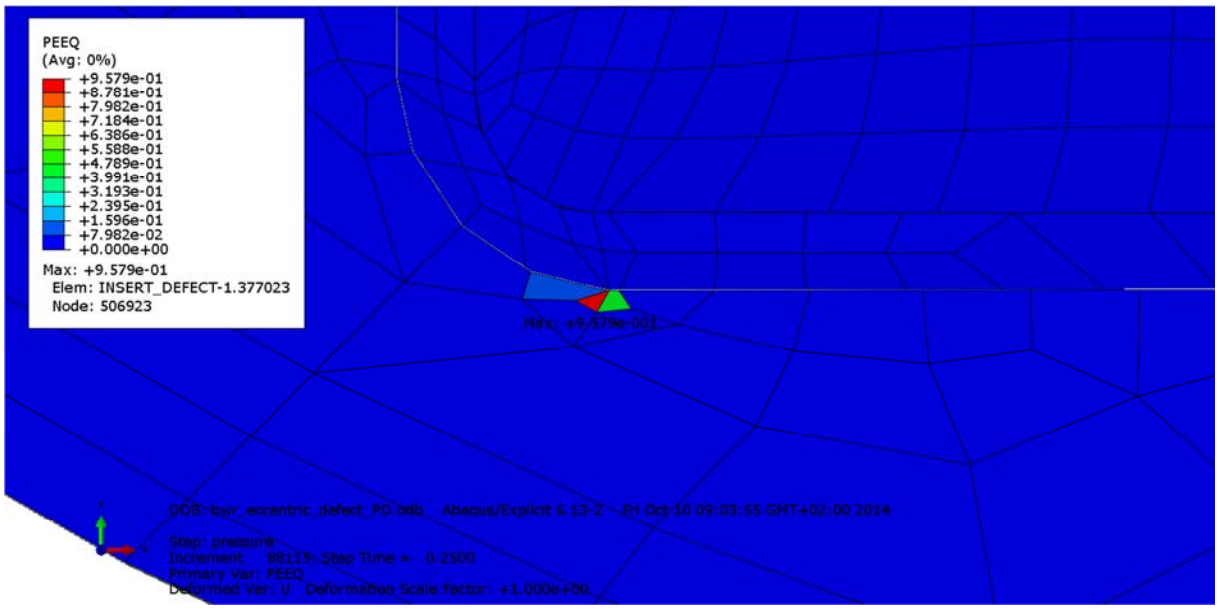

Figure 10-2. *Example of bad elements creating unrealistically high stress and strain magnitudes.*

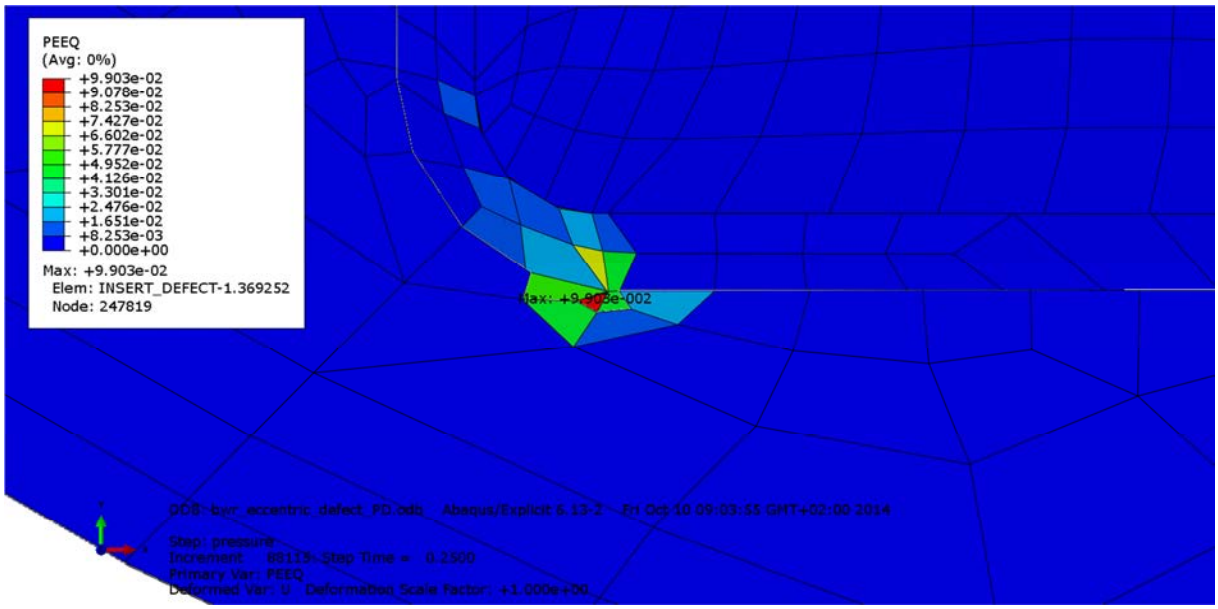

Figure 10-3. *Example of bad elements creating unrealistically high stress and strain magnitudes. The bad elements (red colour, Fig 10-1) have been removed from the plot. Note the decrease in maximum magnitude.*

11 Results for hydrostatic pressure

For each analysis a large amount of results are available, but here only a few representative values are reported. When stress components are plotted, S22 corresponds to the normal stress in the y-direction (lateral) and S33 corresponds to the normal stress in the z-direction (axial). The results are shown in Appendix 1 to 4 for the PWR insert and in Appendix 5 to 8 for the BWR insert. Another finding is that the magnitude quickly decreases after each peak indicating a new stable configuration. This could be interpreted as post-buckling. Also the completely compressed insert represents a stable configuration even though not useful as a container for the spent nuclear fuel.

Sudden increases in the kinetic energy, indicates some instability in the model.

11.1 Limit load based on kinetic energy

The performed study aimed to investigate the safety factor for the insert. The insert should withstand a hydrostatic pressure of 45 MPa (Raiko et al. 2010).
In addition, SKB also explores the possibilities to increase the load in the design premises from 45 MPa to 50 MPa. An assessment on potential the safety factor in relation to such a requirements for the given canister designs is also asked for.
All analyses have been performed using a dynamic approach by monotonically increasing the pressure and then the kinetic energy is used to decide if any instability occurs. Figure 11-1, 11-2 and 11-3 show the kinetic, plastic respectively strain energy versus time for the PWR insert together with applied pressure versus time. Figures 11-14 to11-16 are the corresponding plots for the BWR insert.
The first peak in kinetic energy occurs at about 10 MPa due to initial contact between the copper shell and the insert (initially there is a gap between the copper shell and the insert). Tables 11-1 and 11-2 show a summary of the first instability level based on kinetic energy and also compared with the previous study (Dillström et al. 2010). One finding is that the results agree rather well for inserts based on nominal dimensions, whereas the results differ significantly for inserts based on manufacturing tolerances. The reason for this difference could be explained by the different eccentricity levels (10 mm in the current study and 15 mm in the reference case). Also the cases containing one defect differs which could be explained by different models (the current study is based on a 3D analysis and the reference case is based on a 2D analysis implying much bigger defects).
Besides the structural instability also the stress and strain levels need to be studied.

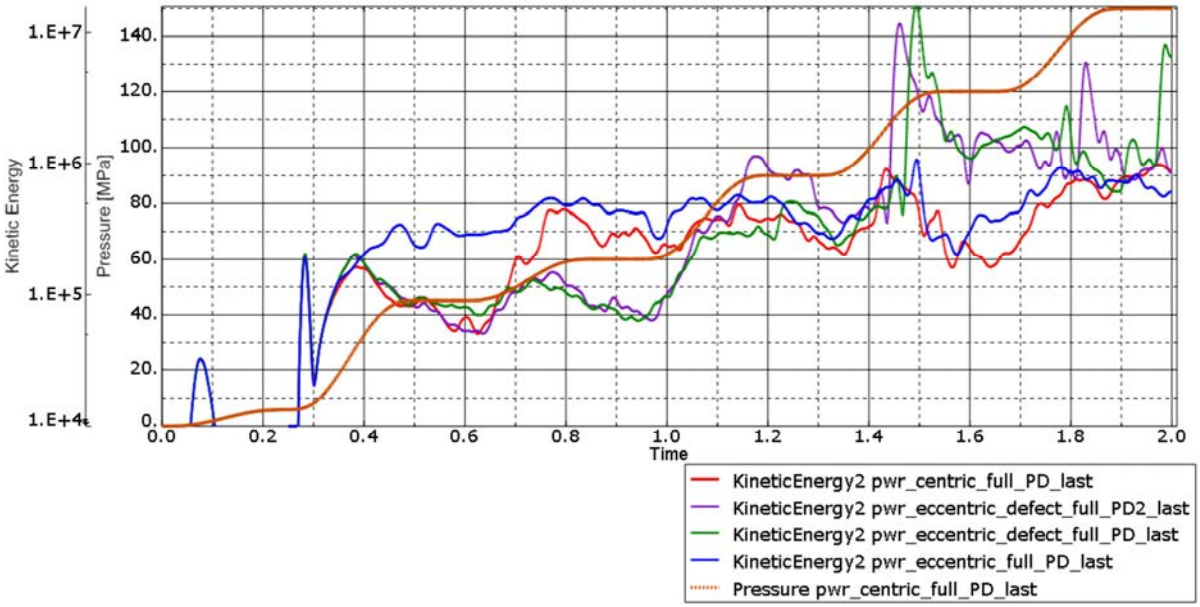

Figure 11-1. *Kinetic energy and pressure versus time [seconds] for the PWR insert.*

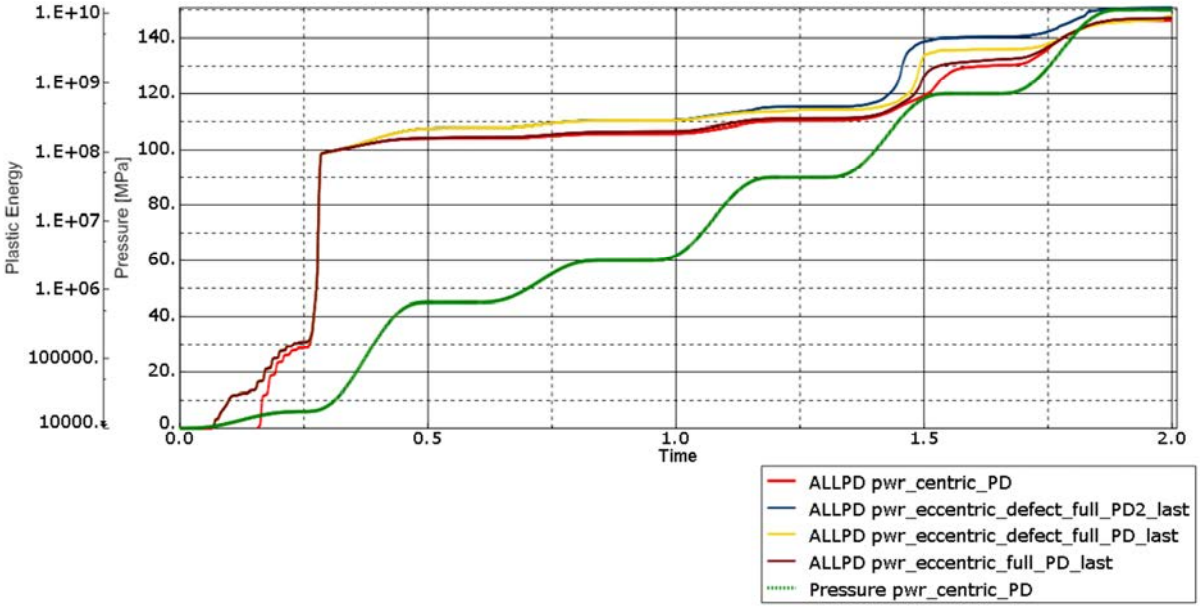

Figure 11-2. *Plastic energy and pressure versus time [seconds] for the PWR insert.*

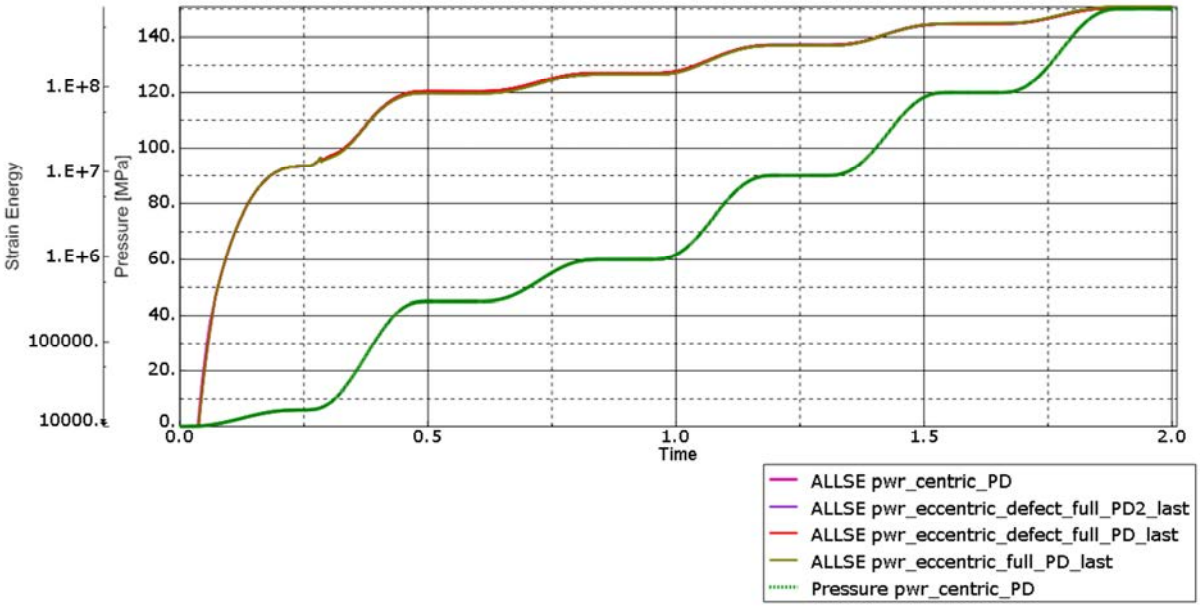

***Figure 11-3**. Strain energy and pressure versus time [seconds] for the PWR insert.*

Figures 11-4 – 11-13 show one plot with energies versus time together with applied pressure versus time and one plot with kinetic energy versus applied pressure focused at the first instability for each analyzes for the PWR insert.

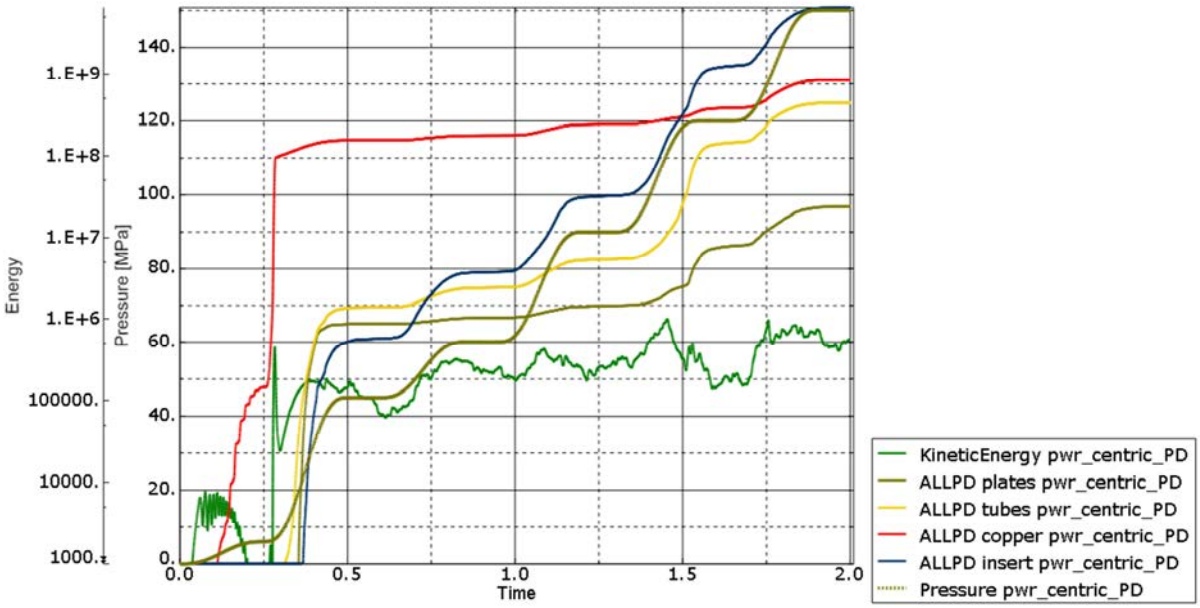

***Figure 11-4**. Kinetic and plastic energy together with pressure versus time [seconds] for the PWR insert for case pwr_centric_full_PD.*

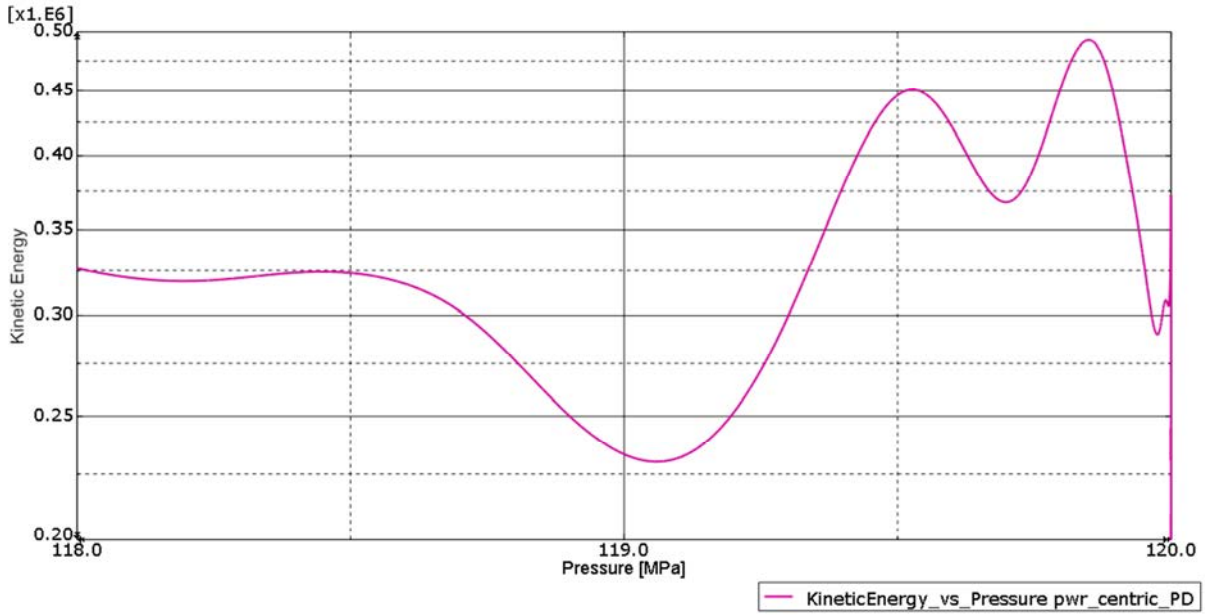

***Figure 11-5**. Kinetic energy versus pressure for the PWR insert for case pwr_centric_full_PD.*

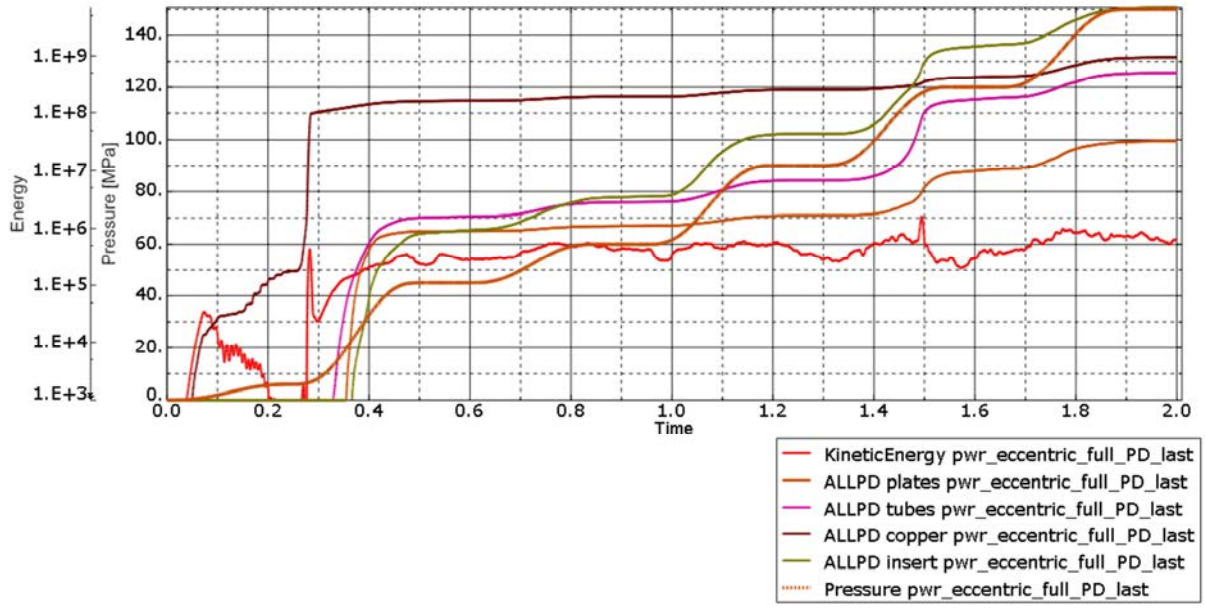

***Figure 11-6**. Kinetic and plastic energy together with pressure versus time [seconds] for the PWR insert for case pwr_eccentric_full_PD.*

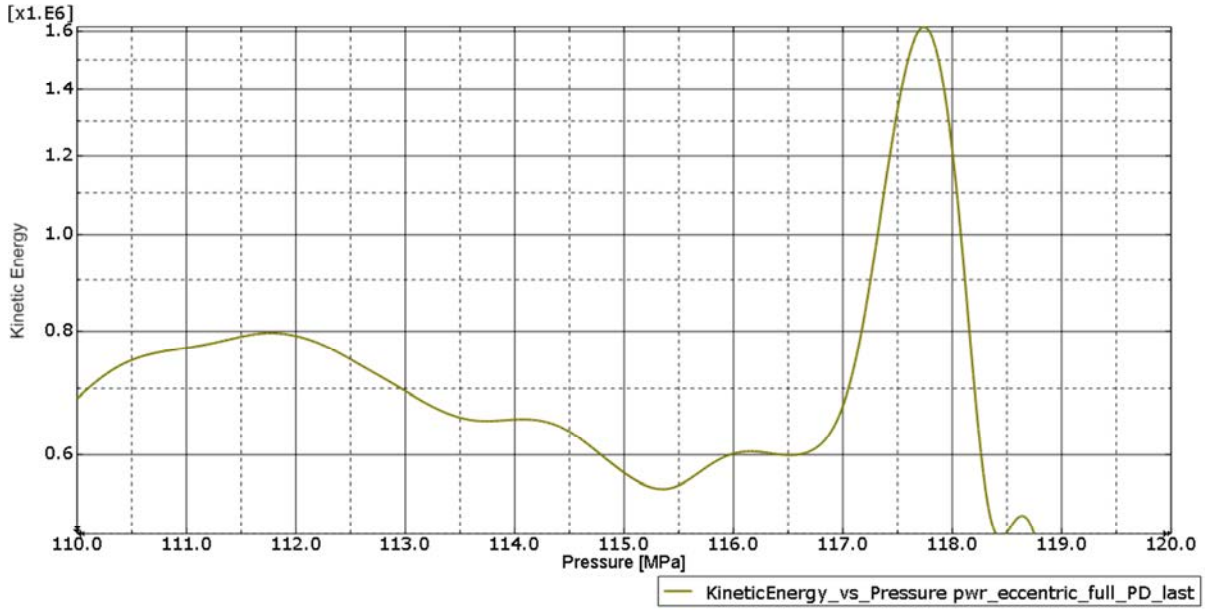

Figure 11-7*. Kinetic energy versus pressure for the PWR insert for case pwr_eccentric_full_PD.*

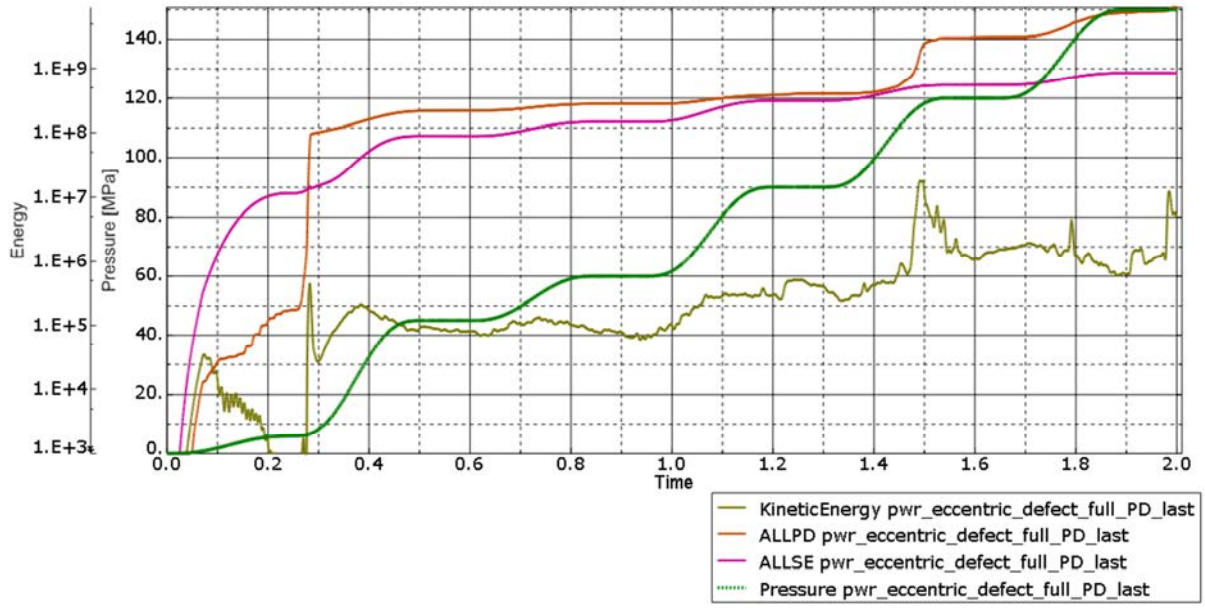

Figure 11-8*. Kinetic and plastic energy together with pressure versus time [seconds] for the PWR insert for case pwr_eccentric_defect_full_PD.*

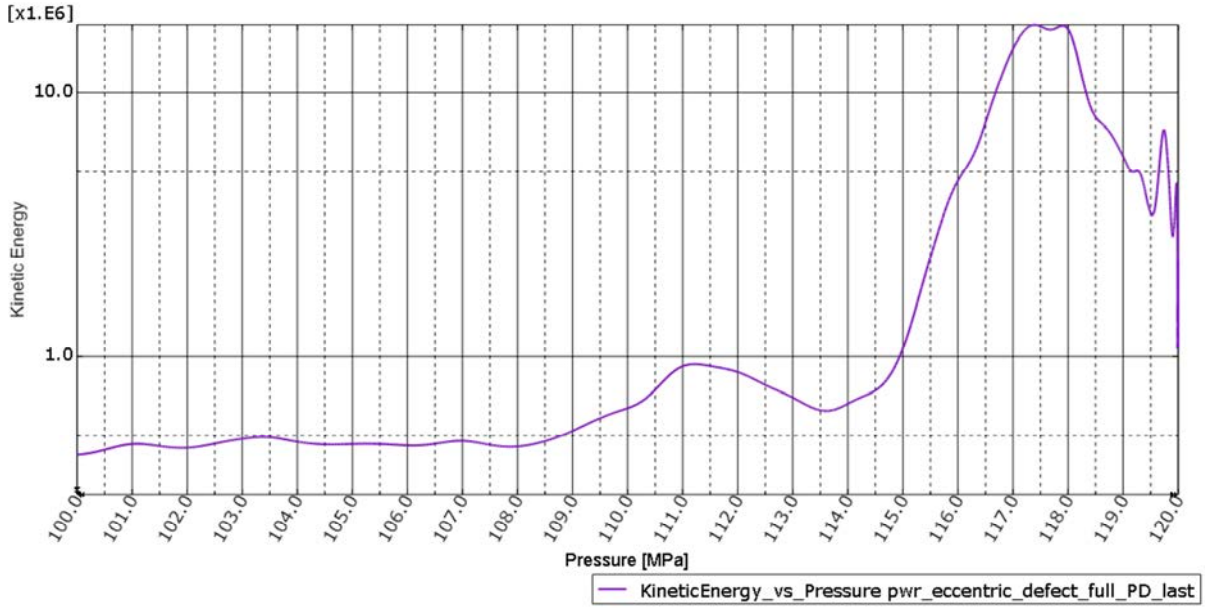

***Figure 11-9**. Kinetic energy versus pressure for the PWR insert for case pwr_eccentric_defect_full_PD.*

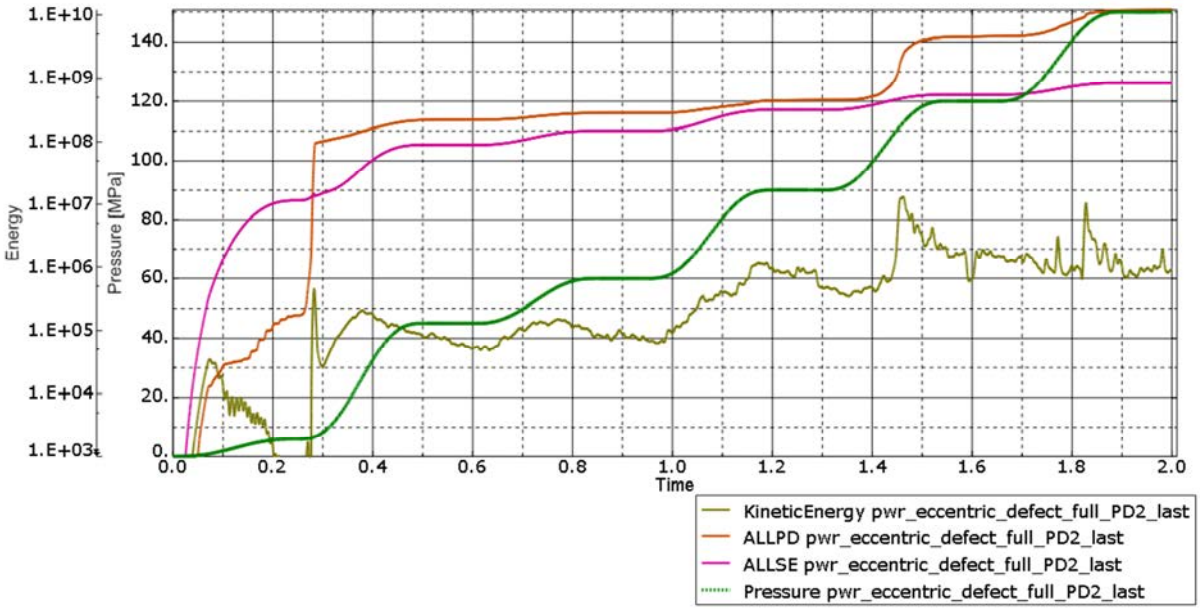

***Figure 11-10**. Kinetic and plastic energy together with pressure versus time [seconds] for the PWR insert for case pwr_eccentric_defect_full_PD2.*

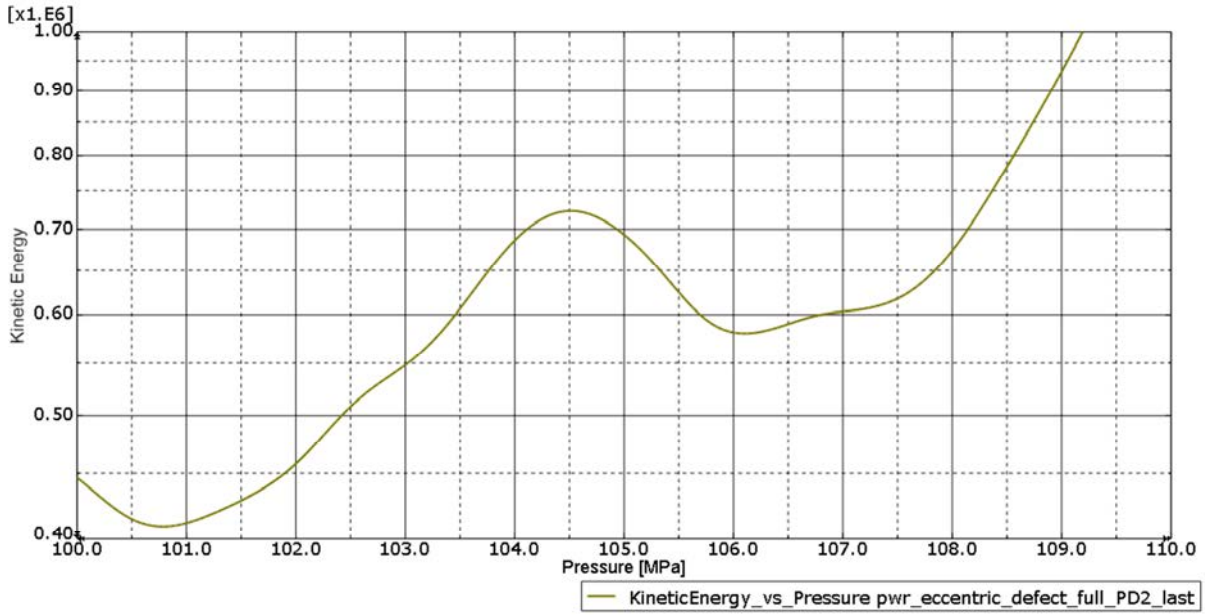

***Figure 11-11**. Kinetic energy versus pressure for the PWR insert for case pwr_eccentric_defect_full_PD2.*

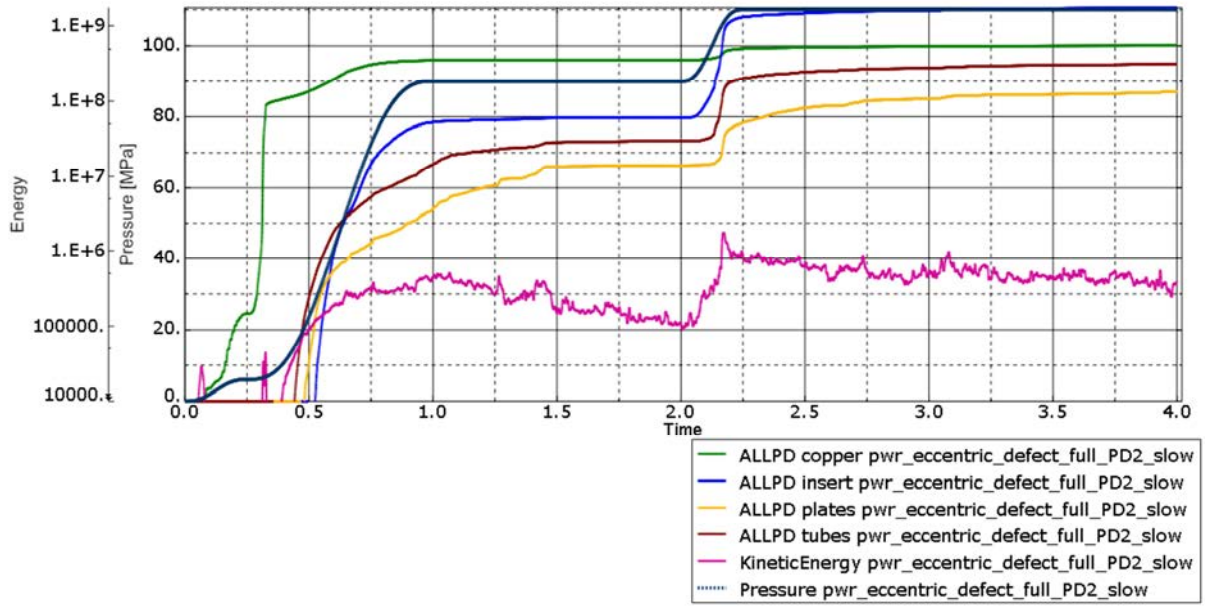

***Figure 11-12**. Kinetic and plastic energy together with pressure versus time [seconds] for the PWR insert for case pwr_eccentric_defect_full_PD2 – slow loading.*

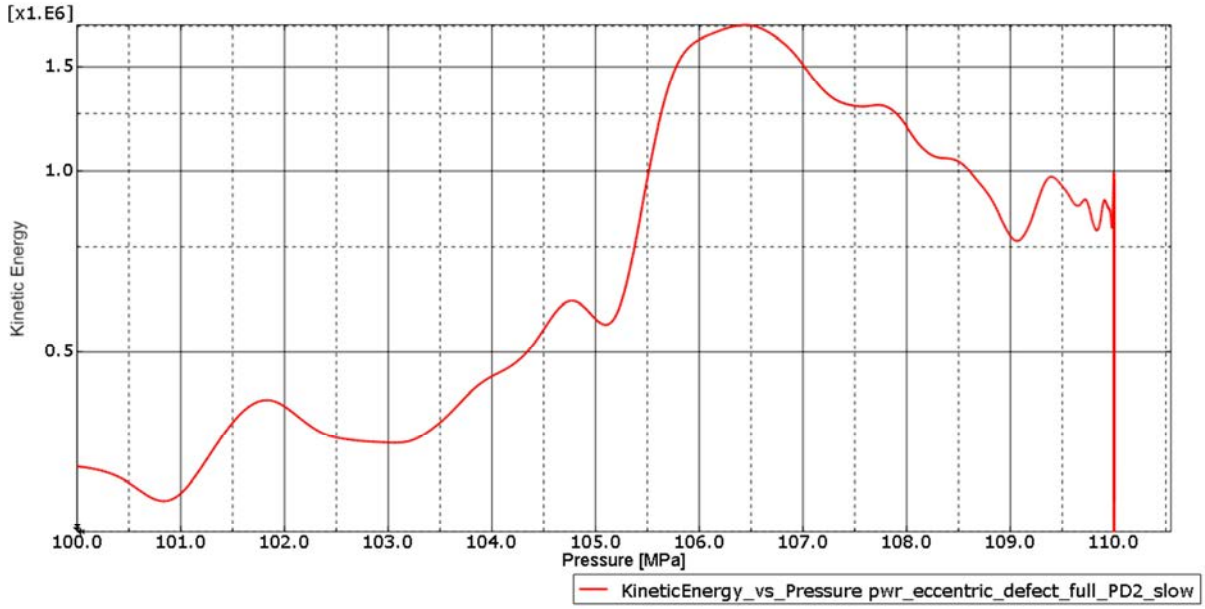

Figure 11-13. *Kinetic energy versus pressure for the PWR insert for case pwr_eccentric_defect_full_PD2 – slow loading.*

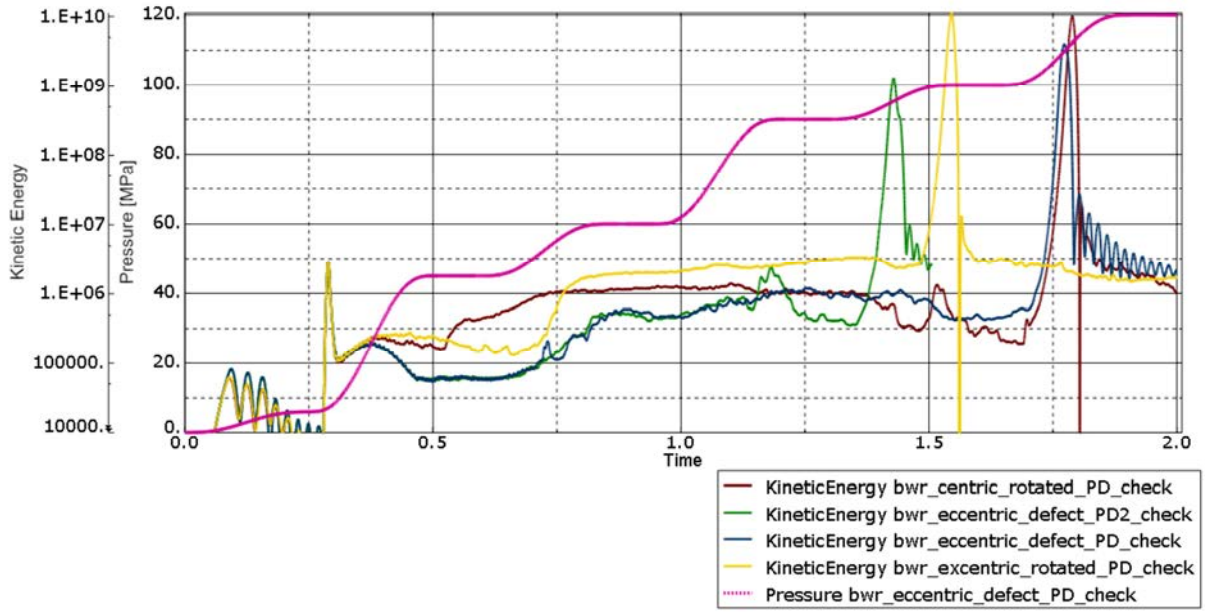

Figure 11-14*. Kinetic energy and pressure versus time [seconds] for the BWR insert.*

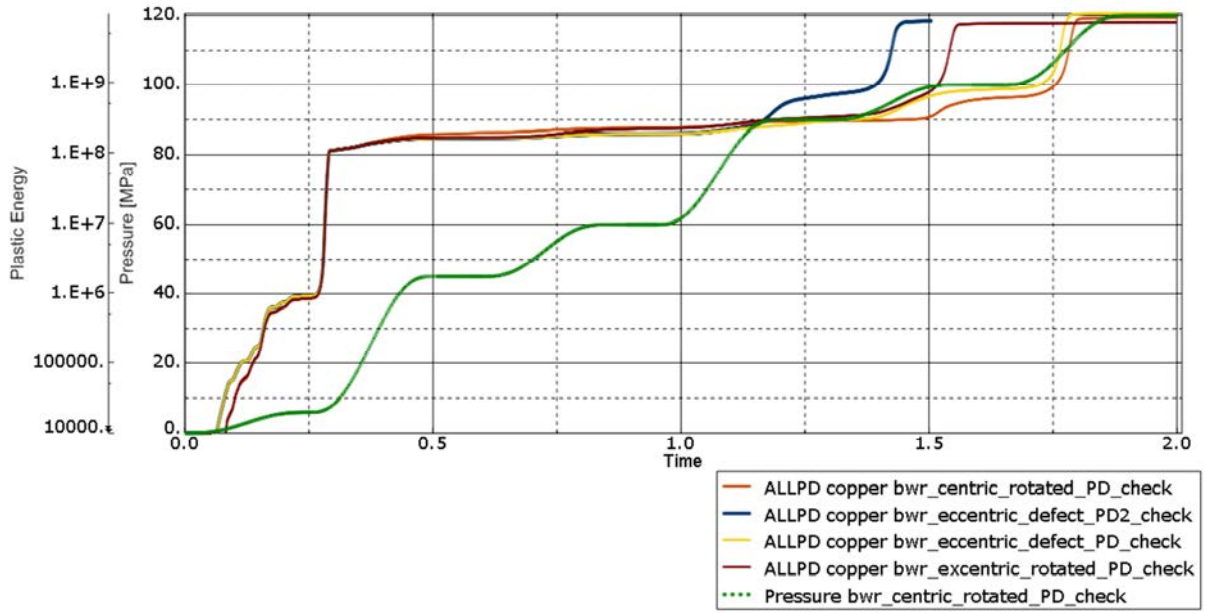

***Figure 11-15**. Plastic energy and pressure versus time [seconds] for the BWR insert.*

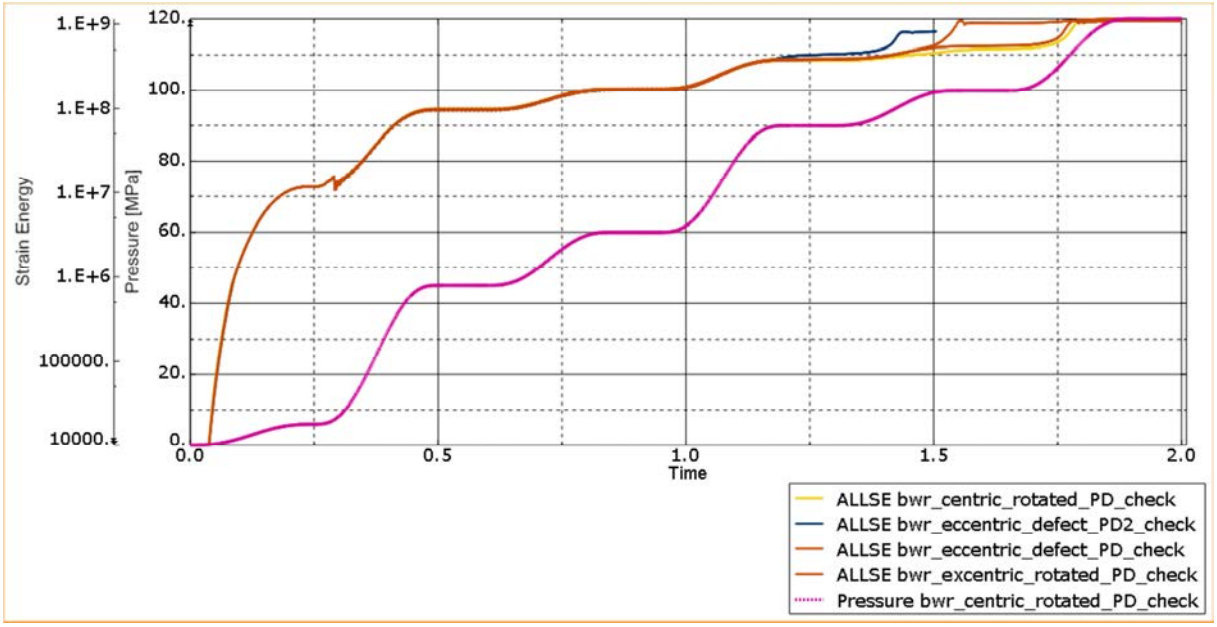

***Figure 11-16**. Strain energy and pressure versus time [seconds] for the BWR insert.*

Figures 11-17 to 11-28 show one plot with energies versus time together with applied pressure versus time and one plot with kinetic energy versus applied pressure focused at the first instability for each analysis for the BWR insert. The case bwr_eccentric_defect_PD2 has rigid body rotation which are very pronounced when the load is increased and thus this effect has been remove as much as possible, see Figures 11-25 to11-28. This makes it much easier to detect the sudden increase in kinetic energy (Figure 11-28).

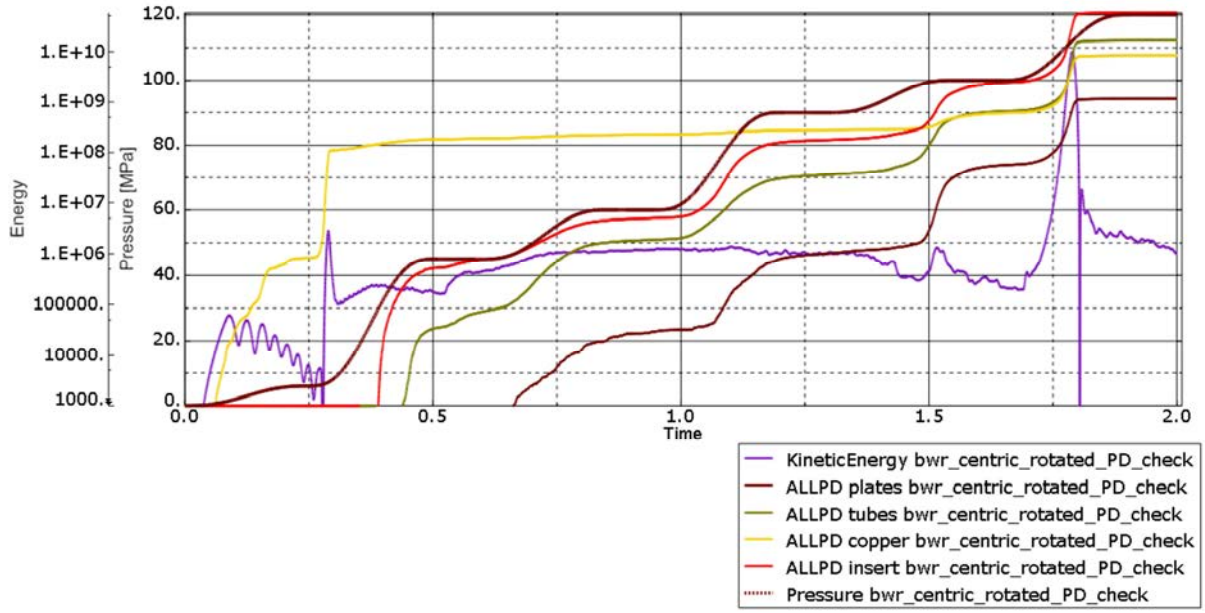

***Figure 11-17**. Kinetic and plastic energy together with pressure versus time [seconds] for the BWR insert for case bwr_centric_rotated_PD.*

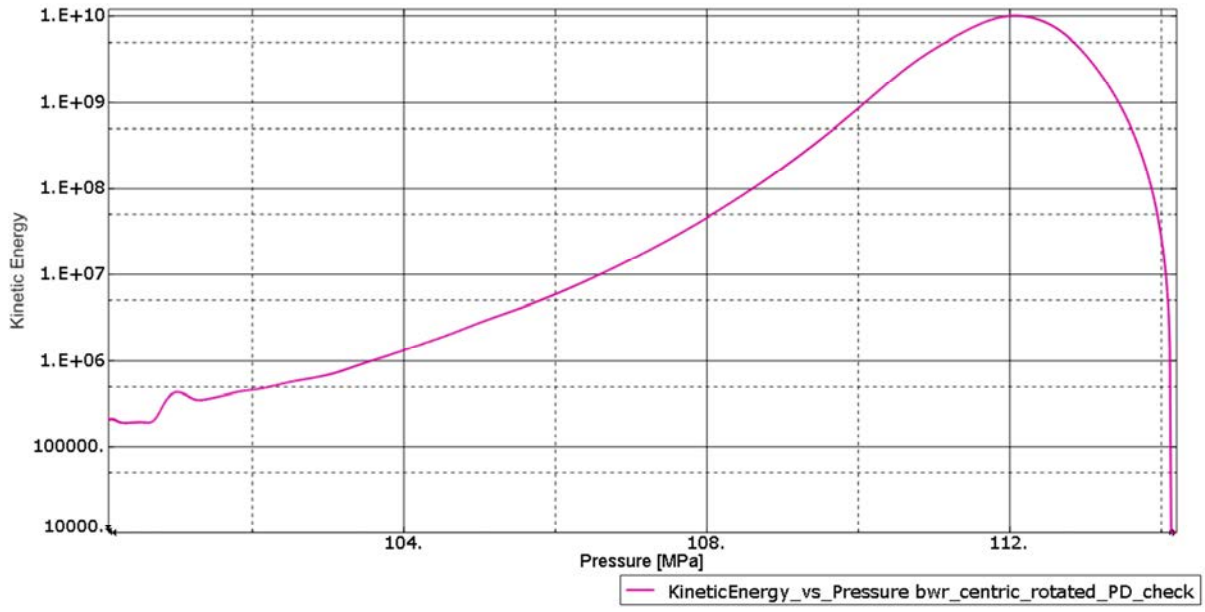

***Figure 11-18**. Kinetic energy versus pressure for the BWR insert for case bwr_centric_rotated_PD.*

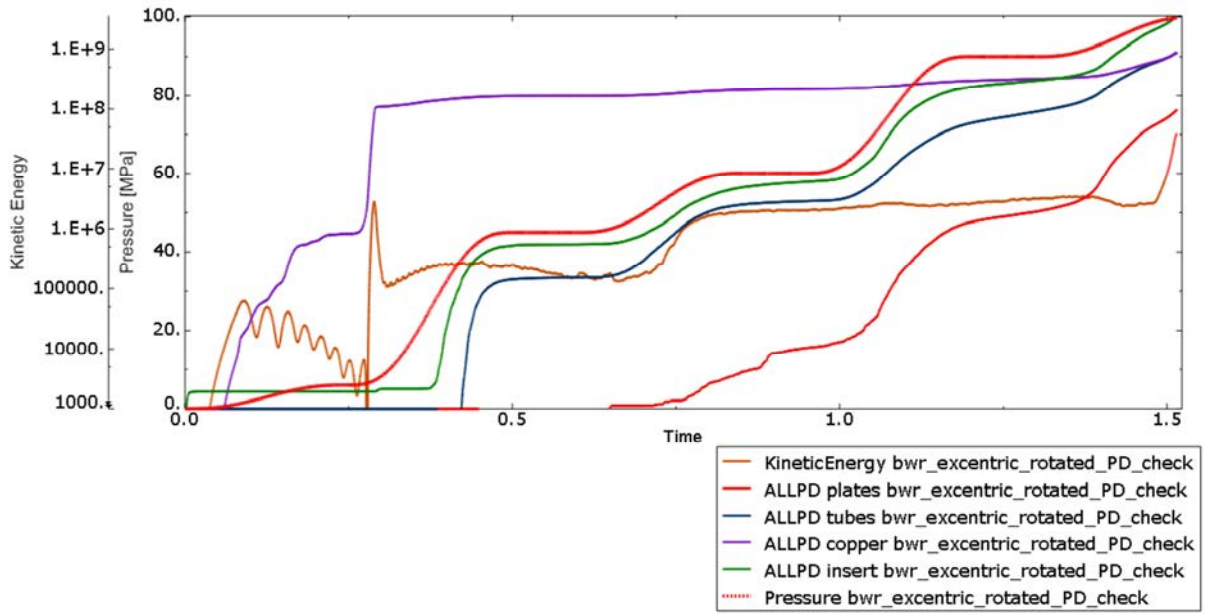

***Figure 11-19**. Kinetic and plastic energy together with the pressure versus time [seconds] for the BWR insert for case bwr_eccentric_rotated_PD.*

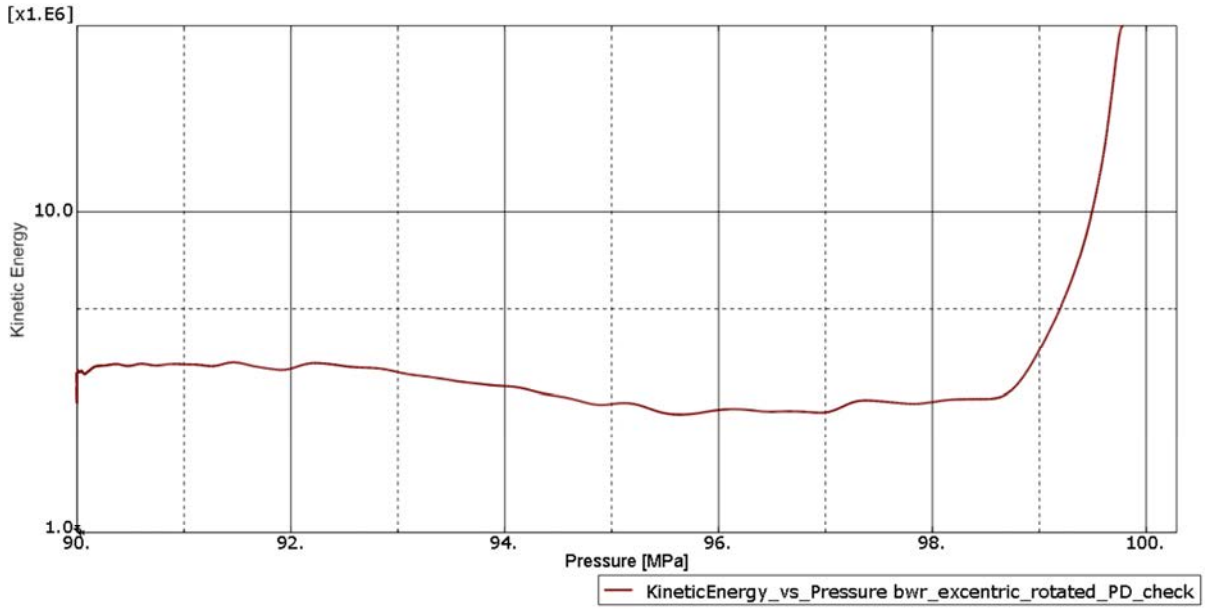

***Figure 11-20**. Kinetic energy versus pressure for the BWR insert for case bwr_eccentric_rotated_PD.*

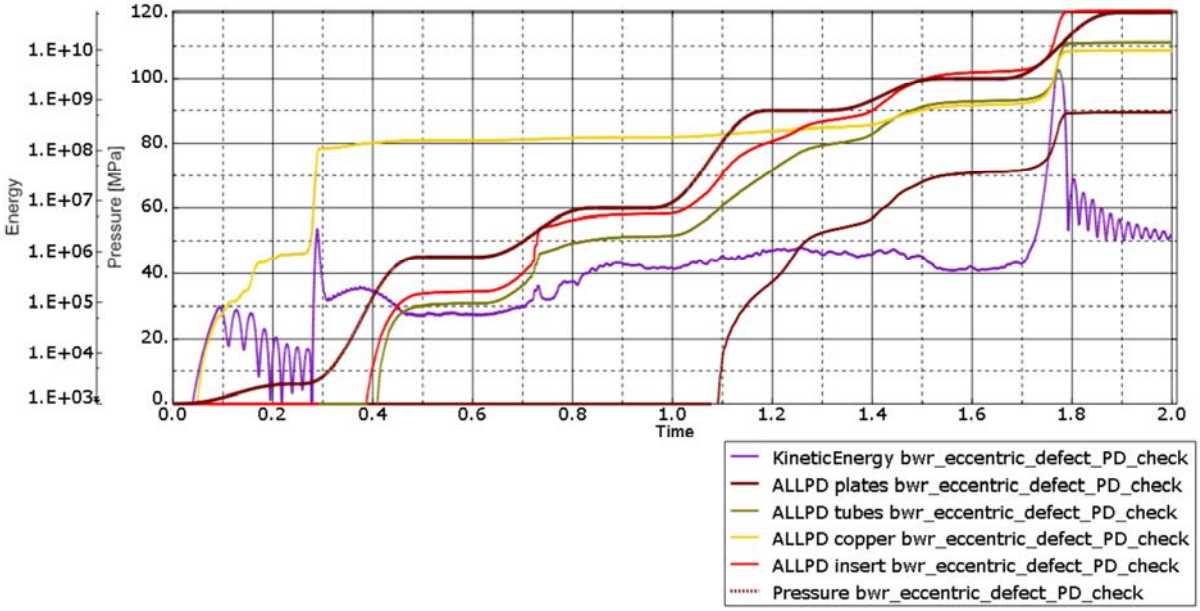

***Figure 11-21**. Kinetic and plastic energy together with pressure versus time [seconds] for the BWR insert for case bwr_eccentric_defect_PD.*

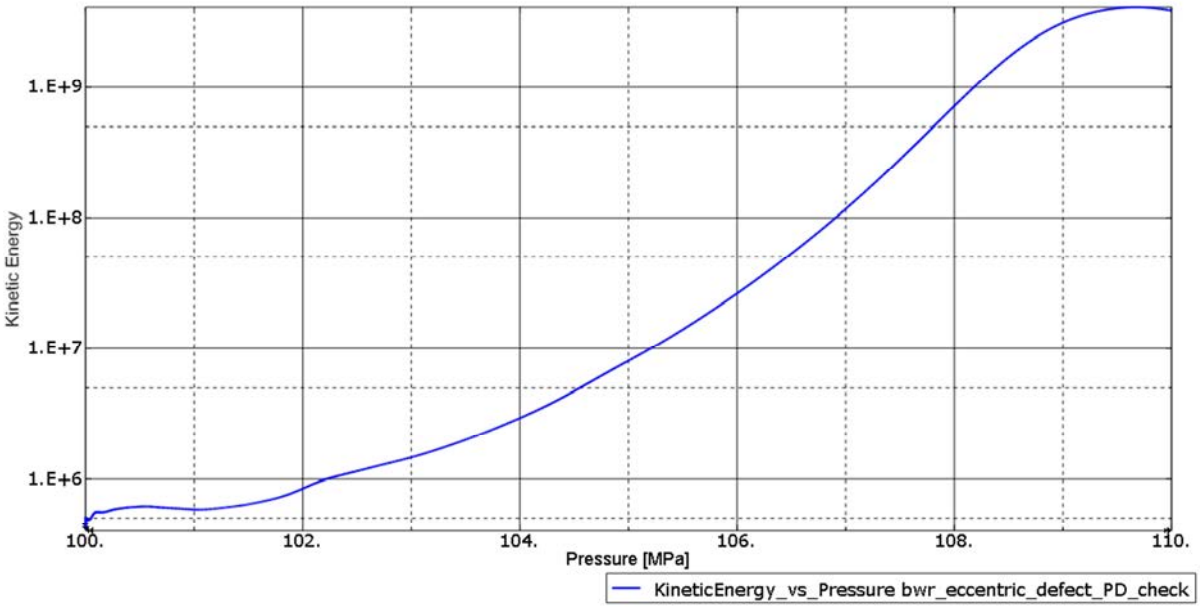

***Figure 11-22**. Kinetic energy versus pressure for the BWR insert for case bwr_eccentric_defect_PD.*

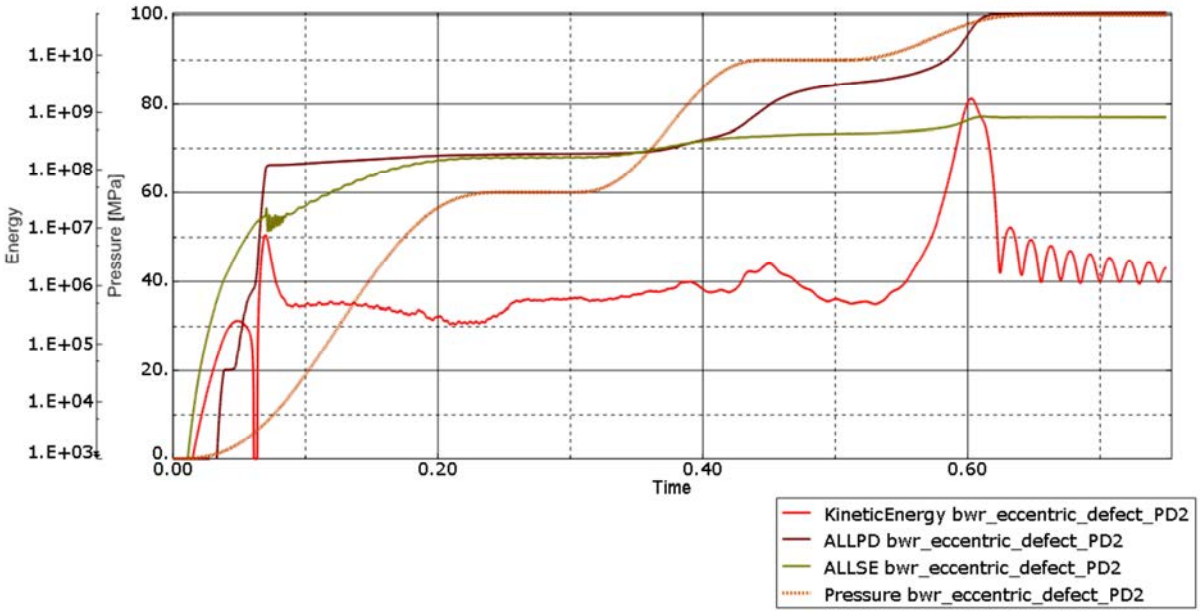

Figure 11-23. *Kinetic and plastic energy together with pressure versus time [seconds] for the BWR insert for case bwr_eccentric_defect_PD2.*

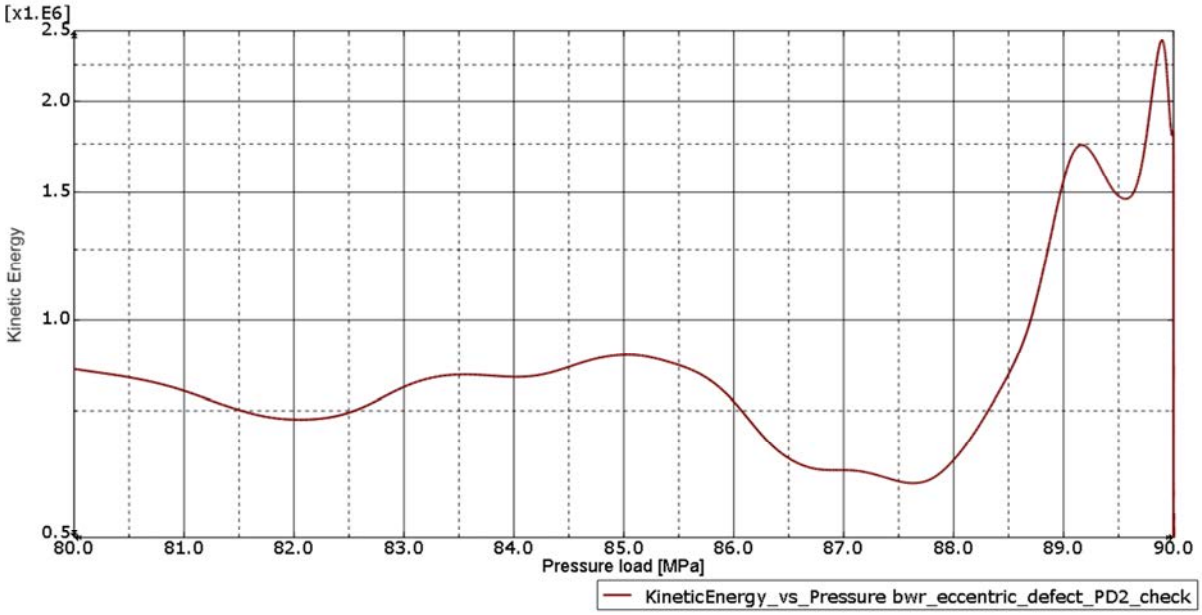

Figure 11-24. *Kinetic energy versus pressure for the BWR insert for case bwr_eccentric_defect_PD2.*

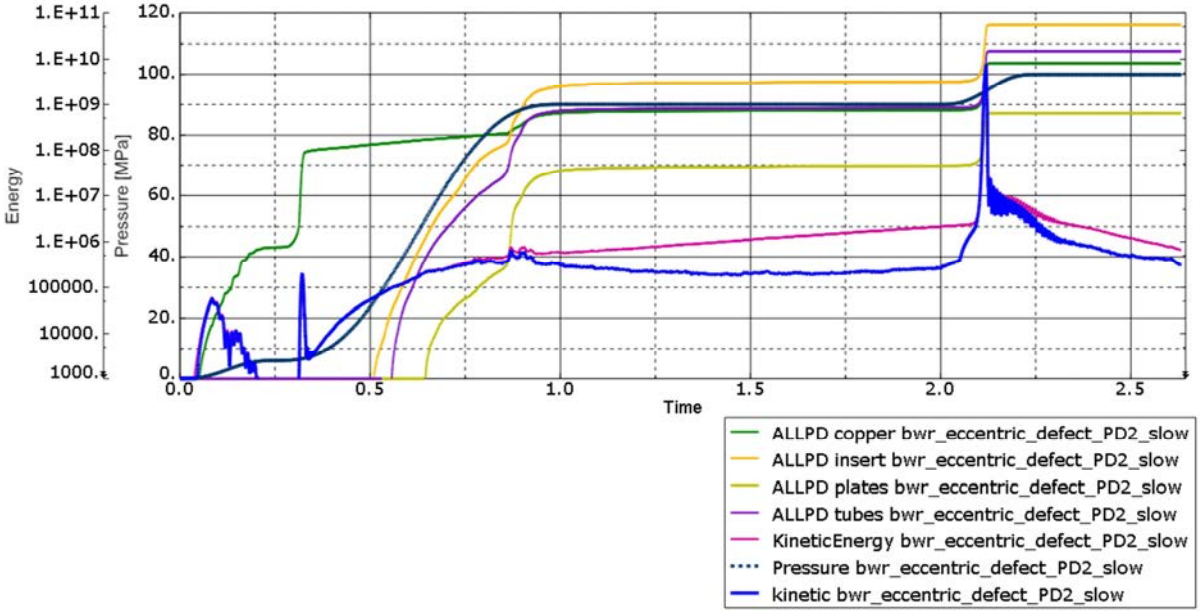

***Figure 11-25**. Kinetic and plastic energy together with pressure versus time [seconds] for the BWR insert for case bwr_eccentric_defect_PD2 – slow loading. Curve labelled "kinetic bwr_eccentric_defect_PD2_slow" corresponds to when rigid body motion is removed.*

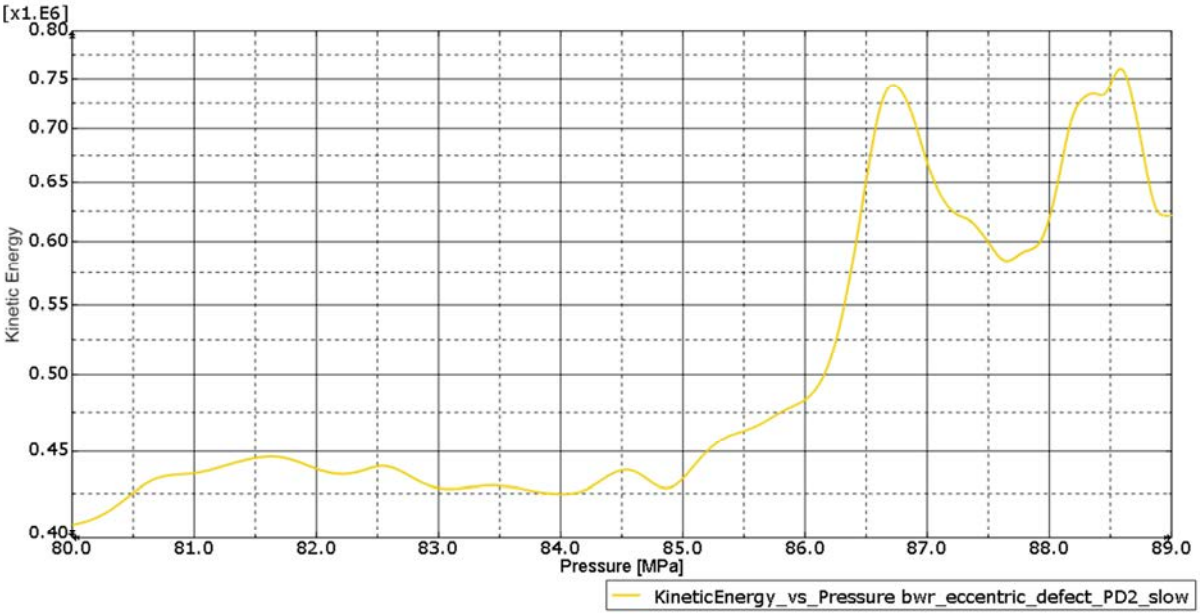

***Figure 11-26**. Kinetic energy versus pressure for the BWR insert for case bwr_eccentric_defect_PD2 – slow loading.*

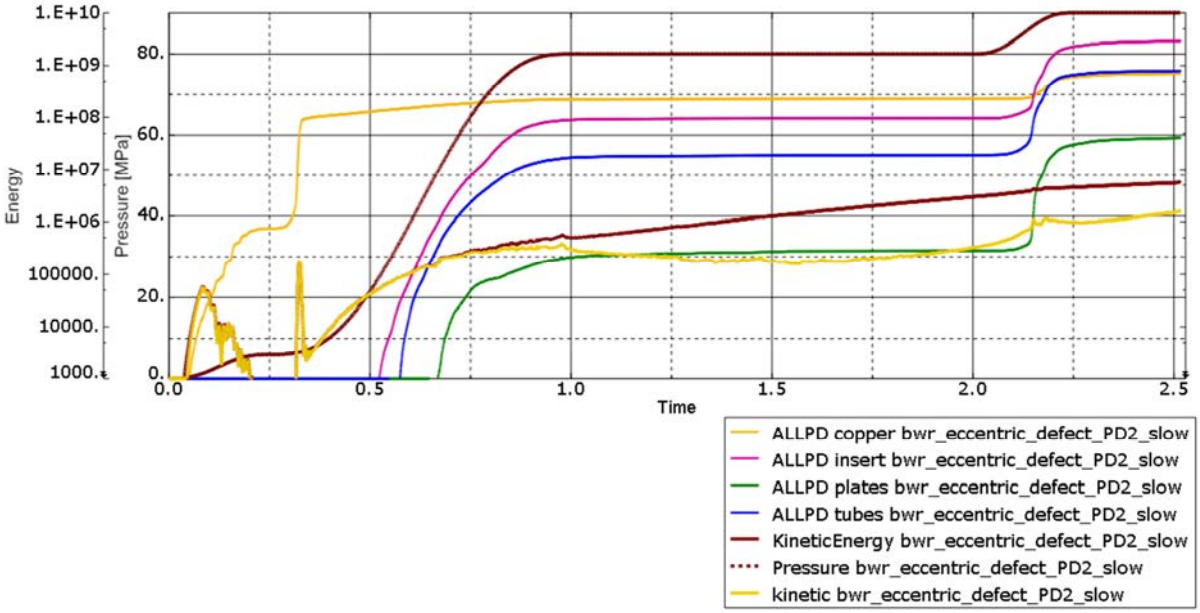

Figure 11-27*. Kinetic and plastic energy together with pressure versus time [seconds] for the BWR insert for case bwr_eccentric_defect_PD2 – slow2 loading. Curve labelled "kinetic bwr_eccentric_defect_PD2_slow" corresponds to when rigid body motion is removed.*

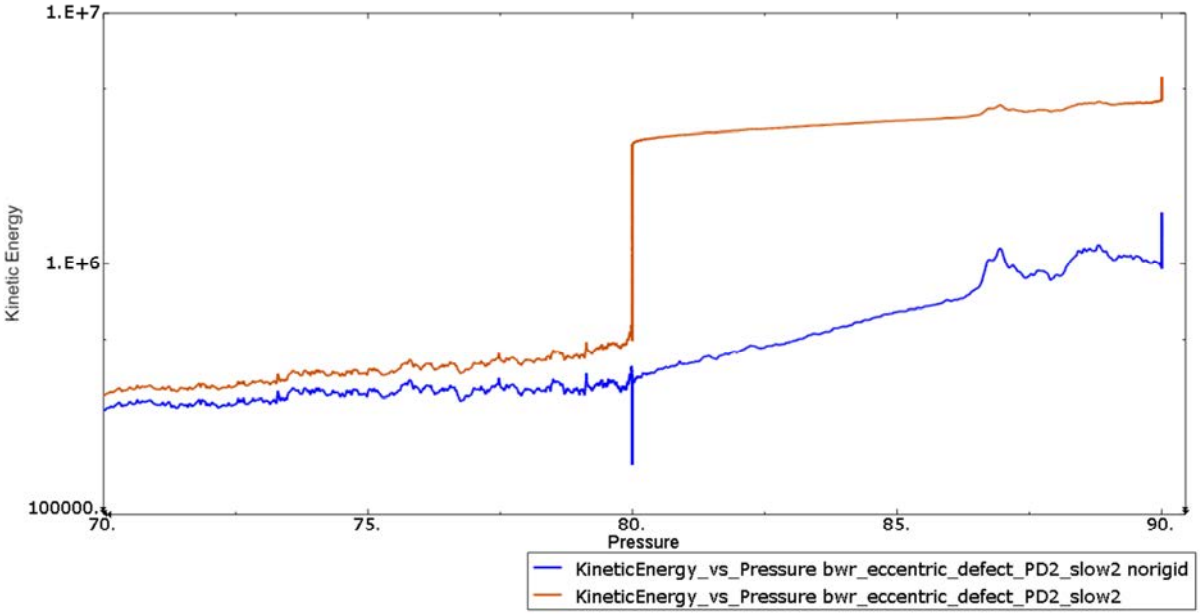

Figure 11-28*. Kinetic energy versus pressure for the BWR insert for case bwr_eccentric_defect_PD2 – slow2 loading. Curve labelled "kinetic bwr_eccentric_defect_PD2_slow2 norigid" corresponds to when rigid body motion is removed.*

11.2 Instability based on ASME

According to ASME VIII (Dillström et al. 2010) the instability can be estimated from sudden change of the slope for applied load versus displacement. The ASME rule is based on linear behaviour up to

the instability and the instability is assumed to occur when the secant has changed by a factor of 2.0, see Figure 11-29.

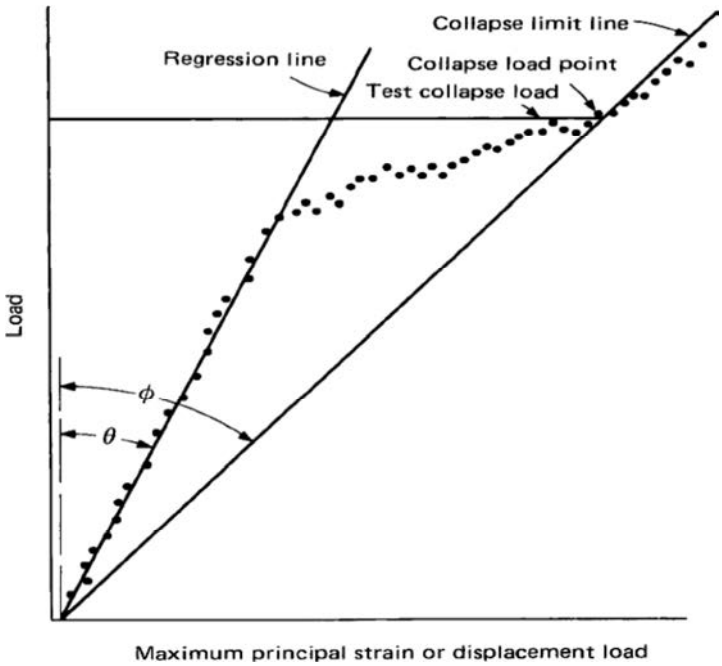

***Figure 11-29**. Definition of collapse load according to ASME VIII (6-153).*

Figures 11-30 to 11-34 show results for the PWR insert. Note that slow loading decreases the stiffness (compare Figure 11-33 and 11-34) but the instability magnitudes are very similar. The inertia effect is obvious where the load magnitude is kept constant which makes it difficult to decide which slope to use for the initial stiffness.

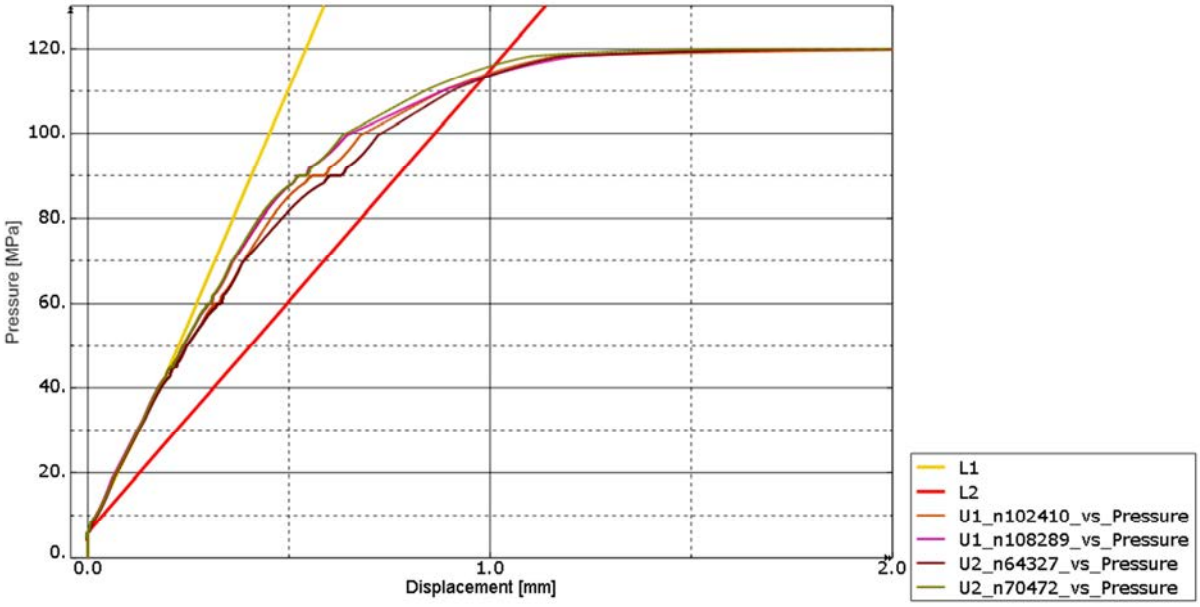

***Figure 11-30**. Instability for case pwr_centric_PD according to ASME VIII (6-153). L1 is the regression line and L2 is the collapse limit line.*

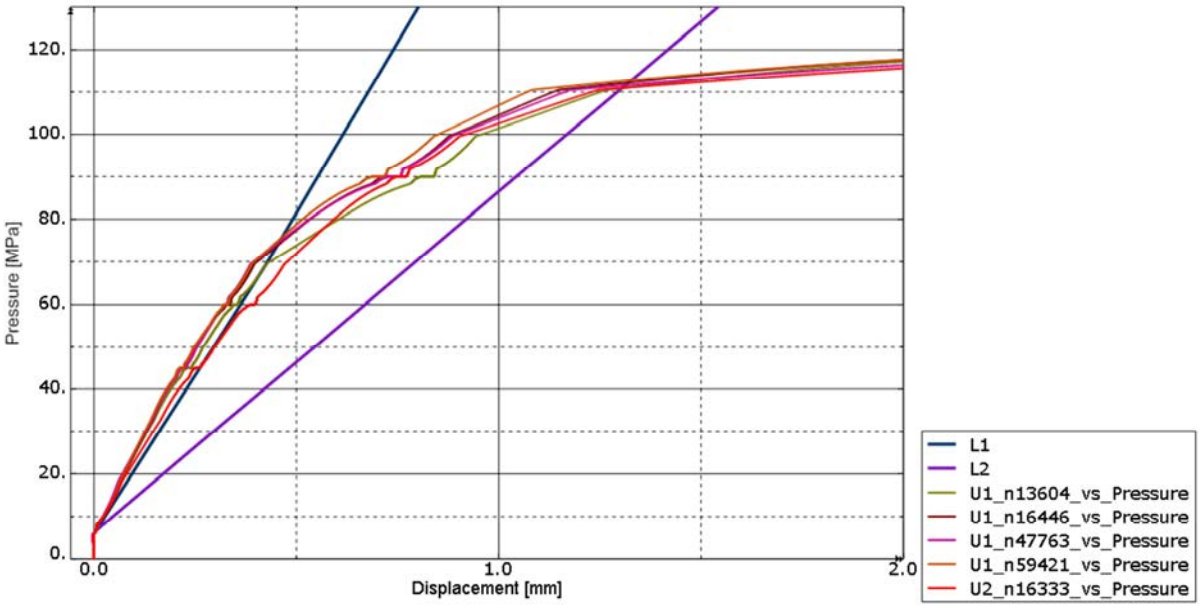

***Figure 11-31**. Instability for case pwr_eccentric_full_PD according to ASME VIII (6-153). L1 is the regression line and L2 is the collapse limit line.*

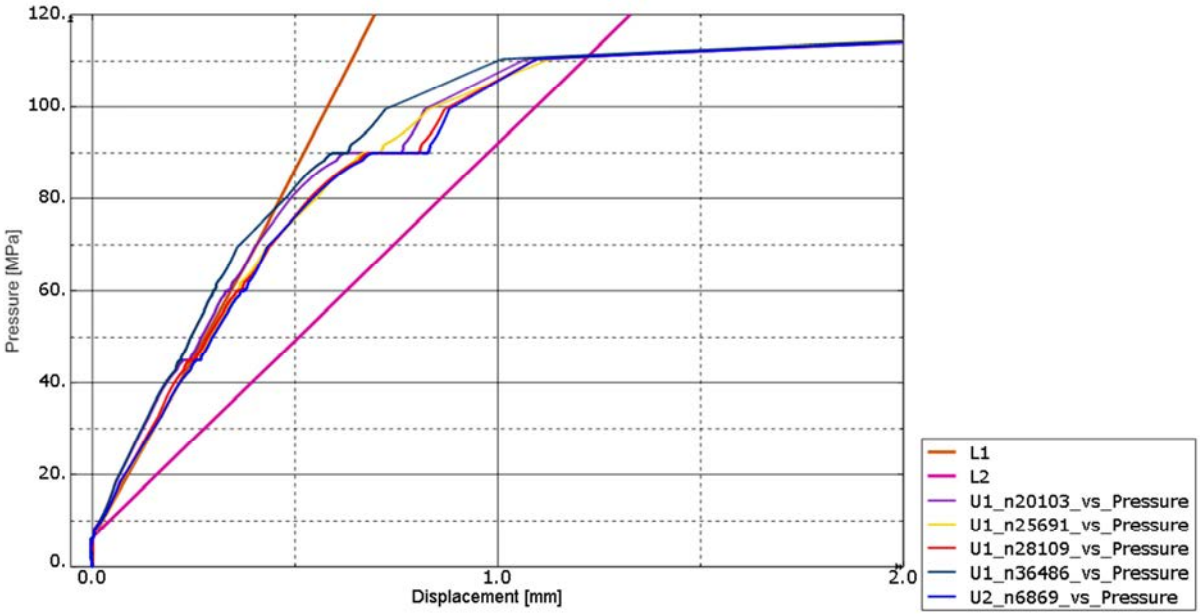

***Figure 11-32**. Instability for case pwr_eccentric_defect_full_PD according to ASME VIII (6-153). L1 is the regression line and L2 is the collapse limit line.*

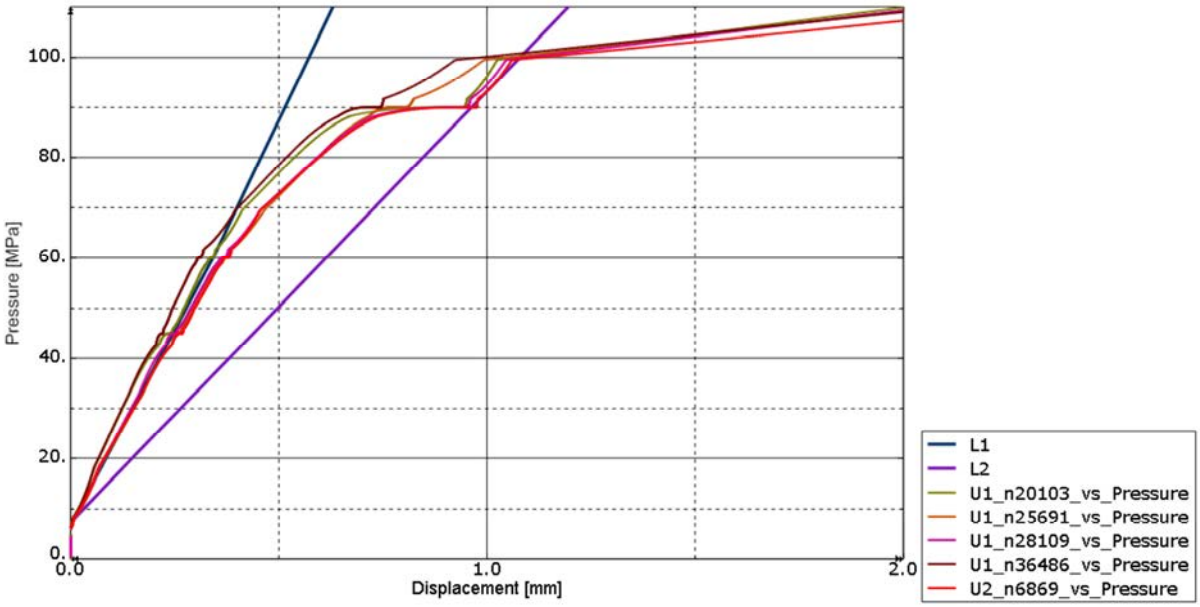

***Figure 11-33**. Instability for case pwr_eccentric_defect_full_PD2 according to ASME VIII (6-153). L1 is the regression line and L2 is the collapse limit line.*

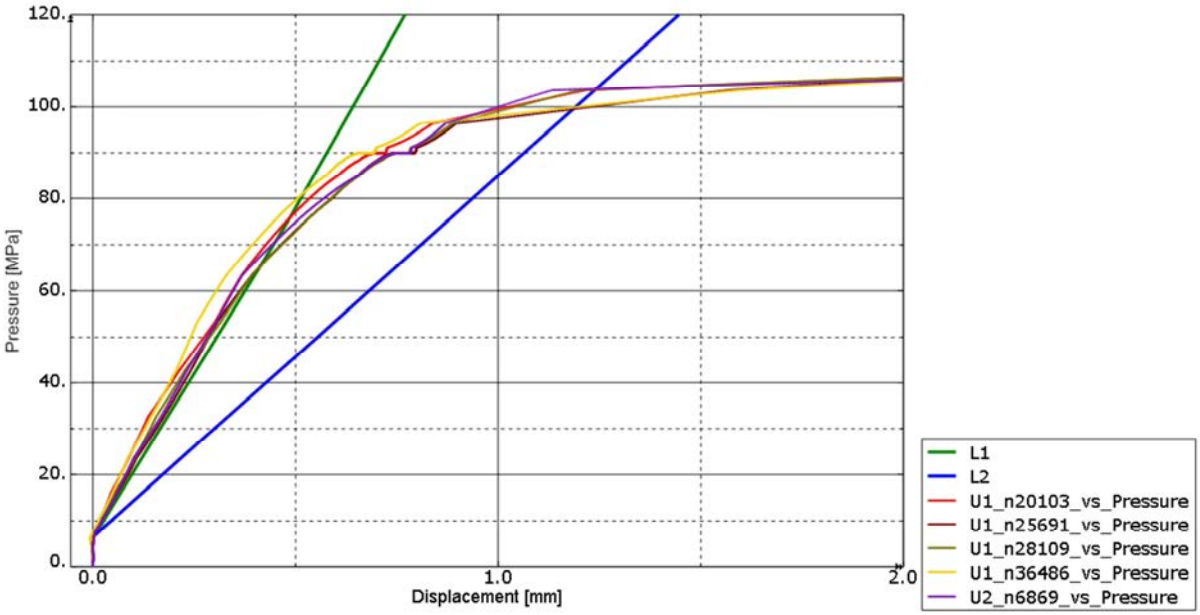

***Figure 11-34**. Instability for case pwr_eccentric_defect_PD2 slow loading according to ASME VIII (6-153). L1 is the regression line and L2 is the collapse limit line.*

Figures 11-35 to 11-39 show results for the BWR insert. For the BWR insert it's more difficult to estimate the instability magnitude following ASME VIII (except for the case with slow loading) mainly due to inertia effects. Instead of using the initial stiffness a rough estimate is made by using the displacement magnitude versus pressure. The case with slow loading also has a decrease of the mass scaling by a factor of 3 which decreases the inertia effect substantially.
For case bwr_eccentric_defect_PD2 the rigid body rotation makes it difficult to define regression line and the collapse limit line. However, a rough compensation for this effect has been used for construction of these lines. Probably, the estimate is more accurate if the rigid body rotation is constrained.

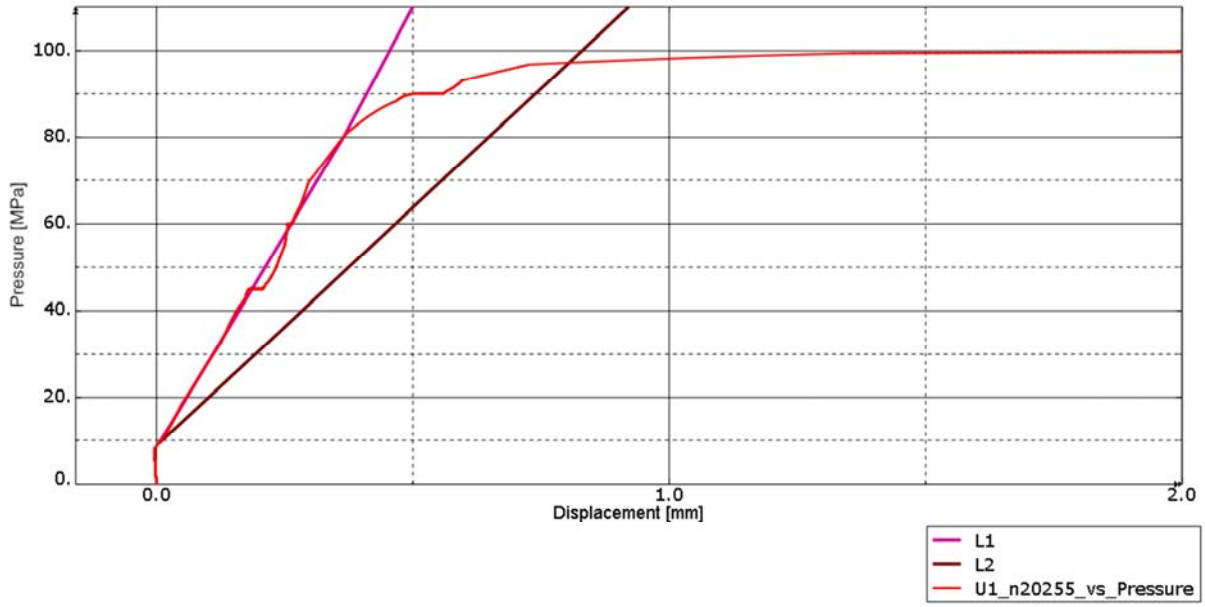

***Figure 11-35**. Instability for case bwr_centric_rotated_PD according to ASME VIII (6-153). L1 is the regression line and L2 is the collapse limit line.*

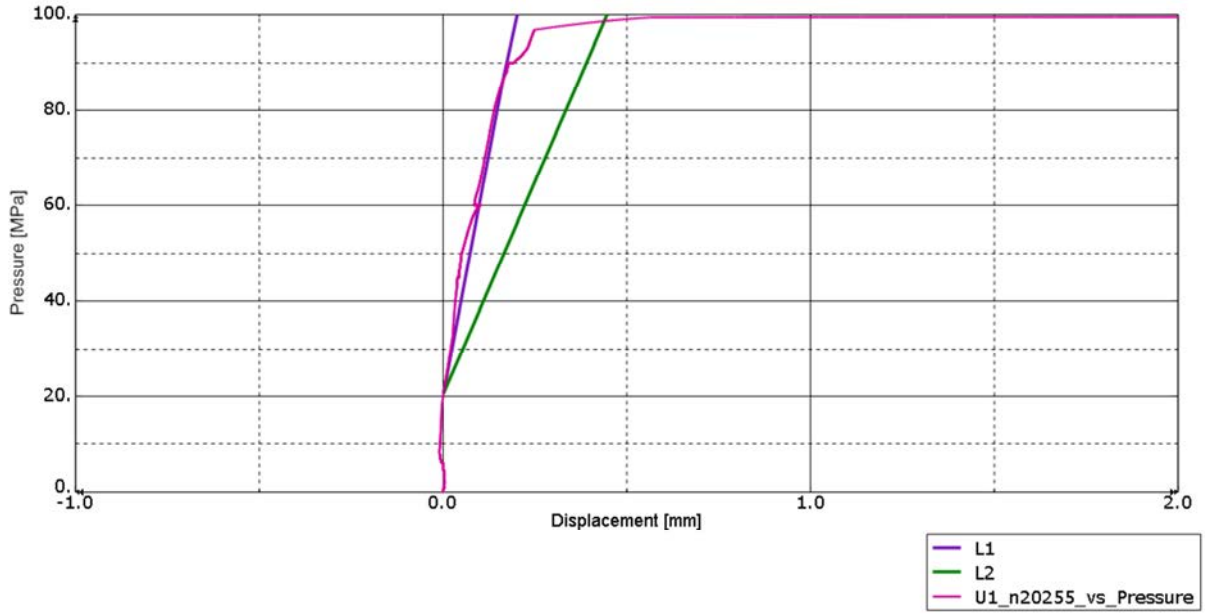

***Figure 11-36**. Instability for case bwr_excentric_rotated_PD according to ASME VIII (6-153). L1 is the regression line and L2 is the collapse limit line.*

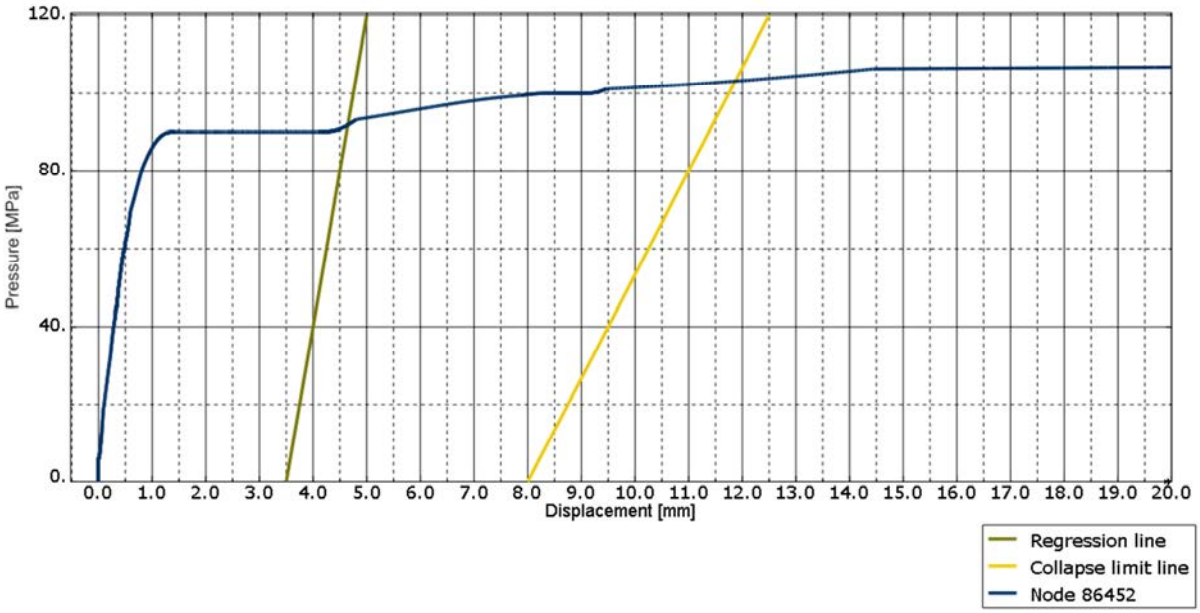

***Figure 11-37**. Instability for case bwr_eccentric_defect_PD according to ASME VIII (6-153). Adjustmenents due to rigid body motion.*

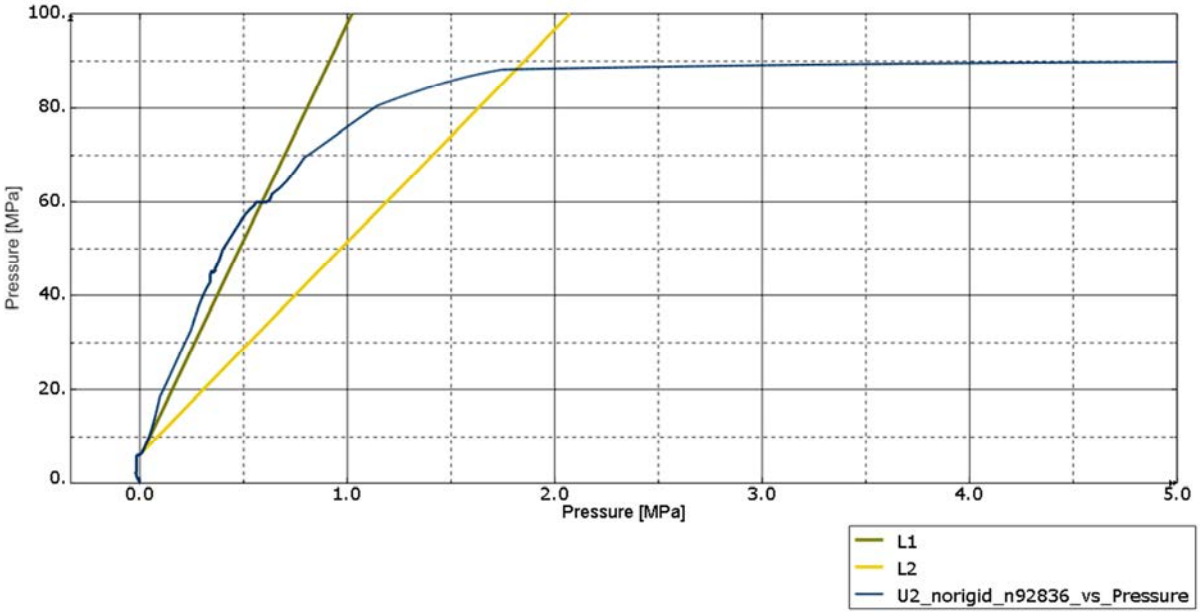

***Figure 11-38**. Instability for case bwr_eccentric_defect_PD2 according to ASME VIII (6-153). L1 is the regression line and L2 is the collapse limit line.*

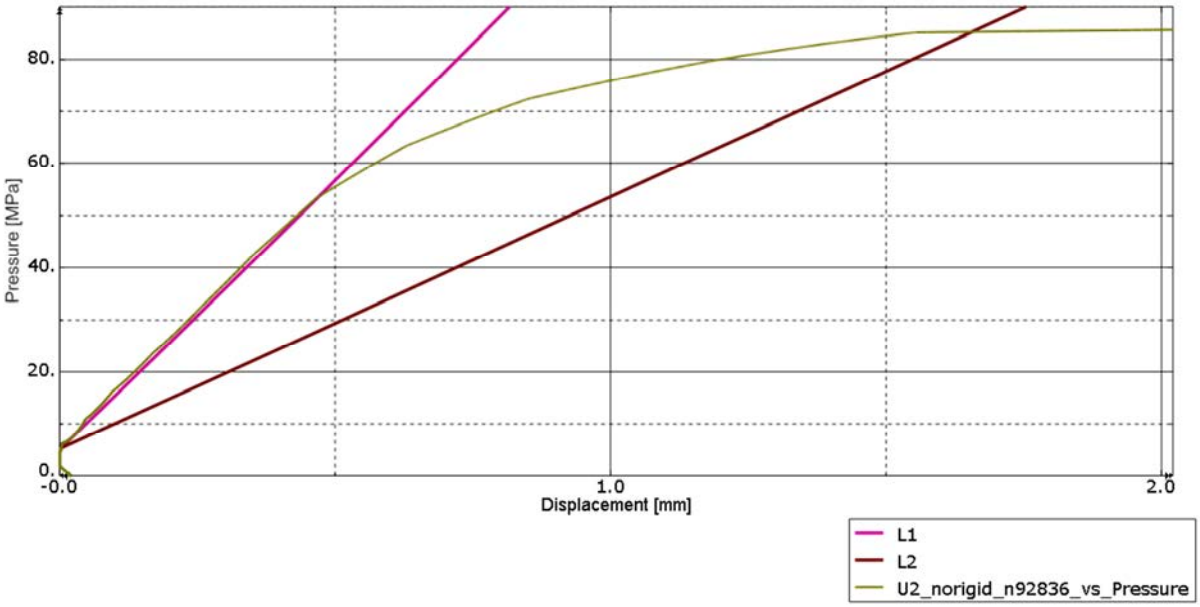

***Figure 11-39**. Instability for case bwr_eccentric_defect_PD2 slow loading according to ASME VIII (6-153). L1 is the regression line and L2 is the collapse limit line.*

Table 11-1 and 11-2 shows the first instability level for the BWR and PWR inserts. For cases eccentric_defect_PD2 two values are reported, the first having the default loading and the second when slow loading is used.

Table 11-1. First instability level for the BWR insert.

Model name	Instability level		Reference (Dillström et al. 2010)
	Based on kinetic energy	Based on ASME	
bwr_centric_rotated	98 MPa	97 MPa	99 MPa
bwr_eccentric_rotated	99 MPa	98 MPa	75 MPa
bwr_eccentric_defect	101 MPa	102 MPa	68 MPa
bwr_eccentric_defect_PD2	88/86 MPa	88/85 MPa	-

Table 11-2. First instability level for the PWR insert.

Model name	Instability level		Reference (Dillström et al. 2010)
	Based on kinetic energy	Based on ASME	
pwr_centric_PD	119 MPa	116 MPa	128 MPa
pwr_eccentric_PD	116 MPa	113 MPa	-
pwr_eccentric_defect_PD	113 MPa	111 MPa	71 MPa
pwr_eccentric_defect_PD2	101/103 MPa	101/104 MPa	-

12 Post buckling

Increasing the load after reaching the first instability the insert finds a new stable configuration, either the insert will be fully compressed and leaves no space for any waste or the insert only gets small deformations leaving enough with space for the waste.
Figures 12-1 to 12-4 show results for the BWR insert (slow loading). Figure 12-1 shows that when the pressure load is kept constant at 90 MPa the kinetic energy slowly increases indicating an unstable behaviour (even though the displaced configuration indicates that a new stable configuration is reached) but after the peak at about 95 MPa the kinetic energy quickly decreases when the pressure load is kept at 100 MPa. The reason for this is that the geometry is compressed to almost a solid body. However, at this load the insert is not useful as a container for the waste, Figure 12-4.

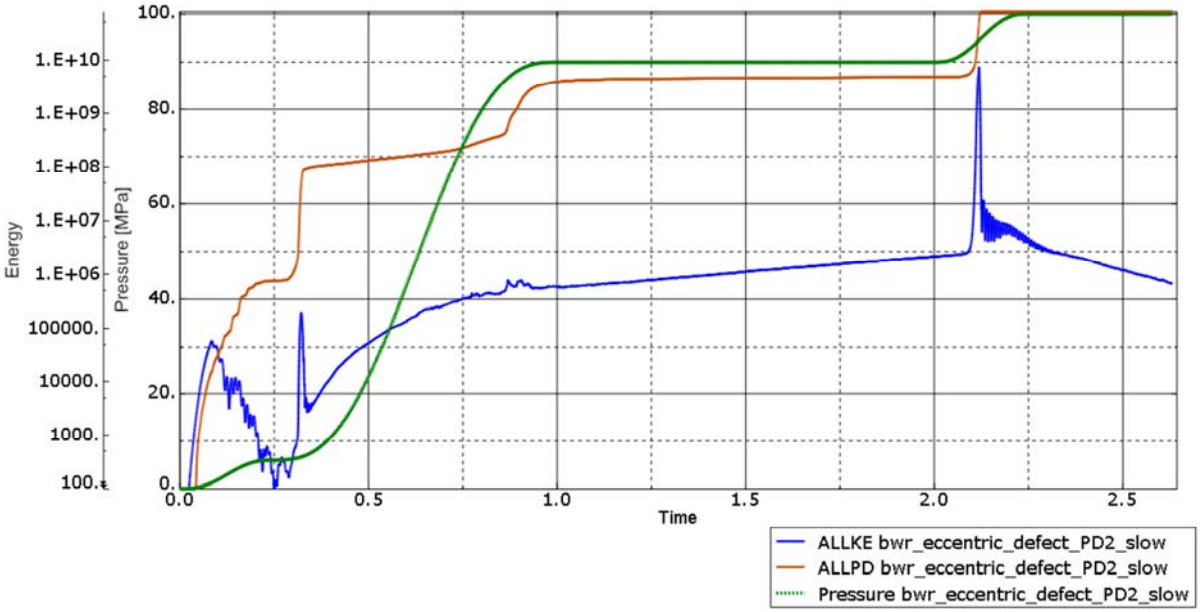

***Figure 12-1**. Energy for case bwr_eccentric_defect_PD2 slow loading.*

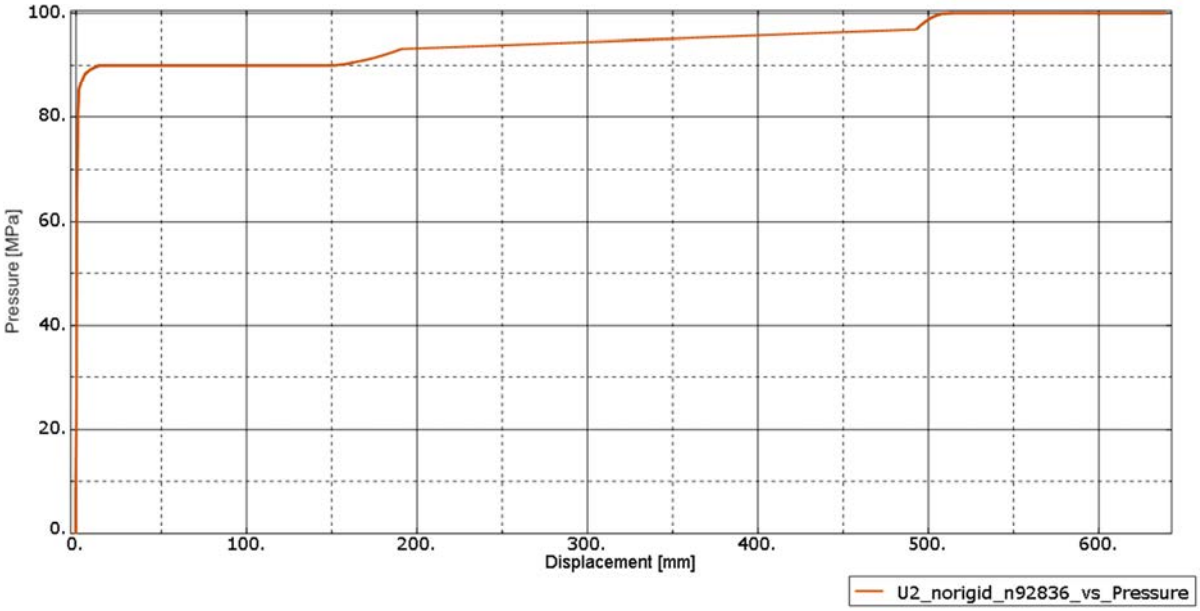

***Figure 12-2**. Displacement versus pressure for case bwr_eccentric_defect_PD2 slow loading.*

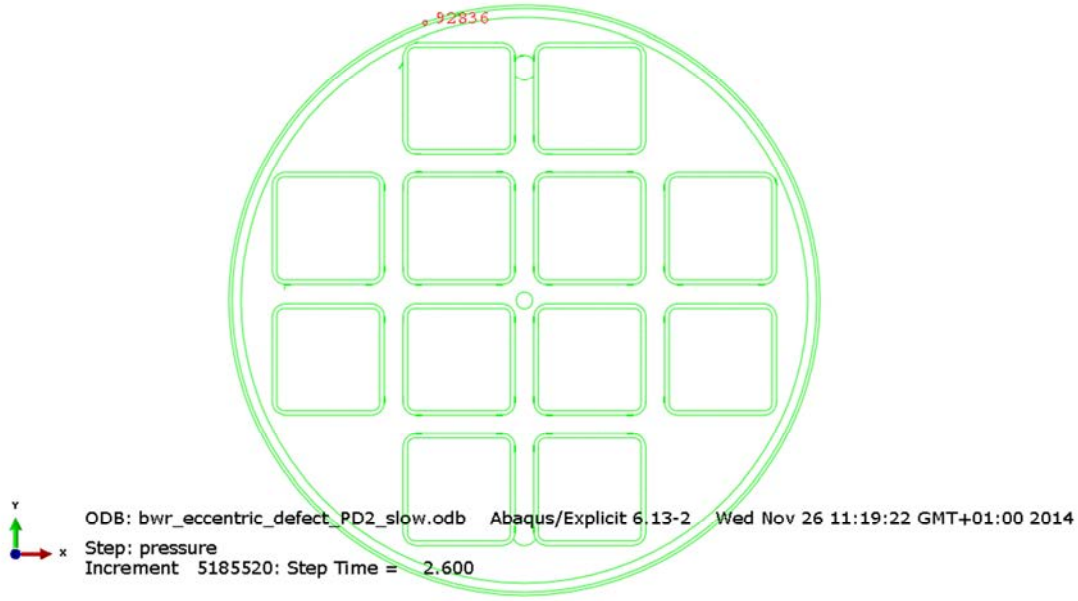

***Figure 12-3**. Selected node for case bwr_eccentric_defect_PD2 slow loading.*

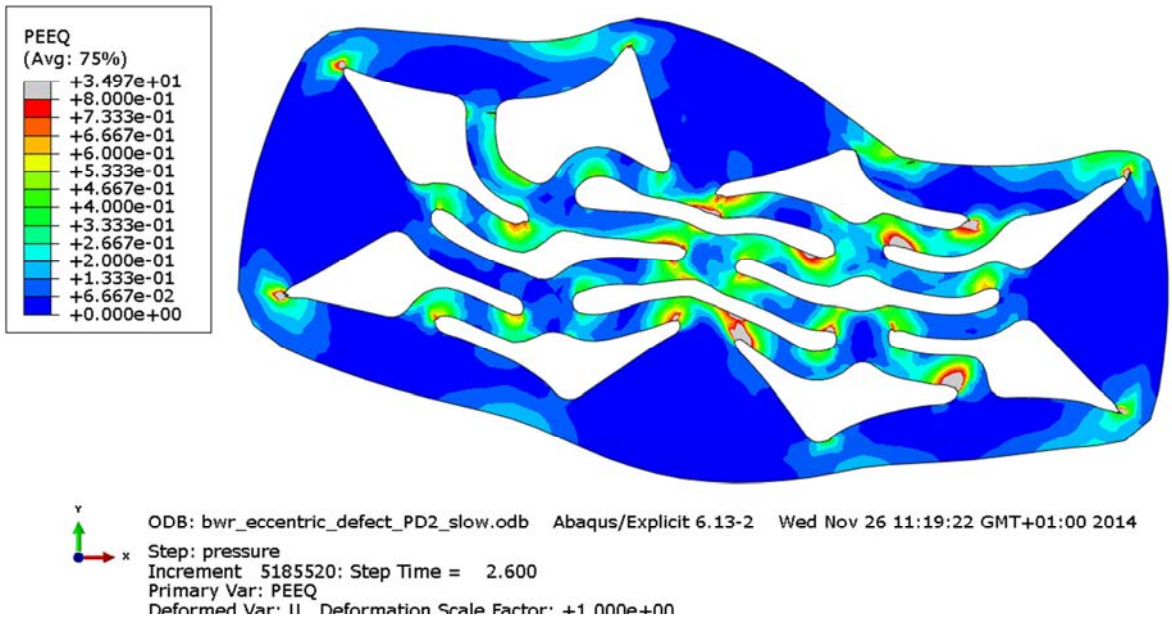

***Figure 12-4**. Displaced geometry with equivalent plastic strain (PEEQ) for case bwr_eccentric_defect_PD2 slow loading.*

Figures 12-5 to 12-8 show results for the PWR insert (slow loading). Figure 12-5 shows that when the pressure load is kept constant at 90 and 110 MP the kinetic energy decreases indicating a stable behaviour. Also the displaced geometry at the end of the analysis, Figure 12-8, indicates that the insert remains as a useful container for the spent fuel and the peak value for PEEQ (plastic equivalent strain) is situated at small regions at the corner for the spent fuel container.

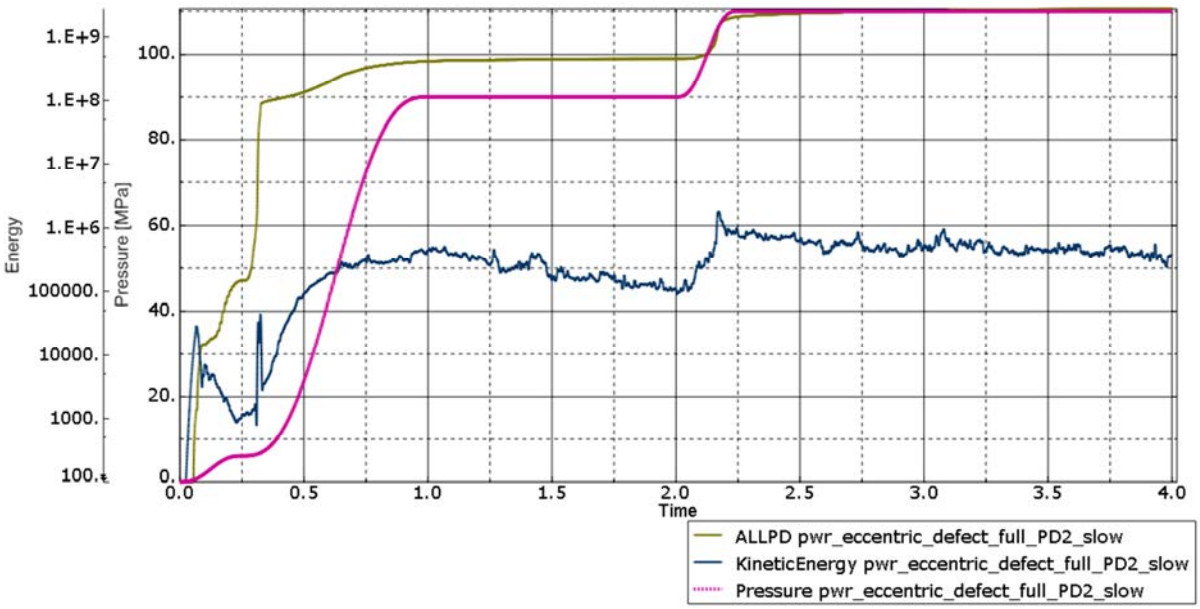

***Figure 12-5**. Energy for case bwr_eccentric_defect_PD2 slow loading.*

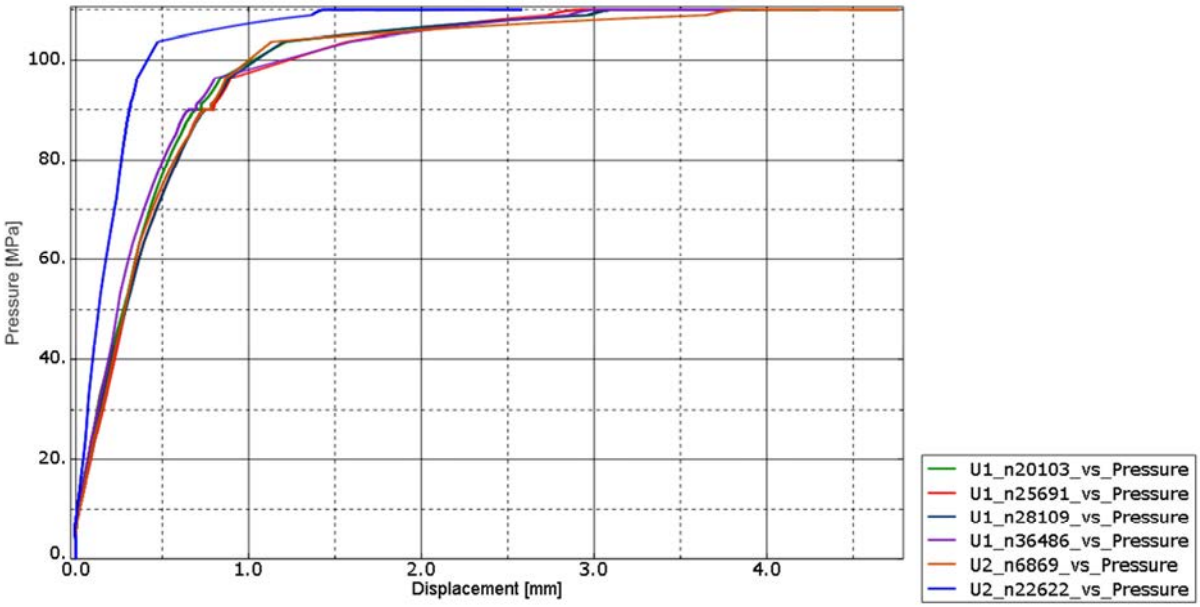

***Figure 12-6**. Displacement versus pressure for case pwr_eccentric_defect_PD2 slow loading.*

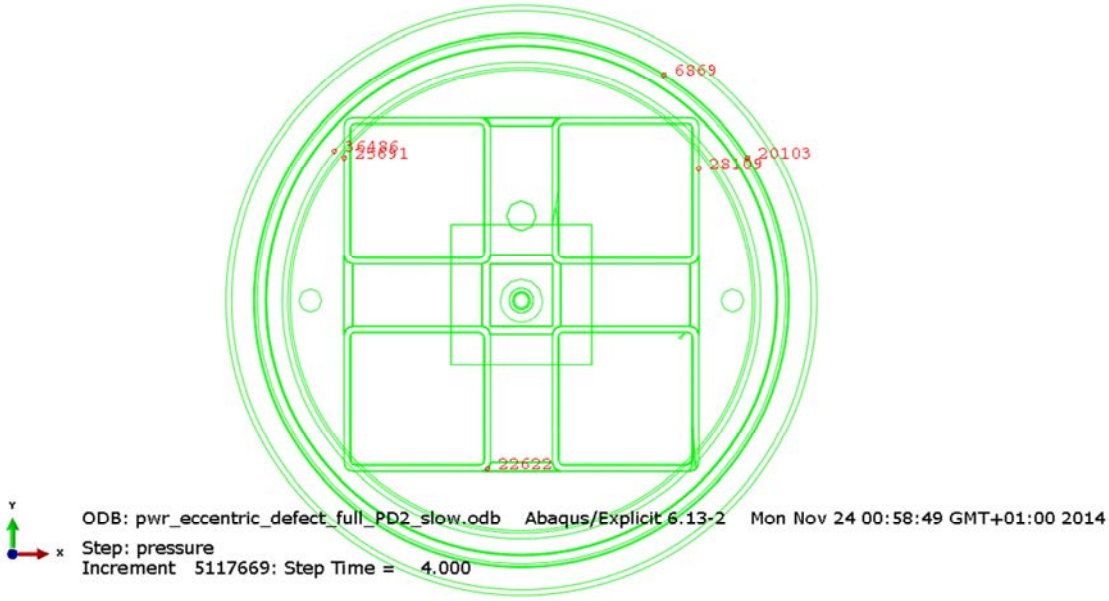

***Figure 12-7**. Selected nodes for case bwr_eccentric_defect_PD2 slow loading.*

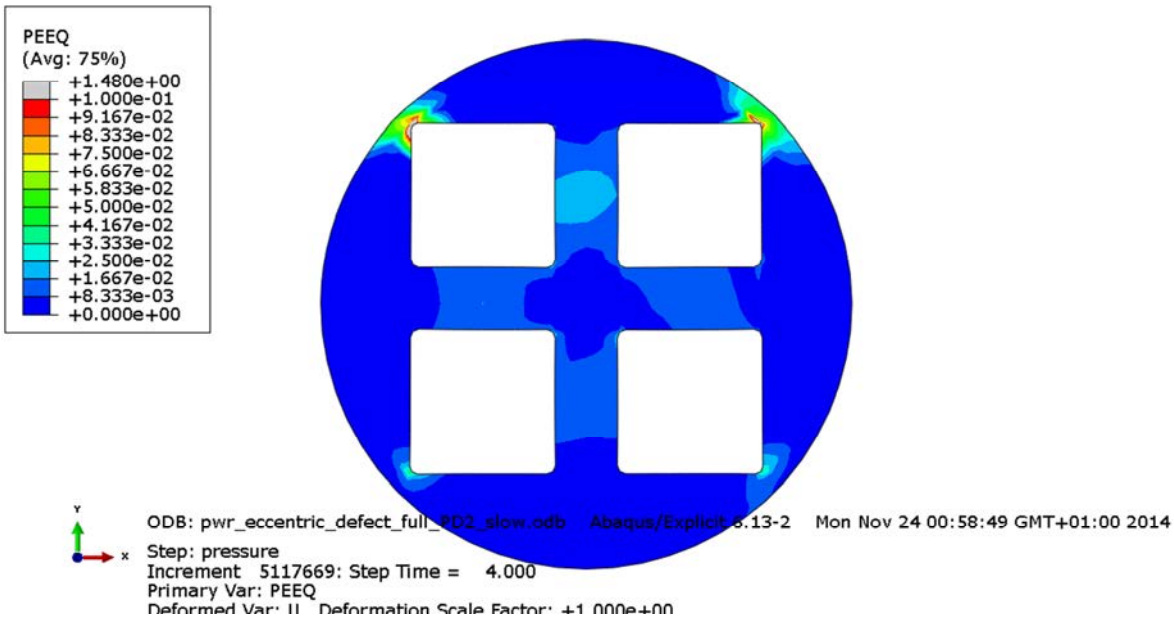

***Figure 12-8**. Plastic equivalent strain (PEEQ) in the insert at the end for case bwr_eccentric_defect_PD2 slow loading.*

13 Uncertainties

The obtained results are based on several assumptions regarding loads and material properties. Also the discretization in the computer model will affect the results. Below, the most important influencing factors are listed:

- All experimental results used for the material calibration have a spread which will imply a range in the values for the properties defining each material model.

- Material properties for nodular cast iron depend on hydrostatic pressure but in this study the material definitions are based on Mises plasticity theory using tensile properties and is taken from Dillström et al. (2010).

- The material properties are not valid for the extreme strain levels at very large deformations obtained when the hydrostatic load is much above the design load. However, this study should be compared with Dillström et al. (2010) and thus the same material definitions have been used for both studies.

- The element mesh is rather fine but nevertheless, too coarse in some regions, especially at the welds and regions with geometric discontinuities. A more refined mesh will probably increase the maximum stress and strain levels. Fortunately, the use of non-linear material properties (such as plasticity) will decrease the sensitivity to the used mesh. The used mesh has been judged to be accurate enough for evaluation of the expected stress and strain magnitudes. If more detailed results are required one possibility is to create sub-models with boundary conditions from the reported global analyzes.

- A better CAD-model defining the geometry should make it possible to improve the mesh quality implying smoother results and allows less mass scaling.

14 Evaluation and conclusions

The results obtained from the hydrostatic pressure analyses could be summarized as follows.

- General findings
    - The first instability occurs at about the same load magnitude when comparing the nominal geometry with the results obtained by Dillström et al. (2010).
    - A stable configuration is achieved for any load until the canister is cut off by the insert lid. However, the stable configuration at extremely high hydrostatic pressure is not useful due to almost completely compressed channel tubes.
    - The PWR insert shows higher acceptable load magnitudes and much less deformations also at an extremely high load magnitude.
    - For all cases the copper shell reach the yield surface already at a low load magnitude (less than 10 MPa) but after reaching complete contact with the insert, the plastic energy is almost constant until the canister gets visible deformations.
    - Plastic energy for the insert and channel tubes follows the applied load magnitude except at instabilities. It could also be noticed that when the configuration is stable the plastic energy doesn't change when the load is kept at a constant magnitude.
    - The last part reaching plasticity is the support plates, about 60-75 MPa for BWR insert and about 30 MPa for PWR insert. The low load magnitude for PWR insert is explained by bad element geometry, see Figure 14-1 (for load magnitude 100 MPa still a very small region has any plastic strains).

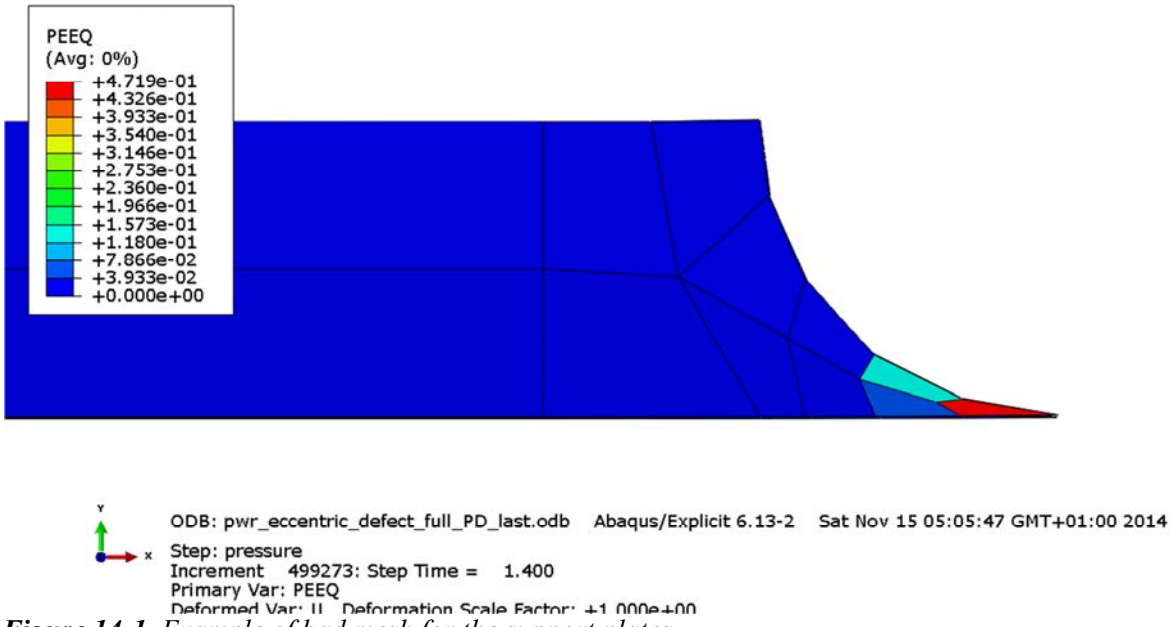

Figure 14-1. *Example of bad mesh for the support plates.*

- Effect of manufacturing tolerances
    - Considering tolerances when creating the model increases stresses/strains in regions where the wall thickness have been reduced but the first instability level is almost

unaffected for the BWR insert but for the PWR insert this has a much more pronounced effect.

- Effect of including defects
    - Including the assumed defect into the insert (cylindric shape) has a non-significant influence on the first instability level both for the BWR and the PWR insert.
- Effect on reducing the yield surface
    - Scaling down the yield surface influences as expected the instability level. The decrease of the first instability level is about 13% which is close to the reduction of the yield surface for the insert.
- Safety factors
    - Inserts having a defect and at the same time a reduced yield surface show the lowest value for the first instability.
        - With a design load of 45 MPa the safety factor is 1.9 for the BWR model using the first instability at 86 MPa. However, the safety factor is increased to about 2.1 if the stable post buckling deformation is acceptable as storage space.
        - Increasing the design load to 50 MPa implies a safety factor for the BWR model between 1.72 to1.85 using the same values for the instability load.
        - The PWR model with 45 MPa as design load has a safety factor of at least 2.4 and has enough storage space also at 120 MPa corresponding to a safety factor 2.7.
        - Increasing the design load to 50 MPa implies a safety factor for the PWR model between 2.0 – 2.4 using the same values for the instability load.

References

ABAQUS, 2013. Version 6.12.1. Dassault Systèmes Simulia Corp.

ASME, 1995. ASME boiler and pressure vessel code. New York: American Society of Mechanical Engineers

Dillström P, Alverlind L, Andersson M, 2010. Framtagning av acceptanskriterier samt skadetålighetsanalyser av segjärnsinsatsen. SKB R-10-11, Svensk Kärnbränslehantering AB.

Hernelind J, 2010. Modelling and analysis of canister and buffer for earthquake induced rock shear and glacial load. SKB TR-10-34, Svensk Kärnbränslehantering AB.

Raiko H, Sandström R, Rydén H, Johansson M, 2010. Design analysis report for the canister. SKB TR-10-28, Svensk Kärnbränslehantering AB.

SKB, 2010. Design, production and initial state of the canister. SKB TR-10-14, Svensk Kärnbränslehantering AB.

SSABDirekt, 2008. Steelfacts Domex 355 MC. Available at http://www.ssabdirect.com. [19 September 2008].

SS-EN 10025-2:2004. Varmvalsade konstruktionsstål – Del 2: Tekniska leveransbestämmelser för olegerade stål (Hot rolled products of structural steels - Part 2: Technical delivery conditions for non-alloy structural steels). Stockholm: Swedish Standards Institute.

Unpublished documents

SKBdoc id, version	Title	Issuer, year
1203875 ver 2.0	Ritningsförteckning för kapselkomponenter. (In Swedish.)	SKB, 2014

Appendix 1 – Plots for bwr_centric_rotated_PD

Plots showing deformed geometry as contour plots for all parts of the BWR model at pressure magnitude 50, 90 and 120 MPa for case bwr_centric_rotated_PD (geometry based on nominal dimensions and centrically positioned channel tubes).

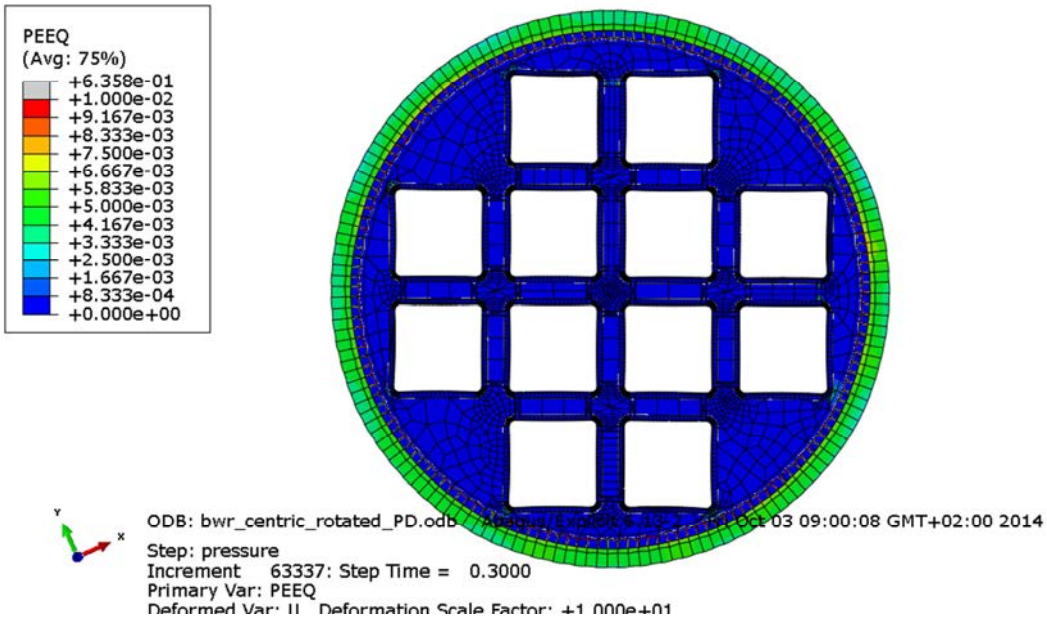

Figure A1-1 *Equivalent plastic strain (PEEQ) with 60 MPa as applied hydrostatic pressure.*

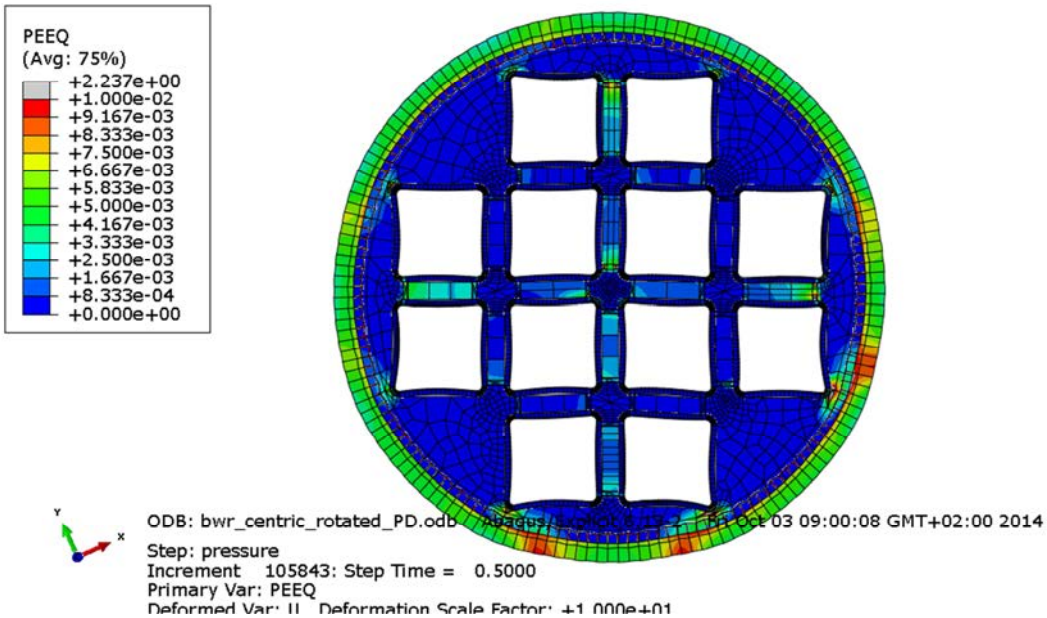

Figure A1-2 *Equivalent plastic strain (PEEQ) with 90 MPa as applied hydrostatic pressure.*

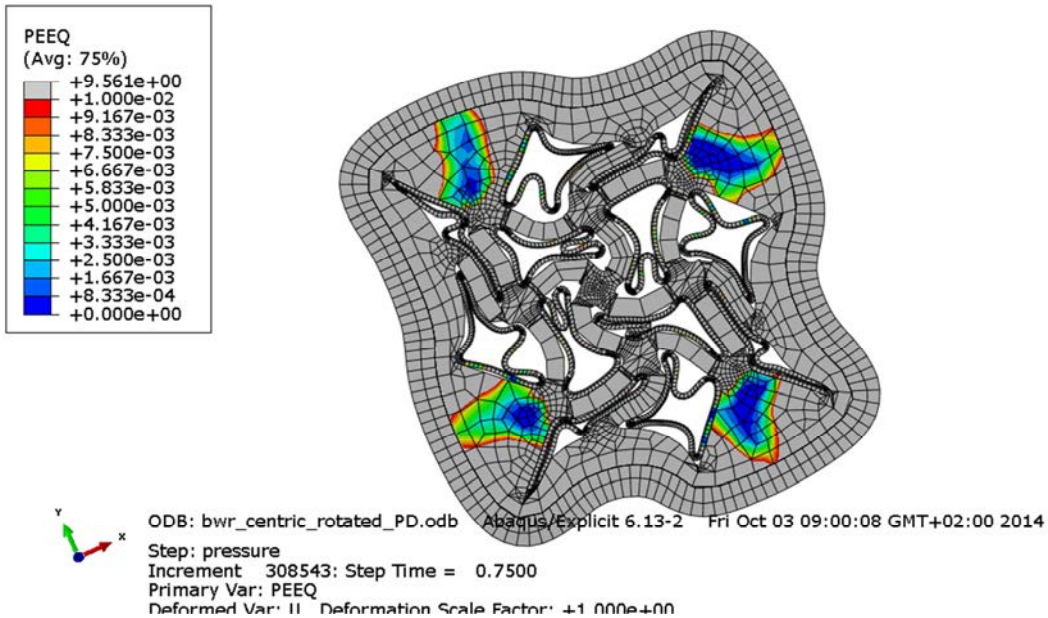

Figure A1-3 *Equivalent plastic strain (PEEQ) with 120 MPa as applied hydrostatic pressure.*

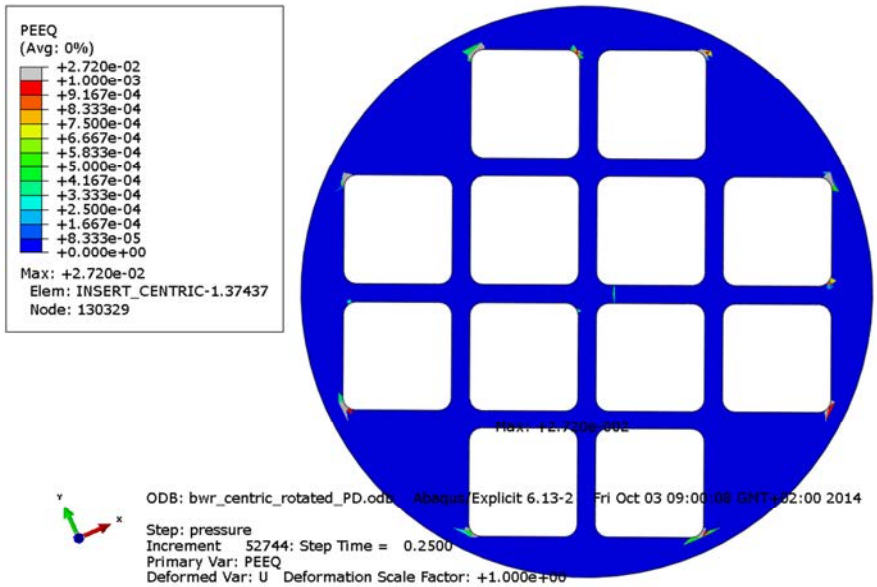

Figure A1-4 *Equivalent plastic strain (PEEQ) for the insert with 60 MPa as applied hydrostatic pressure.*

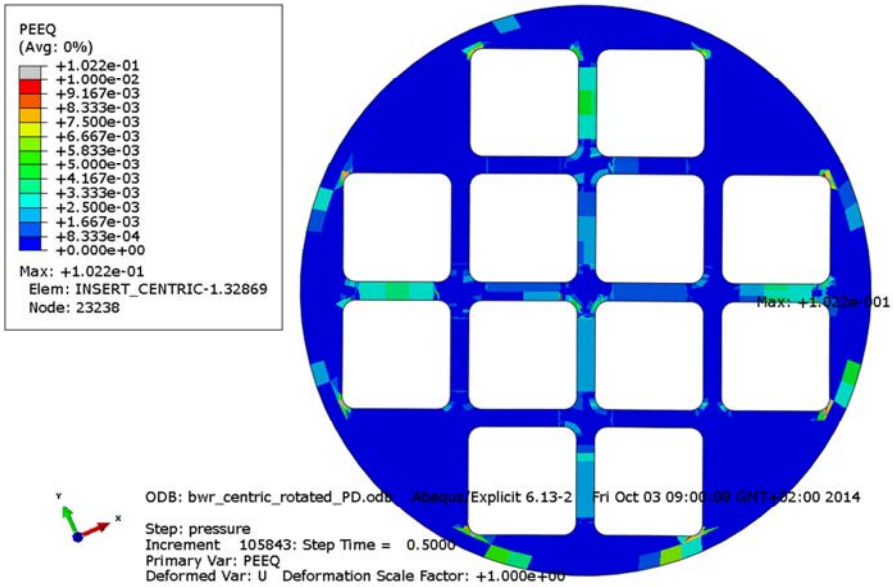

Figure A1-5 *Equivalent plastic strain (PEEQ) for the insert with 90 MPa as applied hydrostatic pressure.*

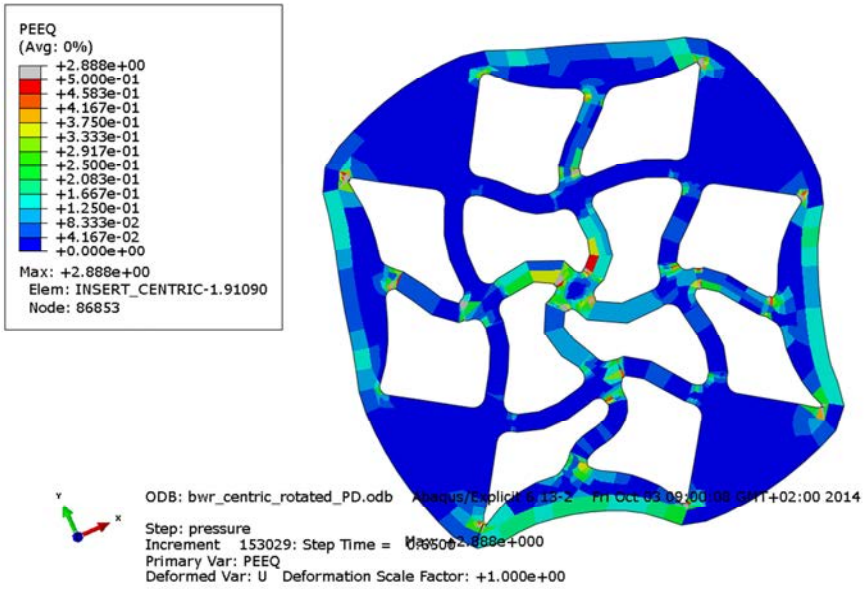

Figure A1-6 *Equivalent plastic strain (PEEQ) for the insert with 120 MPa as applied hydrostatic pressure.*

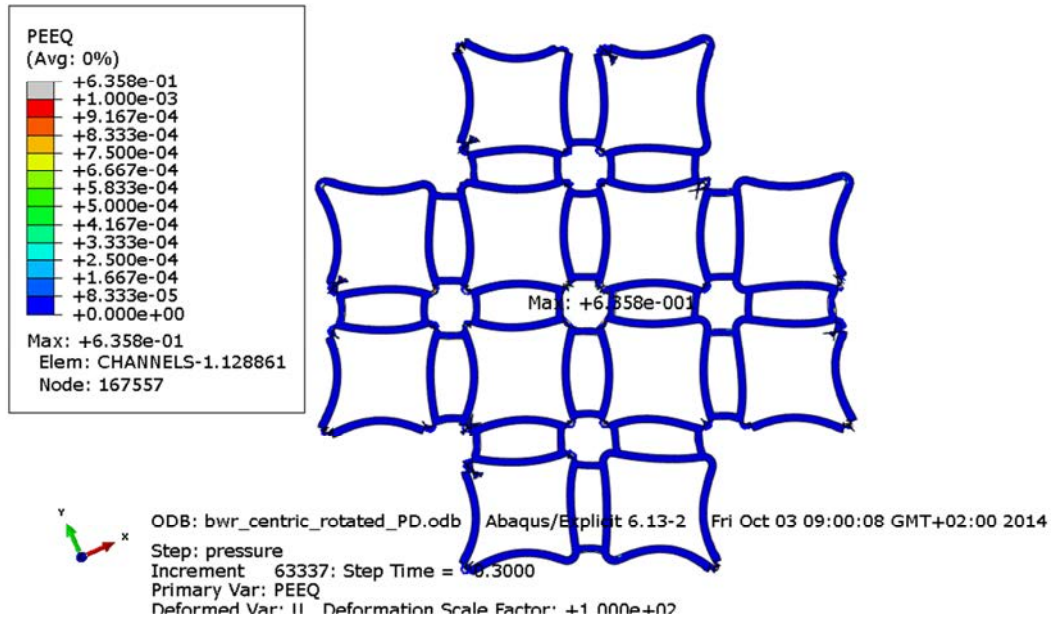

Figure A1-7 *Equivalent plastic strain (PEEQ) for the channel tubes with 60 MPa as applied hydrostatic pressure. Displacements scaled by factor 100.*

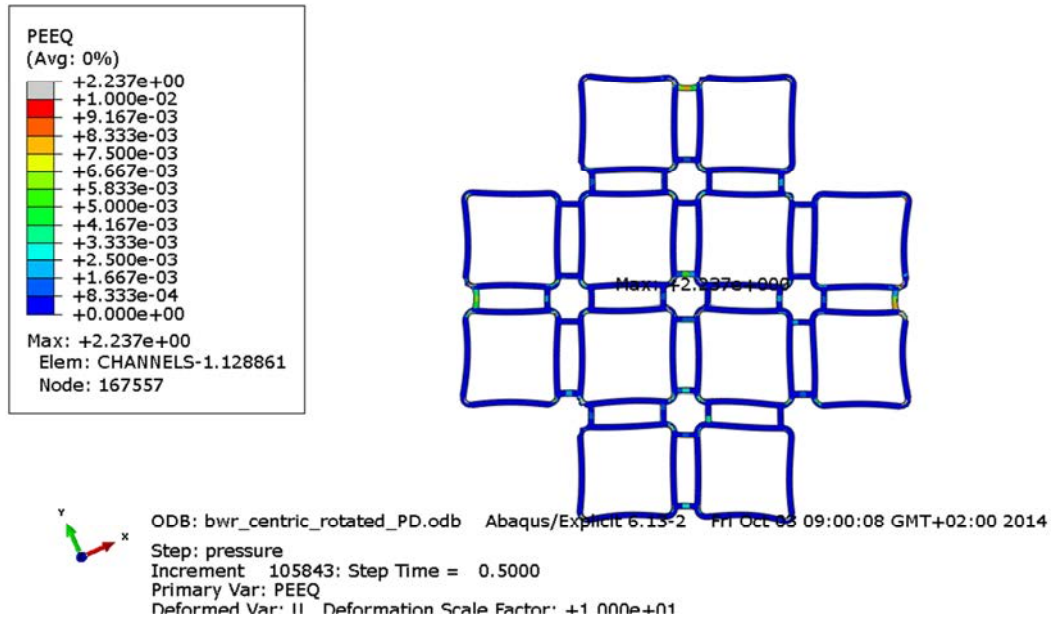

Figure A1-8 *Equivalent plastic strain (PEEQ) for the channel tubes with 90 MPa as applied hydrostatic pressure.*

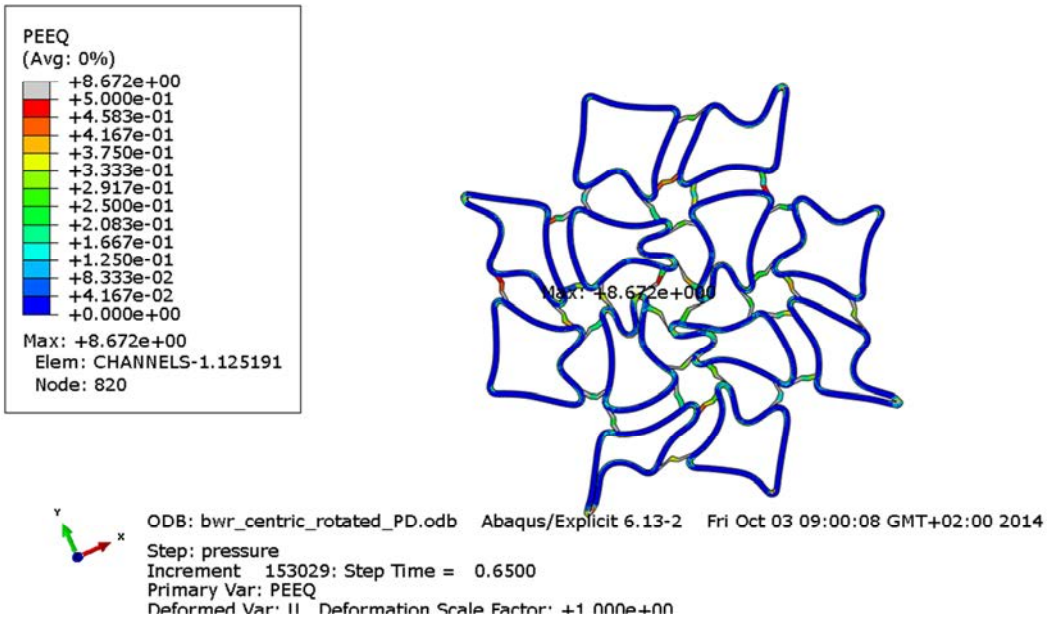

Figure A1-9 *Equivalent plastic strain (PEEQ) for the channel tubes with 120 MPa as applied hydrostatic pressure.*

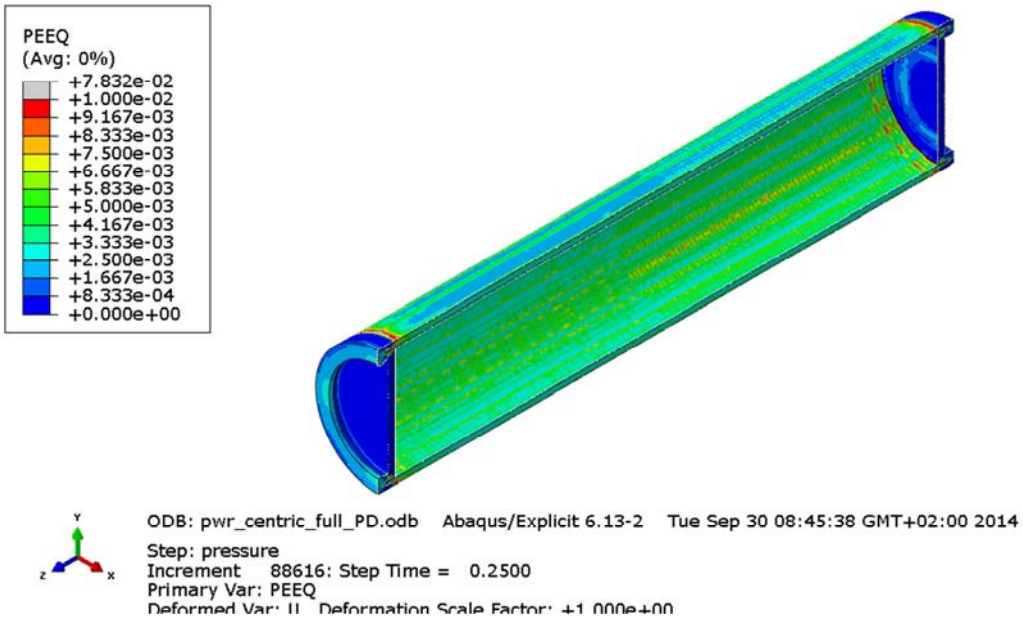

Figure A1-10 *Equivalent plastic strain (PEEQ) for the copper shell with 60 MPa as applied hydrostatic pressure.*

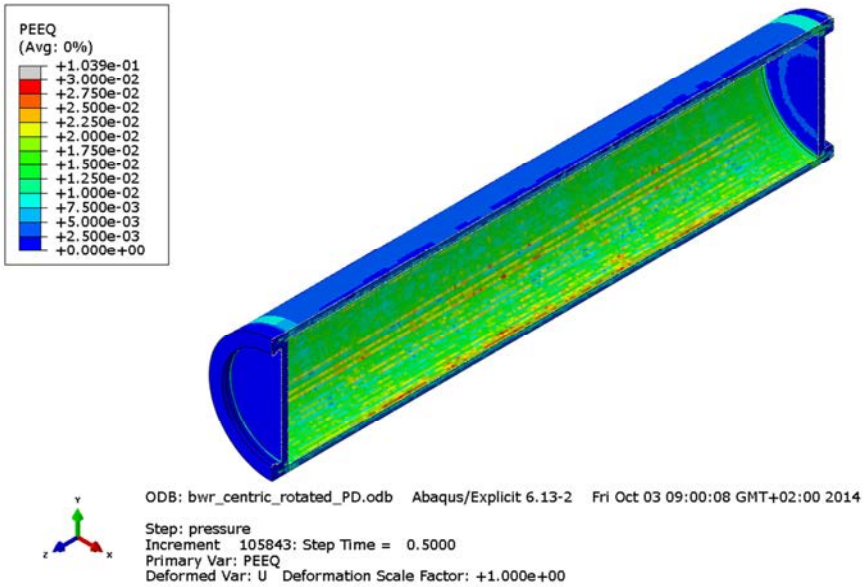

Figure A1-11 *Equivalent plastic strain (PEEQ) for the copper shell with 90 MPa as applied hydrostatic pressure.*

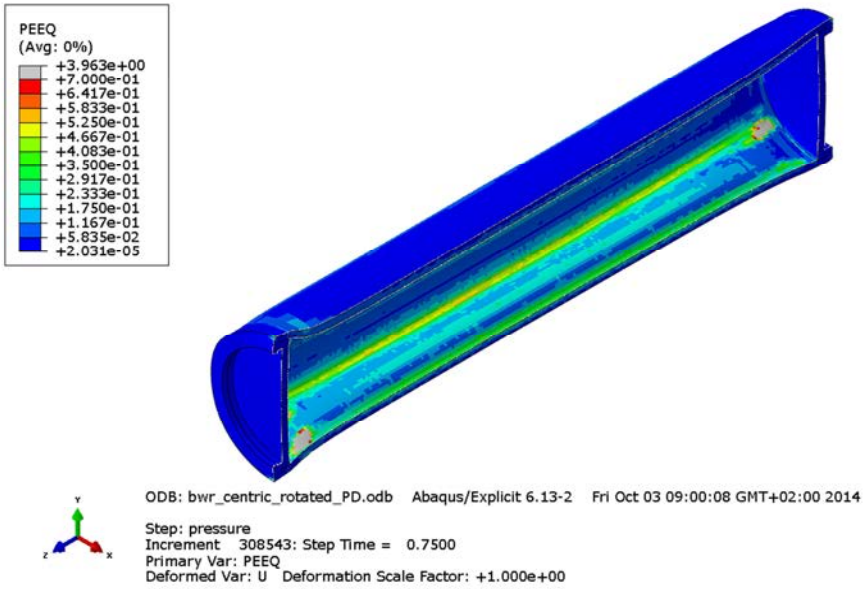

Figure A1-12 *Equivalent plastic strain (PEEQ) for the copper shell with 120 MPa as applied hydrostatic pressure.*

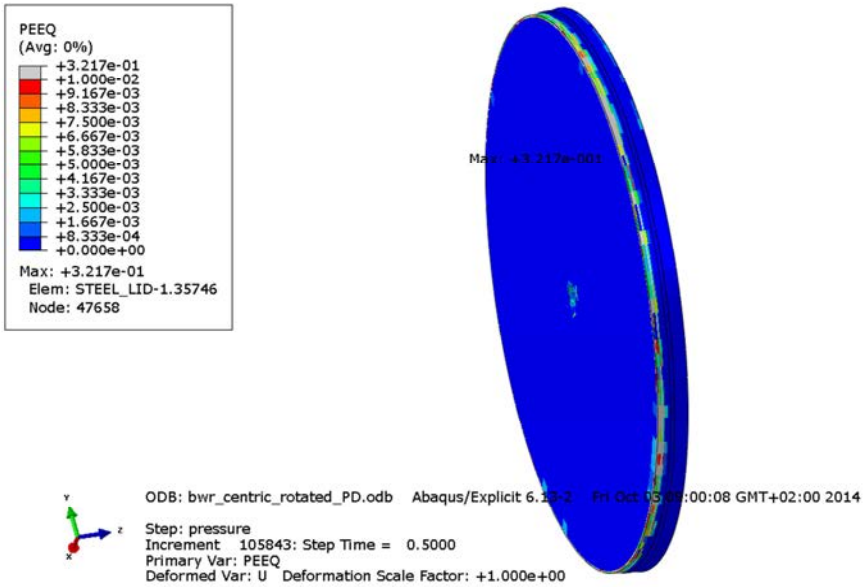

Figure A1-13 *Equivalent plastic strain (PEEQ) for the insert lid with 90 MPa as applied hydrostatic pressure.*

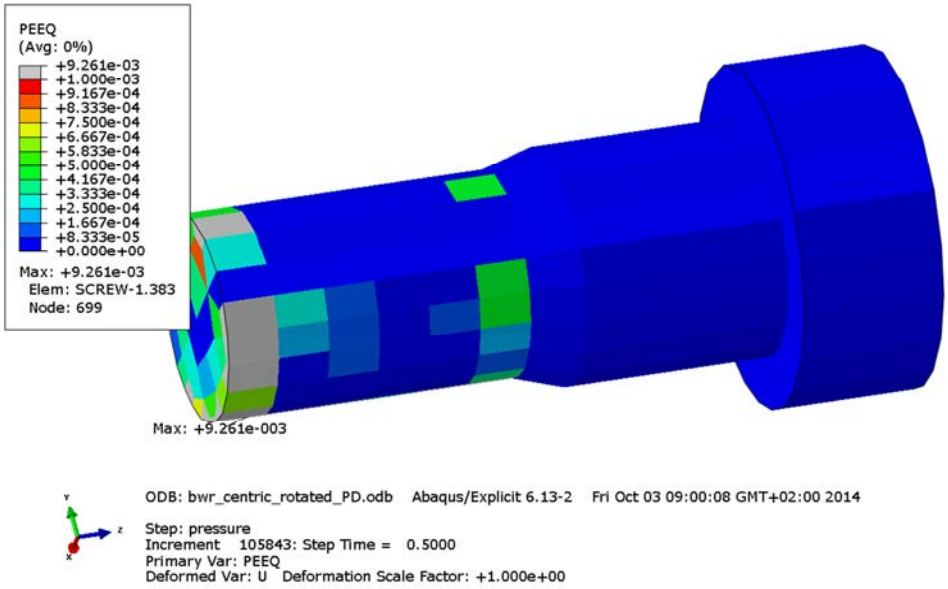

Figure A1-14 *Equivalent plastic strain (PEEQ) for the fixing screw with 90 MPa as applied hydrostatic pressure.*

Appendix 2 – Plots for bwr_excentric_rotated_PD

Plots showing deformed geometry as contour plots for all parts of the BWR model at pressure magnitude 50, 90 and 120 MPa for case bwr_excentric_rotated_PD (geometry based on manufacturing tolerances and eccentrically positioned channel tubes, 10 mm).

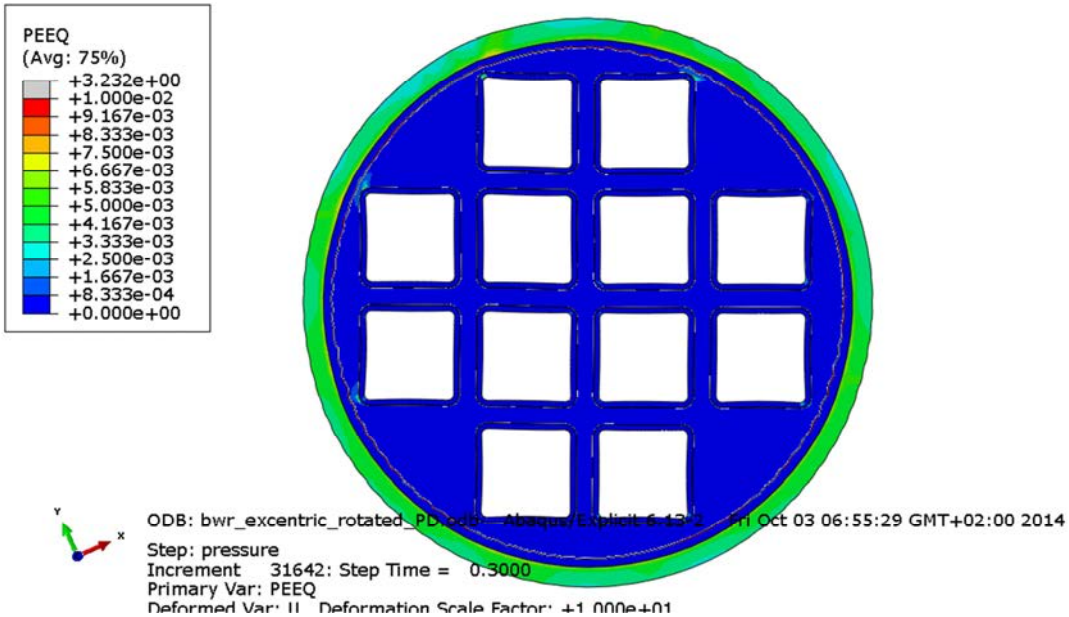

Figure A2-1 *Equivalent plastic strain (PEEQ) with 60 MPa as applied hydrostatic pressure. Deformations scaled by factor 10.*

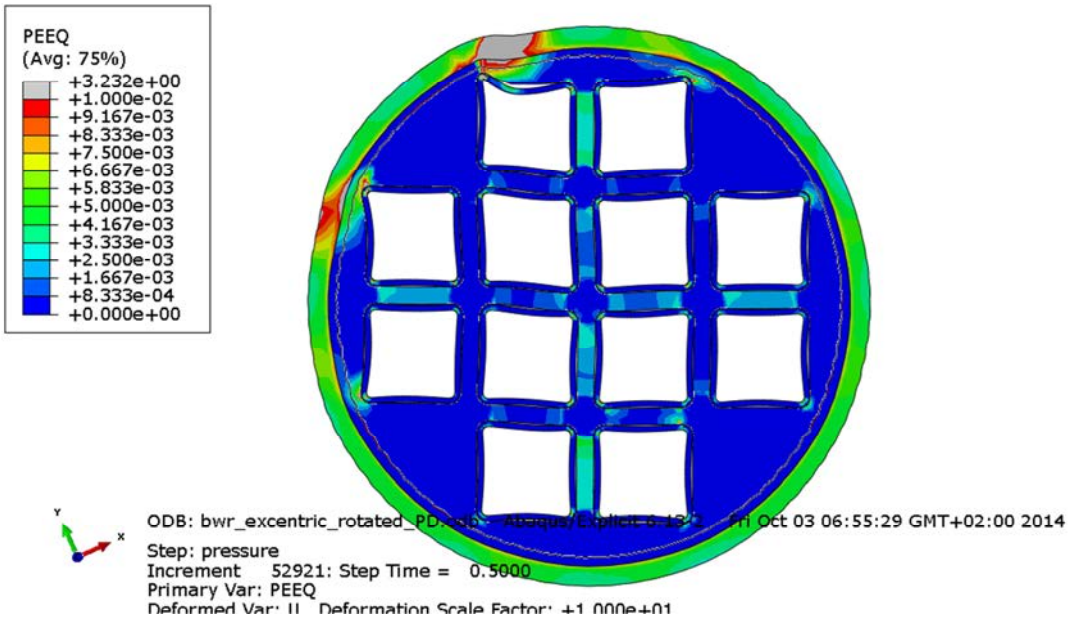

Figure A2-2 *Equivalent plastic strain (PEEQ) with 90 MPa as applied hydrostatic pressure. Deformations scaled by factor 10.*

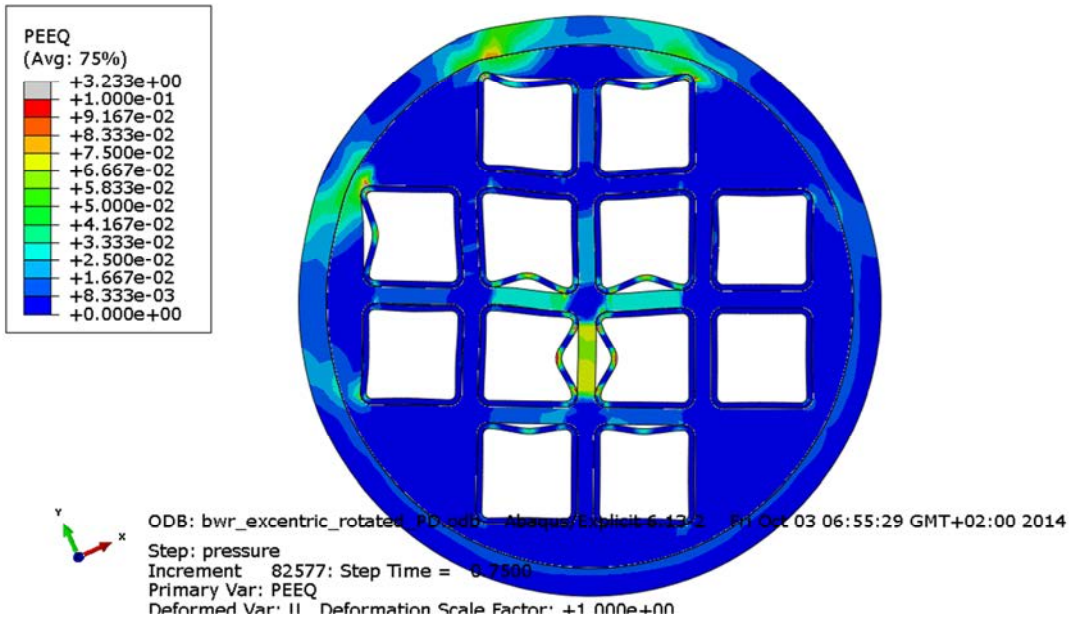

Figure A2-3 *Equivalent plastic strain (PEEQ) with 120 MPa as applied hydrostatic pressure.*

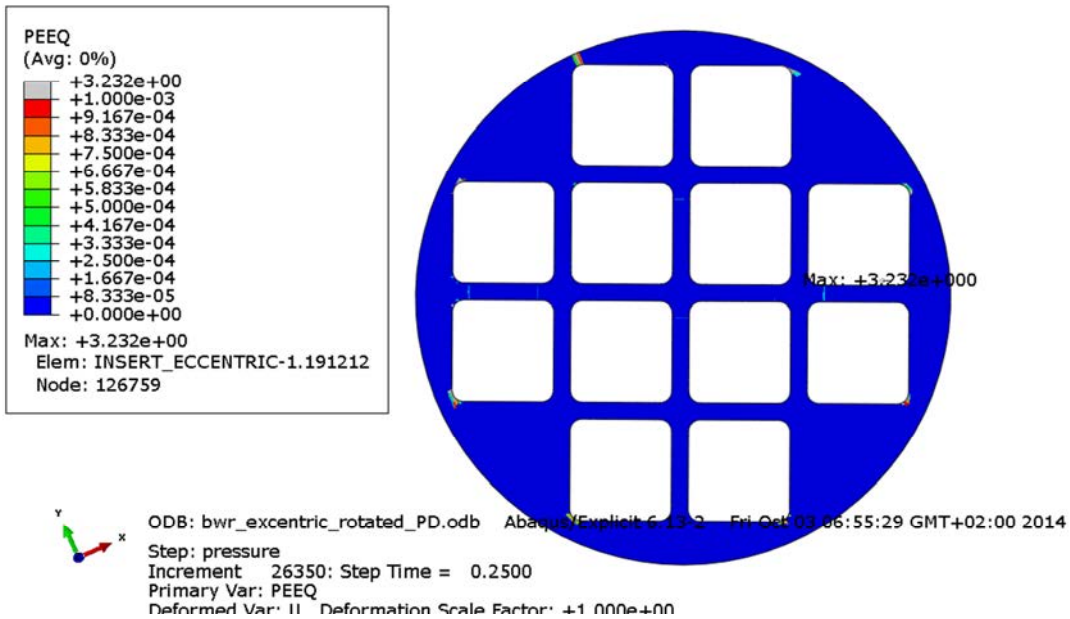

Figure A2-4 *Equivalent plastic strain (PEEQ) for the insert with 60 MPa as applied hydrostatic pressure.*

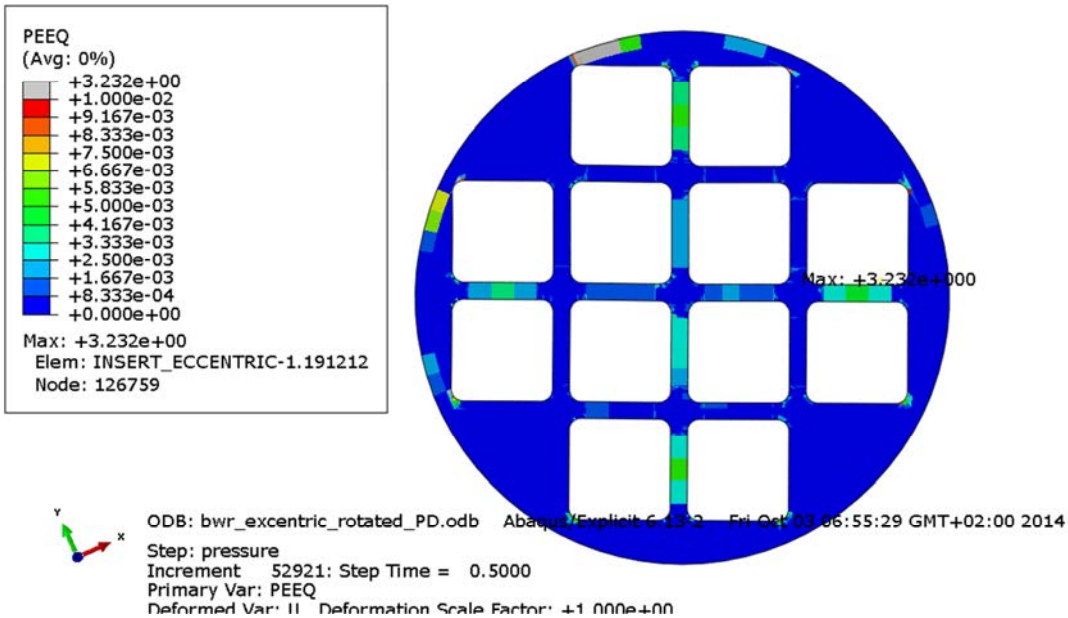

Figure A2-5 *Equivalent plastic strain (PEEQ) for the insert with 90 MPa as applied hydrostatic pressure.*

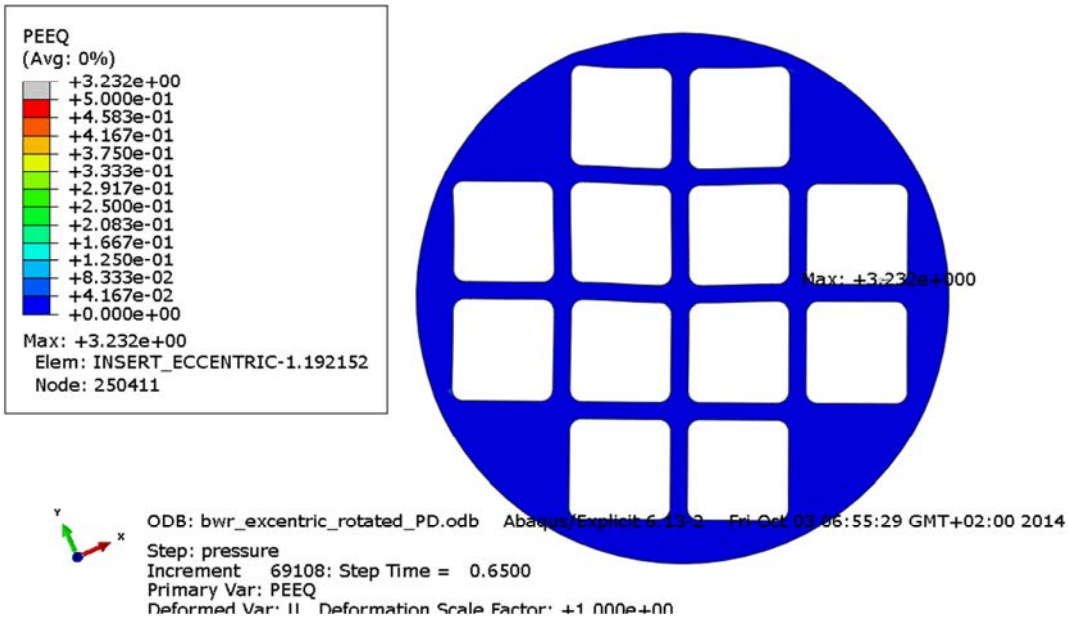

Figure A2-6 *Equivalent plastic strain (PEEQ) for the insert with 120 MPa as applied hydrostatic pressure.*

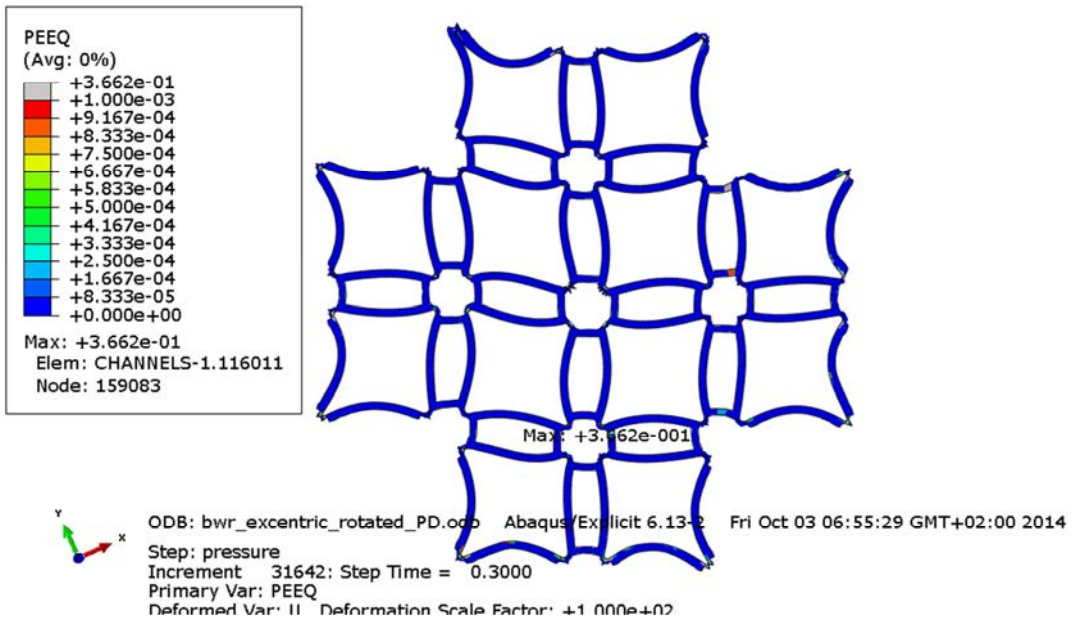

Figure A2-7 *Equivalent plastic strain (PEEQ) for the channel tubes with 60 MPa as applied hydrostatic pressure. Displacements scaled by factor 100.*

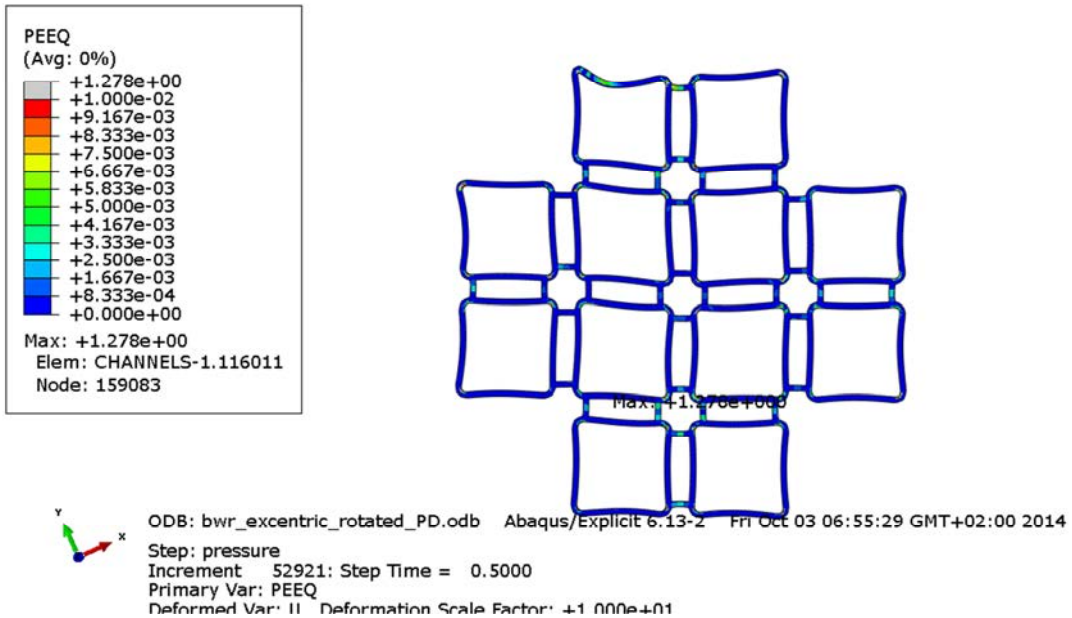

Figure A2-8 *Equivalent plastic strain (PEEQ) for the channel tubes with 90 MPa as applied hydrostatic pressure. Displacements scaled by factor 10.*

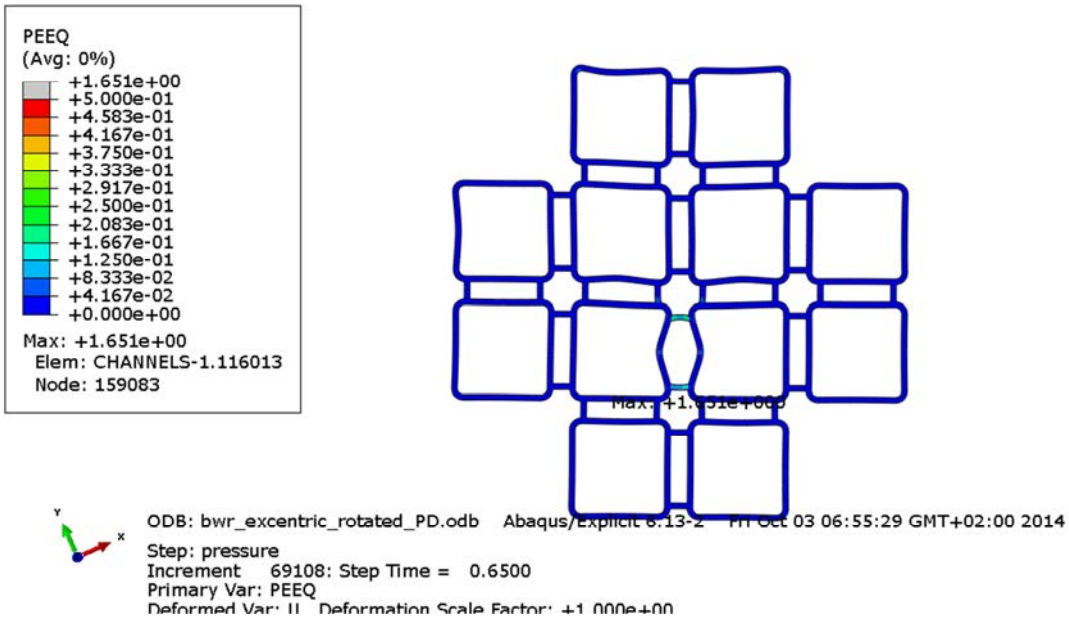

Figure A2-9 *Equivalent plastic strain (PEEQ) for the channel tubes with 120 MPa as applied hydrostatic pressure.*

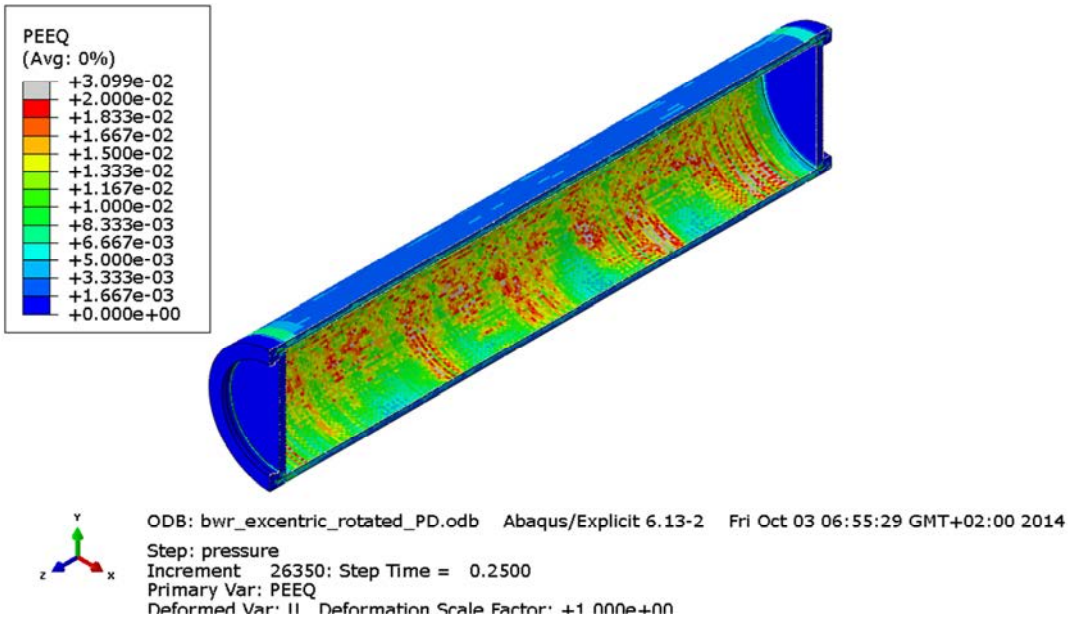

Figure A2-10 *Equivalent plastic strain (PEEQ) for the copper shell with 60 MPa as applied hydrostatic pressure.*

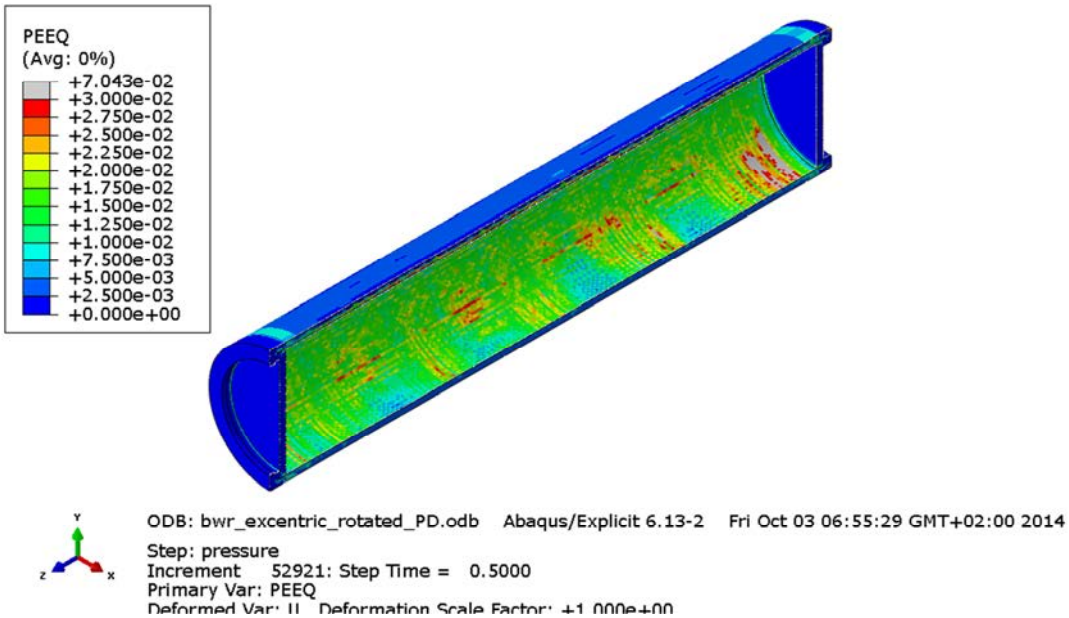

Figure A2-11 *Equivalent plastic strain (PEEQ) for the copper shell with 90 MPa as applied hydrostatic pressure.*

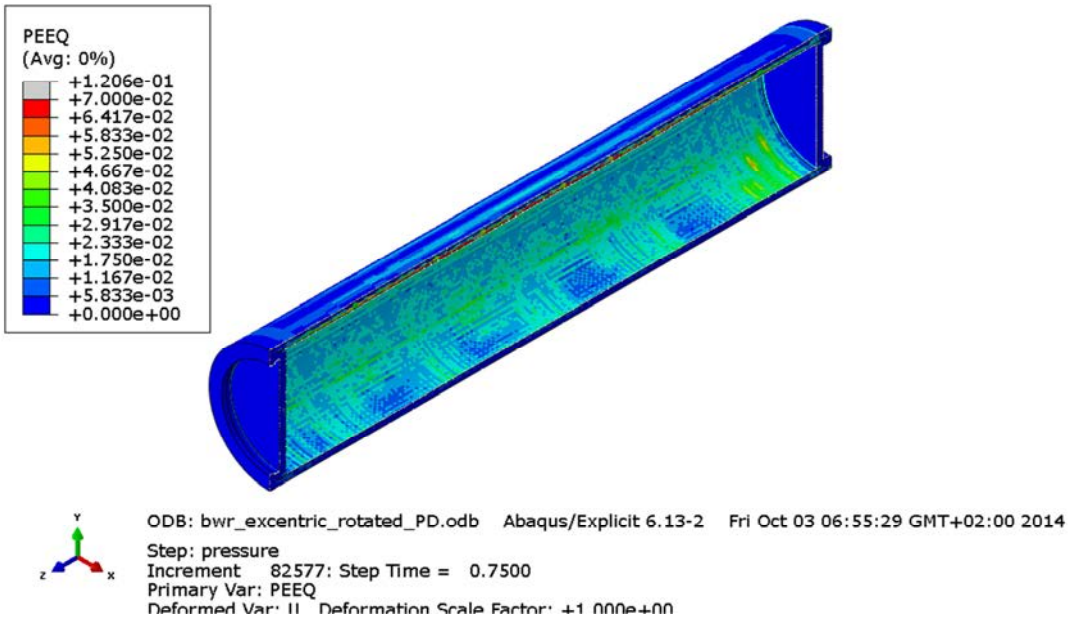

Figure A2-12 *Equivalent plastic strain (PEEQ) for the copper shell with 120 MPa as applied hydrostatic pressure.*

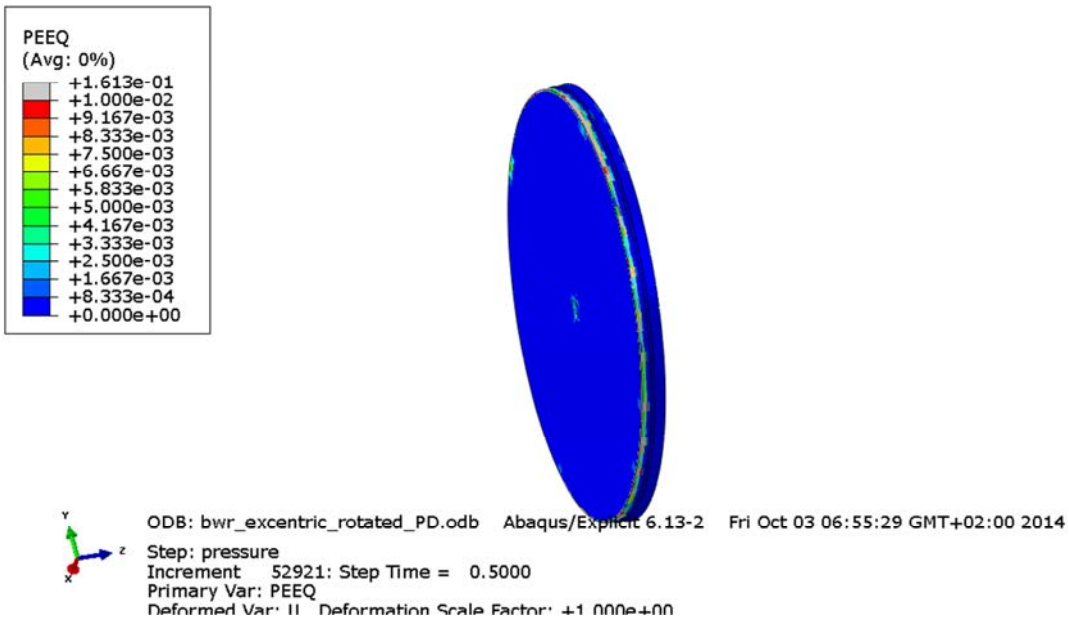

Figure A2-13 *Equivalent plastic strain (PEEQ) for the insert lid with 90 MPa as applied hydrostatic pressure.*

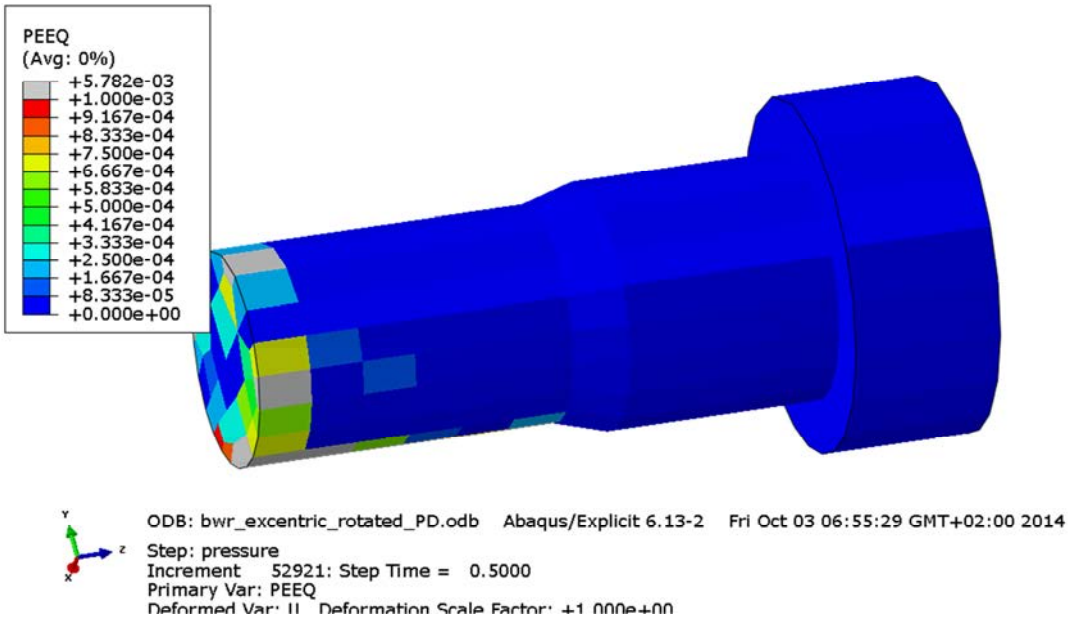

Figure A2-14 *Equivalent plastic strain (PEEQ) for the fixing screw with 90 MPa as applied hydrostatic pressure.*

Appendix 3 – Plots for bwr_eccentric_defect_PD

Plots showing deformed geometry as contour plots for all parts of the BWR model at pressure magnitude 50, 90 and 120 MPa for case bwr_eccentric_defect_PD (geometry based on manufacturing tolerances and eccentrically positioned channel tubes, 10 mm and a cylindrical defect assumed for the insert).

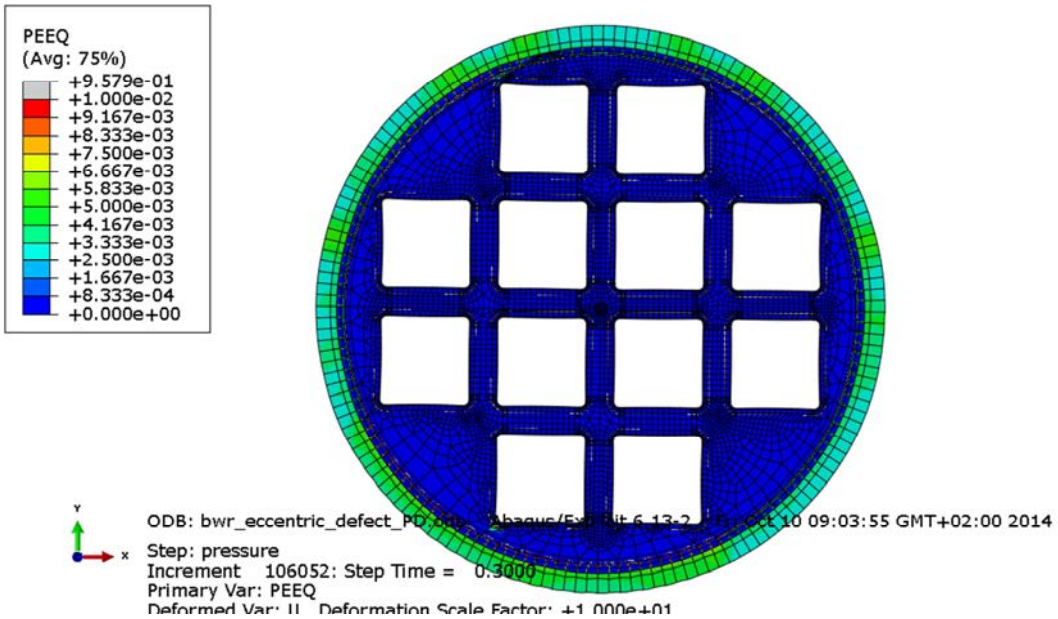

Figure A3-1 *Equivalent plastic strain (PEEQ) with 60 MPa as applied hydrostatic pressure. Displacements scaled by factor 10.*

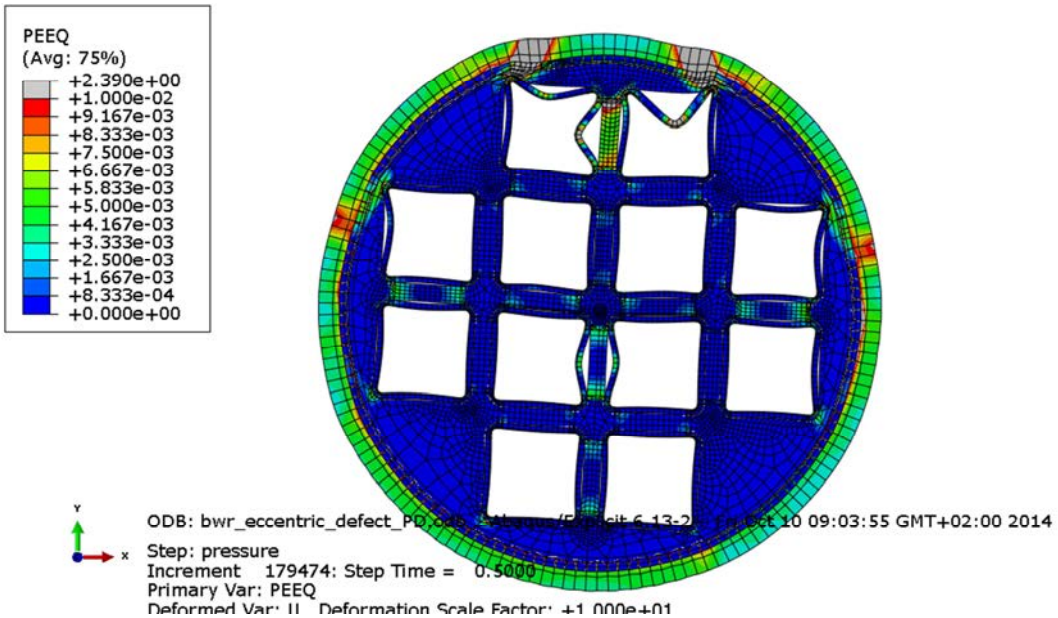

Figure A3-2 *Equivalent plastic strain (PEEQ) with 90 MPa as applied hydrostatic pressure. Displacement scaled by factor 10.*

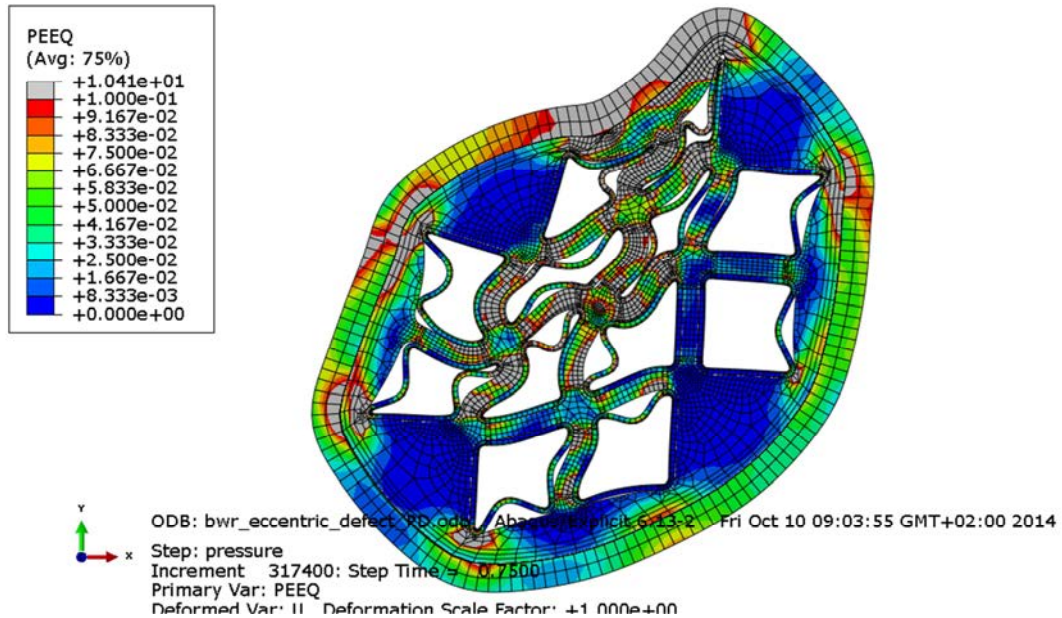

Figure A3-3 *Equivalent plastic strain (PEEQ) with 120 MPa as applied hydrostatic pressure.*

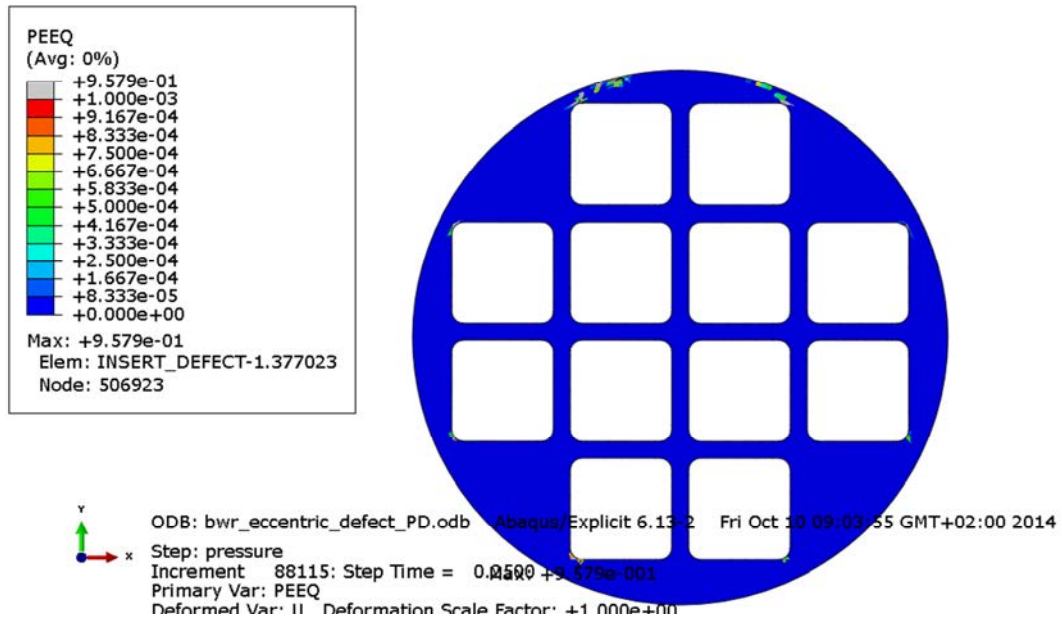

Figure A3-4 *Equivalent plastic strain (PEEQ) for the insert with 60 MPa as applied hydrostatic pressure.*

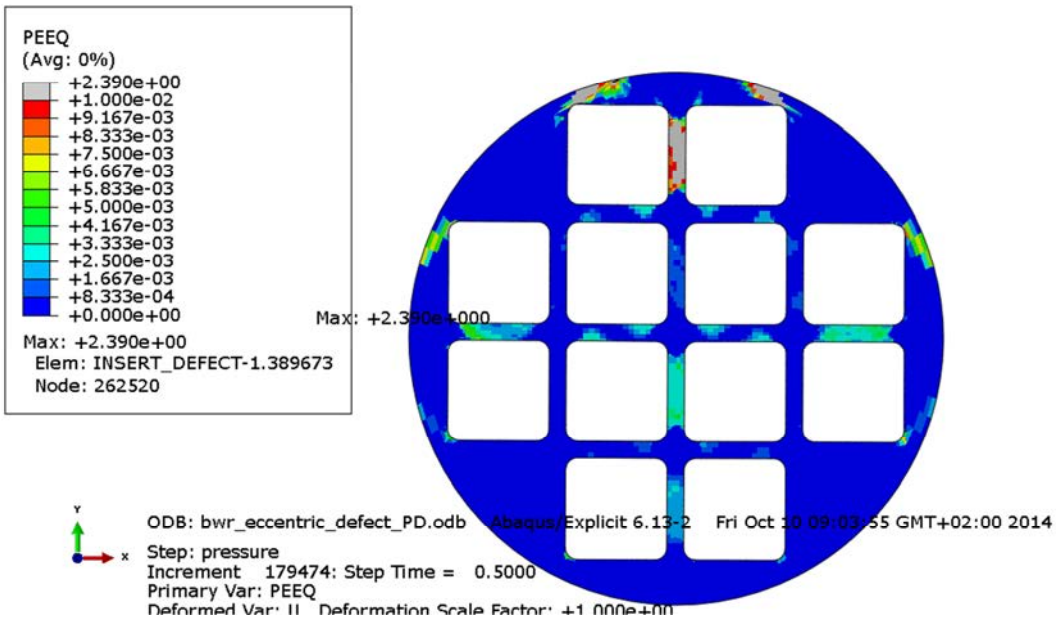

Figure A3-5 *Equivalent plastic strain (PEEQ) for the insert with 90 MPa as applied hydrostatic pressure.*

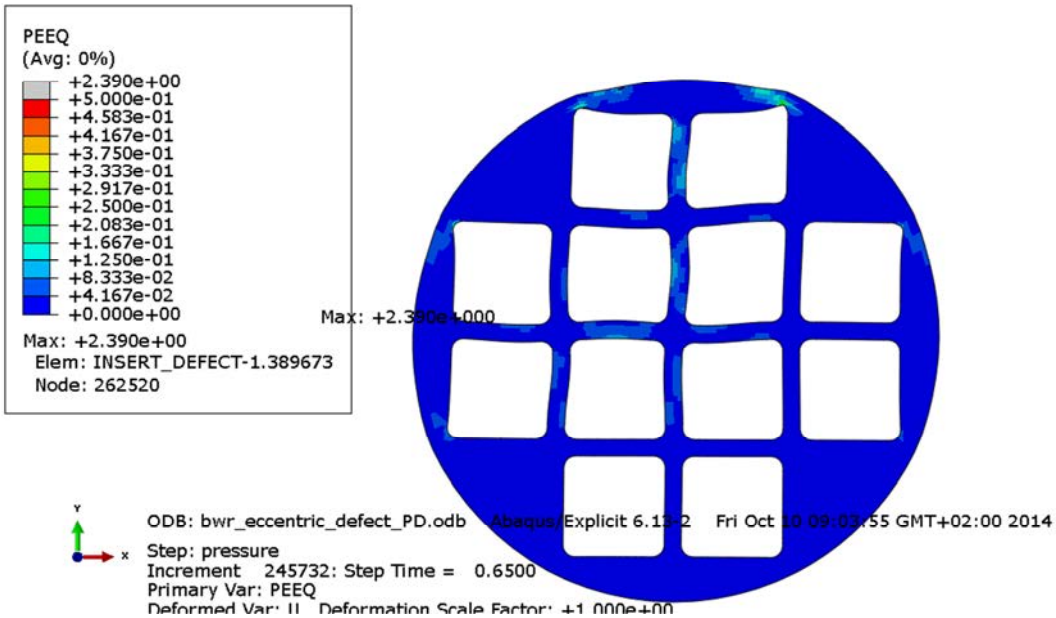

Figure A3-6 *Equivalent plastic strain (PEEQ) for the insert with 120 MPa as applied hydrostatic pressure.*

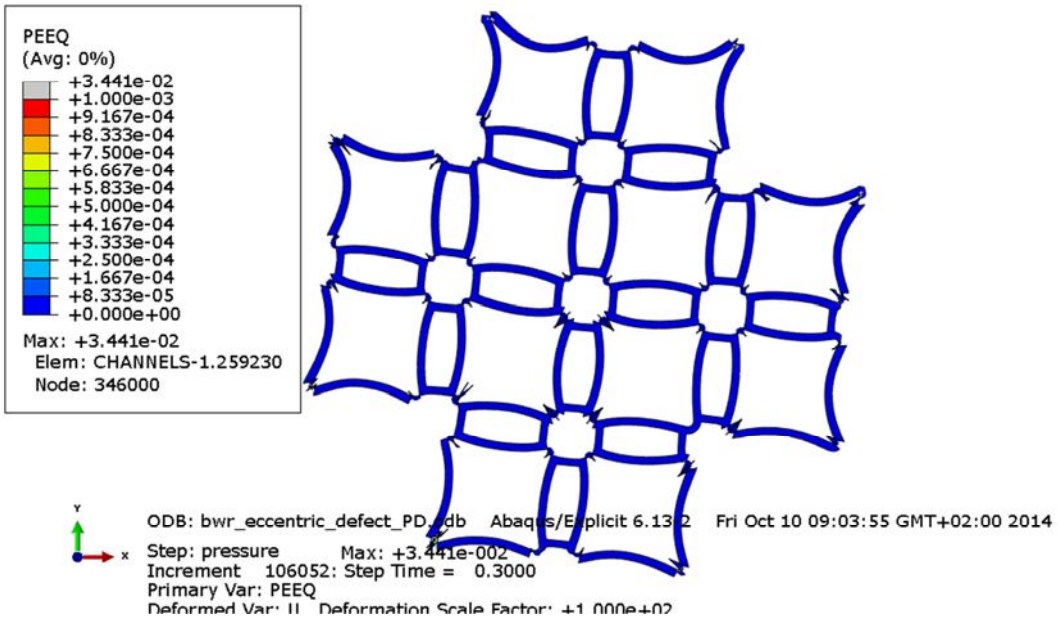

Figure A3-7 *Equivalent plastic strain (PEEQ) for the channel tubes with 60 MPa as applied hydrostatic pressure. Displacement scaled by factor 100.*

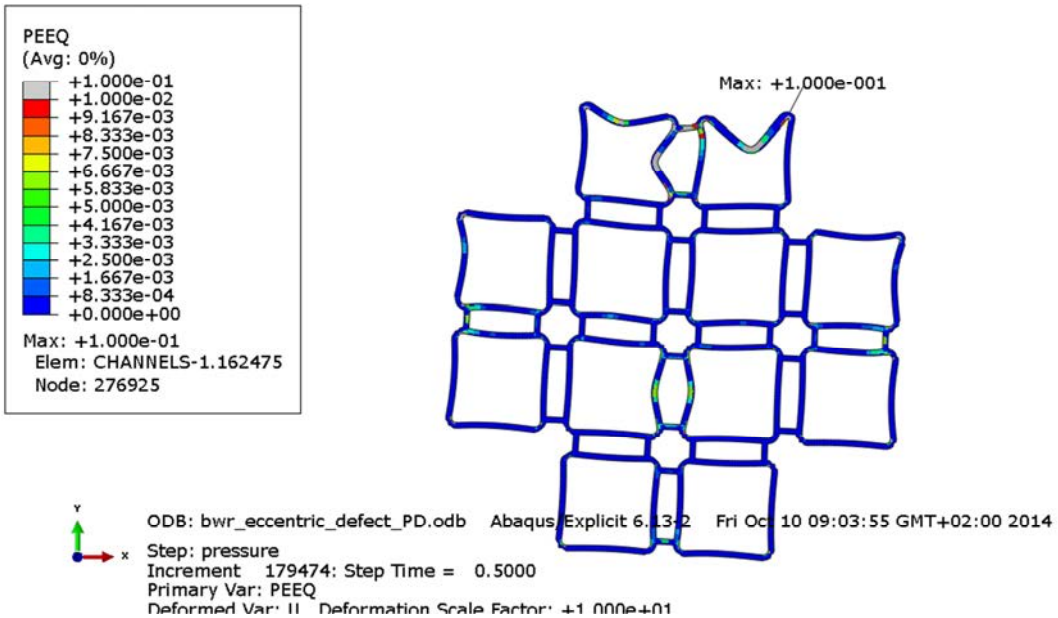

Figure A3-8 *Equivalent plastic strain (PEEQ) for the channel tubes with 90 MPa as applied hydrostatic pressure. Displacements scaled by factor 10.*

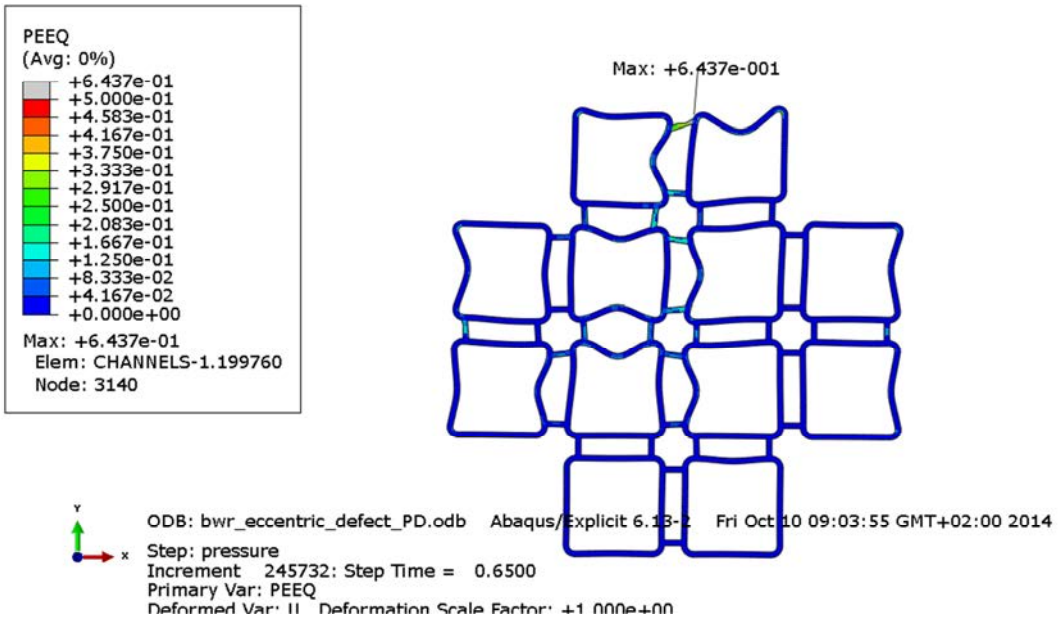

Figure A3-9 *Equivalent plastic strain (PEEQ) for the channel tubes with 120 MPa as applied hydrostatic pressure.*

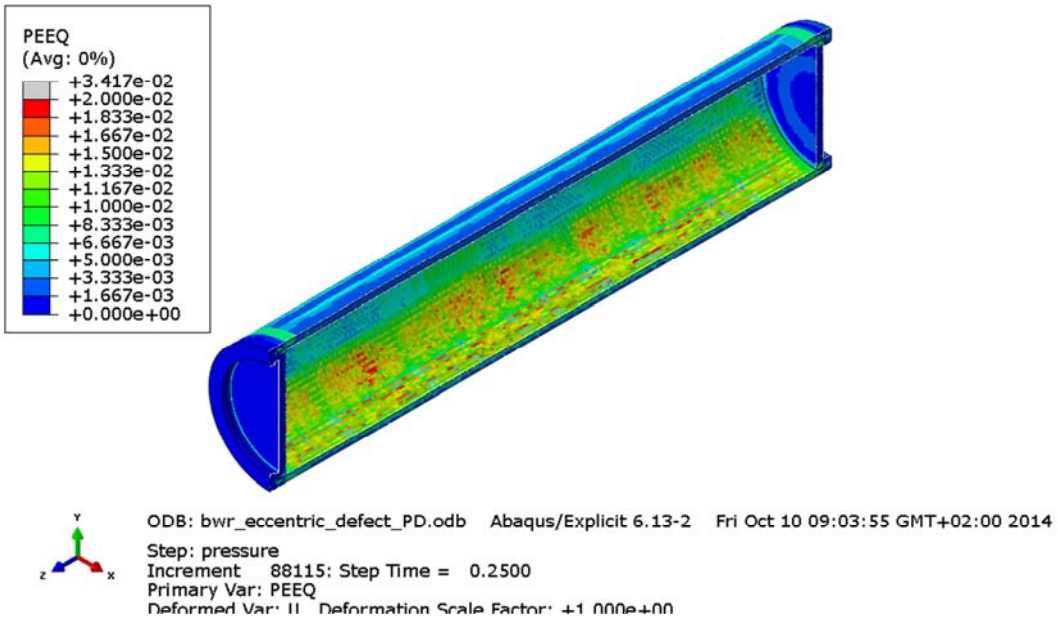

Figure A3-10 *Equivalent plastic strain (PEEQ) for the copper shell with 60 MPa as applied hydrostatic pressure.*

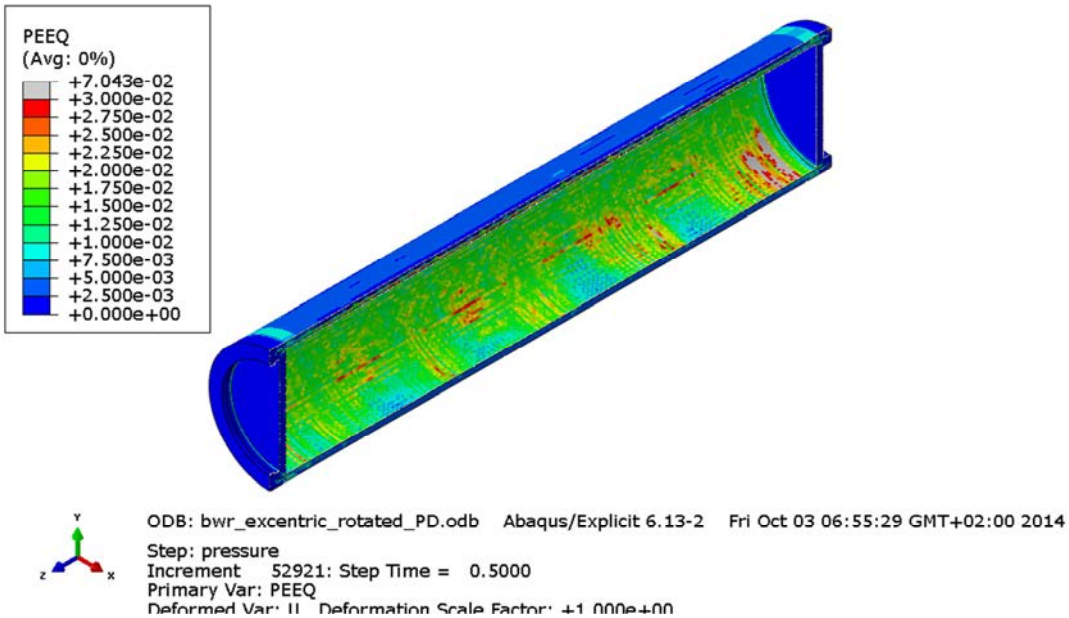

Figure A3-11 *Equivalent plastic strain (PEEQ) for the copper shell with 90 MPa as applied hydrostatic pressure.*

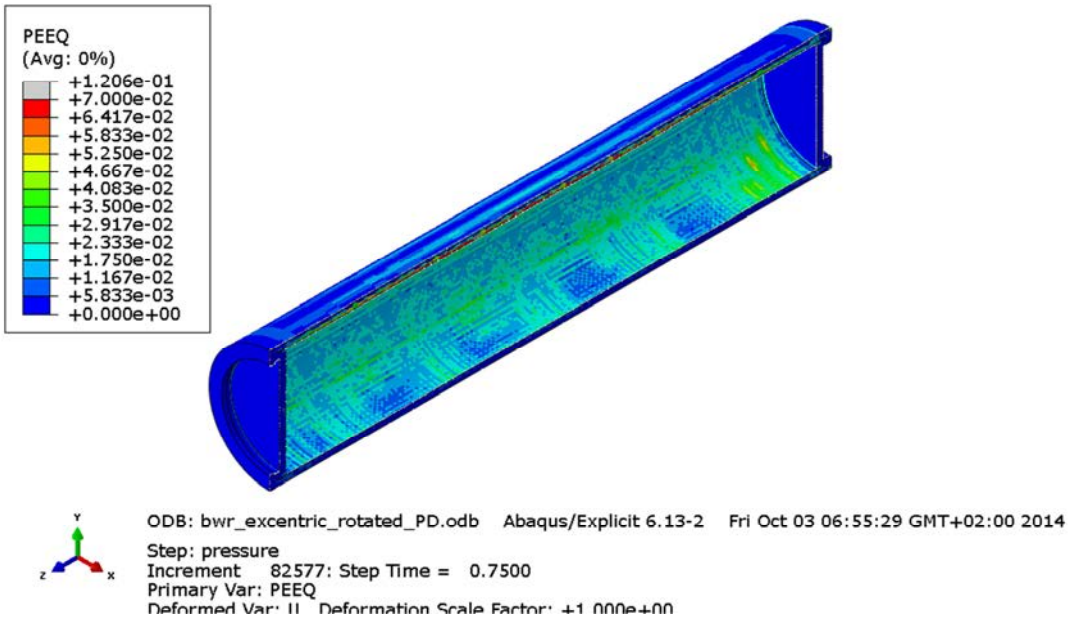

Figure A3-12 *Equivalent plastic strain (PEEQ) for the copper shell with 120 MPa as applied hydrostatic pressure.*

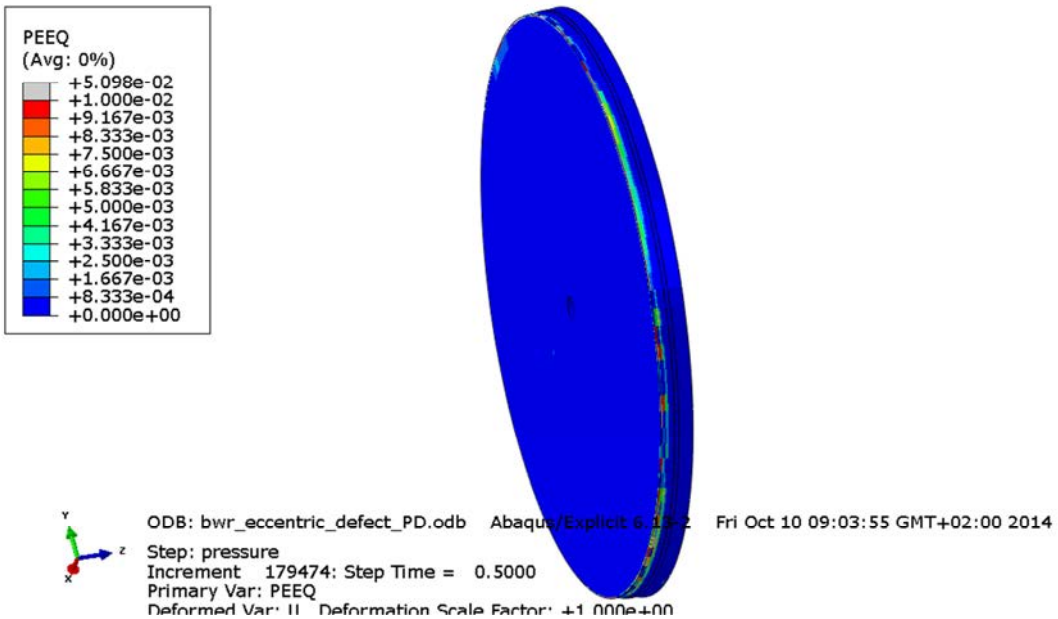

Figure A3-13 *Equivalent plastic strain (PEEQ) for the insert lid with 90 MPa as applied hydrostatic pressure.*

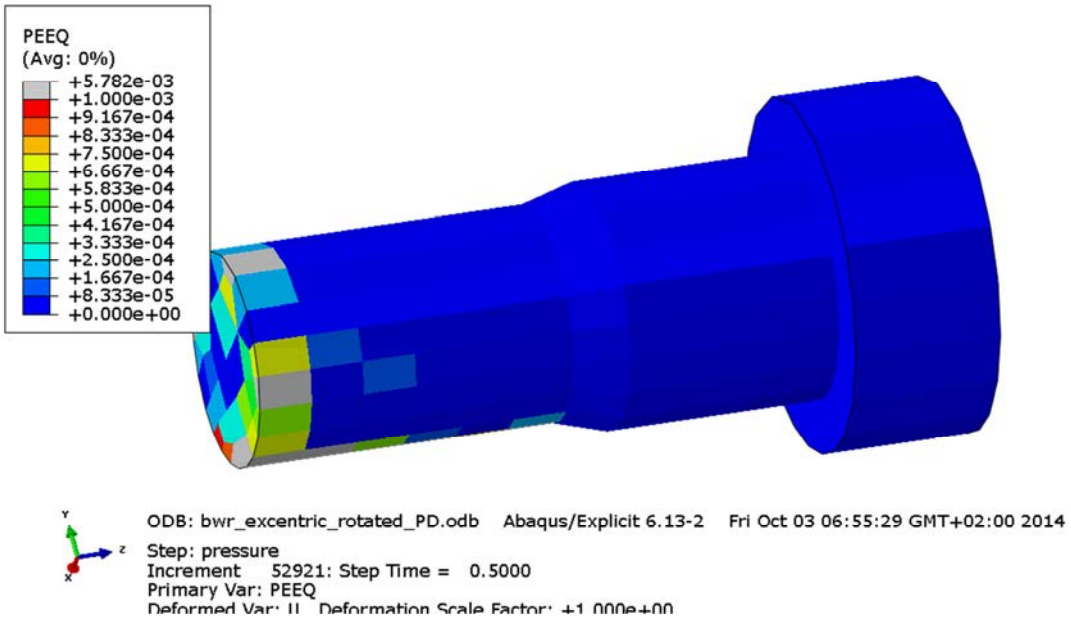

Figure A3-14 *Equivalent plastic strain (PEEQ) for the fixing screw with 90 MPa as applied hydrostatic pressure.*

Appendix 4 – Plots for bwr_eccentric_defect_PD2

Plots showing deformed geometry as contour plots for all parts of the BWR model at pressure magnitude 50, 90 and 120 MPa for case bwr_eccentric_defect_PD (geometry based on manufacturing tolerances and eccentrically positioned channel tubes, 10 mm and a cylindrical defect assumed for the insert). Yield surface for the insert has been reduced by scaling by factor 89%.

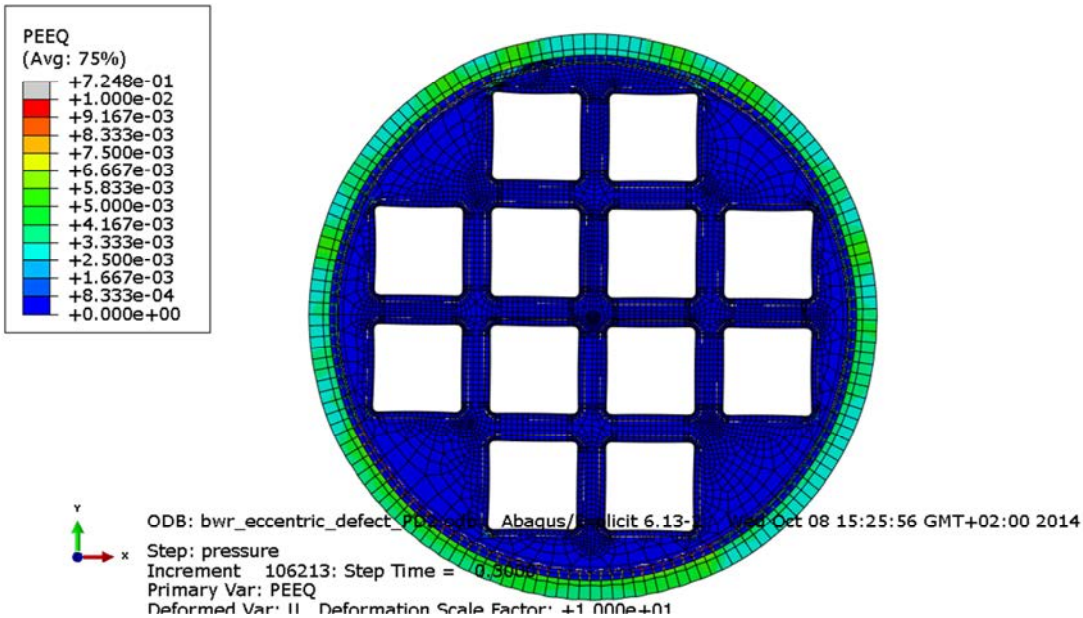

Figure A4-1 *Equivalent plastic strain (PEEQ) with 60 MPa as applied hydrostatic pressure. Displacements scaled by factor 10.*

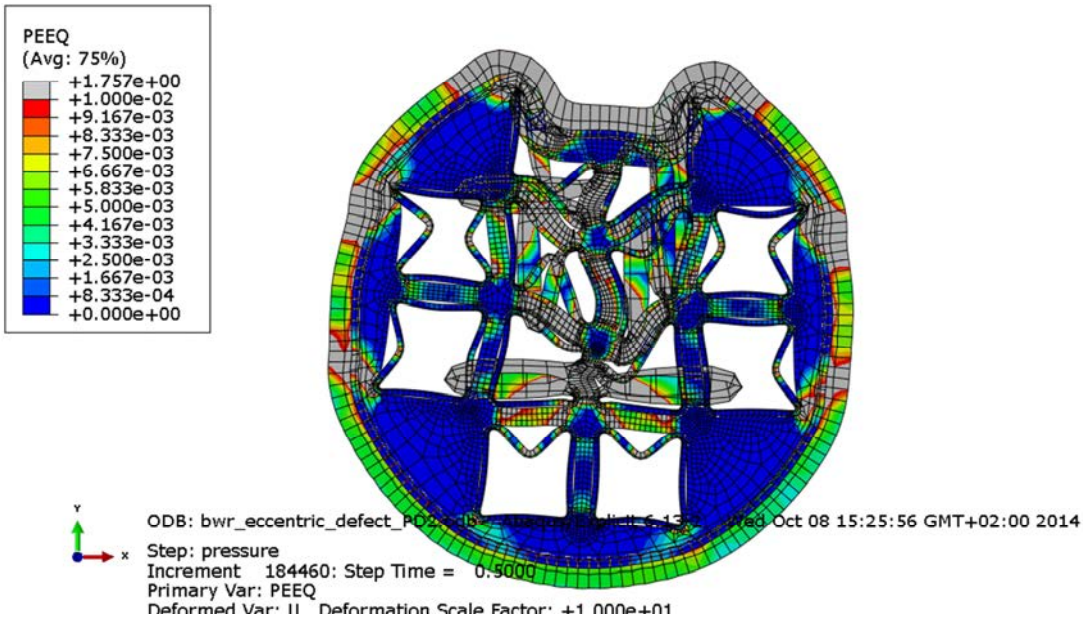

Figure A4-2 *Equivalent plastic strain (PEEQ) with 90 MPa as applied hydrostatic pressure. Displacements scaled by factor 10.*

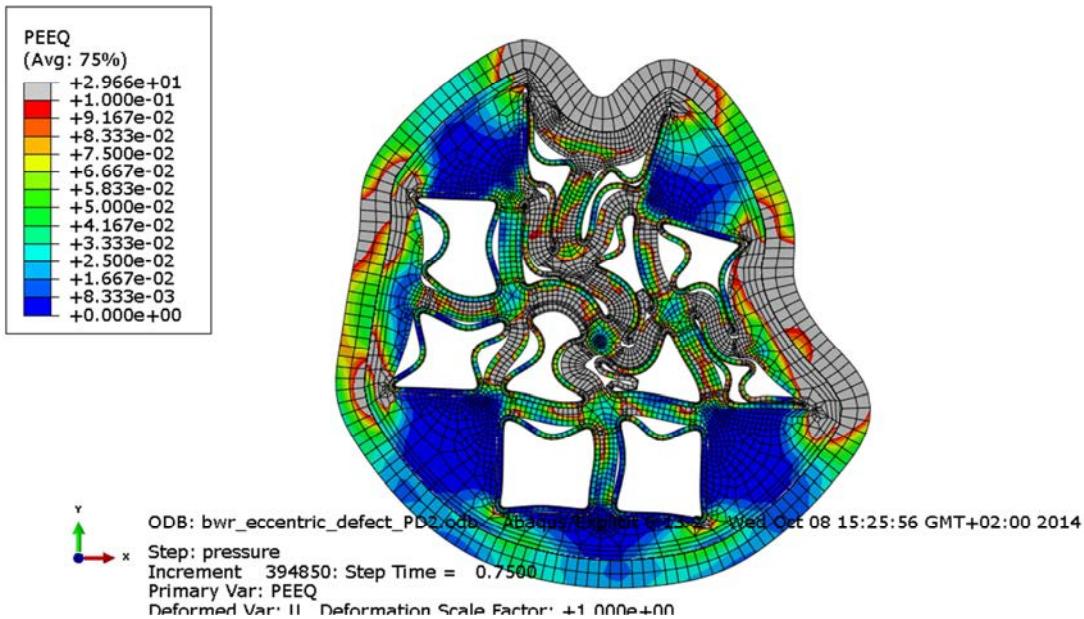

Figure A4-3 *Equivalent plastic strain (PEEQ) with 120 MPa as applied hydrostatic pressure.*

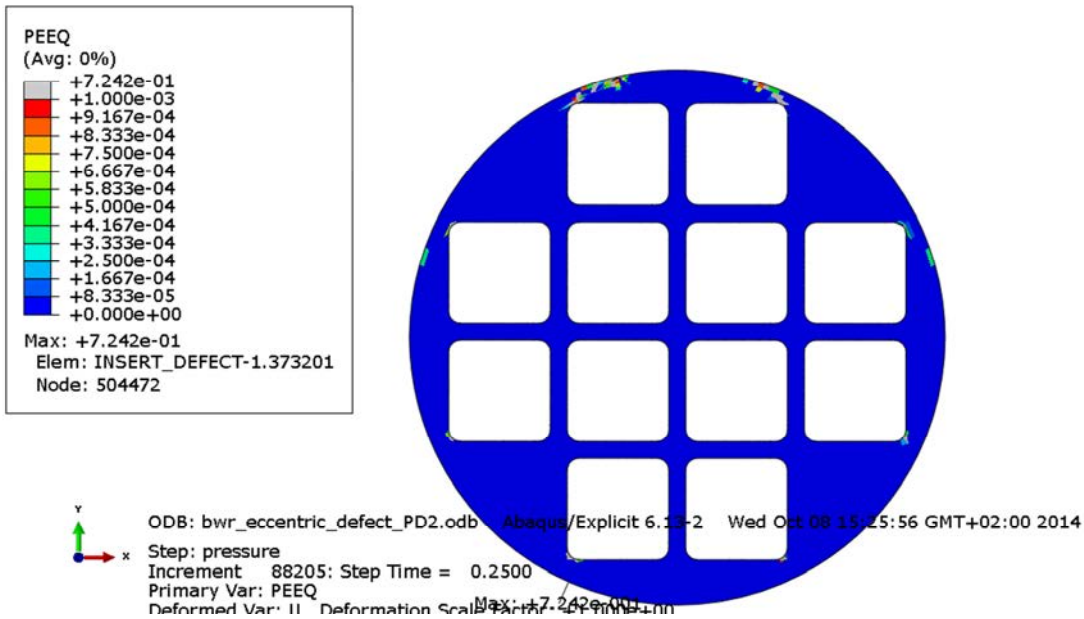

Figure A4-4 *Equivalent plastic strain (PEEQ) for the insert with 60 MPa as applied hydrostatic pressure.*

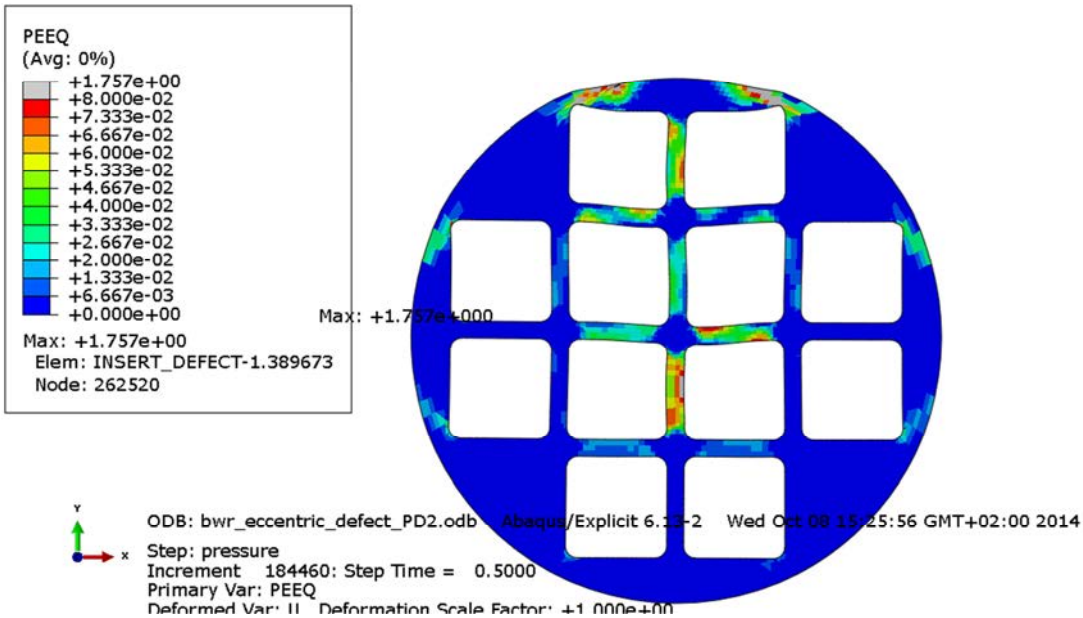

Figure A4-5 *Equivalent plastic strain (PEEQ) for the insert with 90 MPa as applied hydrostatic pressure.*

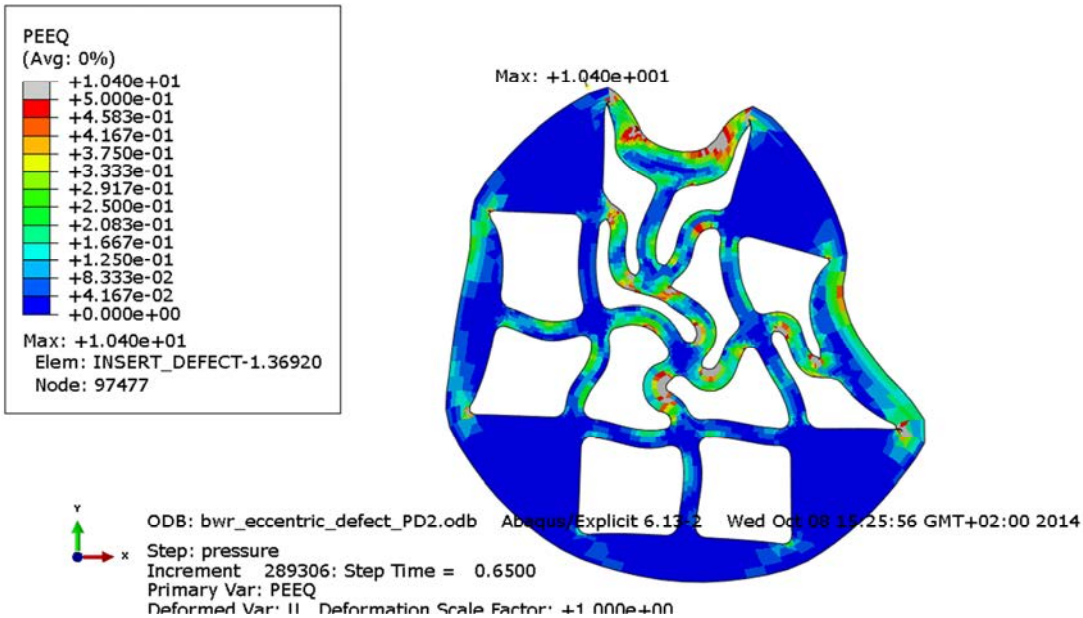

Figure A4-6 *Equivalent plastic strain (PEEQ) for the insert with 120 MPa as applied hydrostatic pressure.*

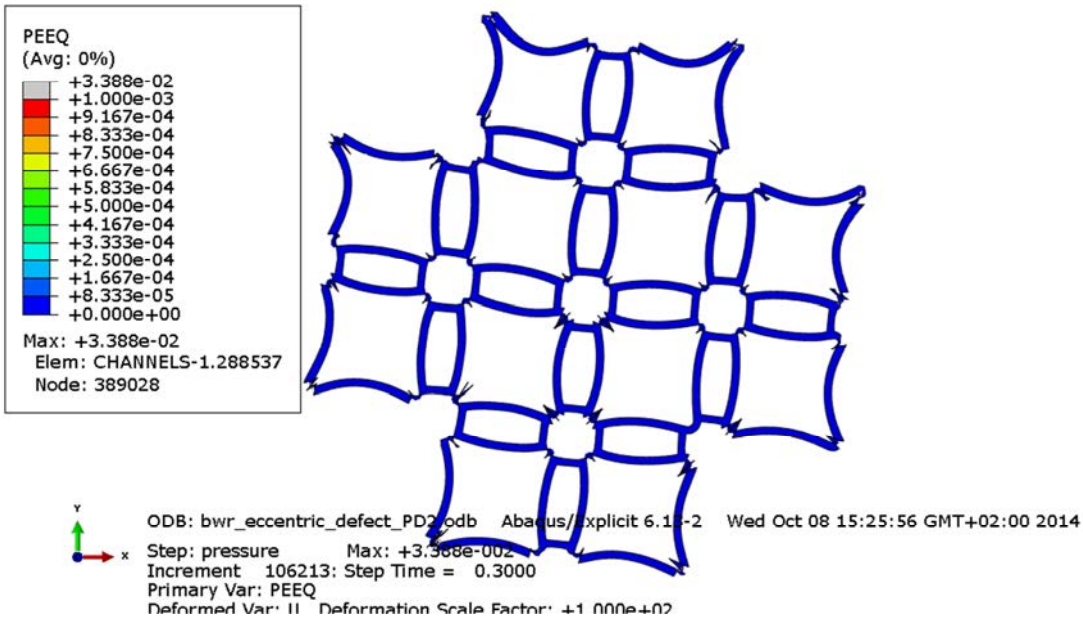

Figure A4-7 *Equivalent plastic strain (PEEQ) for the channel tubes with 60 MPa as applied hydrostatic pressure.*

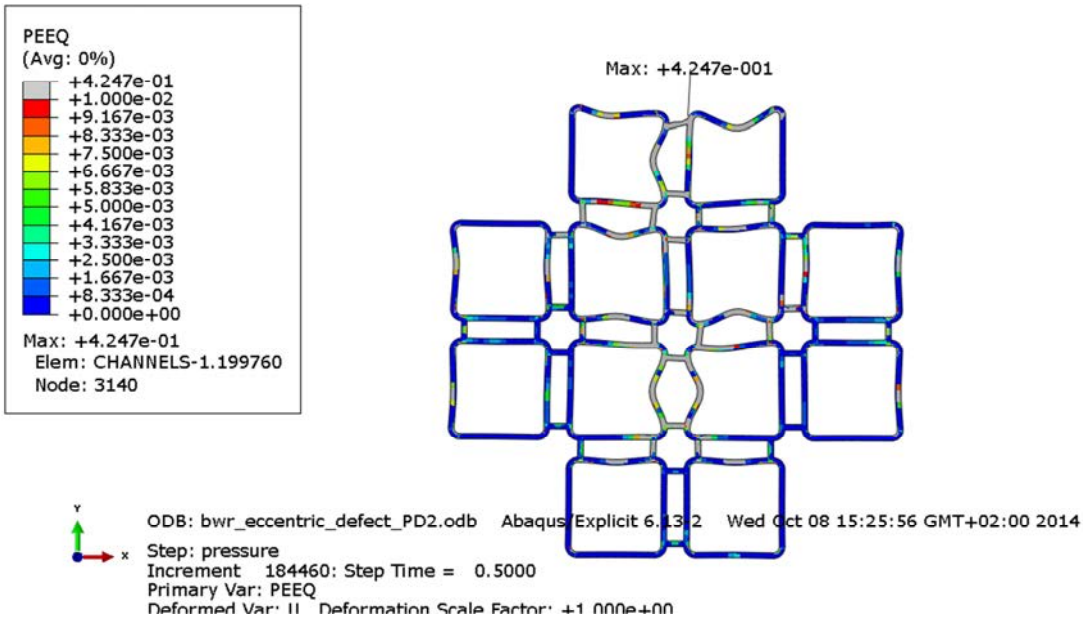

Figure A4-8 *Equivalent plastic strain (PEEQ) for the channel tubes with 90 MPa as applied hydrostatic pressure.*

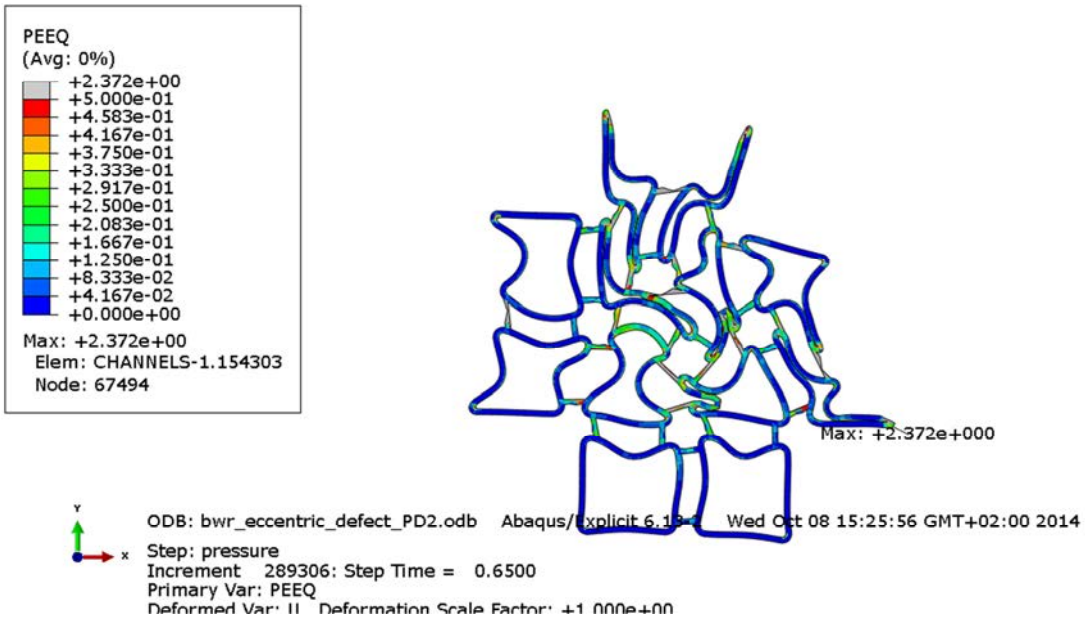

Figure A4-9 *Equivalent plastic strain (PEEQ) for the channel tubes with 120 MPa as applied hydrostatic pressure.*

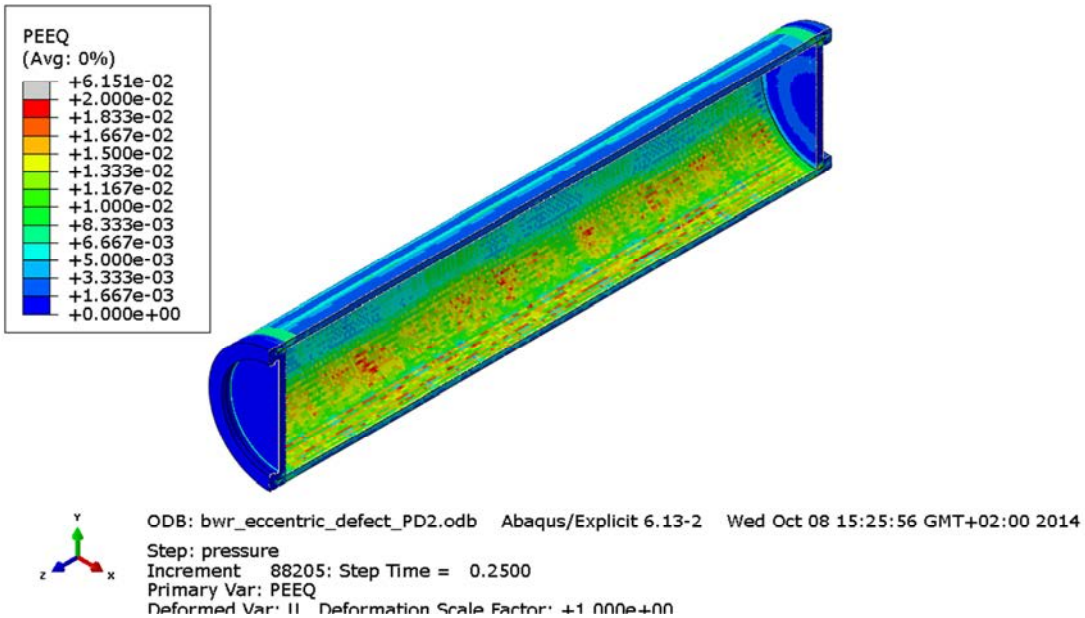

Figure A4-10 *Equivalent plastic strain (PEEQ) for the copper shell with 60 MPa as applied hydrostatic pressure.*

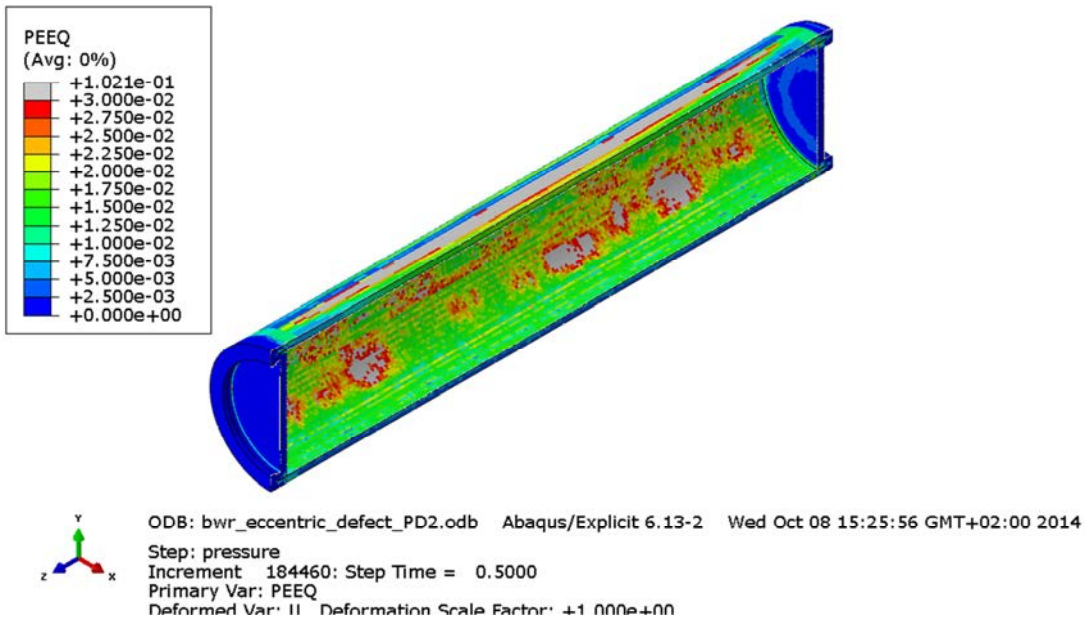

Figure A4-11 *Equivalent plastic strain (PEEQ) for the copper shell with 90 MPa as applied hydrostatic pressure.*

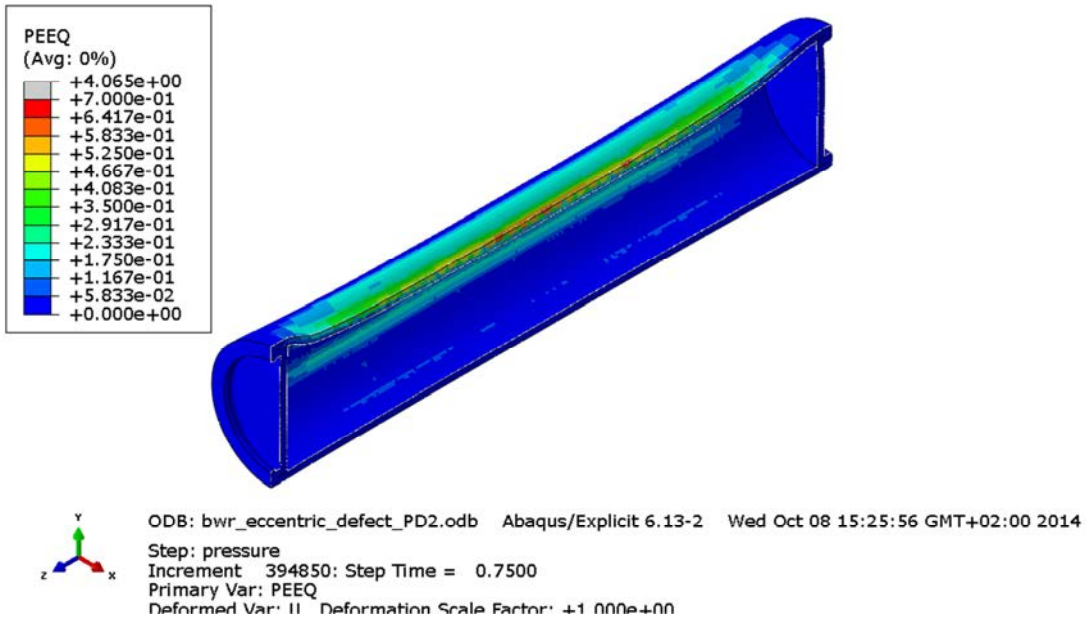

Figure A4-12 *Equivalent plastic strain (PEEQ) for the copper shell with 120 MPa as applied hydrostatic pressure.*

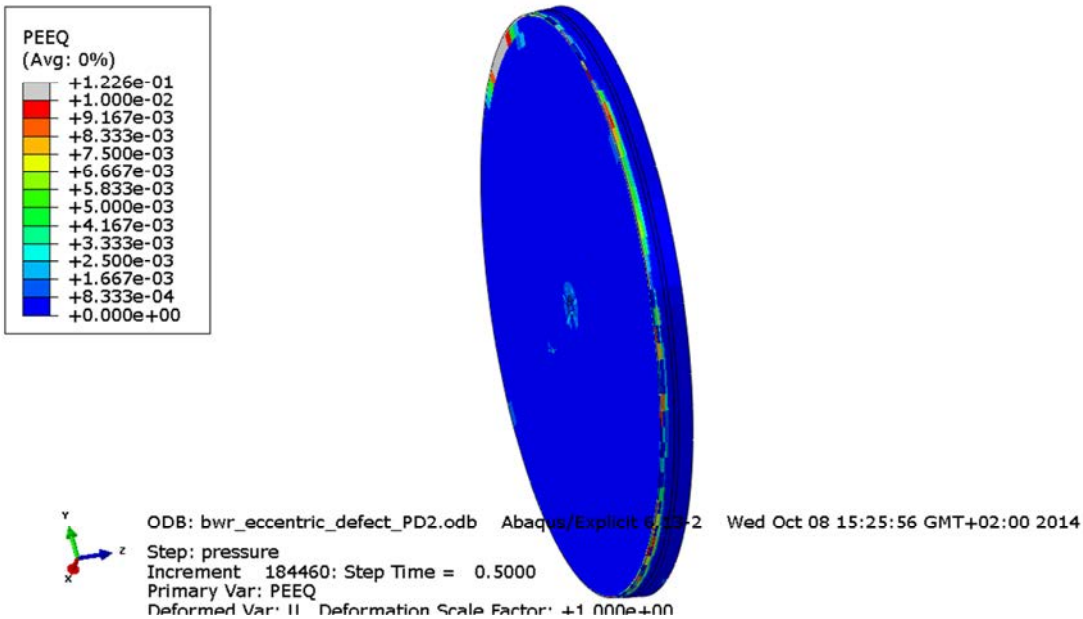

Figure A4-13 *Equivalent plastic strain (PEEQ) for the insert lid with 90 MPa as applied hydrostatic pressure.*

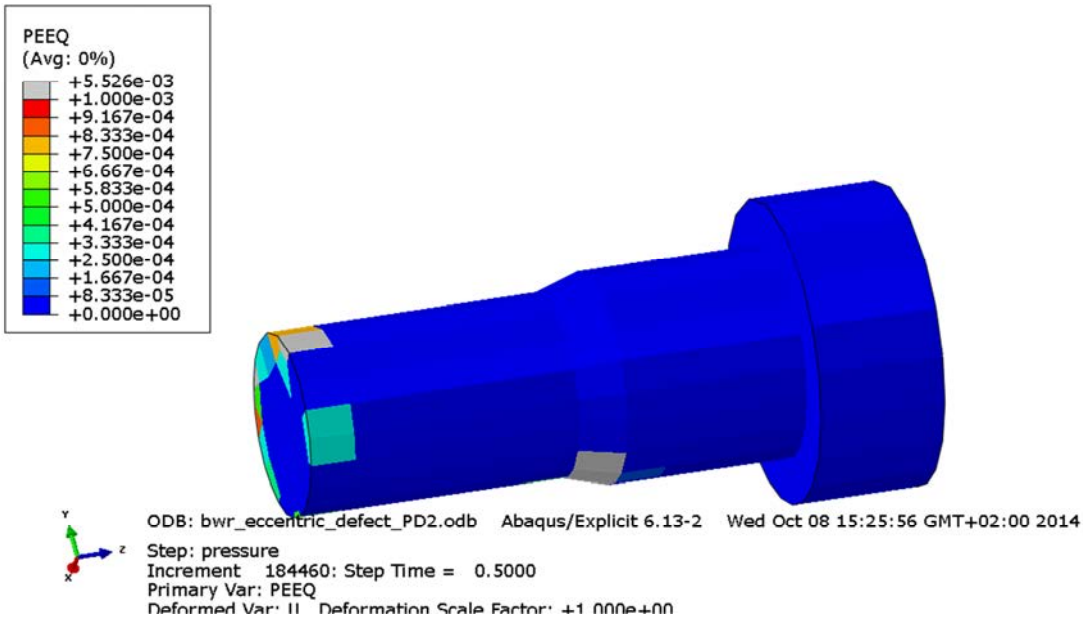

Figure A4-14 *Equivalent plastic strain (PEEQ) for the fixing screw with 90 MPa as applied hydrostatic pressure.*

Appendix 5 – Plots for pwr_centric_full_PD

Plots showing deformed geometry as contour plots for all parts of the PWR model at pressure magnitude 50, 90 and 120 MPa for case pwr_centric_full_PD (geometry based on nominal dimensions and centrically positioned channel tubes).

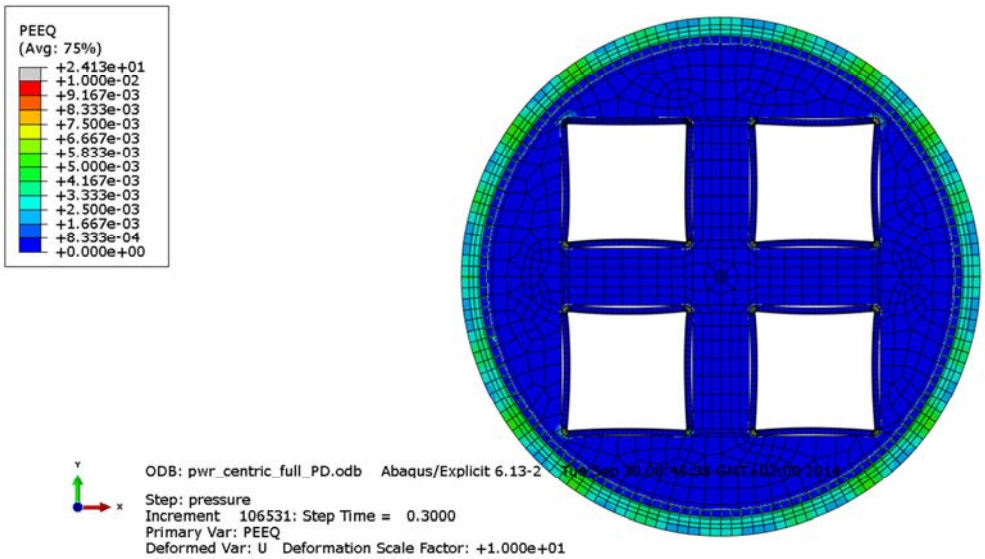

Figure A5-1 *Equivalent plastic strain (PEEQ) with 60 MPa as applied hydrostatic pressure. Displacements scaled by factor 100.*

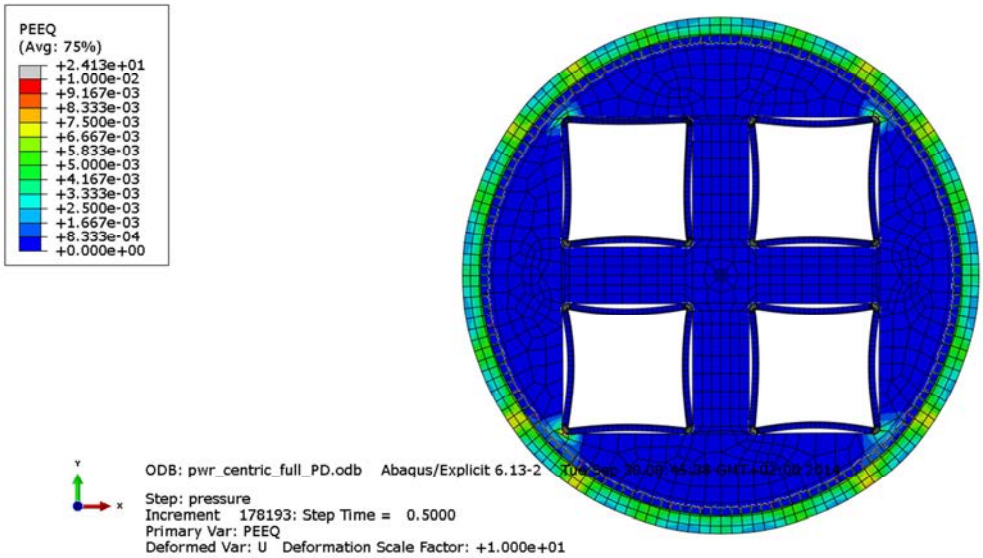

Figure A5-2 *Equivalent plastic strain (PEEQ) with 90 MPa as applied hydrostatic pressure. Displacements scaled by factor 10.*

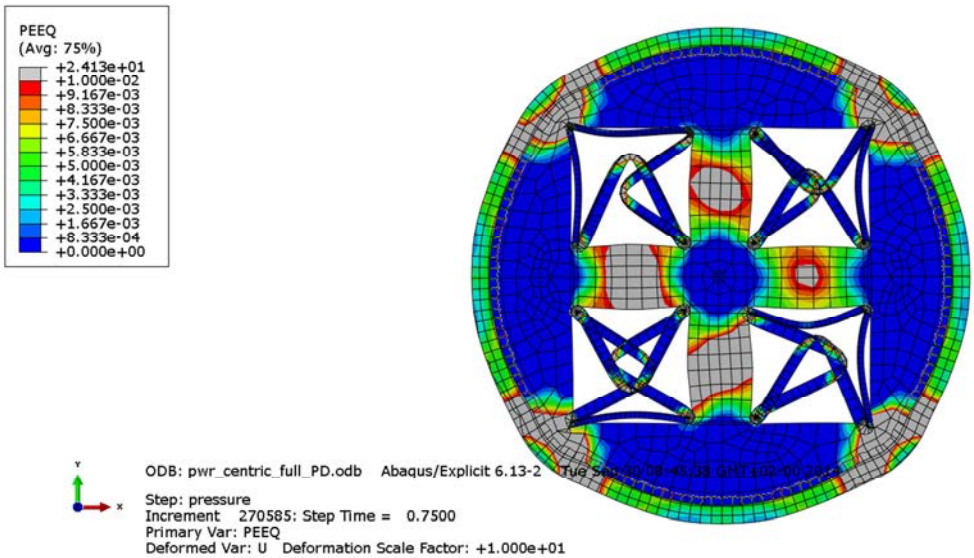

Figure A5-3 *Equivalent plastic strain (PEEQ) with 120 MPa as applied hydrostatic pressure. Displacements scaled by factor 10.*

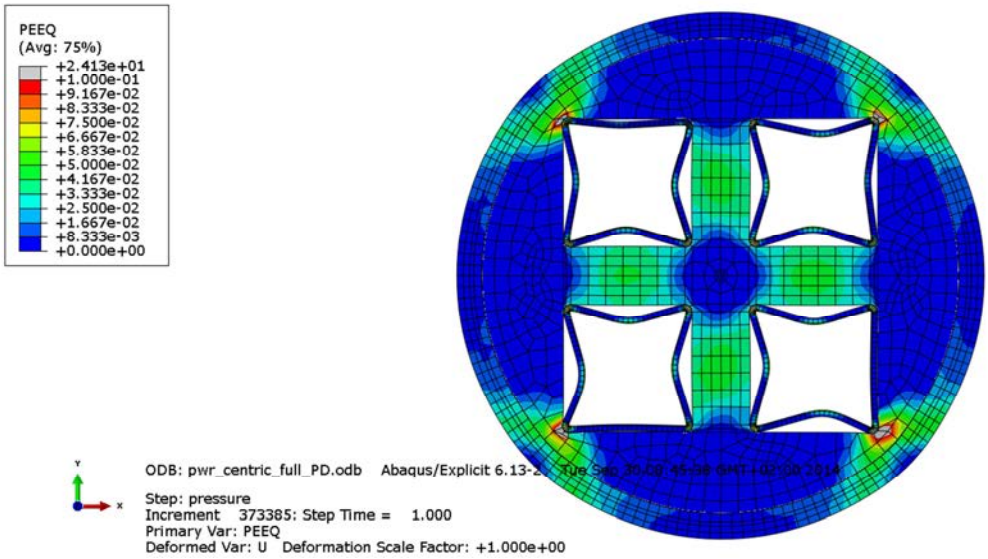

Figure A5-4 *Equivalent plastic strain (PEEQ) with 150 MPa as applied hydrostatic pressure.*

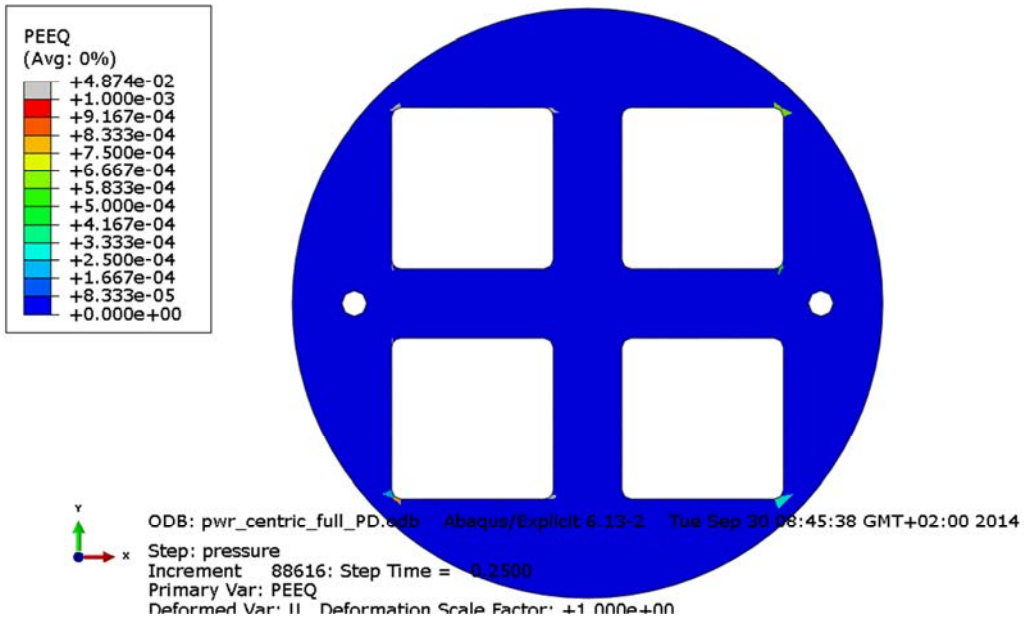

Figure A5-5 *Equivalent plastic strain (PEEQ) for the insert with 60 MPa as applied hydrostatic pressure.*

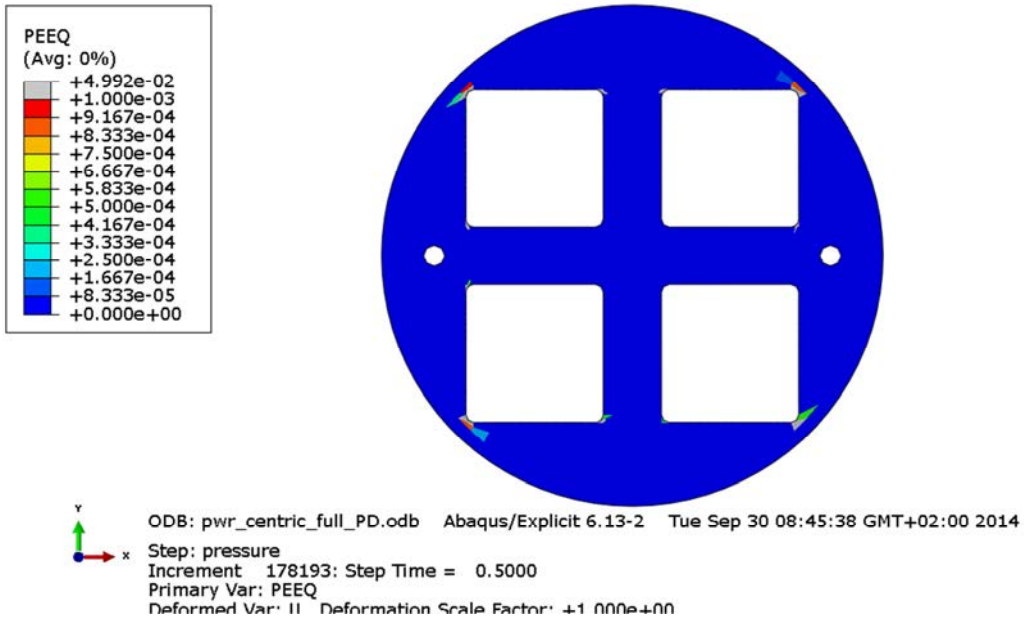

Figure A5-6 *Equivalent plastic strain (PEEQ) for the insert with 90 MPa as applied hydrostatic pressure.*

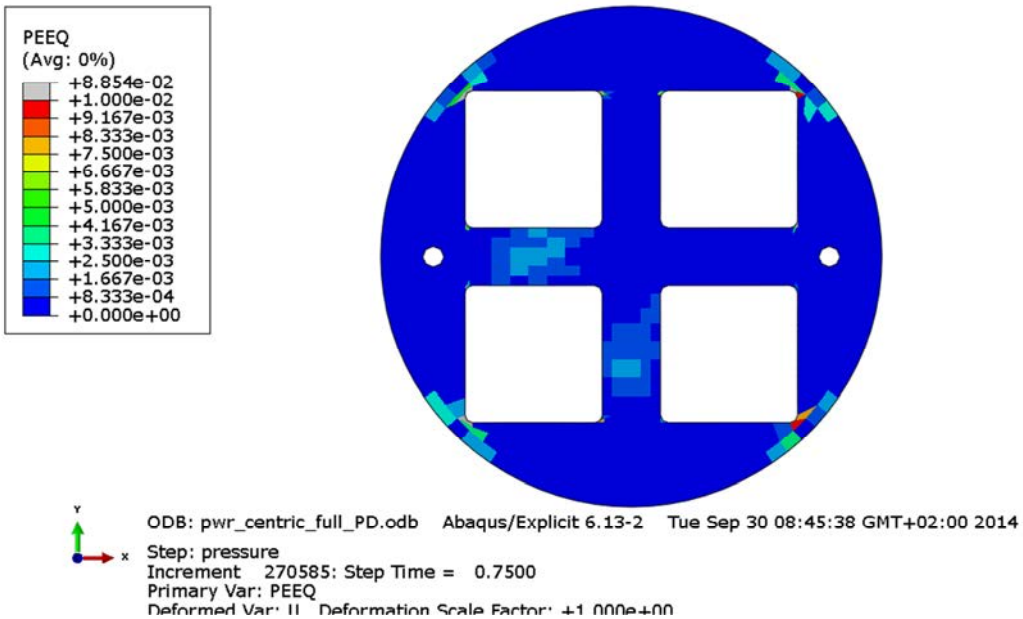

Figure A5-7 *Equivalent plastic strain (PEEQ) for the insert with 120 MPa as applied hydrostatic pressure.*

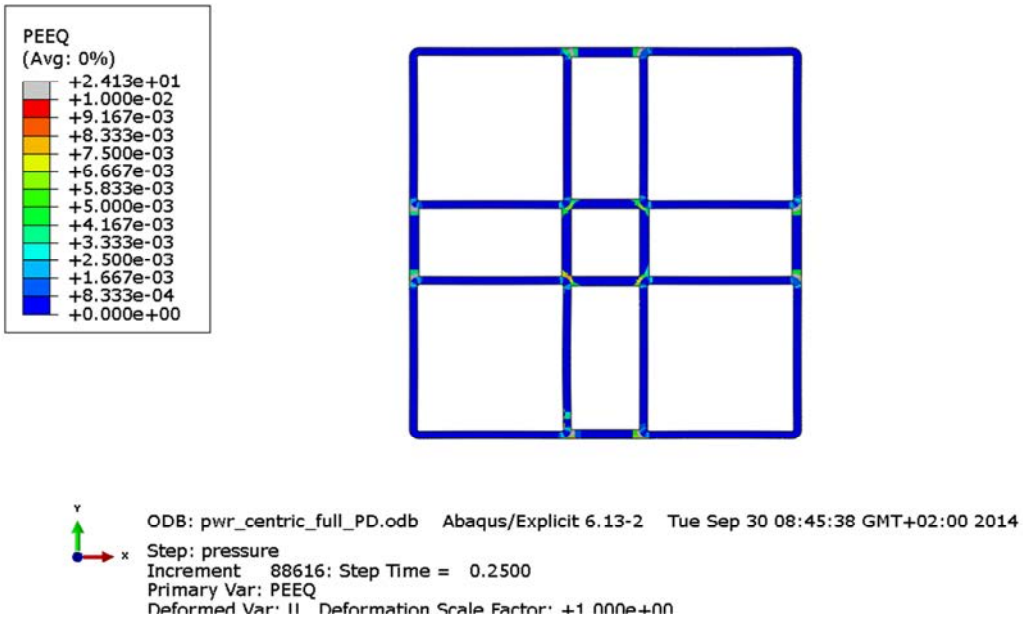

Figure A5-8 *Equivalent plastic strain (PEEQ) for the channel tubes with 60 MPa as applied hydrostatic pressure.*

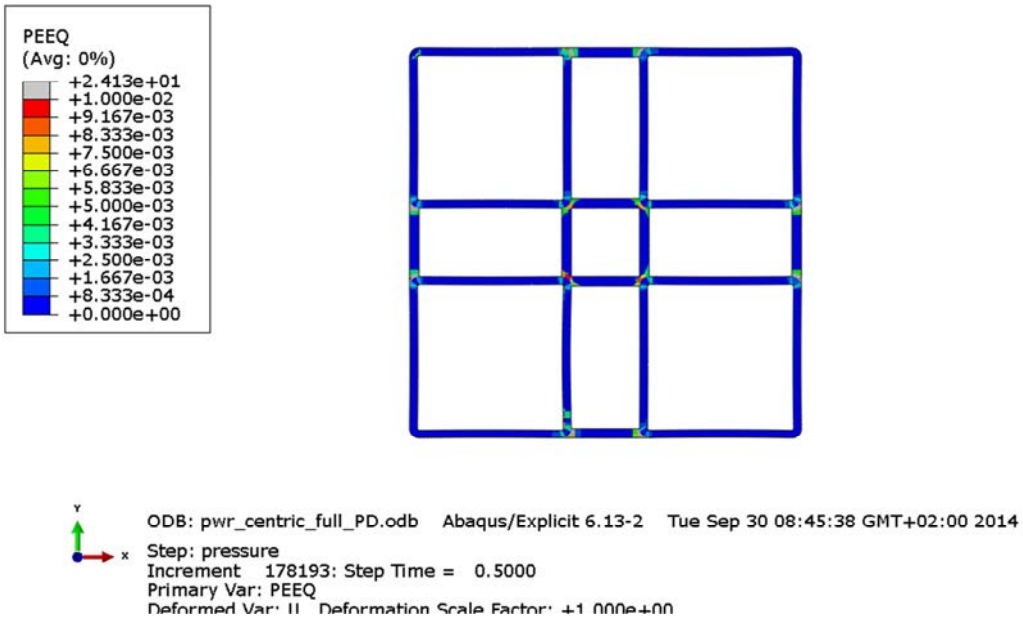

Figure A5-9 *Equivalent plastic strain (PEEQ) for the channel tubes with 90 MPa as applied hydrostatic pressure.*

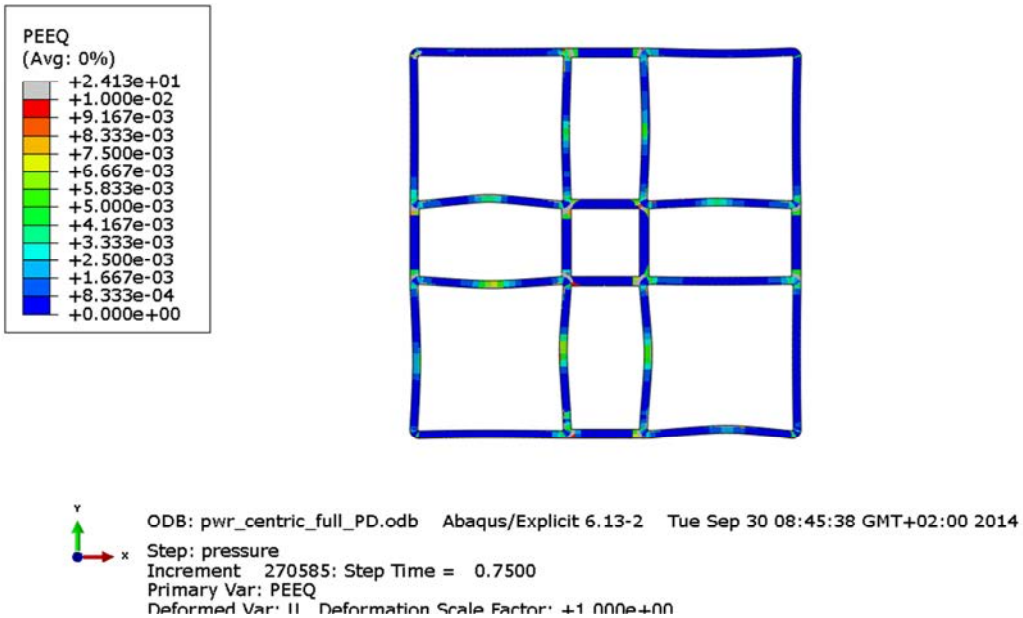

Figure A5-10 *Equivalent plastic strain (PEEQ) for the channel tubes with 120 MPa as applied hydrostatic pressure.*

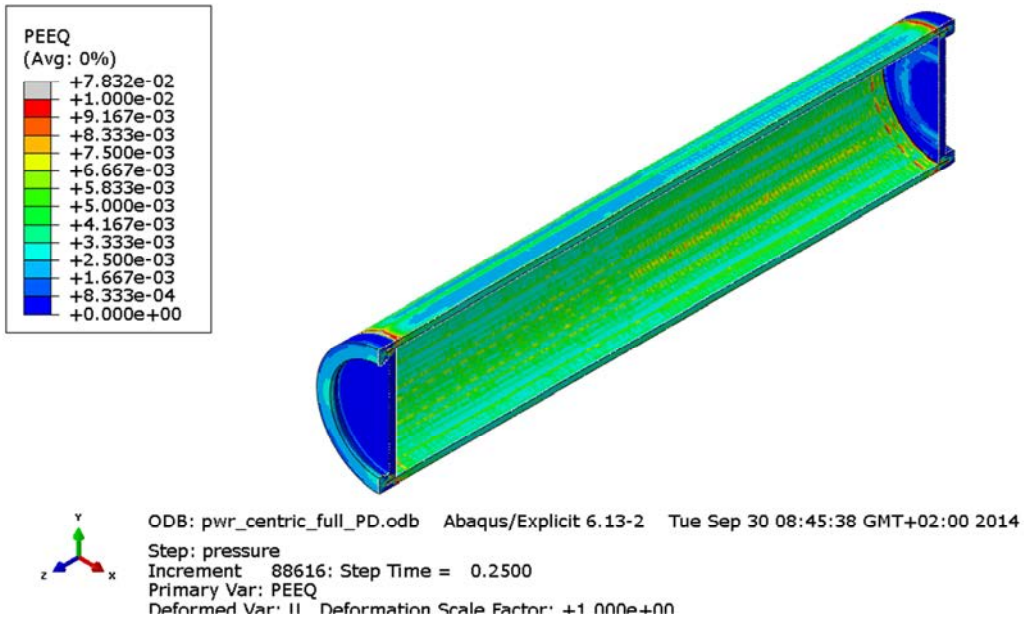

Figure A5-11 *Equivalent plastic strain (PEEQ) for the copper shell with 60 MPa as applied hydrostatic pressure.*

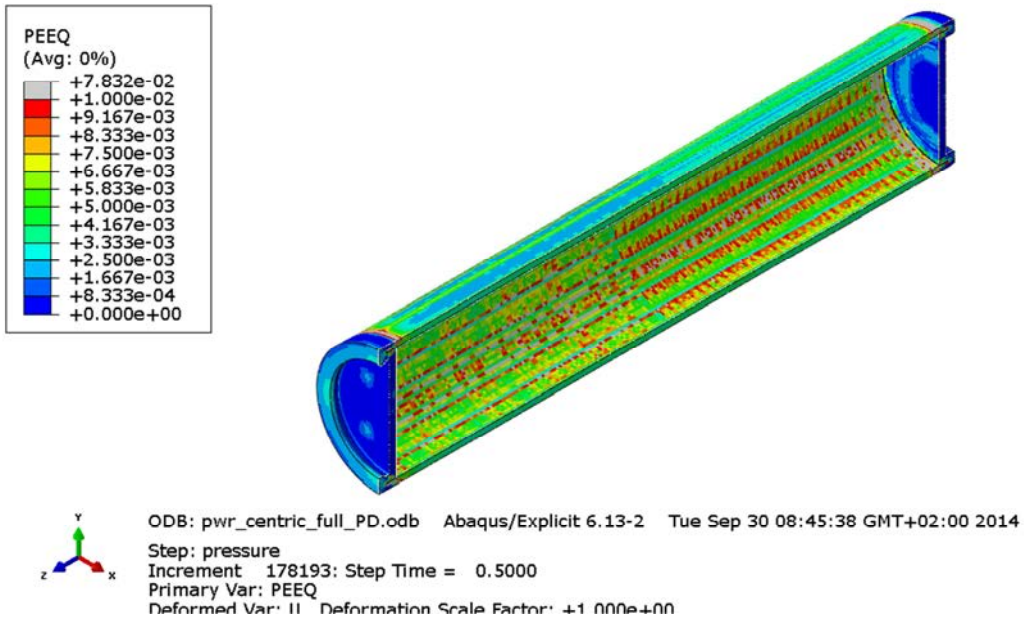

Figure A5-12 *Equivalent plastic strain (PEEQ) for the copper shell with 90 MPa as applied hydrostatic pressure.*

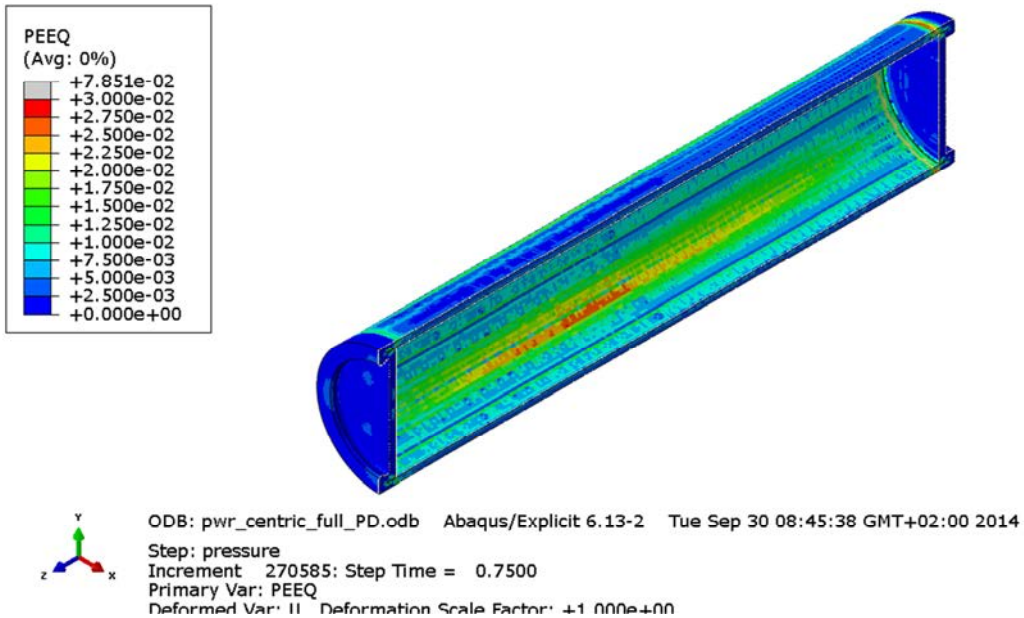

Figure A5-13 *Equivalent plastic strain (PEEQ) for the copper shell with 120 MPa as applied hydrostatic pressure.*

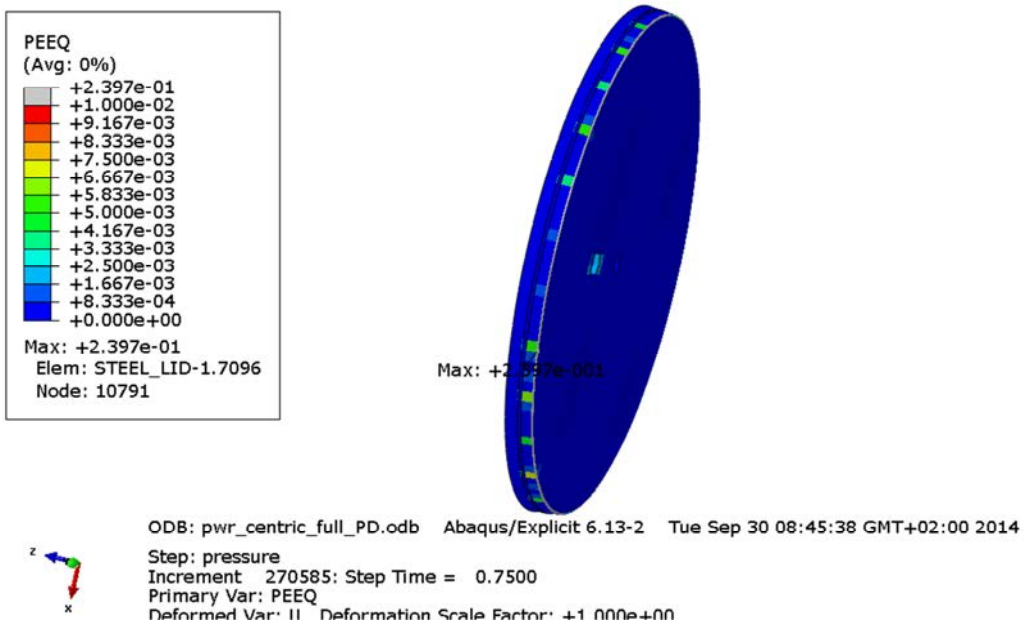

Figure A5-14 *Equivalent plastic strain (PEEQ) for the insert lid with 120 MPa as applied hydrostatic pressure.*

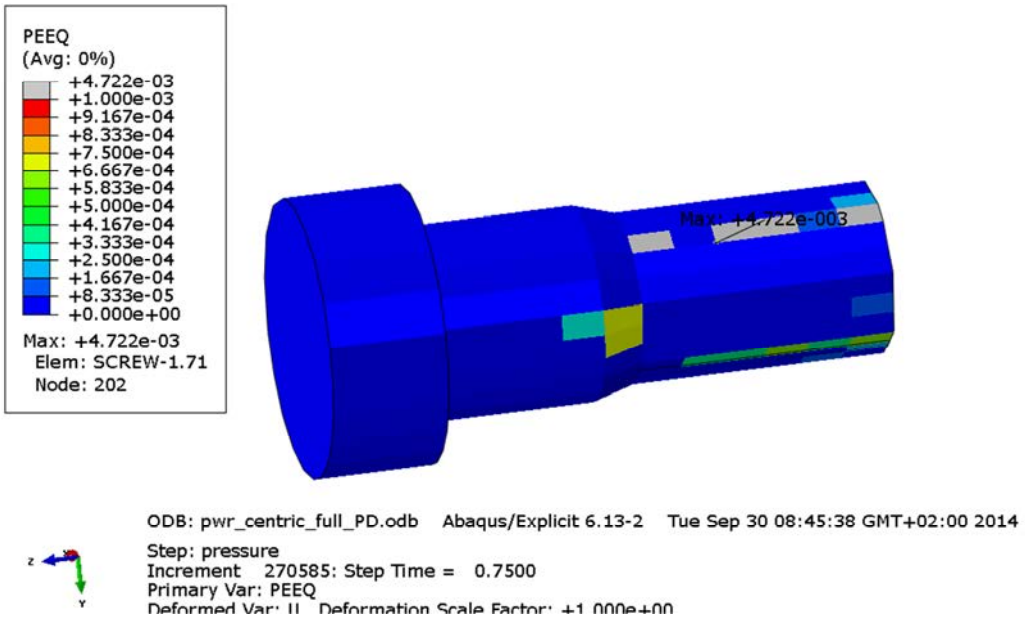

Figure A5-15 *Equivalent plastic strain (PEEQ) for the fixing screw with 120 MPa as applied hydrostatic pressure.*

Appendix 6 – Plots for pwr_eccentric_full_PD

Plots showing deformed geometry as contour plots for all parts of the PWR model at pressure magnitude 50, 90 and 120 MPa for case pwr_eccentric_full_PD (geometry based on manufacturing tolerances and eccentrically positioned channel tubes, 10 mm).

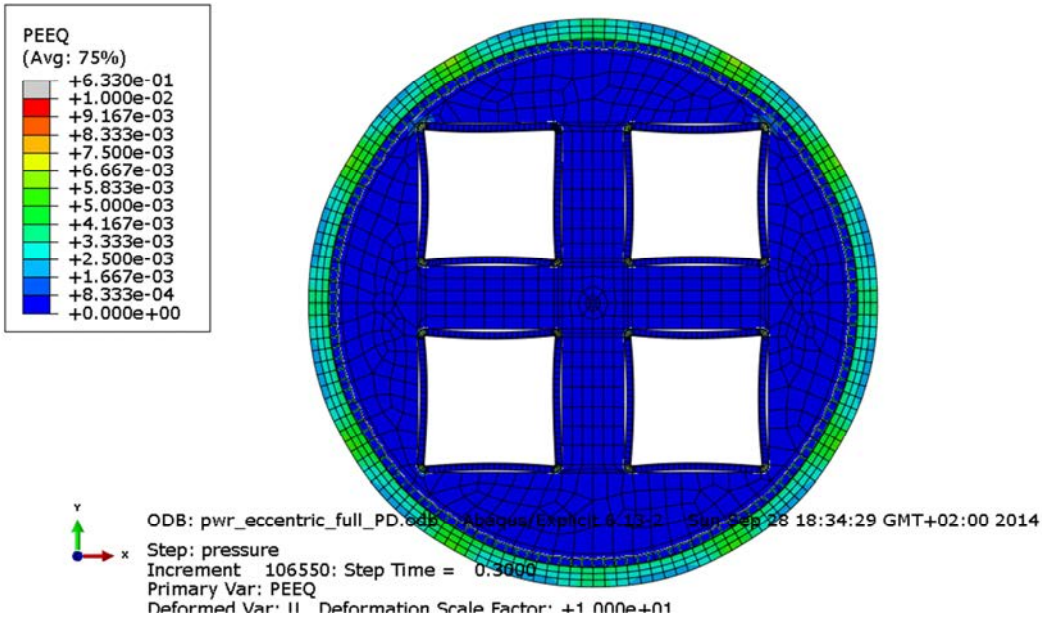

Figure A6-1 *Equivalent plastic strain (PEEQ) with 60 MPa as applied hydrostatic pressure. Displacements scaled by factor 100.*

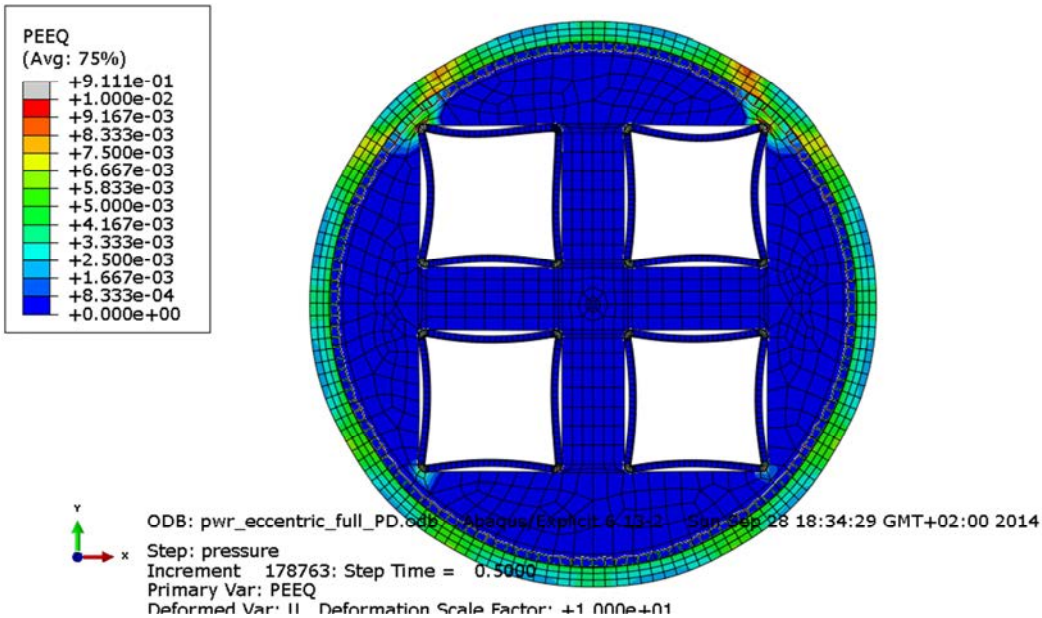

Figure A6-2 *Equivalent plastic strain (PEEQ) with 90 MPa as applied hydrostatic pressure. Displacements scaled by factor 10.*

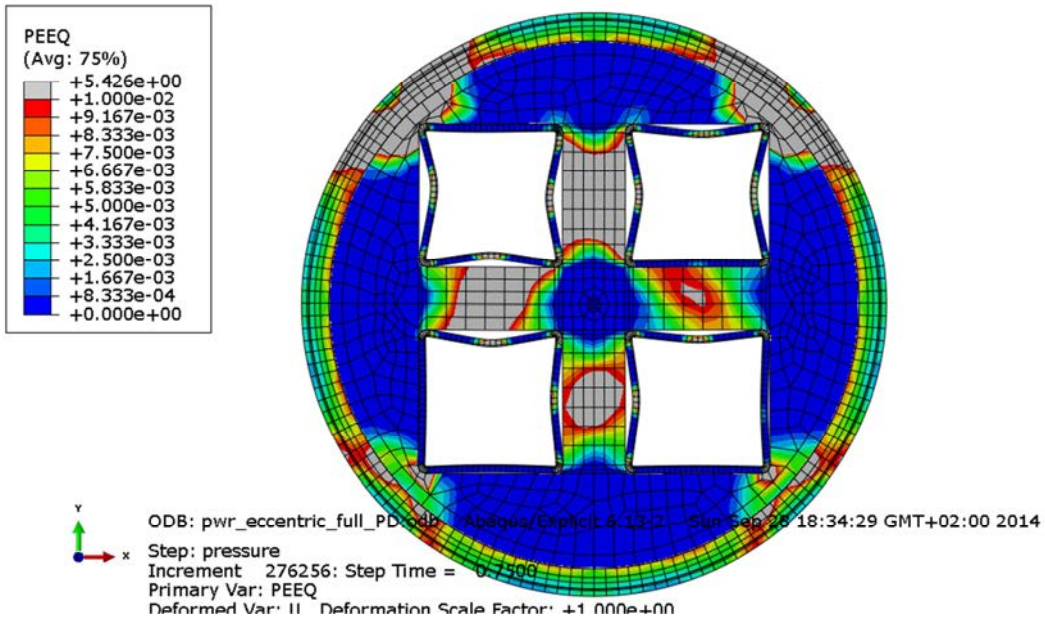

Figure A6-3 *Equivalent plastic strain (PEEQ) with 120 MPa as applied hydrostatic pressure.*

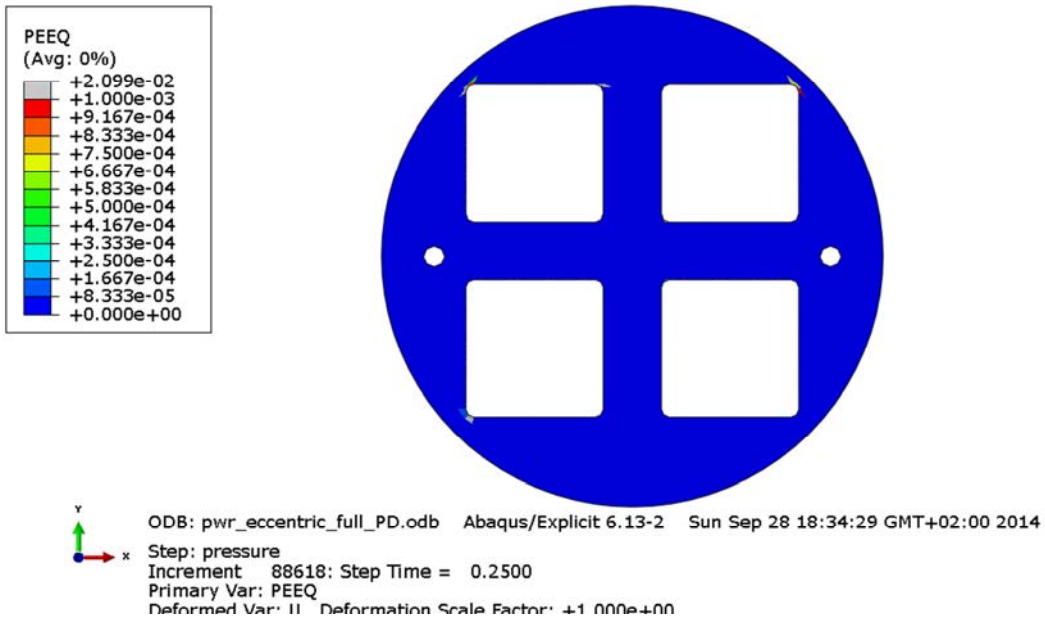

Figure A6-4 *Equivalent plastic strain (PEEQ) for the insert with 60 MPa as applied hydrostatic pressure.*

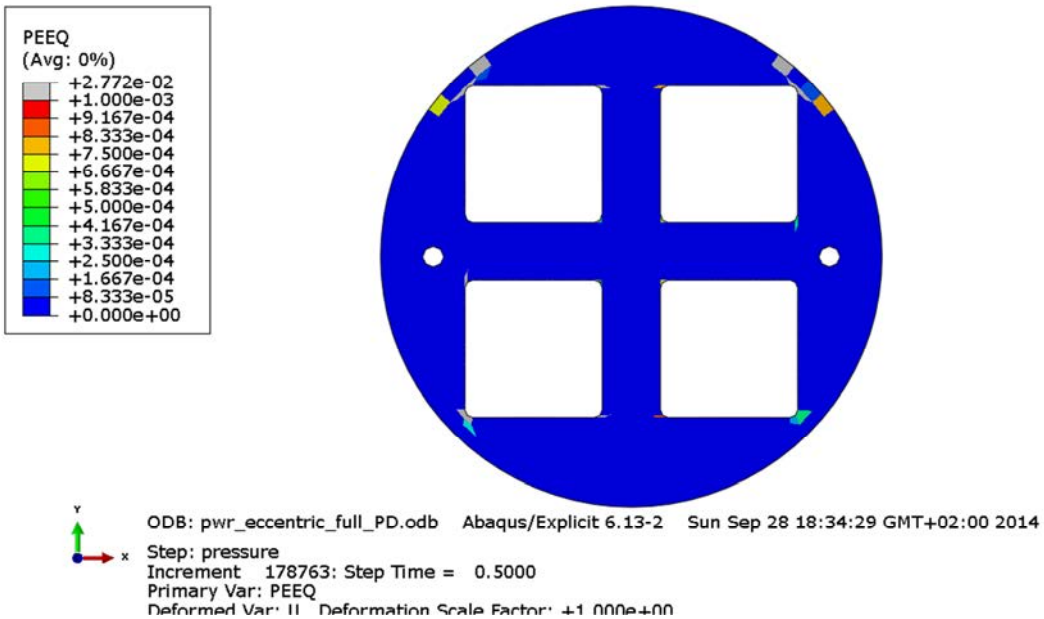

Figure A6-5 *Equivalent plastic strain (PEEQ) for the insert with 90 MPa as applied hydrostatic pressure.*

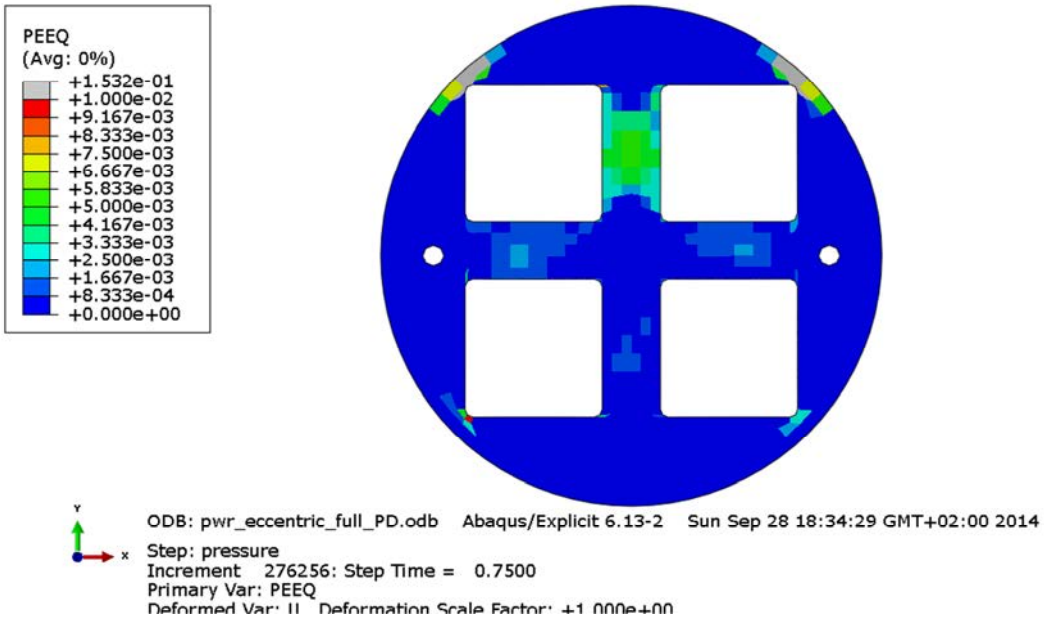

Figure A6-6 *Equivalent plastic strain (PEEQ) for the insert with 120 MPa as applied hydrostatic pressure.*

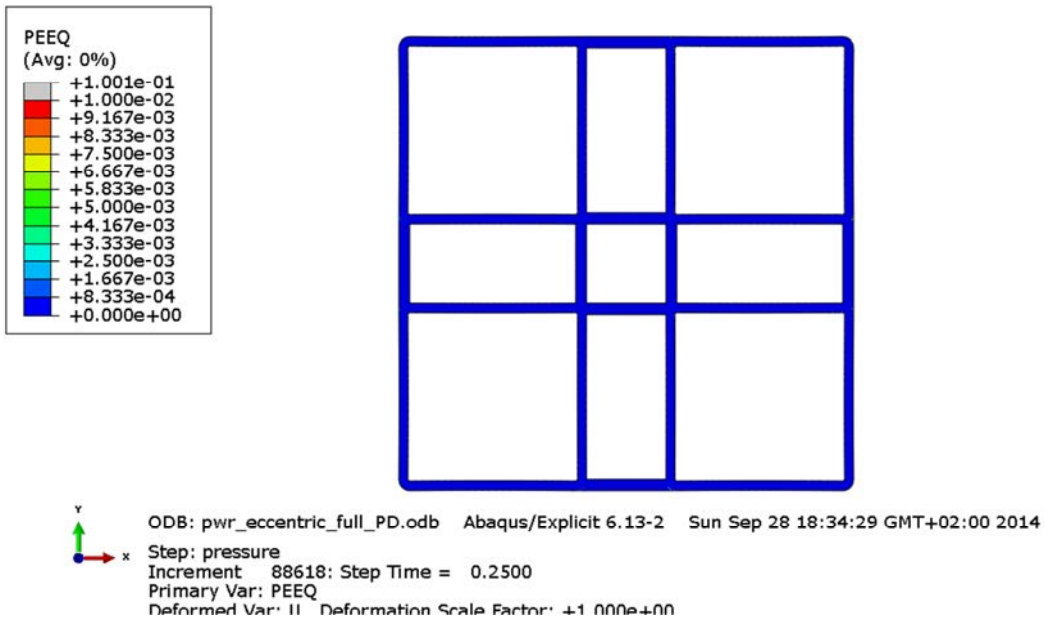

Figure A6-7 *Equivalent plastic strain (PEEQ) for the channel tubes with 60 MPa as applied hydrostatic pressure.*

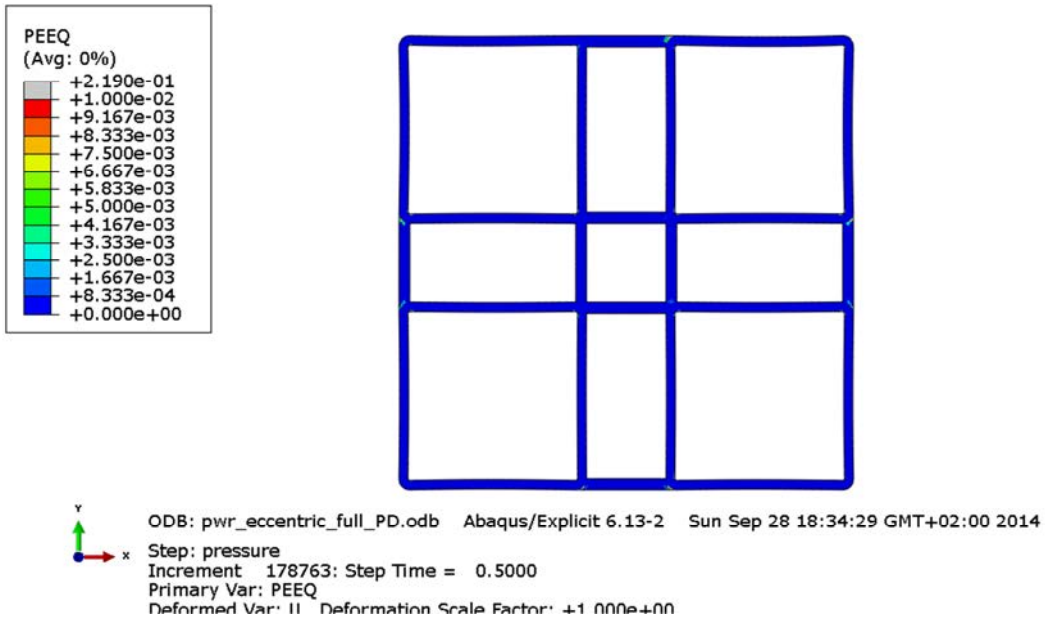

Figure A6-8 *Equivalent plastic strain (PEEQ) for the channel tubes with 90 MPa as applied hydrostatic pressure.*

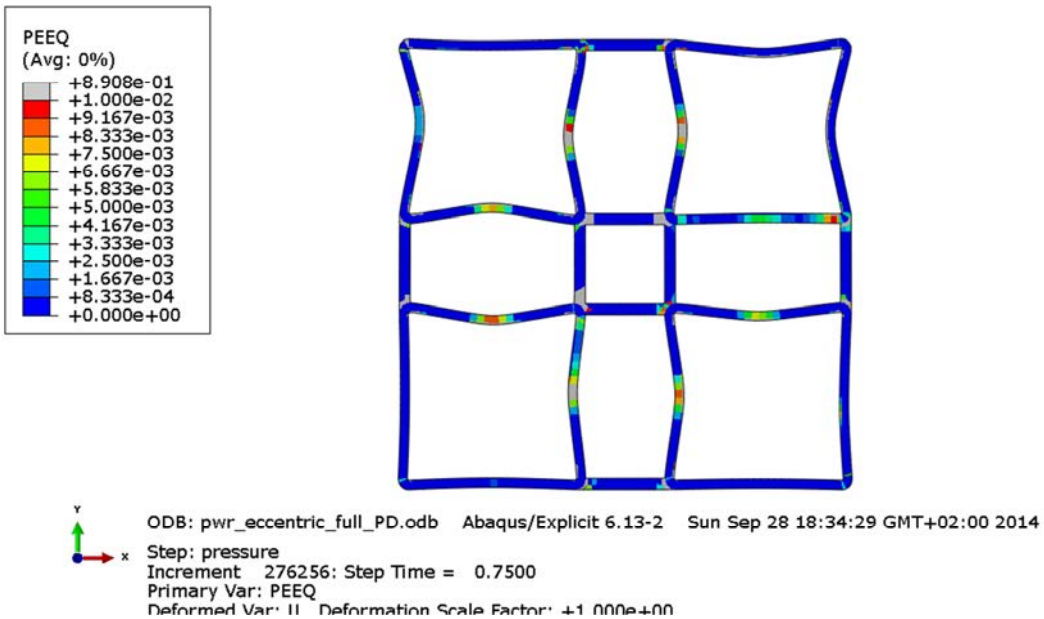

Figure A6-9 *Equivalent plastic strain (PEEQ) for the channel tubes with 120 MPa as applied hydrostatic pressure.*

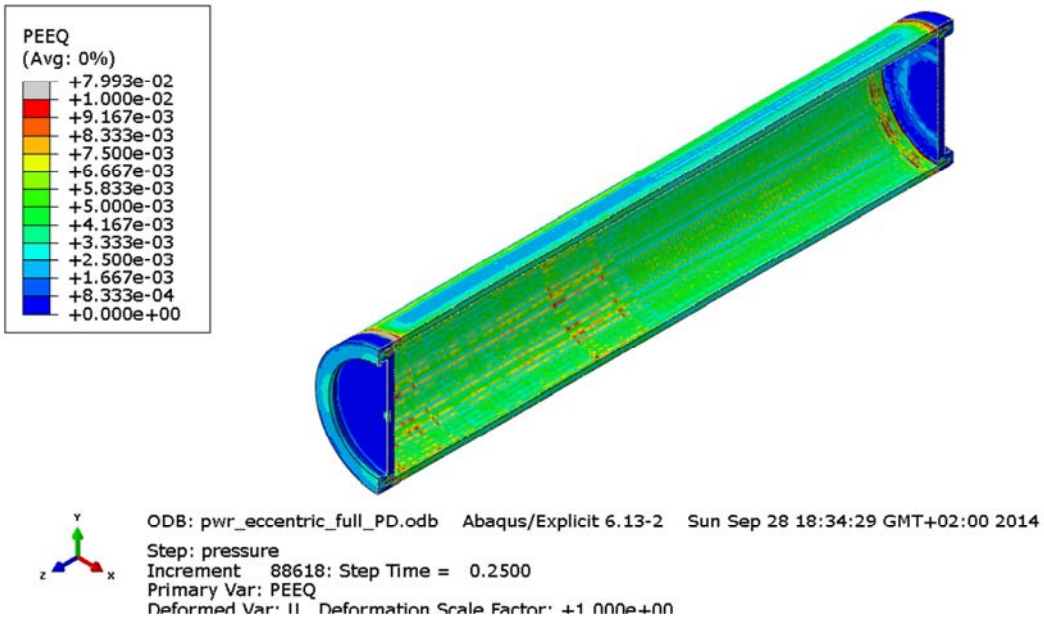

Figure A6-10 *Equivalent plastic strain (PEEQ) for the copper shell with 60 MPa as applied hydrostatic pressure.*

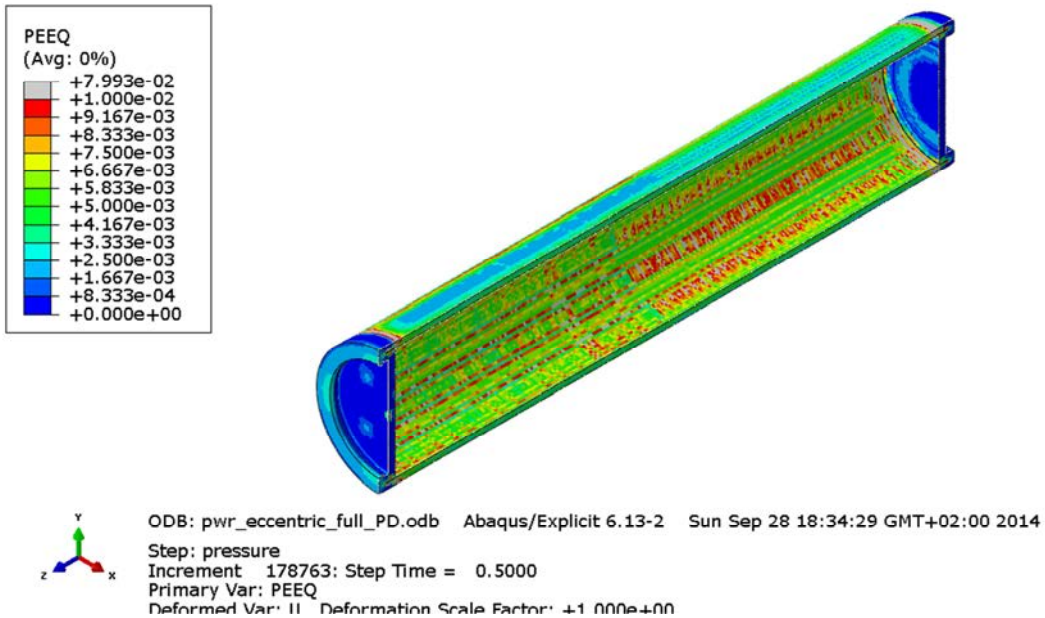

Figure A6-11 *Equivalent plastic strain (PEEQ) for the copper shell with 90 MPa as applied hydrostatic pressure.*

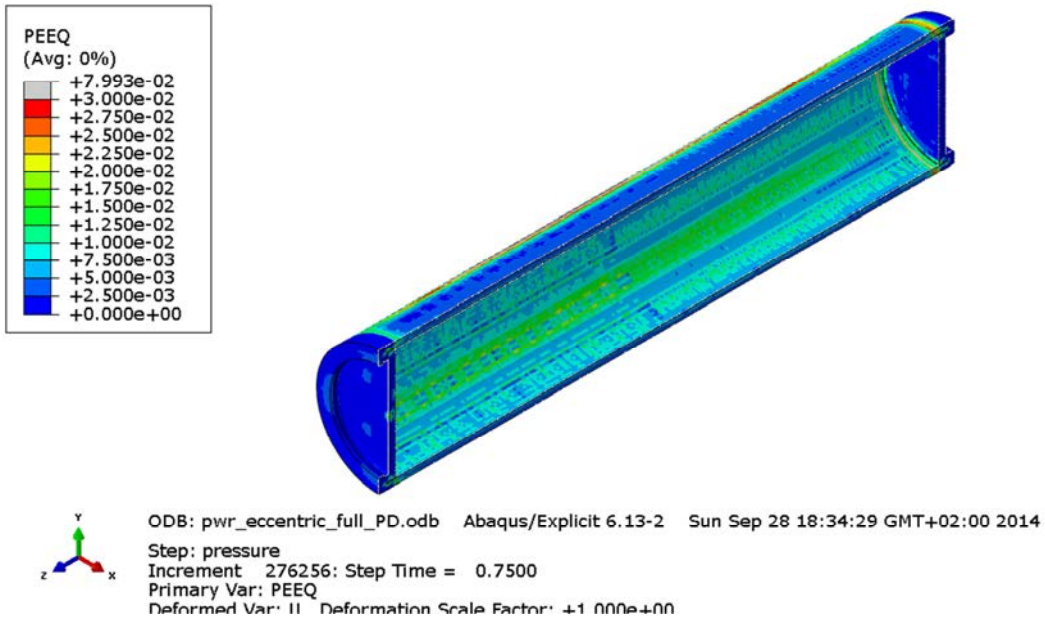

Figure A6-12 *Equivalent plastic strain (PEEQ) for the copper shell with 120 MPa as applied hydrostatic pressure.*

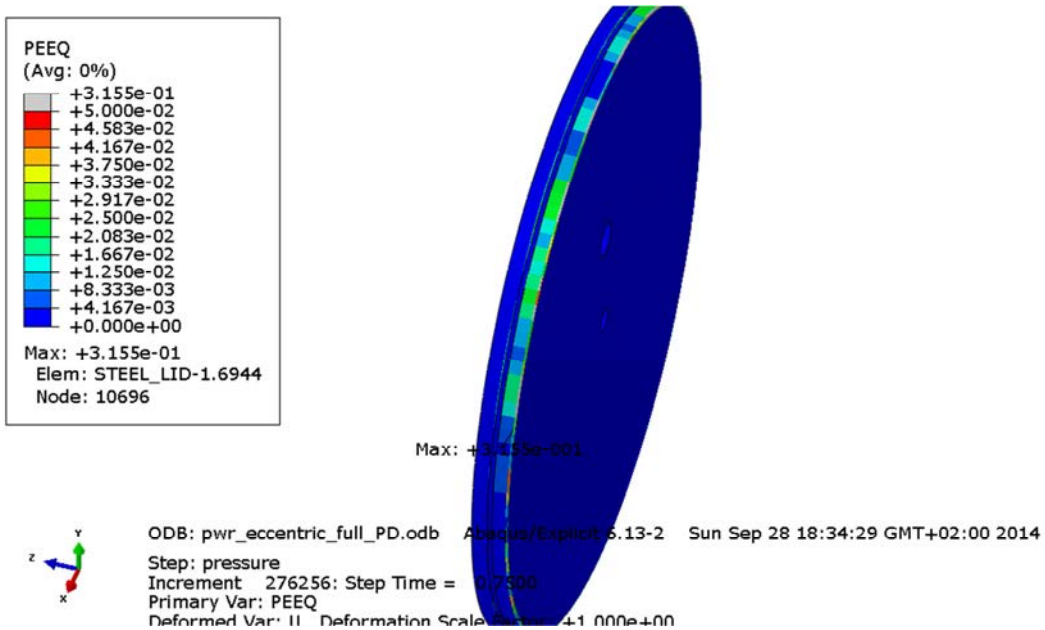

Figure A6-13 *Equivalent plastic strain (PEEQ) for the insert lid with 120 MPa as applied hydrostatic pressure.*

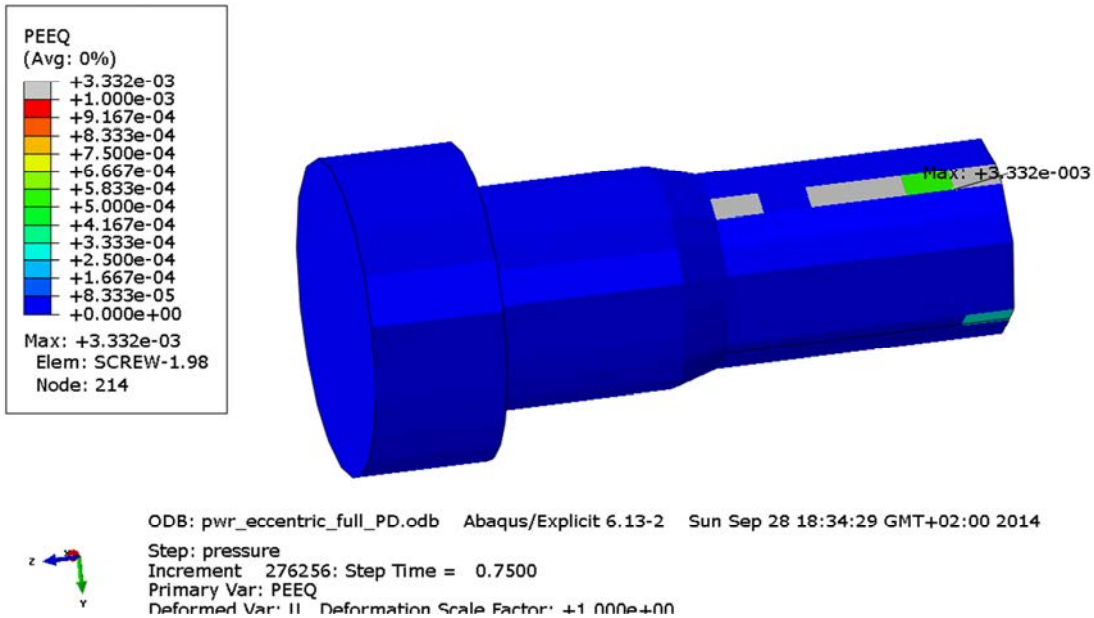

Figure A6-14 *Equivalent plastic strain (PEEQ) for the fixing screw with 120 MPa as applied hydrostatic pressure.*

Appendix 7 – Plots for pwr_defect_full_PD

Plots showing deformed geometry as contour plots for all parts of the PWR model at pressure magnitude 50, 90 and 120 MPa for case pwr_defect_full_PD (geometry based on manufacturing tolerances and eccentrically positioned channel tubes, 10 mm and an assumed cylindrical defect for the insert).

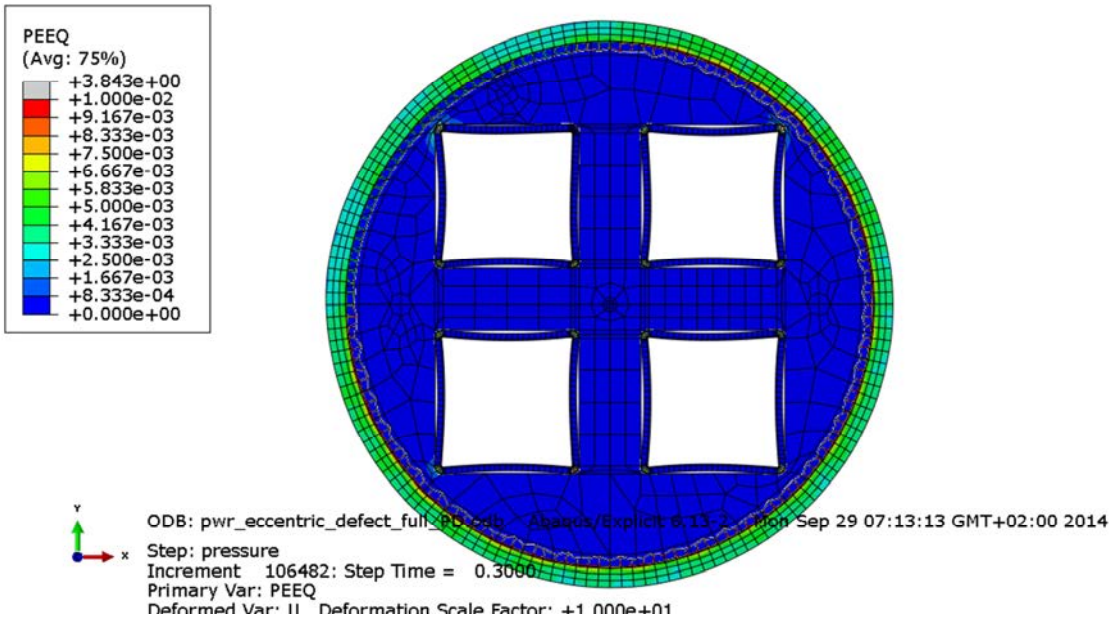

Figure A7-1 *Equivalent plastic strain (PEEQ) with 60 MPa as applied hydrostatic pressure. Displacements scaled by factor 100.*

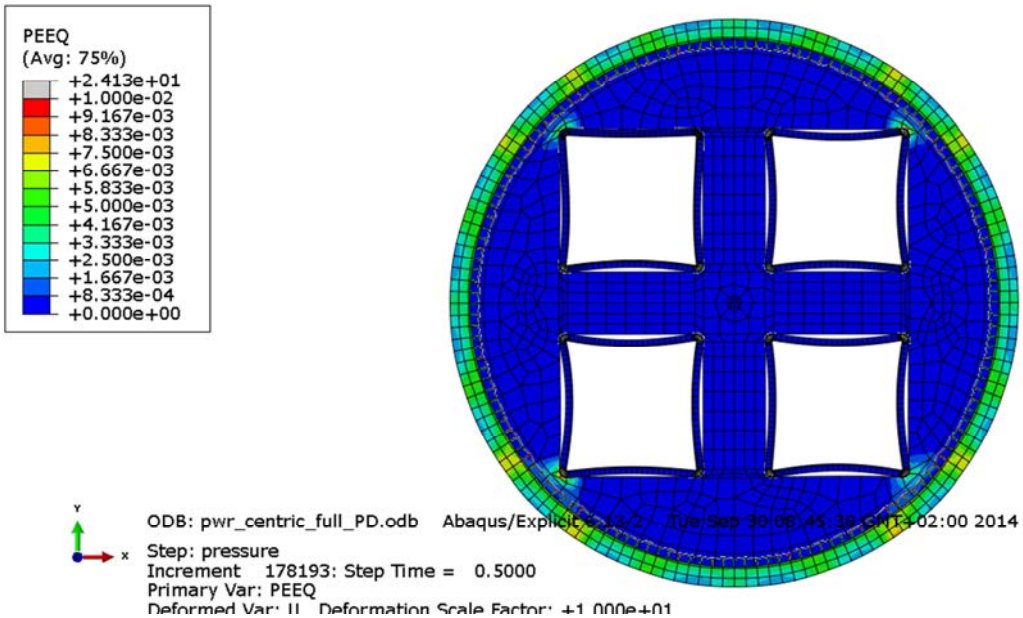

Figure A7-2 *Equivalent plastic strain (PEEQ) with 90 MPa as applied hydrostatic pressure. Displacements scaled by factor 10.*

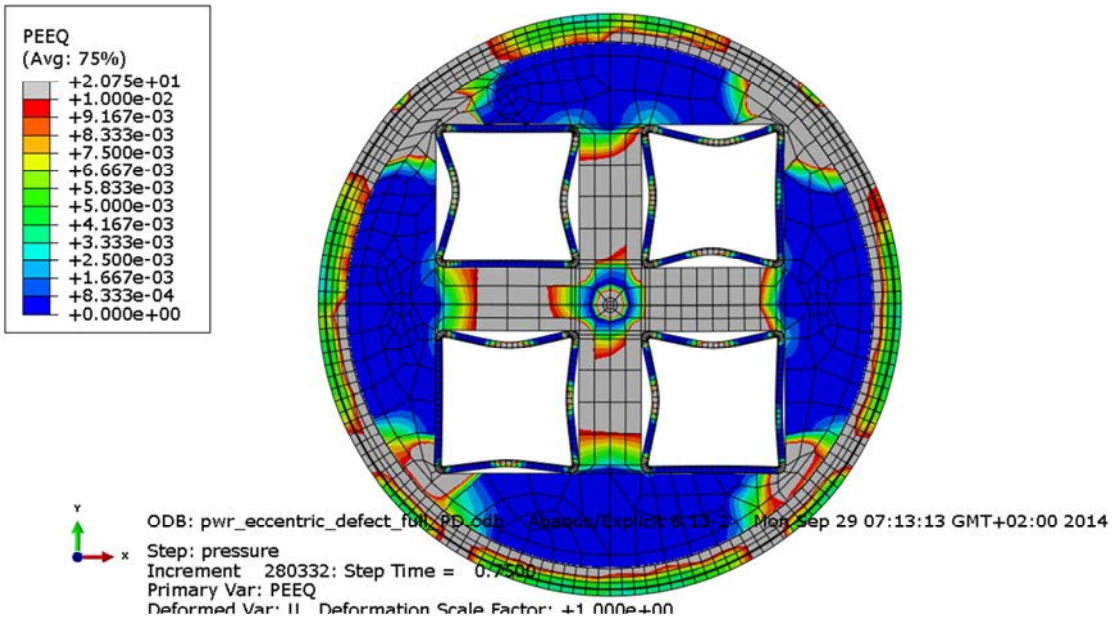

Figure A7-3 *Equivalent plastic strain (PEEQ) with 120 MPa as applied hydrostatic pressure.*

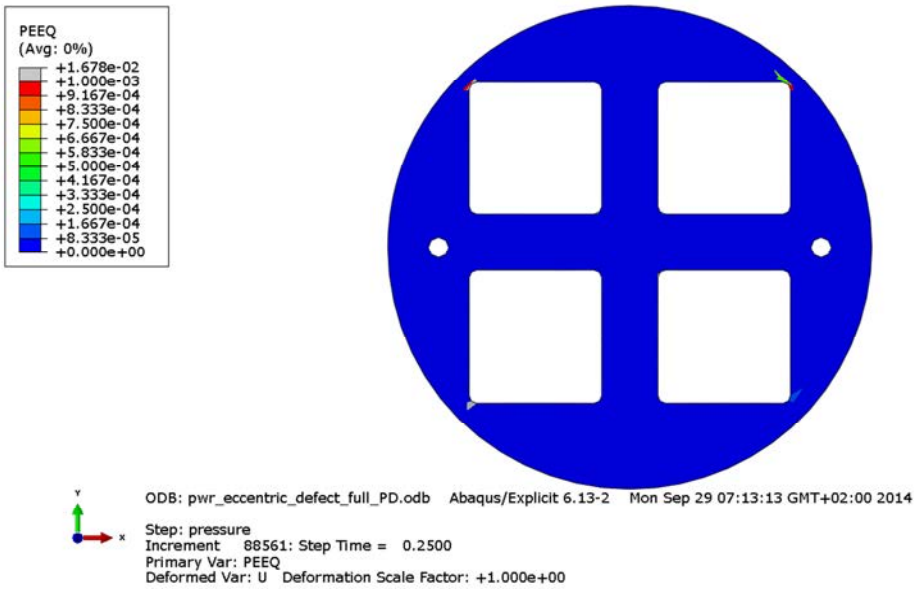

Figure A7-4 *Equivalent plastic strain (PEEQ) for the insert with 60 MPa as applied hydrostatic pressure.*

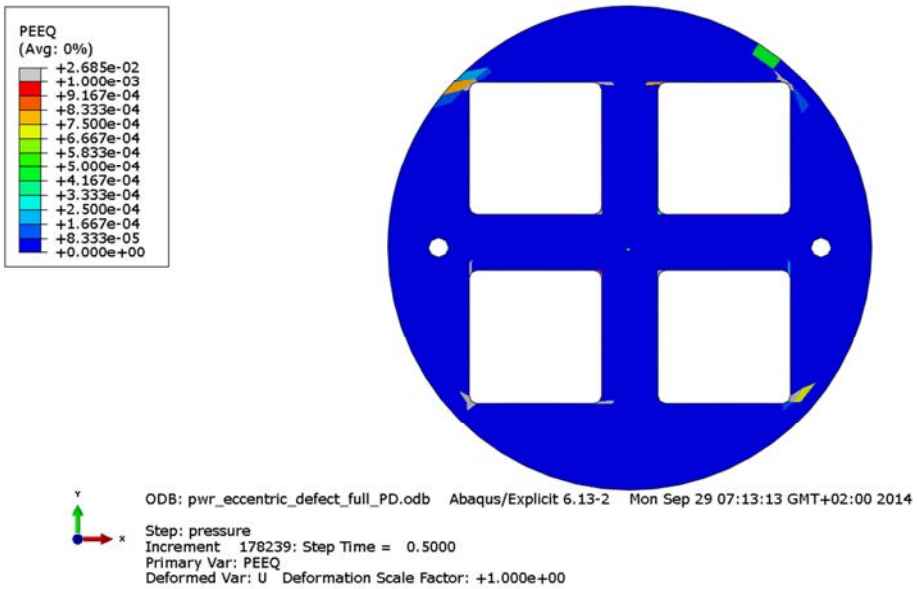

Figure A7-5 *Equivalent plastic strain (PEEQ) for the insert with 90 MPa as applied hydrostatic pressure.*

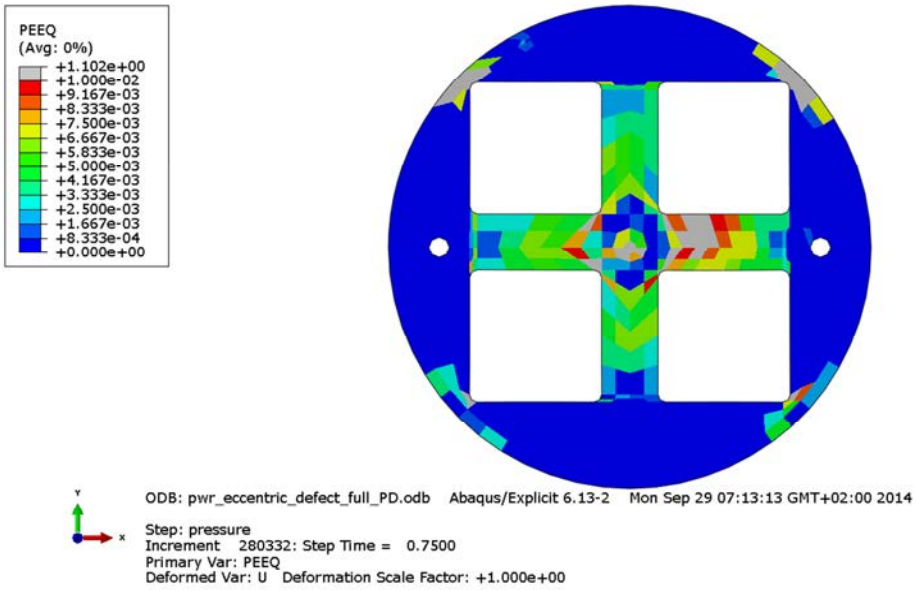

Figure A7-6 *Equivalent plastic strain (PEEQ) for the insert with 120 MPa as applied hydrostatic pressure.*

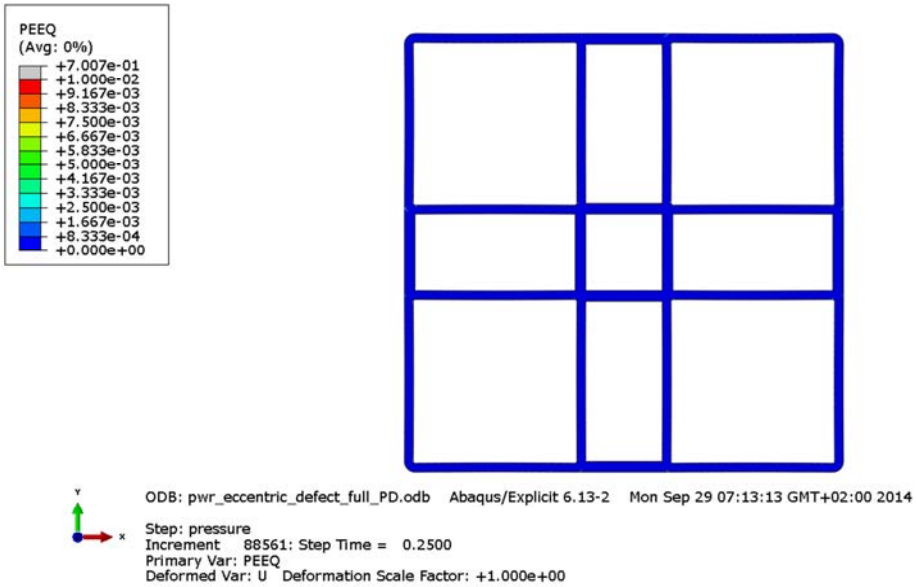

Figure A7-7 *Equivalent plastic strain (PEEQ) for the channel tubes with 60 MPa as applied hydrostatic pressure.*

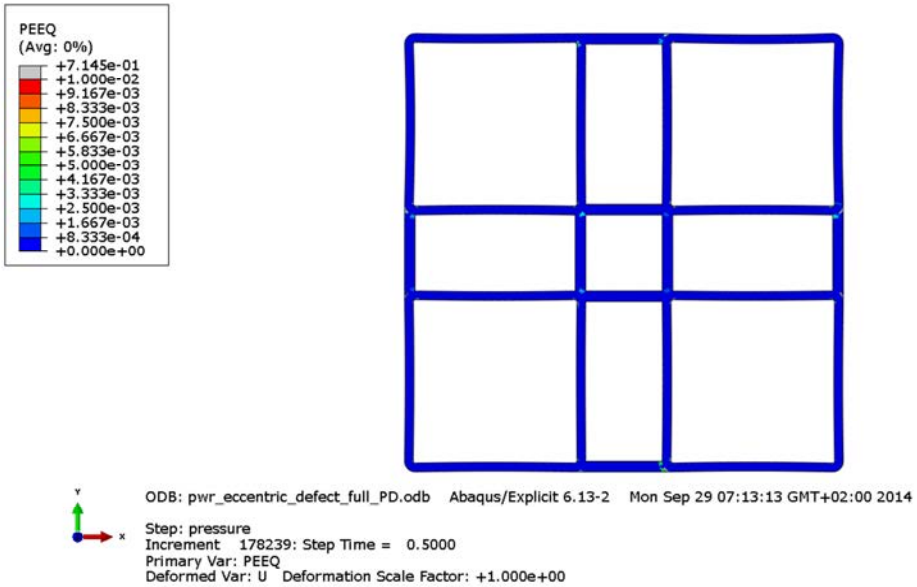

Figure A7-8 *Equivalent plastic strain (PEEQ) for the channel tubes with 90 MPa as applied hydrostatic pressure.*

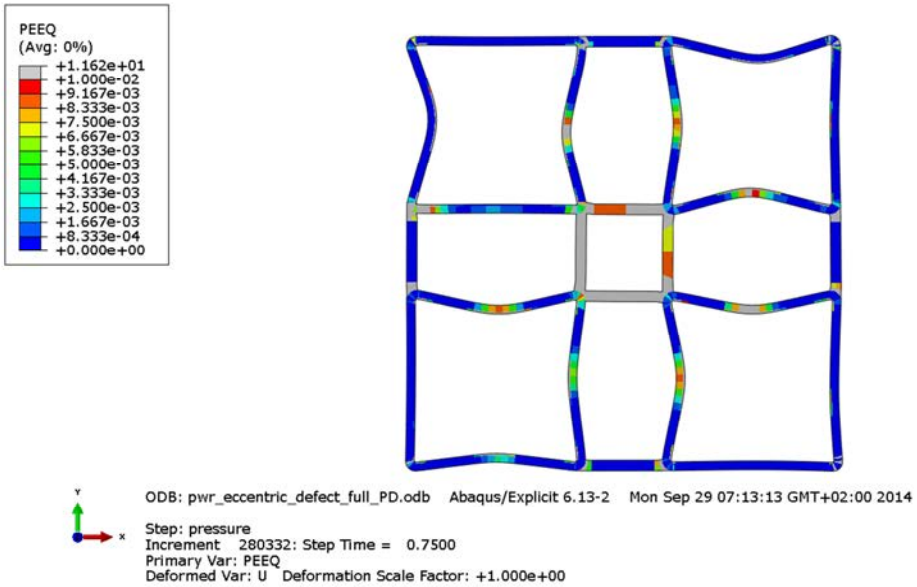

Figure A7-9 *Equivalent plastic strain (PEEQ) for the channel tubes with 120 MPa as applied hydrostatic pressure.*

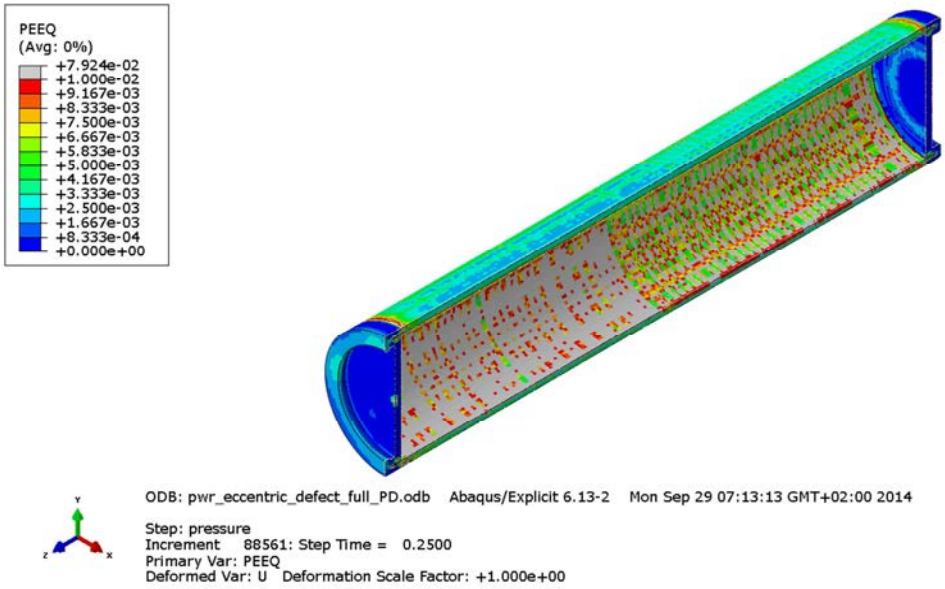

Figure A7-10 *Equivalent plastic strain (PEEQ) for the copper shell with 60 MPa as applied hydrostatic pressure.*

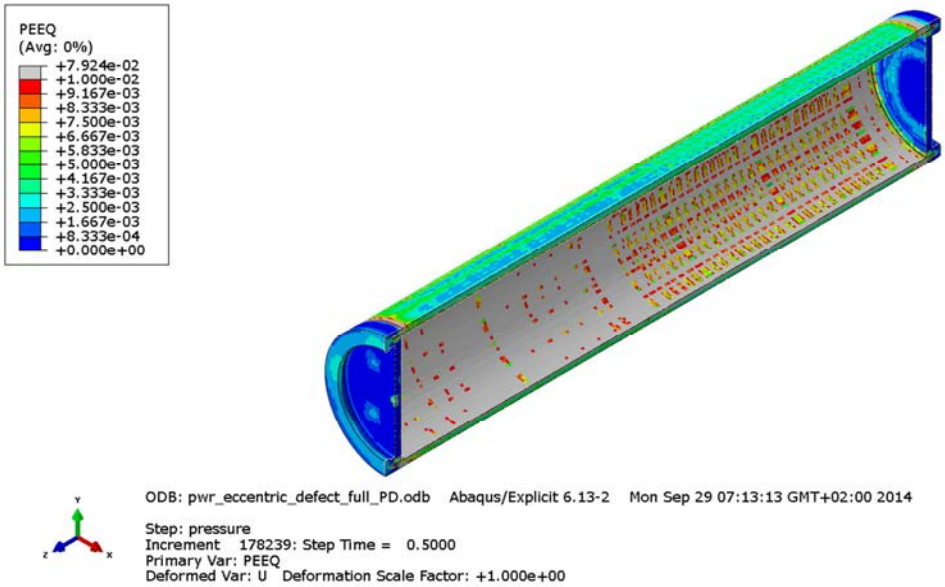

Figure A7-11 *Equivalent plastic strain (PEEQ) for the copper shell with 90 MPa as applied hydrostatic pressure.*

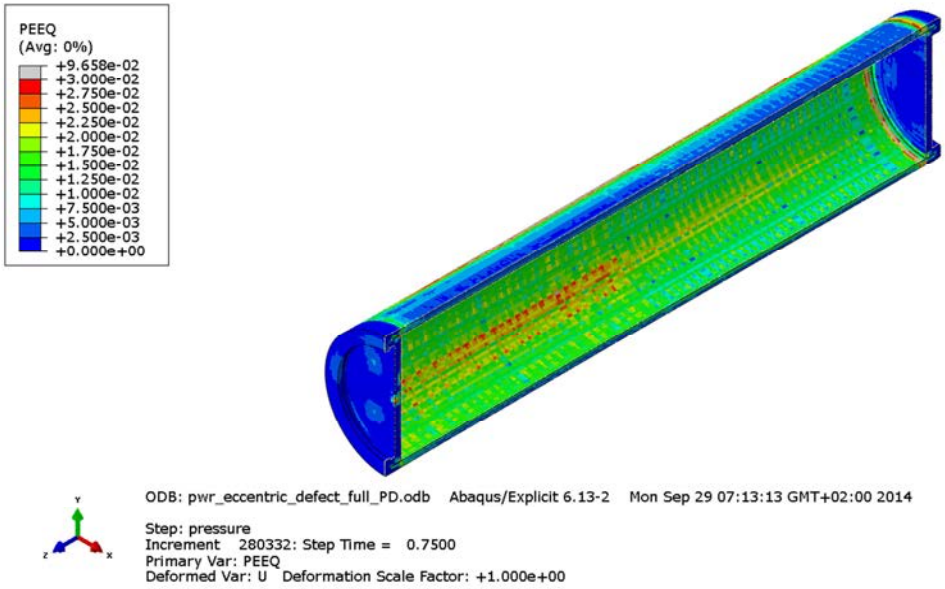

Figure A7-12 *Equivalent plastic strain (PEEQ) for the copper shell with 120 MPa as applied hydrostatic pressure.*

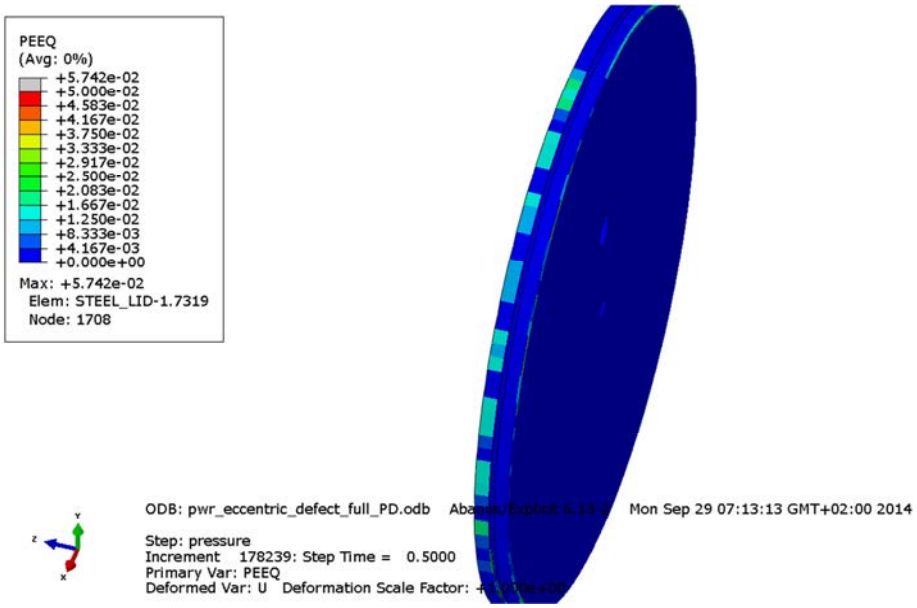

Figure A7-13 *Equivalent plastic strain (PEEQ) for the insert lid with 90 MPa as applied hydrostatic pressure.*

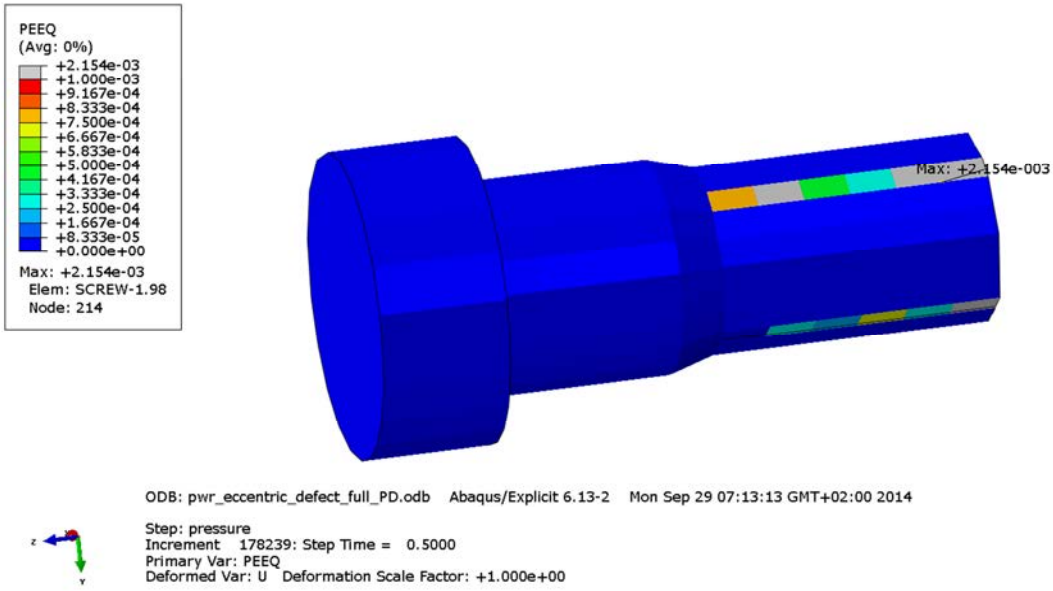

Figure A7-14 *Equivalent plastic strain (PEEQ) for the fixing screw with 90 MPa as applied hydrostatic pressure.*

Appendix 8 – Plots for pwr_defect_full_PD2

Plots showing deformed geometry as contour plots for all parts of the BWR model at pressure magnitude 50, 90 and 120 MPa for case pwr_defect_full_PD2 (geometry based on manufacturing tolerances and eccentrically positioned channel tubes, 10 mm and an assumed cylindrical defect for the insert). Yield surface for the insert has been reduced by scaling by factor 89%.

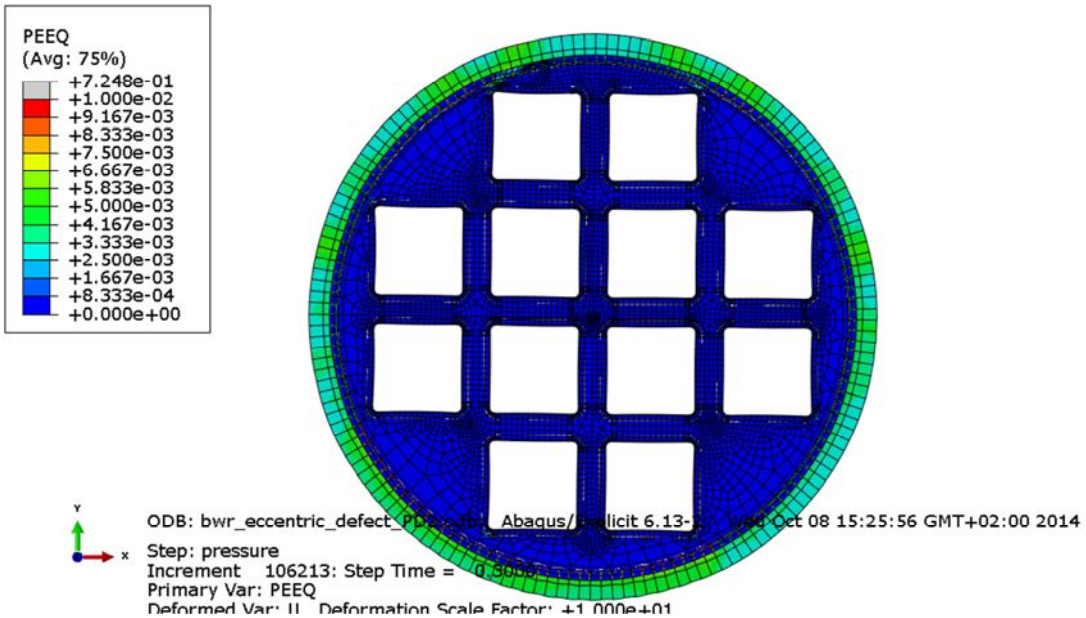

Figure A8-1 *Equivalent plastic strain (PEEQ) with 60 MPa as applied hydrostatic pressure. Displacements scaled by factor 10.*

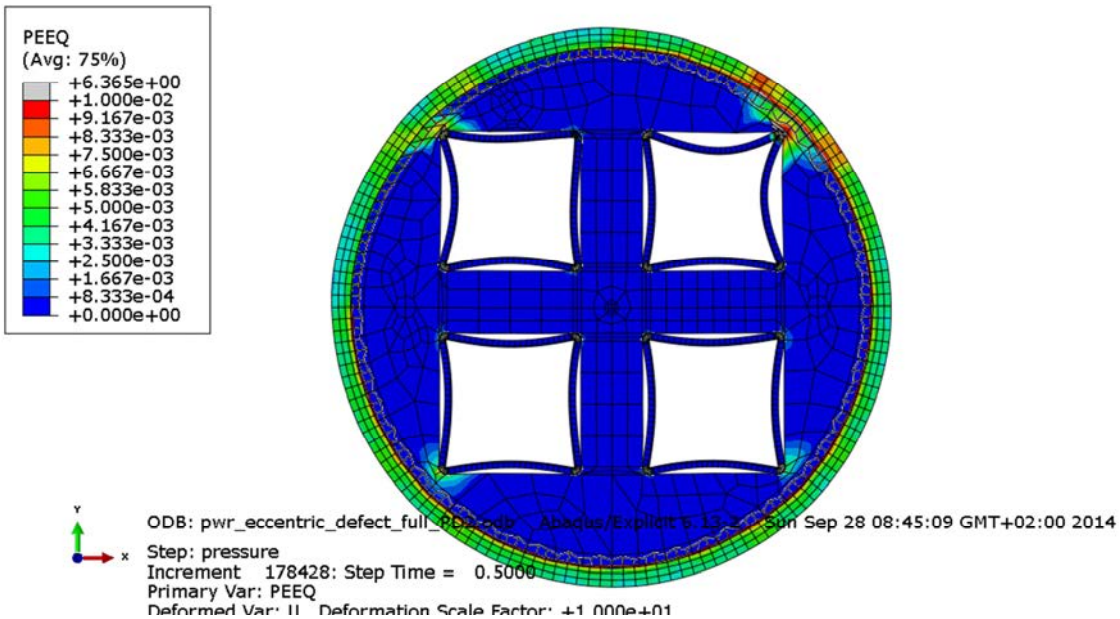

Figure A8-2 *Equivalent plastic strain (PEEQ) with 90 MPa as applied hydrostatic pressure. Displacements scaled by factor 10.*

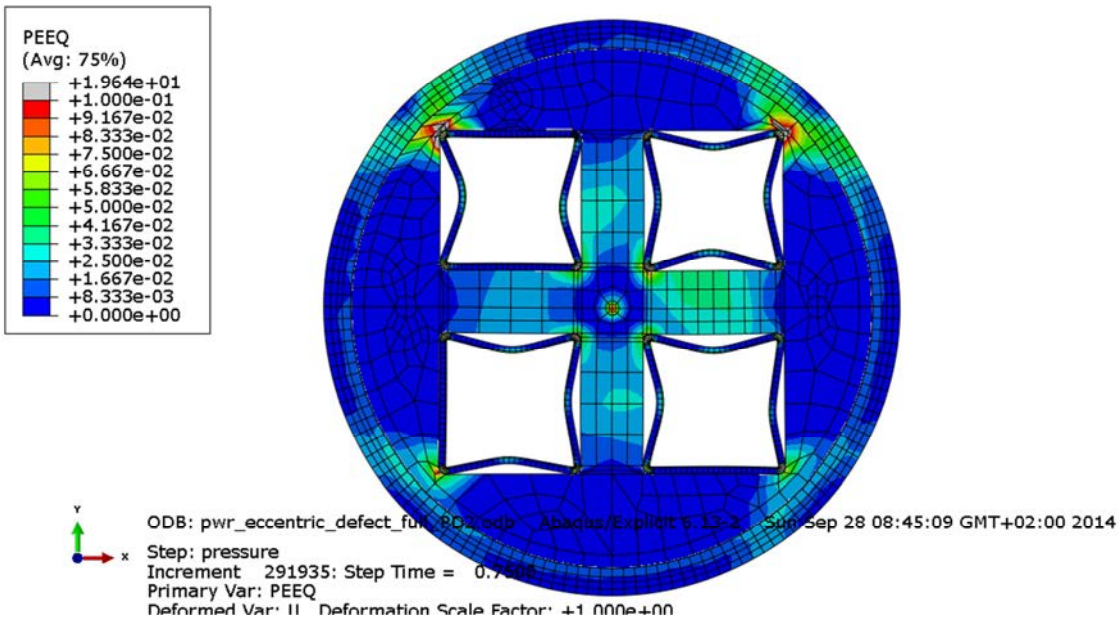

Figure A8-3 *Equivalent plastic strain (PEEQ) with 120 MPa as applied hydrostatic pressure.*

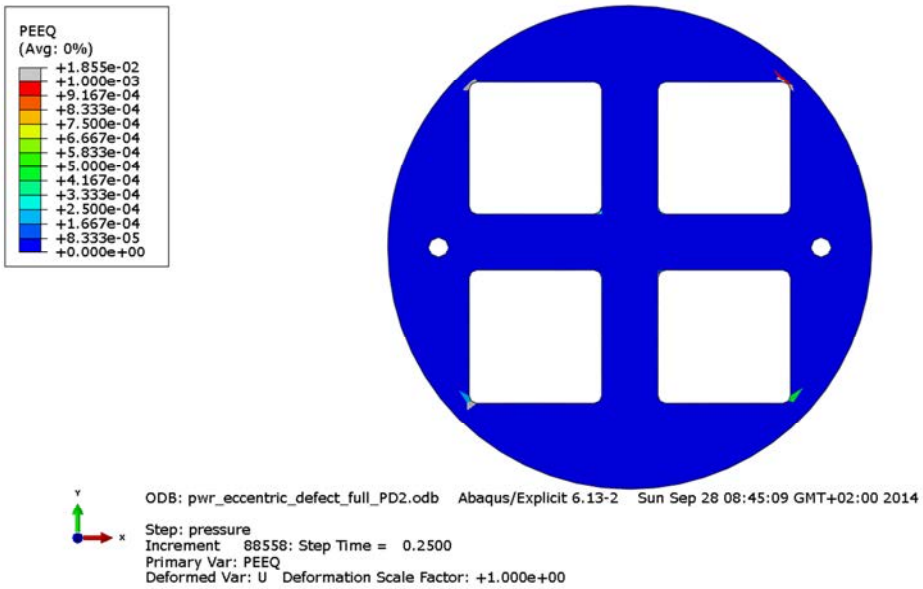

Figure A8-4 *Equivalent plastic strain (PEEQ) for the insert with 60 MPa as applied hydrostatic pressure.*

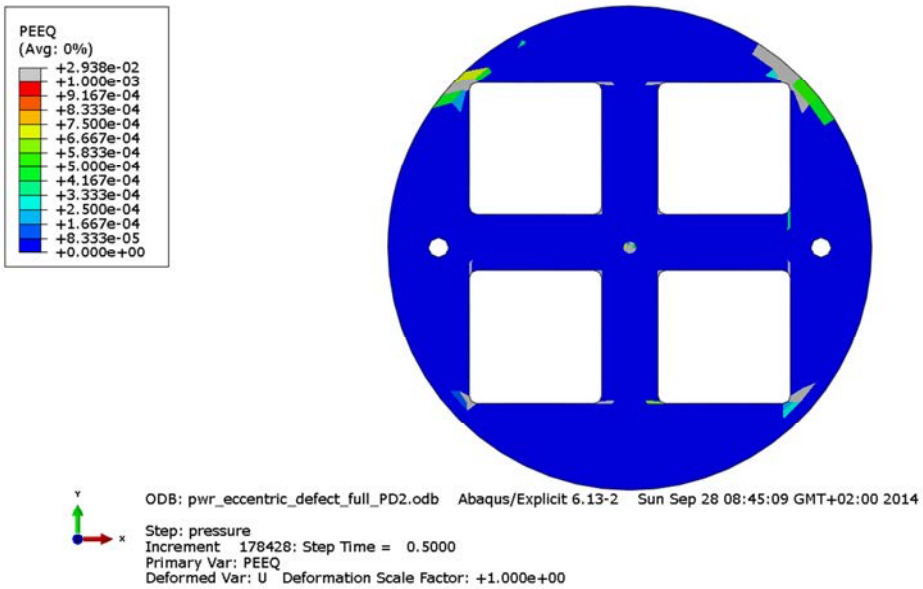

Figure A8-5 *Equivalent plastic strain (PEEQ) for the insert with 90 MPa as applied hydrostatic pressure.*

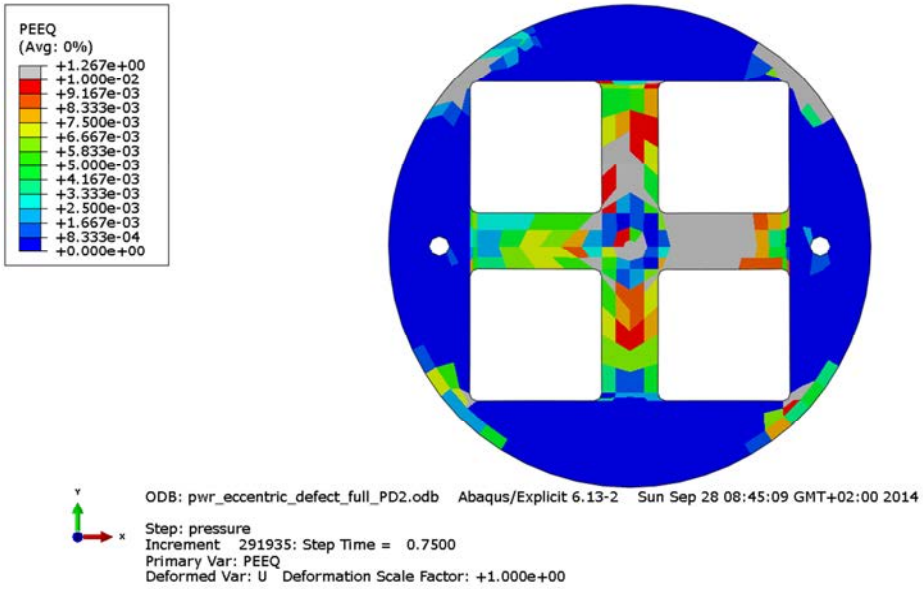

Figure A8-6 *Equivalent plastic strain (PEEQ) for the insert with 120 MPa as applied hydrostatic pressure.*

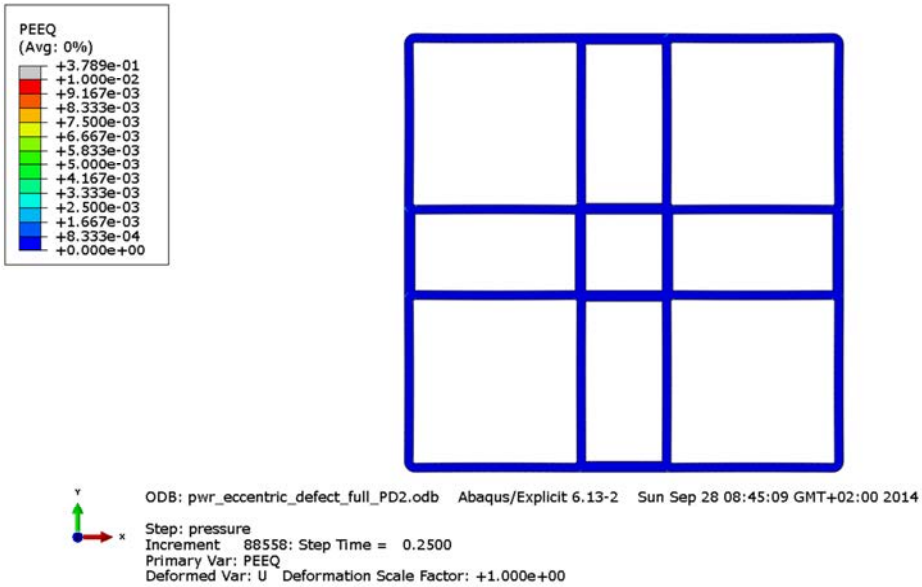

Figure A8-7 *Equivalent plastic strain (PEEQ) for the channel tubes with 60 MPa as applied hydrostatic pressure.*

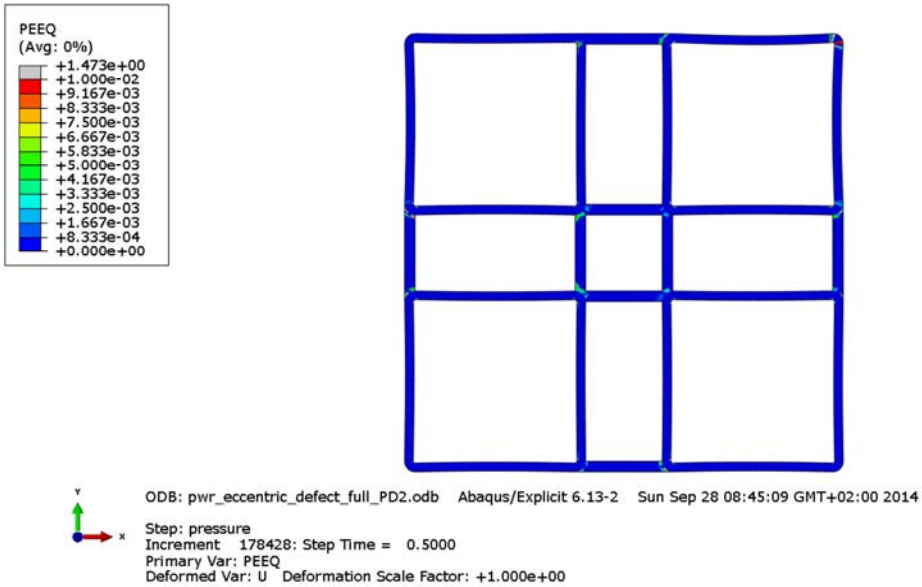

Figure A8-8 *Equivalent plastic strain (PEEQ) for the channel tubes with 90 MPa as applied hydrostatic pressure.*

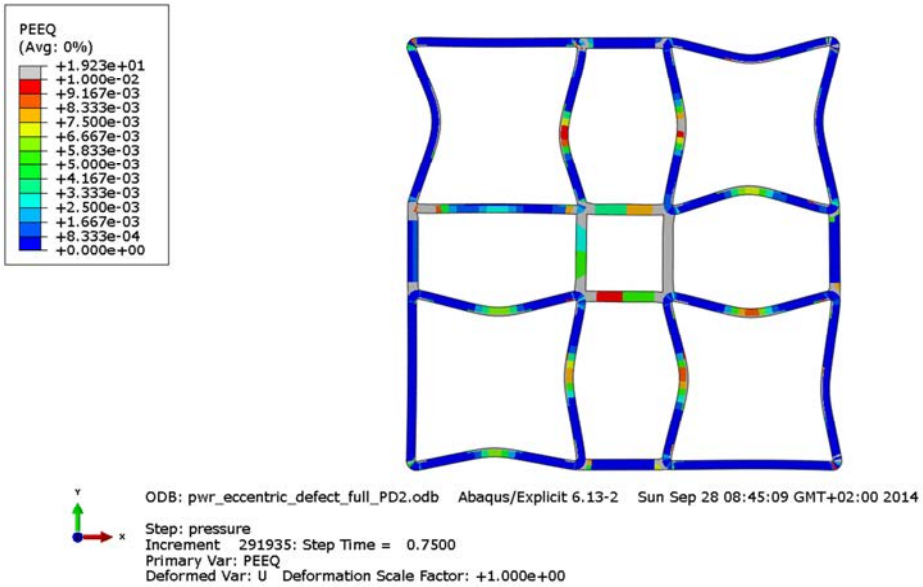

Figure A8-9 *Equivalent plastic strain (PEEQ) for the channel tubes with 120 MPa as applied hydrostatic pressure.*

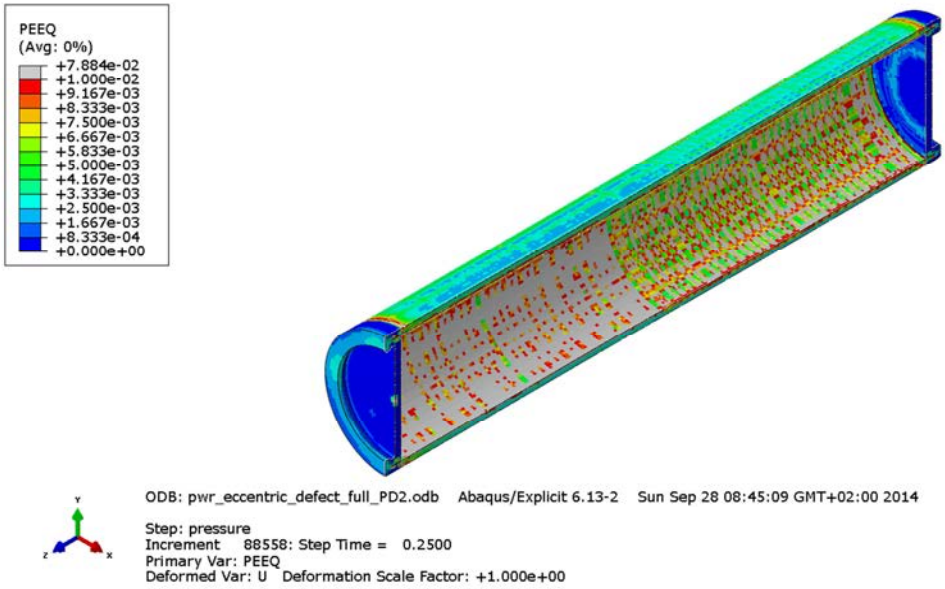

Figure A8-10 *Equivalent plastic strain (PEEQ) for the copper shell with 60 MPa as applied hydrostatic pressure.*

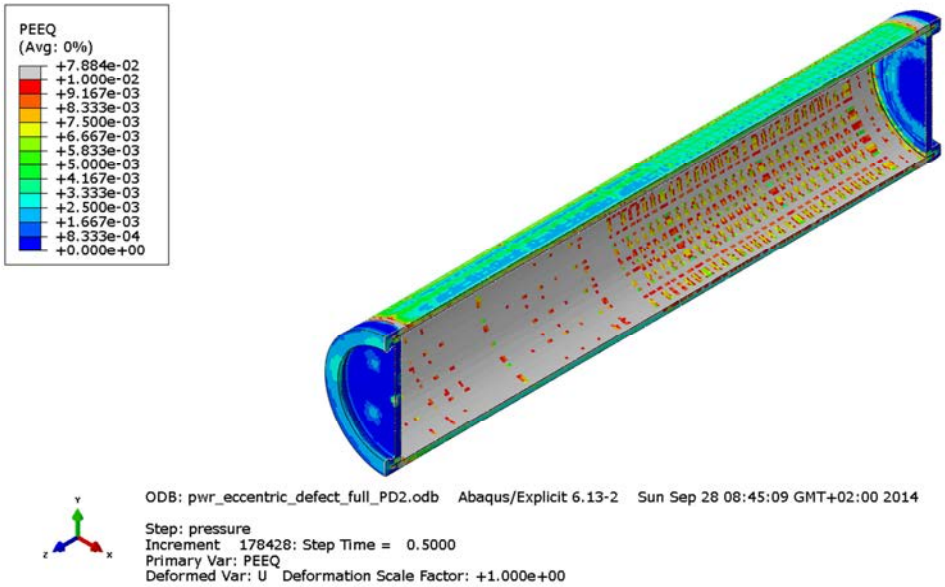

Figure A8-11 *Equivalent plastic strain (PEEQ) for the copper shell with 90 MPa as applied hydrostatic pressure.*

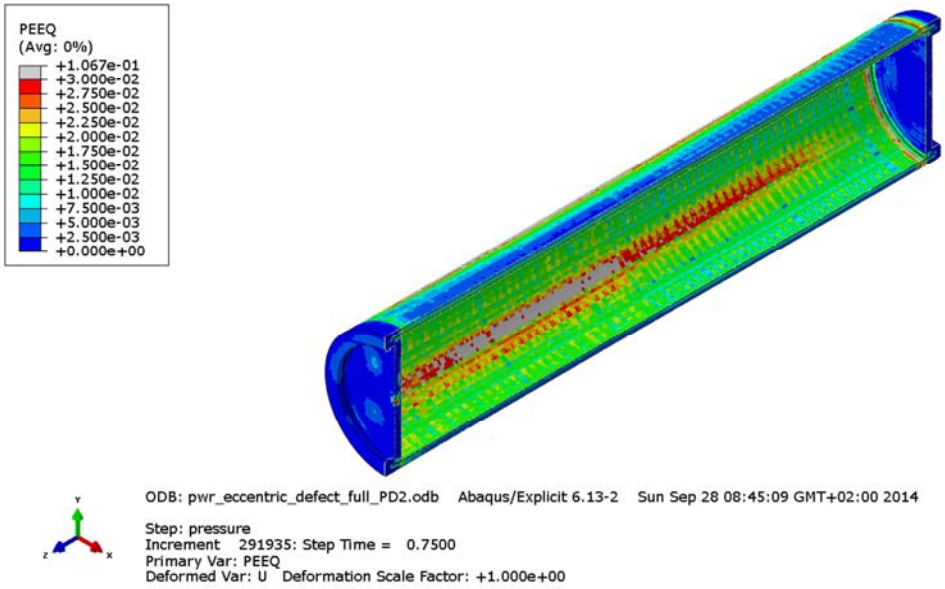

Figure A8-12 *Equivalent plastic strain (PEEQ) for the copper shell with 120 MPa as applied hydrostatic pressure.*

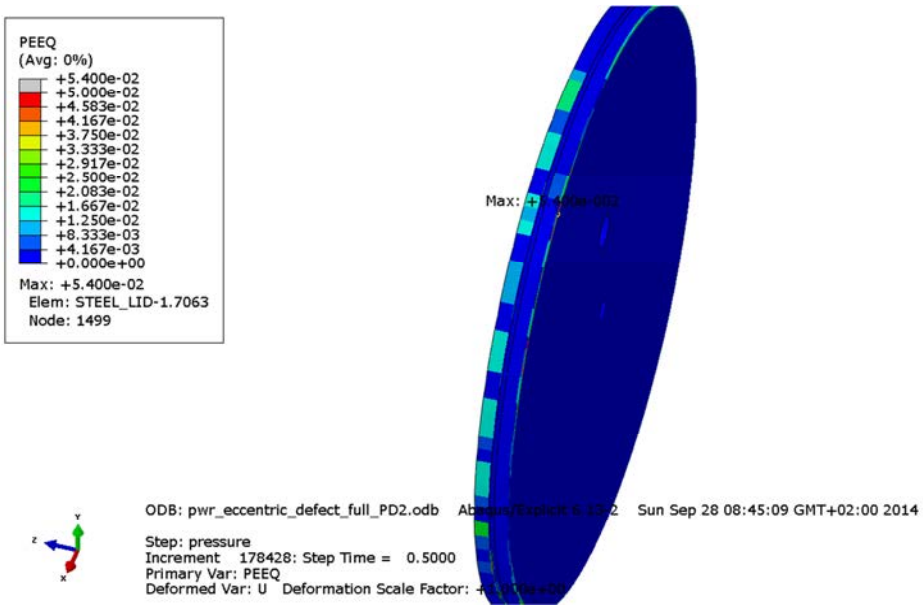

Figure A8-13 *Equivalent plastic strain (PEEQ) for the insert lid with 90 MPa as applied hydrostatic pressure.*

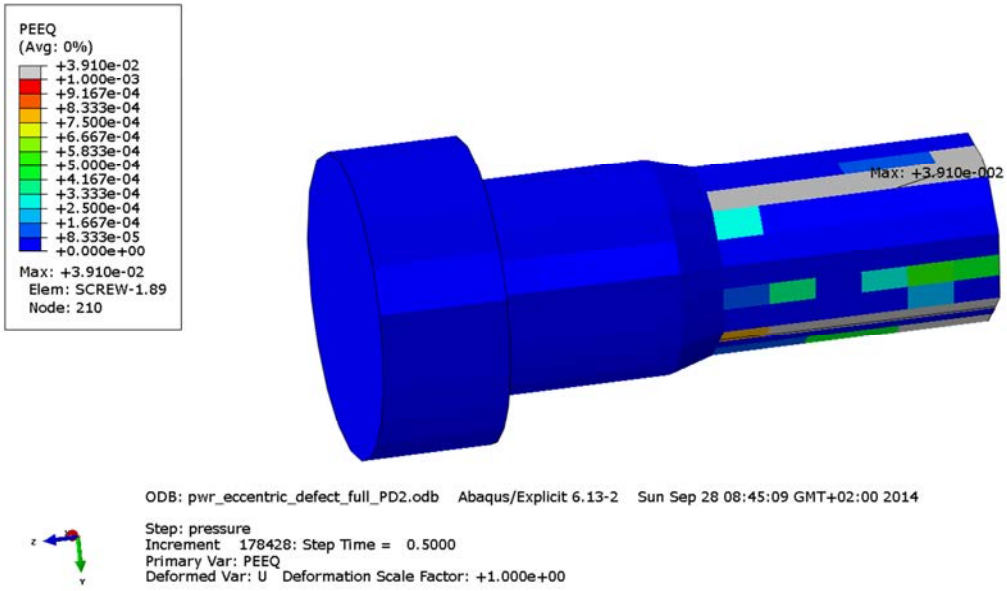

Figure A8-14 *Equivalent plastic strain (PEEQ) for the fixing screw with 90 MPa as applied hydrostatic pressure.*

Appendix 9 – Storage of files

This report is based on the results from a lot of FE-simulations using ABAQUS which is a commercial available code and is thus not stored as part of the work. Below is a short description of files used in the project and directories for storage of these. These files are also stored at SKB.

The files are stored in directories as:

Geometry Input-files Plots Hydrostatic load for detailed BWR/PWR-canisters.docx - this report Scripts

1 – Plot-files used in the report

Contents in C:\Users\jhd\mappar\skb\Detailed_PWR_BWR\hydrostatic\Plots
pwr_defect_mesh.png
pwr_defect.png
bwr_defect_mesh.png
bwr_defect.png
bwr_centric_rotated_PD-peeq_wo_bad_elements.png
bwr_centric_rotated_PD-peeq_bad_elements.png
bwr_centric_rotated_PD-bad_elements.png
bwr_eccentric_defect_PD-peeq_wo_bad_elements.png
bwr_eccentric_defect_PD-peeq_bad_elements.png
bwr_eccentric_defect_PD-bad_elements.png
Pressure_vs_Time-PWR.png
pwr_channels3.png
pwr_channels2.png
pwr_channels.png
pwr_insert-defect_mesh.png
pwr_insert-defect.png
pwr_insert-centric_eccentric.png
bwr_channels3.png
bwr_channels2.png
bwr_channels.png
bwr_insert-defect_mesh.png
bwr_insert-defect.png
bwr_insert-centric_eccentric.png
bwr_insert_channels_view2.png
bwr_steel_lid_view2.png
bwr_screw_view2.png
bwr_channels_view2.png
bwr_channels_top_view2.png
bwr_channels_bot_view2.png
bwr_insert_cut_bot_view2.png
bwr_insert_cut_top_view2.png
bwr_insert_cut_view2.png
bwr_copper_cut_view2.png
bwr_copper_cut_top_view2.png
bwr_copper_cut_bot_view2.png
bwr_all_cut_bot_view2.png
bwr_all_cut_top_view2.png
bwr_all_cut_view2.png
pwr_defect_cut_view2.png
bwr_defect_cut_view_mesh.png
bwr_defect_cut_view.png
bwr_defect_top_view.png
steel_lid.png
steel_lid_mesh.png
screw_mesh.png
screw.png
bwr_insert_all_bot_view.png
bwr_insert_channels_all_top_view.png

bwr_channels_all_mesh_top_view.png
bwr_channels_all_mesh_bot.png
bwr_channels_all_mesh_top.png
bwr_channels_all.png
bwr_insert_cut_mesh_bot.png
bwr_insert_cut_mesh_top.png
bwr_insert_cut.png
bwr_copper_cut_mesh_bot.png
bwr_copper_cut_mesh_top.png
bwr_copper_cut.png
bwr_all_cut_mesh_bot.png
bwr_all_cut_mesh_top.png
bwr_all_cut_mesh1.png
bwr_all_cut.png
bwr_all.png
pwr_insert_channels_view2.png
pwr_steel_lid_view2.png
pwr_screw_view2.png
pwr_channels_view2.png
pwr_channels_top_view2.png
pwr_channels_bot_view2.png
pwr_insert_cut_bot_view2.png
pwr_insert_cut_top_view2.png
pwr_insert_cut_view2.png
pwr_copper_cut_view2.png
pwr_copper_cut_top_view2.png
pwr_copper_cut_bot_view2.png
pwr_all_cut_bot_view2.png
pwr_all_cut_top_view2.png
pwr_all_cut_view2.png
pwr_defect_cut_view_mesh.png
pwr_defect_cut_view.png
pwr_defect_top_view.png
pwr_insert_all_bot_view.png
pwr_insert_channels_all_top_view.png
pwr_channels_all_mesh_top_view.png
pwr_channels_all_mesh_bot.png
pwr_channels_all_mesh_top.png
pwr_channels_all.png
pwr_insert_cut_mesh_bot.png
pwr_insert_cut_mesh_top.png
pwr_insert_cut.png
pwr_copper_cut_mesh_bot.png
pwr_copper_cut_mesh_top.png
pwr_copper_cut.png
pwr_all_cut_mesh_bot.png
pwr_all_cut_mesh_top.png
pwr_all_cut_mesh1.png
pwr_all_cut.png
pwr_all.png

Contents in C:\Users\jhd\mappar\skb\Detailed_PWR_BWR\hydrostatic\Plots

Results

bwr_loading_slow2.png
bwr_loading_slow.png
bwr_eccentric_defect_PD2_slow2-Energies_vs_Time.png
bwr_eccentric_defect_PD2_slow2-ASME.png
bwr_eccentric_defect_PD_check-ASME_special.png
bwr_eccentric_defect_PD2_slow-Energies_vs_Time.png
bwr_eccentric_defect_PD2_check-PlasticEnergy_vs_Time.png
pwr_eccentric_defect_full_PD2_slow-Energies_vs_Time.png
pwr_all-PlasticEnergy_vs_Time.png
pwr_all-StrainEnergy_vs_Time.png
bwr_eccentric_defect_PD_check-ASME_special2.png
bwr_eccentric_defect_PD_check-ASME_node.png
bwr_all-PlasticEnergy_vs_Time.png
bwr_all-KineticEnergy_vs_Time.png
pwr_eccentric_defect_PD2_slow-insert_peeq_end.png
pwr_eccentric_defect_PD2_slow-nodes.png
pwr_eccentric_defect_PD2_slow-Energy_vs_time.png
bwr_eccentric_defect_PD2_slow-insert_peeq_end.png
bwr_eccentric_defect_PD2_slow-node.png
bwr_eccentric_defect_PD2_slow_Energy_vs_time.png
bwr_all-StrainEnergy_vs_time.png
bwr_eccentric_defect_PD2_slow-ASME_disp.png
bwr_eccentric_defect_PD_check-ASME_disp.png
bwr_eccentric_defect_PD2_check-ASME_disp.png
bwr_excentric_rotated_PD_check-ASME_disp.png
bwr_eccentric_defect_PD_slow-insert_peeq_end.png
bwr_centric_rotated_PD_check-ASME_disp.png
pwr_eccentric_full_PD_last-KineticEnergy_vs_Pressure_detail.png
pwr_eccentric_full_PD_last-ASME_disp.png
pwr_eccentric_full_PD_last-Energies.png
pwr_centric_PD-KineticEnergy_vs_Pressure_detail.png
pwr_centric_PD-ASME_disp.png
pwr_eccentric_defect_full_PD_last-ASME_disp.png
pwr_eccentric_defect_full_PD_last-
KineticEnergy_vs_Pressure_detail.png
pwr_eccentric_defect_full_PD2_slow-
KineticEnergy_vs_Pressure_detail.png
pwr_eccentric_defect_full_PD2_slow-ASME_disp.png
pwr_eccentric_defect_full_PD2_last-
KineticEnergy_vs_Pressure_detail.png
pwr_eccentric_defect_full_PD2_last-ASME_disp.png
pwr_eccentric_defect_full_PD2_slow_ASME.png
pwr_slow_loading.png
bwr_centric_rotated_PD_check-KineticEnergy_vs_Pressure_detail.png
bwr_excentric_rotated_PD_check-KineticEnergy_vs_Pressure_detail.png
bwr_eccentric_defect_PD2_last-KineticEnergy_vs_Pressure_detail.png
bwr_eccentric_defect_PD_last-KineticEnergy_vs_Pressure_detail.png
bwr_centric_PD_last-KineticEnergy_vs_Pressure_detail.png

Appendix 1

bwr_centric_rotated_PD-copper_peeq_120MPa.png
bwr_centric_rotated_PD-copper_peeq_90MPa.png
bwr_centric_rotated_PD-copper_peeq_60MPa.png
bwr_centric_rotated_PD-screw-peeq-60MPa.png
bwr_centric_rotated_PD-screw-peeq-90MPa.png
bwr_centric_rotated_PD-screw-peeq-120MPa.png
bwr_centric_rotated_PD-insert_lid-peeq-120MPa.png
bwr_centric_rotated_PD-insert_lid-peeq-90MPa.png
bwr_centric_rotated_PD-insert_lid-peeq-60MPa.png
bwr_centric_rotated_PD-channels-peeq-60MPa.png
bwr_centric_rotated_PD-channels-peeq-90MPa.png
bwr_centric_rotated_PD-channels-peeq-120MPa.png
bwr_centric_rotated_PD-insert-peeq-120MPa.png
bwr_centric_rotated_PD-insert-peeq-90MPa.png
bwr_centric_rotated_PD-insert-peeq-60MPa.png
bwr_centric_rotated_PD-peeq_200MPa.png
bwr_centric_rotated_PD-peeq_150MPa.png
bwr_centric_rotated_PD-peeq_120MPa.png
bwr_centric_rotated_PD-peeq_90MPa.png
bwr_centric_rotated_PD-peeq_60MPa.png
bwr_centric_rotated_PD-peeq1.png
bwr_centric_rotated_PD-peeq_100MPa.png

Appendix 2

bwr_excentric_rotated_PD-copper_peeq_120MPa.png
bwr_excentric_rotated_PD-copper_peeq_90MPa.png
bwr_excentric_rotated_PD-copper_peeq_60MPa.png
bwr_excentric_rotated_PD-screw-peeq-60MPa.png
bwr_excentric_rotated_PD-screw-peeq-90MPa.png
bwr_excentric_rotated_PD-screw-peeq-120MPa.png
bwr_excentric_rotated_PD-insert_lid-peeq-120MPa.png
bwr_excentric_rotated_PD-insert_lid-peeq-90MPa.png
bwr_excentric_rotated_PD-insert_lid-peeq-60MPa.png
bwr_excentric_rotated_PD-channels-peeq-60MPa.png
bwr_excentric_rotated_PD-channels-peeq-90MPa.png
bwr_excentric_rotated_PD-channels-peeq-120MPa.png
bwr_excentric_rotated_PD-insert-peeq-120MPa.png
bwr_excentric_rotated_PD-insert-peeq-90MPa.png
bwr_excentric_rotated_PD-insert-peeq-60MPa.png
bwr_excentric_rotated_PD-peeq_200MPa.png
bwr_excentric_rotated_PD-peeq_150MPa.png
bwr_excentric_rotated_PD-peeq_120MPa.png
bwr_excentric_rotated_PD-peeq_90MPa.png
bwr_excentric_rotated_PD-peeq_60MPa.png
bwr_excentric_rotated_PD-peeq1.png

Appendix 3

bwr_eccentric_defect_PD-copper_peeq_120MPa.png
bwr_eccentric_defect_PD-copper_peeq_90MPa.png
bwr_eccentric_defect_PD-copper_peeq_60MPa.png
bwr_eccentric_defect_PD-screw-peeq-60MPa.png
bwr_eccentric_defect_PD-screw-peeq-90MPa.png
bwr_eccentric_defect_PD-screw-peeq-120MPa.png
bwr_eccentric_defect_PD-insert_lid-peeq-120MPa.png
bwr_eccentric_defect_PD-insert_lid-peeq-90MPa.png
bwr_eccentric_defect_PD-insert_lid-peeq-60MPa.png
bwr_eccentric_defect_PD-channels-peeq-60MPa.png
bwr_eccentric_defect_PD-channels-peeq-90MPa.png
bwr_eccentric_defect_PD-channels-peeq-120MPa.png
bwr_eccentric_defect_PD-insert-peeq-120MPa.png
bwr_eccentric_defect_PD-insert-peeq-90MPa.png
bwr_eccentric_defect_PD-insert-peeq-60MPa.png
bwr_excentric_defect-peeq_200MPa.png
bwr_excentric_defect-peeq_150MPa.png
bwr_excentric_defect-peeq_120MPa.png
bwr_excentric_defect-peeq_90MPa.png
bwr_excentric_defect-peeq_60MPa.png
bwr_excentric_defect-peeq1.png

Appendix 4

bwr_eccentric_defect_PD2-copper_peeq_120MPa.png
bwr_eccentric_defect_PD2-copper_peeq_90MPa.png
bwr_eccentric_defect_PD2-copper_peeq_60MPa.png
bwr_eccentric_defect_PD2-screw-peeq-60MPa.png
bwr_eccentric_defect_PD2-screw-peeq-90MPa.png
bwr_eccentric_defect_PD2-screw-peeq-120MPa.png
bwr_eccentric_defect_PD2-insert_lid-peeq-120MPa.png
bwr_eccentric_defect_PD2-insert_lid-peeq-90MPa.png
bwr_eccentric_defect_PD2-insert_lid-peeq-60MPa.png
bwr_eccentric_defect_PD2-channels-peeq-60MPa.png
bwr_eccentric_defect_PD2-channels-peeq-90MPa.png
bwr_eccentric_defect_PD2-channels-peeq-120MPa.png
bwr_eccentric_defect_PD2-insert-peeq-120MPa.png
bwr_eccentric_defect_PD2-insert-peeq-90MPa.png
bwr_eccentric_defect_PD2-insert-peeq-60MPa.png
bwr_excentric_defect_PD2-peeq_200MPa.png
bwr_excentric_defect_PD2-peeq_150MPa.png
bwr_excentric_defect_PD2-peeq_120MPa.png
bwr_excentric_defect_PD2-peeq_90MPa.png
bwr_excentric_defect_PD2-peeq_60MPa.png
bwr_excentric_defect_PD2-peeq1.png

Appendix 5

pwr_centric_full-screw_peeq_120MPa.png
pwr_centric_full-steel_lid_peeq_120MPa.png
pwr_centric_full-channels_peeq_60MPa.png
pwr_centric_full-channels_peeq_90MPa.png
pwr_centric_full-channels_peeq_120MPa.png
pwr_centric_full-channels_peeq_150MPa.png
pwr_centric_full-channels_peeq_200MPa.png
pwr_centric_full-insert_peeq_200MPa.png
pwr_centric_full-insert_peeq_150MPa.png
pwr_centric_full-insert_peeq_120MPa.png
pwr_centric_full-insert_peeq_90MPa.png
pwr_centric_full-insert_peeq_60MPa.png
pwr_centric_full-copper_peeq_60MPa.png
pwr_centric_full-copper_peeq_90MPa.png
pwr_centric_full-copper_peeq_120MPa.png
pwr_centric_full-copper_peeq_150MPa.png
pwr_centric_full-copper_peeq_200MPa.png
pwr_centric_full_PD-peeq_200MPa.png
pwr_centric_full_PD-peeq_150MPa.png
pwr_centric_full_PD-peeq_120MPa.png
pwr_centric_full_PD-peeq_90MPa.png
pwr_centric_full_PD-peeq_60MPa.png
pwr_centric_full_PD-peeq1.png

Appendix 6

pwr_eccentric_full_PD-screw_peeq_120MPa.png
pwr_eccentric_full_PD-steel_lid_peeq_120MPa.png
pwr_eccentric_full_PD-channels_peeq_60MPa.png
pwr_eccentric_full_PD-channels_peeq_90MPa.png
pwr_eccentric_full_PD-channels_peeq_120MPa.png
pwr_eccentric_full_PD-channels_peeq_150MPa.png
pwr_eccentric_full_PD-channels_peeq_200MPa.png
pwr_eccentric_full_PD-insert_peeq_200MPa.png
pwr_eccentric_full_PD-insert_peeq_150MPa.png
pwr_eccentric_full_PD-insert_peeq_120MPa.png
pwr_eccentric_full_PD-insert_peeq_90MPa.png
pwr_eccentric_full_PD-insert_peeq_60MPa.png
pwr_eccentric_full_PD-copper_peeq_60MPa.png
pwr_eccentric_full_PD-copper_peeq_90MPa.png
pwr_eccentric_full_PD-copper_peeq_120MPa.png
pwr_eccentric_full_PD-copper_peeq_150MPa.png
pwr_eccentric_full_PD-copper_peeq_200MPa.png
pwr_eccentric_full_PD-peeq_200 MPa.png
pwr_eccentric_full_PD-peeq_150 MPa.png
pwr_eccentric_full_PD-peeq_120 MPa.png
pwr_eccentric_full_PD-peeq_90 MPa.png
pwr_eccentric_full_PD-peeq_60 MPa.png
pwr_eccentric_full_PD-peeq1.png

Appendix 7

pwr_eccentric_defect_full_PD-screw_peeq_90MPa.png
pwr_eccentric_defect_full_PD-steel_lid_peeq_90MPa.png
pwr_eccentric_defect_full_PD-channels_peeq_60MPa.png
pwr_eccentric_defect_full_PD-channels_peeq_90MPa.png
pwr_eccentric_defect_full_PD-channels_peeq_120MPa.png
pwr_eccentric_defect_full_PD-channels_peeq_150MPa.png
pwr_eccentric_defect_full_PD-channels_peeq_200MPa.png
pwr_eccentric_defect_full_PD-insert_peeq_200MPa.png
pwr_eccentric_defect_full_PD-insert_peeq_150MPa.png
pwr_eccentric_defect_full_PD-insert_peeq_120MPa.png
pwr_eccentric_defect_full_PD-insert_peeq_90MPa.png
pwr_eccentric_defect_full_PD-insert_peeq_60MPa.png
pwr_eccentric_defect_full_PD-copper_peeq_60MPa.png
pwr_eccentric_defect_full_PD-copper_peeq_90MPa.png
pwr_eccentric_defect_full_PD-copper_peeq_120MPa.png
pwr_eccentric_defect_full_PD-copper_peeq_150MPa.png
pwr_eccentric_defect_full_PD-copper_peeq_200MPa.png
pwr_eccentric_defect_full_PD-screw_peeq_120MPa.png
pwr_eccentric_defect_full_PD-steel_lid_peeq_120MPa.png
pwr_eccentric_defect_full_PD-peeq_200MPa.png
pwr_eccentric_defect_full_PD-peeq_150MPa.png
pwr_eccentric_defect_full_PD-peeq_120MPa.png
pwr_eccentric_defect_full_PD-peeq_90MPa.png
pwr_eccentric_defect_full_PD-peeq_60MPa.png
pwr_eccentric_defect_full_PD-peeq1.png

Appendix 8

pwr_eccentric_defect_full_PD2-screw_peeq_90MPa.png
pwr_eccentric_defect_full_PD2-steel_lid_peeq_90MPa.png
pwr_eccentric_defect_full_PD2-channels_peeq_60MPa.png
pwr_eccentric_defect_full_PD2-channels_peeq_90MPa.png
pwr_eccentric_defect_full_PD2-channels_peeq_120MPa.png
pwr_eccentric_defect_full_PD2-channels_peeq_150MPa.png
pwr_eccentric_defect_full_PD2-channels_peeq_200MPa.png
pwr_eccentric_defect_full_PD2-insert_peeq_200MPa.png
pwr_eccentric_defect_full_PD2-insert_peeq_150MPa.png
pwr_eccentric_defect_full_PD2-insert_peeq_120MPa.png
pwr_eccentric_defect_full_PD2-insert_peeq_90MPa.png
pwr_eccentric_defect_full_PD2-insert_peeq_60MPa.png
pwr_eccentric_defect_full_PD2-copper_peeq_60MPa.png
pwr_eccentric_defect_full_PD2-copper_peeq_90MPa.png
pwr_eccentric_defect_full_PD2-copper_peeq_120MPa.png
pwr_eccentric_defect_full_PD2-copper_peeq_150MPa.png
pwr_eccentric_defect_full_PD2-copper_peeq_200MPa.png
pwr_eccentric_defect_full_PD2-peeq_200MPa.png
pwr_eccentric_defect_full_PD2-peeq_150MPa.png
pwr_eccentric_defect_full_PD2-peeq_120MPa.png
pwr_eccentric_defect_full_PD2-peeq_90MPa.png
pwr_eccentric_defect_full_PD2-peeq_60MPa.png
pwr_eccentric_defect_full_PD2-peeq1.png

2 – Input files used for the simulations

Each analysis is started by abaqus job=input-file (w/o .inp) double cpus=16.

Contents in C:\Users\jhd\mappar\skb\Detailed_PWR_BWR\hydrostatic\Input-files

```
pwr_eccentric_full_PD_last.inp
pwr_eccentric_defect_full_PD_last.inp
pwr_eccentric_defect_full_PD2_last.inp
bwr_eccentric_defect_PD2_check.inp
bwr_eccentric_defect_PD_check.inp
bwr_excentric_rotated_PD_check.inp
pwr_centric_PD.inp
bwr_centric_rotated_PD_check.inp
pwr_eccentric_defect_full_PD2_slow.inp
bwr_eccentric_defect_PD2_slow_old.inp
bwr_eccentric_defect_PD2_slow.inp
```

4 – Scripts used for post-processing

Used inside ABAQUS/CAE or by abaqus cae startup=script.py after appropriate editing of job-name inside the script-file.

Contents in C:\Users\jhd\mappar\skb\Detailed_PWR_BWR\hydrostatic\Scripts

```
KineticEnergy_wo_rigid.py       - script for kinetic energy wo rigid body rotation
filter_energy.py                - script for filtering kinetic energy
pwr_centric_PD.py               - script for PWR insert (Appendices)
bwr_centric_PD.py               - script for BWR insert (Appendices)
bwr_geom_plots.py               - script for BWR insert (geometry plots)
pwr_geom_plots.py               - script for PWR insert (geometry plots)
```

5 – Geometry definitions

Contents in C:\Users\jhd\mappar\skb\Detailed_PWR_BWR\hydrostatic\Geometry

```
pwr2_pressure.cae                          - ABAQUS/CAE database (PWR insert)
bwr_full_pressure.cae                      - ABAQUS/CAE database (BWR insert)
bwr_full_pressure.jnl                      - ABAQUS/CAE journal files (BWR insert)
pwr2_pressure.jnl                          - ABAQUS/CAE journal files (BWR insert)
bwr_correct_test_pressure.cae              - ABAQUS/CAE journal files (PWR insert)
bwr_correct_test_pressure.jnl              - ABAQUS/CAE journal files (BWR insert)
bwr_correct_test_pressure_old.jnl          - ABAQUS/CAE journal files (BWR insert)
pwr_pressure.jnl                           - ABAQUS/CAE journal files (PWR insert)
bwr_correct_test.jnl                       - ABAQUS/CAE journal files (BWR insert)
bwr_pressure.cae                           - ABAQUS/CAE database (BWR insert)
bwr_pressure.jnl                           - ABAQUS/CAE journal files (BWR insert)
bwr_correct_pressure.cae                   - ABAQUS/CAE database (BWR insert)
bwr_correct_pressure.jnl                   - ABAQUS/CAE journal files (BWR insert)
```

CAD-geometries received from SKB:

```
IDE-00015.pdf
IDE-00015.stp
IDE-00015-001.pdf
IDE-00015-21.pdf
IDE-00015-211.pdf
IDE-00015-001.stp
IDE-00015-21.stp
IDE-00015-211.stp
IDE-00025-131.stp
IDE-00025-13.stp
IDE-00015-121.stp
```